AD-772 604

THE DYNAMIC RESPONSE OF THE SPINE DURING + G_z ACCELERATION

P. Prasad, et al

Wayne State University

Prepared for:

Office of Naval Research

30 November 1973

DISTRIBUTED BY:

NTIS

National Technical Information Service
U. S. DEPARTMENT OF COMMERCE
5285 Port Royal Road, Springfield Va. 22151

Best Available Copy

AD-772 604

SECURITY CLASSIFICATION OF THIS PAGE (When Data Entered)

REPORT DOCUMENTATION PAGE

READ INSTRUCTIONS BEFORE COMPLETING FORM

1. REPORT NUMBER N00014-69-A-0235-0001	2. GOVT ACCESSION NO.	3. RECIPIENT'S CATALOG NUMBER
4. TITLE (and Subtitle) THE DYNAMIC RESPONSE OF THE SPINE DURING $+G_z$ ACCELERATION		5. TYPE OF REPORT & PERIOD COVERED Annual Report 6. PERFORMING ORG. REPORT NUMBER
7. AUTHOR(s) P. Prasad, A.I. King		8. CONTRACT OR GRANT NUMBER(s) N00014-69-A-0235-0001
9. PERFORMING ORGANIZATION NAME AND ADDRESS Wayne State Univ., Biomechanics Res. Ctr. 428 Med. Science Bldg., 1400 Chrysler Fwy Detroit, Michigan		10. PROGRAM ELEMENT, PROJECT, TASK AREA & WORK UNIT NUMBERS 105-540 (Code 444)
11. CONTROLLING OFFICE NAME AND ADDRESS Dept. of The Navy, Ofc. of Naval Research Medicine and Dentistry (Code 444) Arlington, Virginia 22217		12. REPORT DATE November 30, 1973 13. NUMBER OF PAGES 257
14. MONITORING AGENCY NAME & ADDRESS (if different from Controlling Office) SAME AS ABOVE		15. SECURITY CLASS. (of this report) Unclassified 15a. DECLASSIFICATION/DOWNGRADING SCHEDULE

16. DISTRIBUTION STATEMENT (of this Report)

Approved for public release; distribution unlimited

17. DISTRIBUTION STATEMENT (of the abstract entered in Block 20, if different from Report)

18. SUPPLEMENTARY NOTES

19. KEY WORDS (Continue on reverse side if necessary and identify by block number)

Impact acceleration, spinal load, facets, vertebrae, mathematical model, experimental verification

20. ABSTRACT (Continue on reverse side if necessary and identify by block number)

This report reviews previous results and presents qualitative as well as quantitative experimental evidence of the existence of a dual load path in the human spine--one through the intervertebral disc and the other through the articular facets. A 78 degree-of-freedom mathematical model is proposed. Its results compare favorably with those from experimental measurements on three cadaveric spines subjected to $+G_z$ acceleration.

DD FORM 1 JAN 73 1473 EDITION OF 1 NOV 65 IS OBSOLETE

SECURITY CLASSIFICATION OF THIS PAGE (When Data Entered)

THE DYNAMIC RESPONSE OF THE SPINE
DURING + G_z ACCELERATION

TO

DEPARTMENT OF THE NAVY
OFFICE OF NAVAL RESEARCH
MEDICINE AND DENTISTRY (CODE 444)
ARLINGTON, VIRGINIA 22217

ia

BIOMECHANICS RESEARCH
CENTER

November 30, 1973

N00014-69-A-0235-0001

THE DYNAMIC RESPONSE OF THE SPINE DURING + G_z ACCELERATION

P. Prasad and A.I. King
Wayne State University
Department of Mechanical Engineering Sciences
428 Medical Science Building
1400 Chrysler Freeway
Detroit, Michigan 48202

November 30, 1973

Annual Report for Period 15 March 1972 - 31 July 1973

Department of the Navy
Office of Naval Research
Medicine and Dentistry (Code 444)
Arlington, Virginia 22217

FOREWORD

This study was conducted by the Biomechanics Research Center of Wayne State University, Detroit, Michigan. The work was sponsored by the Medicine and Dentistry Program of the Office of Naval Research (Code 444), under Contract No. N00014-69-A-0235-0001.

The principal investigator was Professor Albert I. King and the project engineer was Dr. Priyaranjan Prasad. The contract was monitored by Lieutenant Commander Kenneth H. Dickerson, MSC, USN of ONR. The guidance and assistance provided by Capt. C. L. Ewing, MC, USN and Dr. D. J. Thomas of NAMRL, Detachment No. 1, Michoud Station, New Orleans, Louisiana are gratefully acknowledged.

SUMMARY

This report reviews the results obtained under this contract prior to this reporting period to set the background for the qualitative and quantitative documentation of the role of the articular facets during + G_z acceleration.

Experimental evidence, based on nearly 400 cadaver runs made on a vertical accelerator, is presented to prove the existence of dual load paths in the human spine - one through the intervertebral disc and one through the posterior structures in the articular facets. Utilizing the above fact, a method is shown and verified experimentally to increase the threshold of spinal fracture due to + G_z acceleration of the spine.

A 78 degree-of-freedom mathematical model and its experimental verification on three cadaveric spines is presented to simulate the dynamic response of the human spine during + G_z acceleration. The design and use of an intervertebral load cell to measure axial force and moment developed within the spine during + G_z acceleration is also presented.

TABLE OF CONTENTS

LIST OF FIGURES

LIST OF FIGURES (cont'd)

LIST OF FIGURES (cont'd)

LIST OF FIGURES (cont'd)

LIST OF FIGURES (cont'd)

LIST OF TABLES

LIST OF TABLES (cont'd)

CHAPTER I

INTRODUCTION

Several hypotheses have been advanced to explain the anterior wedging fractures of vertebrae during ejections of pilots from jet aircraft. Most of the proposed explanations consider the peak acceleration values, the rate of onset of acceleration, and consider the vertebral column as a single structure or a series of single structures having failure stress levels which when exceeded result in vertebral body fracture. These theories consider basically a symmetrical weight distribution in the mid-sagittal plane of the human body, and hence do not take into account the rotation of the vertebral column. Vulcan and King [20] showed that the vertebral column was subjected to significantly high bending strains due to the eccentricity of the location of the center of gravity of head and torso, with respect to that of the vertebral column, resulting in a forward rotation of head and torso during + G_z acceleration. Due to this bending of the vertebral column, the strains developed in the vertebral column during + G_z acceleration were the highest along the anterior aspects of the vertebral bodies. Orne and Liu [15] studied the phenomenon with a multi degree-of-freedom mathematical model of the human spine.

Using the bending theory of the vertebral column it would be possible, by altering the initial configuration of the spine with respect to the acceleration vector, to decrease the bending moments on the anterior aspects of the vertebral bodies, hence increasing the threshold of fracture. Hence, depending on whether the acceleration vector is before or behind the center of mass, anterior or posterior wedge compression fractures respectively would occur if the failure limit in anterior or posterior bending is exceeded. After studying eighty ejection vertebral fracture cases, Ewing [4] noted that almost all were anterior compression fractures; only one was a posterior compression fracture. Hence, he advanced the following hypothesis [5]:

> "Posterior compression of the vertebral column in the thoraco-lumbar area is limited by the articular facets of the vertebrae while anterior compression is not limited."

This suggested a way of preventing anterior vertebral compression fracture. By proper hyperextension of the spine a configuration between adjacent vertebrae would be achieved that would allow anterior wedging fracture to occur only if the spinous processes connecting the articular facets to the vertebral bodies are fractured or if the ligaments binding the articular facets together are torn. Also, by hyperextending the spine it would be possible to induce a pretension in the anterior aspects of the vertebral bodies hence increasing the bending moment and axial force required to cause failure of the anterior surfaces. Moreover, by hyperextension of the spine, it would be possible to reduce the strains developed on the anterior aspects of the vertebral bodies by shifting the center of gravity of the torso with respect to the acceleration vector, hence allowing lesser relative angular rotation of adjacent vertebrae as compared to a normally erect spine.

Experiments were carried out to verify the hypothesis and its corollaries. The following chapters describe the experiments carried out.

CHAPTER II

DETERMINATION OF THE OPTIMUM SHAPE AND OPTIMUM LOCATION OF A HYPEREXTENSION DEVICE

1. Introduction

The first phase of the study was to obtain the best location and shape of a hyperextension device which will reduce the peak strains experienced by the vertebrae when the device is not used. The criteria used to determine the optimum location and geometry of the hyperextension block were as follows:

(a) The block and its location should cause the greatest overall reduction in compressive strain levels in the vertebrae.

(b) Tensile strains in any of the vertebra were considered unacceptable, because tension in the vertebral body implies severe compressive loading on the posterior structures and may cause hyperextension fractures.

2. Experimental Procedures

A total of six cadavers were instrumented and subjected to caudocephalad acceleration. Table 1 provides a list of the cadavers used and the number of runs carried out on each specimen. Selection of the cadavers were made on the basis of age, cause of death, and body weight. Those over 70 years of age were rejected and if the cause of death appeared to

TABLE 1

List of Cadavers and

Number of Runs Carried Out

Run No.	Cadaver No.	Age at Death	Cause of Death
*	1494	59	pulmonary embolism
1-28	1580	47	chronic alcoholism
29-48	1582	60	pneumonia
49-50	1459	63	carcinoma
51-57	1536	68	pulmonary edema
58-80	1471	66	pneumonia

*2 unnumbered runs

have a considerable effect on the strength of the vertebral column, the cadaver was not used. Roentgenographic examination of the column was carried out on suitable specimens. Lateral and A-P views were examined for pre-existing fractures or other abnormalities. Spines with abnormal curvatures and those which showed a high degree of calcium depletion or were arthritic were rejected.

(a) Geometry of the hyperextension devices:

The hyperextension devices consisted of wooden blocks which were fastened to the seat back with two countersunk carriage bolts. The height of the blocks from the seat pan was adjustable from 5" - 20" above the seat. Four of the blocks used were 6" wide with different height and thickness. One block was semi-circular, 3" in diameter and 6" wide. Table 2 shows the dimensions of the blocks used.

(b) Instrumentation of vertebral bodies:

The procedure for instrumenting the cadavers consisted of evisceration of the abdominal viscera and the installation of foil-type strain gages on the anterior and lateral aspects of the vertebral bodies. In every cadaver, the three vertebrae gaged were T12, L2 and L4. The method of installation of the strain gages is described below.

The vertebral bodies to be gaged were cleaned by cutting and scraping off the ligaments around it, taking care that the surface of the bones was not damaged. A minimum area of the bone was exposed to ensure some continuity of the ligaments on the bodies. The exposed surfaces of the bones were then

TABLE 2

Description of Hyperextension Devices

Block No.	Shape	Thickness (in)	Height (in)	Width (in)
1	Rectangular parallelepiped	2.25	6.0	6.0
2	Rectangular parallelepiped	3.00	6.0	6.0
3	Semicircle	3.00	6.0	6.0
4	Rectangular parallelepiped	3.00	4.0	6.0
5	Rectangular parallelepiped	2.25	4.0	6.0

cleaned and dried using acetone and freon. Foil type strain gages, 0.125" gage length, were then installed on the cleaned surfaces using Eastman 910 adhesive and catalyst as bonding agents. The installed gages were then tested for resistance to ground. A minimum of 500 megohms of resistance to ground ensured long-lasting and noise-free gages. The installed gages were then coated with Gagekote #3 to ensure insulation from body fluids. The leads from the gages were carefully tied down by sutures to a disc to prevent the gages from being ripped off during the experiment.

One gage was mounted on the anterior surface of the vertebral body as close as possible to the mid-sagittal plane. The lateral gages were mounted in pairs, one on each side of the body, placed as closely as possible in the same coronal plane. The output of the left and right gages was summed to eliminate the effects of lateral bending. All gages were installed with their sensitive axis parallel to the axis of the vertebral body, and all leads were pre-soldered to the gage terminals.

(c) Description of accelerator and instrumentation:

The tests were carried out on a vertical accelerator, housed in an 8-story elevator shaft of the School of Medicine, at Wayne State University. The sled is accelerated over a stroke of 8 feet and then gradually brought to rest by air brakes over some 30 to 40 feet. The acceleration pulse is approximately trapezoidal in shape, the rate of onset and the magnitude of the plateau being variable. Details of the accelerator have been described by Patrick [16].

The restraint system consisted of an automotive lap belt under a regular U.S.A.F. lap belt and shoulder harness combination and leg straps. The wrists were tied together and anchored to the seat base by means of a single rope going through an eye bolt in the seat base and looping around the U.S.A.F. lap belt. This was done so that no load was transmitted on the arm rest, and to prevent the lap belt from creeping up on the cadaver during pretensioning of the shoulder harness. The head was unrestrained.

The electronic instrumentation consisted of 12-channels of bridge balance and carrier amplifier units (Heiland) and a 24-channel light-beam recorder (Visicorder). The sled was equipped with a 50-g strain gage accelerometer (Statham A6-50) and the shoulder harness load was monitored by a 1,000-lb. strap load cell.

After the cadaver had been placed in the chair, the lead wires from the strain gages were connected to form diagonally opposite arms of a 4-arm Wheatstone bridge. The other two arms consisted of 121-ohm high-stability precision resistors. This configuration results in the summing of the output of the two gages. The anterior gage formed a two-arm bridge with a 121-ohm resistor. The other 2 arms were provided by the bridge balance unit.

(d) Experimental runs:

The lap belt was always snugly tightened and restrained from being pulled upwards by the equivalent of an inverted V-strap described in the previous section. The shoulder harness was pre-loaded to 35 lb. tension before each run. Although the head was unrestrained, its initial position was kept approximately vertical by means of masking tape that broke once the head started rotating.

The level of the applied acceleration was 10 g at an onset rate of approximately 300 g/sec. The low acceleration level was used to avoid vertebral fracture and to allow completion of a long series of runs on each cadaver. The acceleration was reduced to 8 g for Cadaver 1471 since it was the oldest among the ones tested.

In order to compare the reduction in vertebral strain resulting from the use of the hyperextension device, at least two runs without the block were carried out on each cadaver. Generally the first and last runs were without the block. For Cadaver 1471, a no-block run was made after each block was tested to monitor more closely the change in strain gage output caused by a change in spinal configuration.

For the convenience of identification of gages, the following symbols will be used in the subsequent sections of this paper:

The prefix A denotes a gage mounted on the anterior surface of a vertebra, e.g., AT12 is the gage on the anterior surface of T12. The prefix D denotes gages mounted on the lateral surface of the vertebra. Strain values of DL2 represent the average output of the two gages on the lateral surface of L2 on either side of AL2. An attempt was made to install these gages near the neutral axis of the vertebra so that their output indicated mostly axial compression.

After each run, a lateral roentgenogram of the spine was taken. Experimentation was discontinued if fracture occurred. In some cases, the x-rays were developed after the completion of several runs. If fracture occurred in one of these runs, the data from all post-fracture runs were discarded.

[illegible]. Summary of Experimental Data

A total of 52 runs were made on six cadavers. Of these, [illegible] runs on 3 cadavers constitute the bulk of the data reported. Runs 49-57 on Cadavers 1459 and 1536 represent incomplete series due to fracture of vertebral bodies. The raw data of typical runs are shown in Figures 2.1 - 2.3.

The vertebral strains sustained in those runs without blocks show the familiar [illegible] reported by Vulcan and King [19]. An example of these control runs is given in Figure 2.1. Figure 2.2 is a typical run with a 2-1/4" thick block opposite L1. Note the disappearance of the second peak and compare with Figure 2.1 to see the reduction in strains on all gages. On Cadaver [illegible], the AL4 gage was malfunctioning, hence its record is meaningless. Figure 2.3 is an example of tension developing in the early part of the acceleration pulse.

Block No. 1 (2.25 × 6 × 6) was used in 12 runs at various locations. In Cadaver 1580 and 1582, when the centerline of the block was placed opposite the L3-L4 disc (Cadaver 1580), L3, L2-L3 disc and L2, the anterior surface of T12 (AT12) was in tension.

By increasing the thickness of the block to 3" (Block No. 2, 3 × 6 × 6), it was observed that AT12 went into tension when the block was opposite the L1-L2 disc, L3-L4 disc and L5 in Cadaver 1580, and opposite T11 and T12 in Cadaver 1471. AL2 went into tension when the block was 2" below L5. In 3 out of 9 cases, a reduction in compressive strain, without any vertebra going into tension, was observed.

There were 12 runs with the semi-circular block (No. 3, 6 in. in diameter and 3" thick). For Cadaver 1580, AT12 went into tension with the block opposite T12-L1 disc, L1-L2 disc, and L3-L4 disc. There was an increase in compression in AT12 and DT12 with the block 2 in. below L5, but there was a marked reduction in compressive strain in AL4. AL2 went into tension when the block was opposite L5. Hence all the 5 runs with this block displayed undesirable characteristics. The results for Cadaver 1582 were slightly better. Opposite L3 and L2-L3 disc, tension developed in AT12, but there was a slight reduction in compressive strain for all gages with the block opposite L2 and T12-L1 disc. In Cadaver 1471, there was an overall reduction in strain when the block was opposite T11 and T12, but AT12 developed tension with the block opposite L1.

The results from Block No. 4 (3 × 4 × 6), were also unsatisfactory. For Cadaver 1580, AT12 developed tension with the block opposite the T12-L1 disc, L1-L2 disc and L3-L4 disc, and DT12 showed an increase in compressive strain when the block was 2" below L5. For Cadaver 1582, with the block opposite T11, an increase in compressive strain for all gages was observed. However, opposite L1, there was a general reduction in strain on all gages. For Cadaver 1471, AT12 developed tension with the block opposite T11. There was a slight reduction in strain when it was opposite the T10-T11 disc.

The results from Block No. 5 (2.25 × 4 × 6) were encouraging. In Cadaver 1582, there was an overall reduction in compressive strain for all gages when the block was placed between T12 and L2. There was a minimal increase in strain when it was located opposite T11. Similarly, for Cadaver 1471, a good overall reduction in strain was obtained with the block opposite T11, T12 and L1.

4. Analysis of Data

The data from Cadavers 1580, 1582 and 1471 were read off the records, converted to strain, compared with the control runs, and the percentage change in strain computed in terms of a reduction in compression. The reduction was tabulated for each block and listed in Tables 3 through 7. The description of the results in the previous section is given in quantitative terms in these tables. In order to evaluate the relative merits of these blocks, Table 8 was prepared using the runs in which no tension was developed and no increase in compression was noted. This procedure reduced the number of runs from 50 to 21. The average percentage decrease in compressive strain was computed for the anterior and lateral gages separately and an overall average was then obtained. It can be seen from Table 8 that the 2-1/4" blocks show a larger reduction than the 3" ones, and in the former group the best location is opposite L1 for every cadaver. An exception is

TABLE 3

Analysis of Data from Block No. 1 (2.25"×6"×6")

Run #	Location of Block	% Reduction in Peak Strain					
		AT12	DT12	AL2	DL2	AL4	DL4
3	below L5	4.52	22.0	64.0	24.8	84.5	35.6
4	L5	62.0	50.0	89.0	24.8	57.6	53.5
5	L3-L4 disc	125.0	66.0	75.5	7.96	33.0	33.0
6	L1-L2 disc	58.8	64.2	48.5	34.6	25.4	34.8
7	T12-L1 disc	51.5	47.5	31.2	24.8	6.7	16.9
44	L2-L3 disc	105.0	24.2	108.0	21.0	35.9	42.0
45	L2	105.0	31.0	81.0	27.6	35.9	42.0
46	T12-L1 disc	41.3	22.4	72.0	25.0	58.5	34.2
47	L3	103.0	43.0	138.0	21.0	119.0	47.4
66	T11	28.0	57.3	45.0	34.8	*	28.8
67	T12	41.0	53.4	67.3	50.0	*	45.2
68	oppos. L1	45.0	73.0	85.5	67.3	*	56.2

*indicates a malfunctioning strain gage

TABLE 4

Analysis of Data from Block No. 2 (3"×6"×6")

Run #	Location of Block	% Reduction in Peak Strain					
		AT12	DT12	AL2	DL2	AL4	DL4
8	2" below L5	34.1	40.0	115.0	24.8	85.0	42.4
11	L5	118.0	69.5	93.0	36.2	64.5	62.0
12	L3-L4 disc	151.0	75.0	66.5	42.5	43.2	52.5
13	L1-L2 disc	112.5	66.5	48.0	41.5	28.8	37.2
14	T12-L1 disc	71.2	68.0	41.6	31.8	17.0	31.4
78	T11	102.0	59.0	57.0	48.5	*	41.5
79	T12	105.0	61.8	82.0	72.0	*	47.8

*indicates a malfunctioning strain gage

TABLE 5

Analysis Data from Block No. 3 (semicircular block, 6" dia, 3" thick)

Run #	Location of Block	% Reduction in Peak Strain AT12	DT12	AL2	DL2	AL4	DL4
17	2" below L5	-16.2	-12.1	20.3	13.4	97.0	19.7
18	L5	32.4	16.8	131.0	21.8	68.5	58.0
19	L3-L4 disc	119.0	59.5	92.0	20.8	56.8	50.5
20	L1-L2 disc	143.0	66.0	67.0	50.0	47.0	38.2
21	T12-L1 disc	105.0	58.5	4.7	13.9	28.4	0.0
40	L3	101.0	32.8	72.0	33.0	5.65	40.8
41	L2-L3 disc	103.0	34.5	64.0	27.6	39.6	36.8
42	T12-L1 disc	27.2	15.5	56.3	13.2	20.8	27.6
43	L2	37.5	29.3	54.0	29.0	28.3	44.6
70	L1	106.0	71.5	54.9	50.5	*	40.0
71	T12	41.0	60.7	36.2	36.3	*	22.8
72	T11	42.3	43.0	21.5	17.6	*	14.3

*indicates a malfunctioning strain gage

TABLE 6

Analysis of Data from Block No. 4 (3"×4"×6")

Run #	Location of Block	% Reduction in Peak Strain AT12	DT12	AL2	DL2	AL4	DL4
22	below L5	0.0	-18.9	61.0	35.8	95.0	48.3
23	L5	0.52	21.0	123.0	24.3	54.5	59.5
24	L3-L4 disc	142.0	54.0	93.5	49.5	45.5	64.0
25	L1-L2 disc	150.0	71.4	50.6	43.0	35.0	60.6
26	T12-L1 disc	105.0	56.3	35.0	29.4	0.0	25.8
31	T11	-18.6	-12.4	-28.0	-22.0	-42.8	-25.6
32	T12	-50.0	-3.4	6.25	2.4	7.2	11.6
34	L1	16.3	19.0	34.4	22.0	17.9	42.0
35	L2	103.0	31.0	37.5	17.0	32.2	44.2
75	T10-T11 disc	25.9	35.6	5.0	8.0	*	3.0
76	bottom T11	108.0	63.0	40.0	47.0	*	38.0

*indicates a malfunctioning strain gage

TABLE 7

Analysis of Data from Block No. 5 (2.25"×4"×6")

Run #	Location of Block	% Reduction in Peak Strain AT12	DT12	AL2	DL2	AL4	DL4
36	L2	10.5	26.7	40.6	19.5	39.2	44.0
37	L1	30.2	6.9	50.0	34.2	28.6	42.0
38	T12	19.8	1.72	50.0	14.6	0.0	18.6
39	T11	10.5	-3.45	3.12	-2.4	-3.4	-7.0
60	T11	43.2	39.4	34.5	34.1	*	31.4
61	top of T12	48.6	66.6	57.0	48.3	*	38.9
62	L1	41.3	66.6	78.5	60.0	*	40.6
63	L1-L2 disc	103.0	83.4	88.0	60.0	*	47.3

*indicates a malfunctioning strain gage

TABLE 8

Analysis of Data for Runs in Which

Tension Was Not Developed

Block No.	Run No.	Location of Block Centerline	Average Ant. Gages	Strain Reduction (%) Lat. Gages	Overall
1	3	2" below L5	51.00	27.46	39.23
	4	L5	69.53	42.73	56.13
	6	L1-L2 disc	44.26	41.20	42.73
	7	T12-L1 disc	29.80	29.73	29.76
	46	T12-L1 disc	57.26	27.20	42.23
	66	T11	36.50	40.30	38.40
	67	T12	54.15	49.60	51.87
	68	L1	65.25	65.50	65.37
2	14	T12-L1 disc	43.26	43.73	43.50
3	42	T12-L1 disc	34.80	18.75	26.80
	43	L2	39.93	34.30	37.12
	71	T12	38.60	40.00	39.30
	72	T11	31.90	25.00	28.45
4	34	L1	22.86	27.70	25.28
	75	T10-T11 disc	15.45	15.53	15.49
5	36	L2	30.10	30.06	30.08
	37	L1	36.26	27.30	31.81
	38	T12	23.26	11.64	17.54
	60	T11	38.85	34.96	36.91
	61	Top of T12	52.80	51.26	52.03
	62	L1	59.90	51.26	55.58

found in Cadaver 1580 using Block No. 1. In this case, a large decrease of 89% in AL2 in Run No. 4, with the block opposite L5, indicated that the L5 location was better than L1. However, the other cadavers show definitely that L1 is the optimum location. Further consideration of the overall reduction at L1 for Blocks 1 and 5 shows that the decrease is 50.1% for Block No. 1 (Runs 6, 46, and 68) and 43.7% for Block No. 5 (Runs 37 and 62). The difference is quite small considering the large biological variations among cadavers and the small sample size. The consistent indications that L1 is the best location using either Block No. 1 or 5 is the major conclusion of this phase of the study.

5. Discussion and Conclusions

The primary objective of selecting the shape of the hyperextension device and its optimum location has been achieved. The data reported from the three cadavers used show that the block should be about 2 in. thick, 4 to 6 in. in height and that its centerline should be opposite L1.

Before the start of this series of experiments, it was expected that the lateral gages would show an increase in strain when the anterior gages showed a decrease. This was based on the hypothesis of a more evenly distributed loading of the vertebral bodies when the hyperextension device was used. However, in all cases the lateral gages, too, showed a marked decrease in strains. This brings up the question of whether the vertical force is being transmitted through the block or through the posterior structures of the vertebrae.

The segments of vertebrae from the cadavers tested were excised and examined radiologically to detect fractures of any posterior structures. However, none was found.

The development of tension on the anterior surface of the vertebrae is another problem which requires further investigation. An examination of the primary and secondary curvatures of the vertebral column, shown in Figure 2.4, reveals that, if the block is placed between L2 and L5, it forces the lumbar vertebrae forward of the center of gravity of the torso which is located about 1/4 to 1/2" in front of the anterior surface of T9 (see Ref. [19]). It can be seen from the data that the tensile stresses occur at the beginning of the acceleration pulse, before the upper torso has had a chance to begin its forward rotation. Also, the strap load dropped from its initial pretension (see Figure 2.3) during the early part of the acceleration pulse. This suggests a slight backward rotation of the upper torso during that period. Forward flexion of the torso immediately causes the gages to go into compression. By placing the block opposite L1, the forward displacement of the segment from T12 to L4 is just enough to reduce the compressive strain on the anterior surface without the development of tension. With the block opposite the lower thoracic vertebrae, the center of gravity of the upper torso is pushed farther forward, causing a greater eccentric loading of the spine, which results in an increase in compressive strain. The question of whether the ungaged vertebrae above T12 would go into tension when the block is at its optimum location for the T12 to L4 segment is still unanswered. However, the primary thoracic curve would tend to prevent tension of the anterior surfaces.

TABLE 9

Variation of Breaking Strength with Age

Age (years)	Median Breaking Strength (kp^*/cm^2)
20 - 30	107
30 - 40	98
40 - 50	76
50 - 60	77
over 60	43

* kp is a unit of force,

1 kp = 1 kilogram force

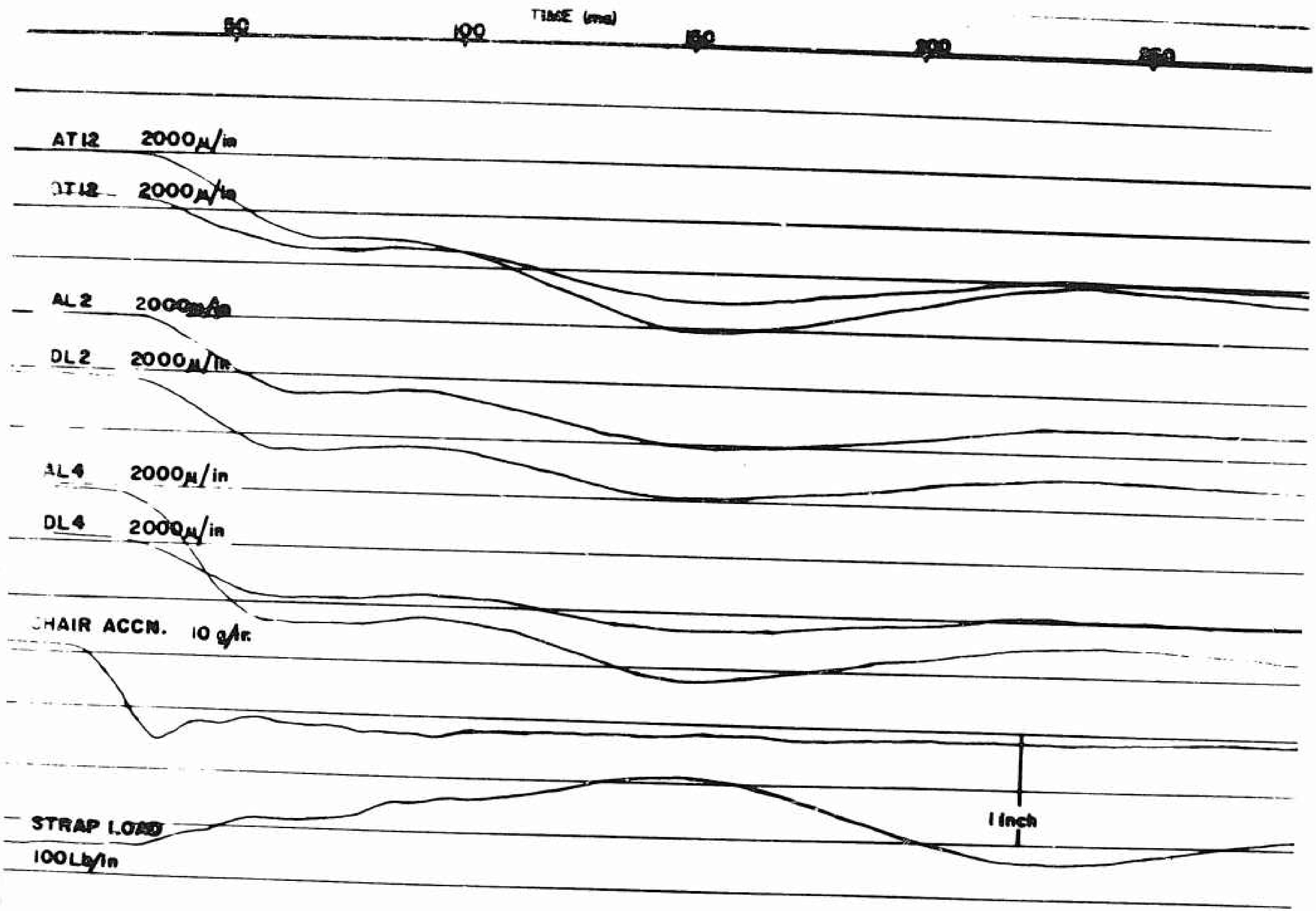

Fig. 2.1. Oscillograph Record of Run 69, Cadaver 1471, No Block

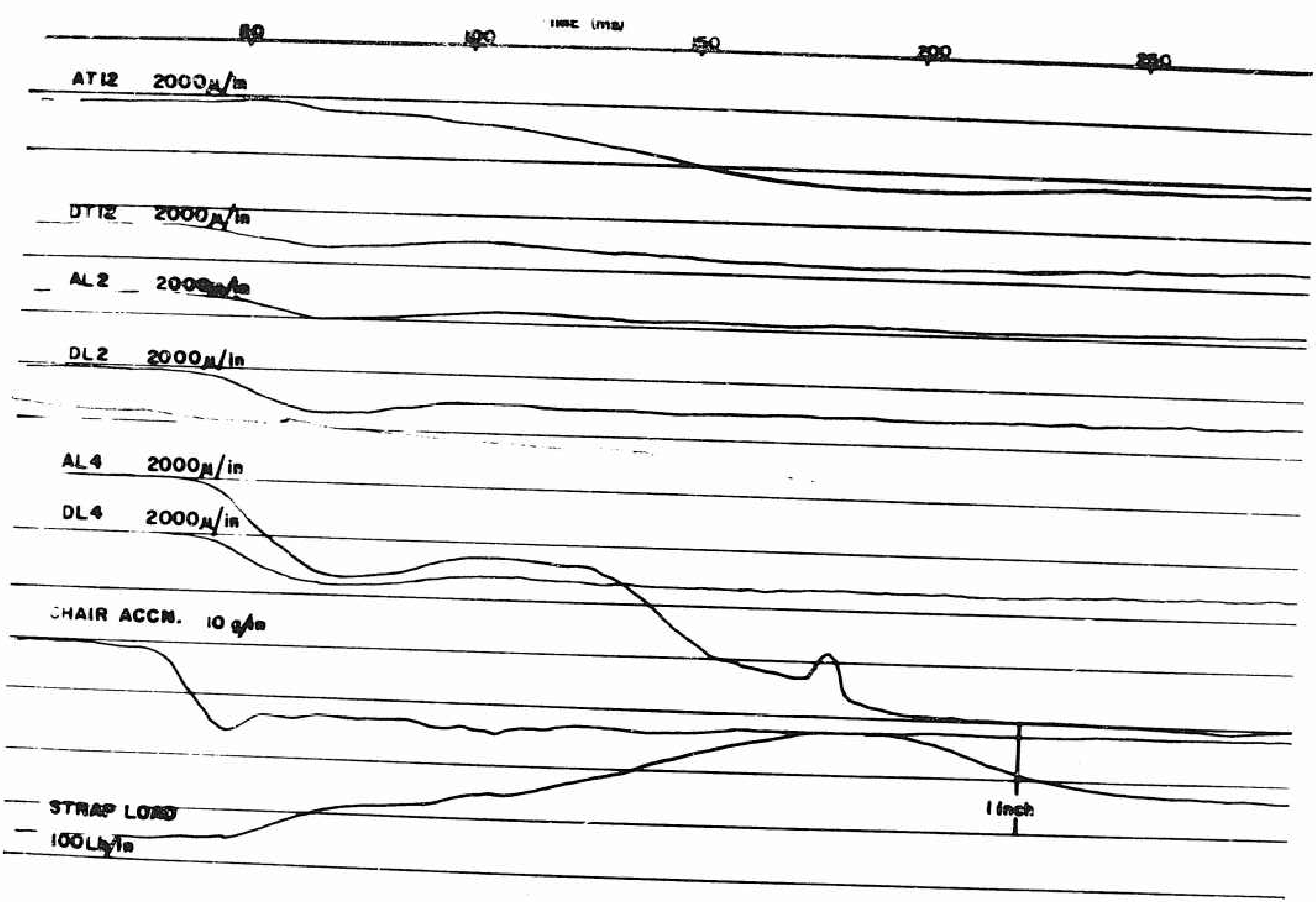

Fig. 2.2. Oscillograph Record of Run 62, Cadaver 1471, Block No. 5

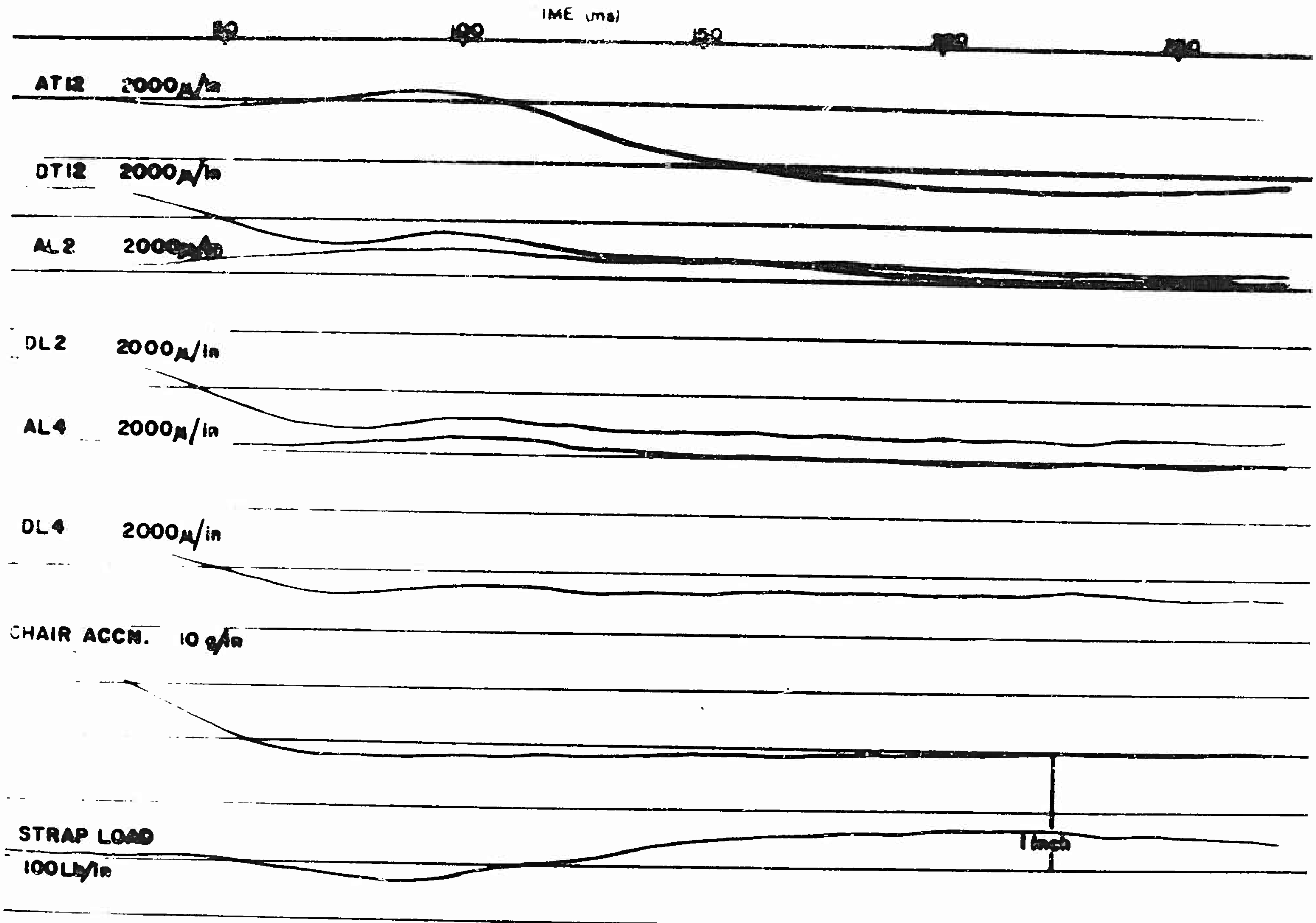

Fig. 2.3. Oscillograph Record of Run 47, Cadaver 1582, Block No. 1

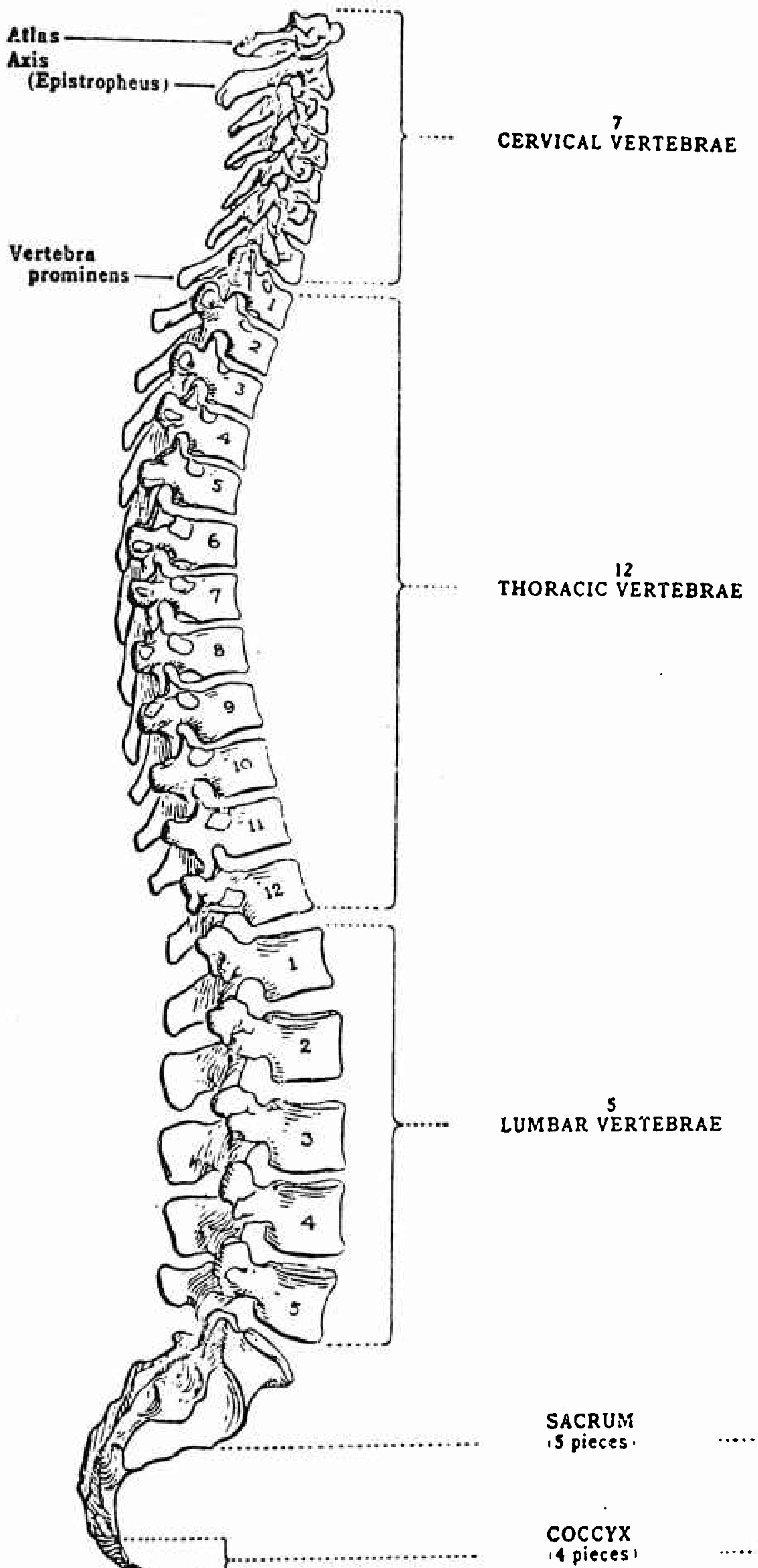

Fig. 2.4. Curvature of the Vertebral Column

CHAPTER III

EFFECTIVENESS OF THE HYPEREXTENSION DEVICE

1. Introduction

With the determination of an optimum geometry and the location of the hyperextension device, it was decided to document the effectiveness of the device used. The hyperextension block that produced the greatest strain reduction, described in Chapter II ($2\frac{1}{4}$" × 6" × 4"), was used opposite the best location, i.e., the block centerline was opposite L1. A total of 12 cadavers were subjected to 75 runs using three different restraint configurations or spinal modes. In the hyperextended mode, in which the block was used, and in the erect mode with no block, the shoulder strap pretension was set at 30 lbs. For runs in the flexed mode, the harness was loosely attached to the torso and the cadaver was restrained essentially by the lapbelt only.

The verification of the effectiveness of the block was carried out by the following methods of data analysis:

(a) An analysis of the acceleration levels at fracture for each mode.

(b) A study of the mode in which fracture occurred when two or more modes were run on the same cadaver.

(c) A comparison of strains in the flexed, erect, and hyperextended mode.

2. Experimental Procedures

Of the 12 cadavers used in this study, 3 were run under all three modes, 5 were tested in the erect and hyperextended modes and 4 were run in the hyperextended mode only. Table 1 contains the pertinent data on the cadavers used. Strain gages were installed on the lower thoracic and the lumbar vertebrae and the runs were carried out at increasing g-levels until fracture occurred. If more than one spinal mode was to be run, the order in which the modes were tested at any given g-level was picked at random for each cadaver.

The procedure for the preparation of the cadavers, the installation of the gages, and the roentgenographic techniques employed were as discussed in the previous chapter.

In Cadavers 1584 and 1615, an anterior gage and a pair of lateral gages were installed on T12, L2, and L4. There was also an anterior gage on L1 and an additional pair of gages on the posterior aspects of L2 in Cadaver 1615. For the next 8 cadavers, according to the order listed in Table 1, an anterior gage was installed on each of the vertebra from T11 to L4. It was felt that the monitoring of the strain along the anterior aspects of all 6 vertebrae was more important than the measurement of strain along the lateral aspects of 3 of the vertebrae. In the last two cadavers, (Nos. 125 and 127), only the anterior aspect of L4 was gaged and the abdominal cavity was not eviscerated. The principal purpose was to maintain integrity of the anterior ligament along the major portion of the vertebral column. The

TABLE 1

List of Cadavers Used

Date	Run No.	Cadaver No.	Age at Death	Cause of Death
9/16/69	81-93	1584	61	unknown
9/24/69	94-99	1615	63	sub-hepatic abscess
10/27/69	100-103	1634	61	CO asphyxia
11/22/69	104-107	1665	49	tuberculosis
12/18/69	108-114	930	60	carcinoma of the tongue
1/21/70	115-121	017	54	unknown
1/28/70	122-130	002	63	congestive heart failure
3/ 3/70	131-135	061	57	cirrhosis of the liver
3/ 4/70	136-140	062	56	pneumonia
4/ 1/70	141-144	095	64	pneumonia, hemophilia
4/22/70	145-150	125	62	unknown
5/13/70	151-155	127	64	cardiovascular atherosclerosis

retention of the abdominal viscera can only affect the fracture level adversely since some of this weight is borne by the spine. To identify the location of the gages, the prefix A is used for anterior gages and D for lateral gages. Posterior gages on the posterior aspects of the body near the neural arch are denoted by the prefix DD.

The input acceleration was a ramp-shaped pulse with a rate of onset of approximately 300 to 500 g-sec. and a plateau varying from 4.5 to 24.5g. The duration of the input pulse varied from about 150-350 msec. and was dependent on the acceleration level, since the total stroke length of the accelerating piston was fixed at 8 feet.

3. Summary of Experimental Data

The data will be presented under three headings:

(a) Fracture g-level and spinal mode at fracture

(b) Strain histories in the various spinal modes

(c) Examination of spinal segments

(a) Fracture g-level and spinal mode at fracture:

The acceleration levels at fracture and the spinal mode in which fracture occurred are listed in Table 2. The number of modes tested and the order in which the testing was carried out and the fractured vertebrae are also given. It can be seen that when the cadaver was subjected to all three spinal modes, vertebral fracture always occurred in the flexed mode. Similarly, when the erect and hyperextended modes were tested, fracture occurred in the erect mode. Cadavers 125 and 127 were not eviscerated and strain gages were installed only on

TABLE 2

Fracture Levels and Spinal Modes

Cadaver No.	Age (yrs)	Acceleration (g)	Spinal Mode at Fracture	No. of Modes Tested	Order of Testing*	Fractured Vertebrae
1584	61	11.0	erect	2	1-2	T12
1615	63	7.5	erect	2	1-2	T10
1634	61	5.5	erect	2	1-2	T11
1665	49	7.0	flexed	3	3-2-1	L2
930	60	11.0	flexed	3	3-2-1	T11
017	54	9.0	flexed	3	2-1-3	L2 & L4
002	63	14.0	erect	2	2-1	T9
061	57	14.0	erect	2	2-1	T11
062	56	18.0	hyperextended	1	-	T12-L1 separation
095	64	20.0	hyperextended	1	-	hypertension frac. of superior end plate of T12 & L2
125	62	24.5	hyperextended	1	-	no fracture
127	64	12.0	hyperextended	1	-	T8

*Mode No.	Mode
1	hyperextended
2	erect
3	flexed

the anterior aspect of L4. The anterior ligament was left intact along the major portion of the vertebral column in an effort to prevent hyperextension fractures when the block was used. Such fractures occurred in Cadavers 062 and 095 which were run solely in the hyperextended mode and were instrumented with strain gages on the anterior aspect of each of the vertebrae from T11 to L4. Cadaver 125 sustained 24.5g and its spine showed no fracture. Due to an accelerator system malfunction, a higher g-level run was delayed for a few days. Unfortunately, the body was claimed by relatives while repairs to the accelerator were being made and no further data could be obtained from this specimen. The same procedure was followed in the experiments on Cadaver 127. Compression fracture of T8 occurred at 12g and there was no evidence of hyperextension fracture.

(b) Strain histories in the various spinal modes:

Some typical strain-time histories resulting from runs in the 3 spinal modes are given to demonstrate the difference in levels of strain among these modes. Figures 3.1 and 3.2 are examples of two runs at 11g on Cadaver 1584 in the hyperextended and erect modes respectively. Fracture of T12 occurred in the erect mode at the instant the shoulder harness load reached a maximum and all strain gages indicated peak values. The sharp drop-off in the T12 strain trace, shown in Figure 3.2, is a reliable indicator of fracture which was subsequently confirmed by roentgenographic examination.

Of particular interest is a record of a hyperextension fracture of T12 and L2 in Cadaver 095 at 20g. This is depicted in Figure 3.3. The instant of fracture was about 120 msec. after the end of the acceleration pulse. The cadaver was undergoing a 6-9g deceleration when the fracture took place. Figure 3.4 is a 24.5g run in the hyperextended mode. There was no fracture. The 2 strain gages on the anterior aspect of L4 were labelled as RAL4 and LAL4 for the right and left gages. In this cadaver the anterior ligament was intact.

A strain-time history in the flexed mode is shown in Figure 3.5. It is believed to be the first of its kind to be reported. There are the customary first and second peaks as reported by Vulcan and King [19] although the first peak is not very well defined in Figure 3.5. This is due to the relatively low rate of onset used for this series of experiments and to the extensive effect of bending on the strain gage output. The phenomenon to be noted in the data is a third strain peak occurring at the end of the acceleration pulse. Its magnitude is generally greater or equal to the second peak. The strap load cell indicated that the torso did not rotate forward far enough to cause any significant force in the shoulder harness. However, when fracture occurred, there was a sharp rise in the shoulder strap load as shown in Figure 3.6 for a different cadaver.

The development of tension in the vertebral bodies during the initial 60 msec. of the acceleration pulse occurred in several runs with the spine in the hyperextended mode.

Generally, the magnitude was less than 300μ. It was impossible to eliminate tensile strains from the vertebrae of Cadaver 062. The block location was changed several times to no avail. At 18g, with the block opposite T12, a hyperextension fracture of L1 occurred. The analog data are shown in Figure 3.7. In the erect mode, the vertebrae were usually in compression throughout the acceleration pulse. However, tension did develop during several runs on Cadavers 002 and 061. The tensile strains were all below 700μ.

A summary of the data for the 12 cadavers used are given in Tables 3 through 14. For the last two cadavers, (Nos. 125 and 127), L4 was the only vertebra gaged for reasons stated previously.

(c) Examination of spinal segments:

Some typical roentgenograms of spinal segments removed from cadavers after fracture had occurred are shown in Figures 3.8 through 3.12. Cadavers 930 and 017 were run in all three modes. Fractures resulted in the flexed mode. Figure 3.8 shows an anterior wedge fracture of T11 of Cadaver 930 and Figure 3.9 shows compression fractures of L2 and L4. An anterior compression fracture of T11 of Cadaver 061 is shown in Figure 3.10 and wedge fractures of T9 and T10 of Cadaver 1615 are shown in Figure 3.11. These fractures resulted from runs in the erect mode. Figure 3.12 is an example of a hyperextension fracture resulting from an 18g run in the hyperextended mode. Cadaver 062 sustained a separation of the superior end plate of L1. Similar fractures occurred in Cadaver 095 which was also run

TABLE 3

Summary of Data on Cadaver 1584

Hyperextension Device: Block No. 1 (2-1/4"×6"×6"), centerline of block located opposite L1

Run No.	Accel. (g)	Peak Strain Data (Microstrain) AT12	DT12	AL2	DL2	AL4	DL4	Shoulder Harness Tension (lb.)	Spinal Mode	Pemarks
81	4.5	650	590	130	300	300	460	72	hyperext.	
82	4.5	2550	1020	470	500	620	700	72	erect	
83	7.5	3610	1510	280	560	800	960	158	hyperext.	
84	7.5	6600	2200	920	1080	1400	1640	124	erect	
85	11.0	3960	2200	400	920	1240	1360	280	hyperext.	
86*	11.0	6100	2400	1000	1320	1760	1800	278	erect	fx. of ant. lip of sup. end-plate of T12

*indicates peak strain values at instant of fracture are tabulated for the run

TABLE 4

Summary of Data on Cadaver 1615

Hyperextension Device: Block No. 1 (2-1/4"×6"×6"), centerline of block located opposite L1

Run No.	Accel. (g)	Peak Strain Data (Microstrain) AT12	DT12	AL2	DL2	AL4	DL4	AL1	DDL2†	Should. Harn. Tension (lb.)	Spinal Mode	Remarks
94	4.9	1320	1120	360	1000	700	1080	-	800	90	hyperext.	block centerline 1" below L1, AL1 gage not hooked up
95	4.9	1500	1080	1040	1360	820	-	1000	860	62	erect	DL4 trace lost - disconnected lead
96	7.5	3000	2000	860	2120	1350	1940	1450	1600	190	hyperext.	
97	7.5	-	2080	2300	2740	1940	2480	2120	1720	112	erect	T12 traces lost due to connector malfunction crushing fx. of T10
98	11.3	4000	2700	2540	3600	2800	3320	3040	2400	305	hyperext.	crushing fx. of T9, T10, T11
99*	11.3	4520	3080	4040	4500	3800	3920	3800	2660	235	erect	crushing fx. of T9, T10 and T11, extensive crushing of T11

†indicates gage on posterior aspect of L2

*indicates peak strain values at instant of fracture are tabulated for this run

TABLE 5

Summary of Data on Cadaver 1634

Hyperextension Device: Block No. 1 (2-1/4"×6"×6"), centerline of block located opposite L1

Run No.	Accel. (g)	Peak Strain Data (Microstrain) AT11	AT12	AL1	AL2	AL3	AL4	Shoulder Harness Tension (lb.)	Spinal Mode	Remarks
100	5.0	4100†	1850	1220	1300	#	2140	78	hyperext.	hyperext. device centerline 1/2" above L1
101	5.0	4500†	1880	1180	880	#	1480	174	erect	
102	5.5	3800	2360	1020	400	#	1350	90	hyperext.	hyperext. device centerline opposite L1
103	5.5	8280†	6280	4000	3440	#	4800	168	erect	marked anterior compression fx. of T11

†indicates strains may be larger than value stated due to galvanometer deflections over 4 inches

#indicates strain gage malfunction

TABLE 6

Summary of Data on Cadaver 1665

Hyperextension Device: Block No. 2 (2-1/4"×4"×6"), centerline of block located opposite L1

Run No.	Accel. (g)	Peak Strain Data (Microstrain) AT11	AT12	AL1	AL2	AL3	AL4	Shoulder Harness Tension (lb.)	Spinal Mode	Remarks
104	4.0	3140	3720	3860	2540	3550	2860	0	flexed	
105	4.0	1900	2080	1580	920	1240	880	92	erect	
106	4.0	1120	1400	740	160	310	420	113	hyperext.	
107	7.0	4260	5700	6600	6200	5500	4900	0	flexed	wedging fx. of L2 & slight wedging of L1

TABLE 7

Summary of Data on Cadaver 930

Hyperextension Device: Block No. 1 (2-1/4"×6"×6"), centerline of block located opposite L1

Run No.	Accel. (g)	Peak Strain Data (Microstrain) AT11	AT12	AL1	AL2	AL3	AL4	Shoulder Harness Tension (lb.)	Spinal Mode	Remarks
108	4.6	3070	2500	3000	1670	840	700	0	flexed	
109	4.6	2060	1650	1960	960	650	470	68	erect	
110	4.6	1980	1740	1570	480	160	320	82	hyperext.	
111	7.6	6360	4520	6520	3640	2200	1480	0	flexed	
112	7.6	6100	4740	6740	3120	2060	1460	96	erect	
113	7.6	4000	2900	3360	2320	560	540	168	hyperext.	
114*	12.0	6960	4640	7360	3200	1920	1400	0	flexed	compression fracture of T11

*indicates peak strain values at instant of fracture are tabulated for the run

TABLE 8

Summary of Data on Cadaver 017

Hyperextension Device: Block No. 2 (2-1/4"×4"×6"), centerline of block located opposite L2

Run No.	Accel. (g)	Peak Strain Data (Microstrain) AT11	AT12	AL1	AL2	AL3	AL4	Shoulder Harness Tension (lb.)	Spinal Mode	Remarks
115	4.5	2700	840	1270	1000	1180	820	122	hyperext.	Block No. 1 opp. L1 Block too high up, change to Block No. 2
116	4.5	2520	820	1320	1280	1660	1020	84	erect	
117	4.5	2360	660	1180	900	1440	840	118	hyperext.	
118	4.5	3280	1050	2740	3660	-†	-†	85	flexed	
119	9.0	6620	2740	3760	4100	5000	2600	-	erect	load cell leads broke off during run
120	9.0	5900	2000	2760	1840	1520	800	188	hyperext.	
121*	9.0	6800	2200	4080	4560	13600	7200	304	flexed	compression fracture of L2 and L4

*indicates peak strain values at instant of fracture are tabulated for this run

†indicates strains in excess of linear range of galvanometers

TABLE 9

Summary of Data on Cadaver 002

Hyperextension Device: Block No. 2 (2-1/4"×4"×6"), centerline of block located opposite L1

Run No.	Accel. (g)	Peak Strain Data (Microstrain) AT11	AT12	AL1	AL2	AL3	AL4	Shoulder Harness Tension (lb.)	Spinal Mode	Remarks
122	4.6	2780	1860	1400	940	700	560	94	erect	
123	4.6	2560	1740	760	520	840	1180	100	hyperext.	block opposite T11
124	4.6	2920	2260	1080	350	540	1060	134	hyperext.	block opposite T12
125	4.6	2980	2260	1440	940	400	310	83	erect	
126	4.6	2940	2000	740	260	180	940	114	hyperext.	block opposite L1
127	9.0	6480	5160	4200	3080	2400	1420	214	erect	
128	9.0	6880	4400	3360	1720	1400	2160	260	hyperext.	block opposite L1
129	12.0	8960	6240	6960	4360	3600	2240	286	erect	Jerk extremely low Valve malfunction
130	14.0	9120	6480	6880	4640	3840	3360	-	erect	Strap data lost due to calibration signal interference. Compression fracture of T9

TABLE 10

Summary of Data on Cadaver 061

Hyperextension Device: Block No. 2 (2-1/4"×4"×6"), centerline of block located opposite L1

Run No.	Accel. (g)	Peak Strain Data (Microstrain) AT11	AT12	AL1	AL2	AL3	AL4	Shoulder Harness Tension (lb.)	Spinal Mode	Remarks
131	4.5	3220	1920	1430	950	1540	†	100	erect	
132	4.5	1180	640	260	100	150	†	100	hyperext.	
133	9.0	4880	3840	3300	2550	4100	†	250	erect	estimate shoulder harness tension
134	9.0	4360	3200	1640	0	100	†	+	hyperext.	
135*	14.0	16000#	6000	3880	3200	4400	†	+	erect	compression fracture of T11

*indicates peak strain values at instant of fracture are tabulated for this run

†data erratic due to malfunction of bridge balance unit

#indicates strain in excess of linear range of galvanometer

+data lost due to calibration signal interference

TABLE 11

Summary of Data on Cadaver 062

Hyperextension Device: Block No. 2 (2-1/4"×4"×6"), centerline of block located opposite T12

Run No.	Accel. (g)	Peak Strain Data (Microstrain) AT11	AT12	AL1	AL2	AL3	AL4	Shoulder Harness Tension (lb.)	Spinal Mode	Remarks
136	4.5	1410	1040	450	200	140	100	100	hyperext.	block opposite L1
137	8.9	3280	2400	1660	360	200	640	198	hyperext.	block 1/2" above L1
138	14.0	5200	4680	4000	2300	700	1300	250	hyperext.	block 3/4" above L1, oppos. T12-L1 disc
139	14.0	5320	4640	3700	2300	1960	2700	-*	hyperext.	block 1-1/2" above L1, opposite T12
140	18.0	5680	#	600	240	320	1920	-*	hyperext.	block 1-1/2" above L1, opposite T12 Hyperext. fracture of L1

#data lost due to broken leads during the run

*data lost due to galvanometer excursion beyond the edge of the recording paper

TABLE 12

Summary of Data on Cadaver 095

Hyperextension Device: Block No. 2 (2-1/4"×4"×6"), centerline of block located opposite L1

Run No.	Accel. (g)	Peak Strain Data (Microstrain) AT11	AT12	AL1	AL2	AL3	AL4	Shoulder Harness Tension (lb.)	Spinal Mode	Remarks
141	4.2	620	750	460	460	240	300	93	hyperext.	
142	8.6	1100	520	760	840	510	600	160	hyperext.	
143	14.5	3000	2340	2480	2540	1620	1460	338	hyperext.	
144	20.0	3600	2200	2500	3520	2140	2040	550	hyperext.	hypertension fracture of T12 and L2

TABLE 13

Summary of Data on Cadaver 125

Hyperextension Device: Block No. 2 (2-1/4"×4"×6"), centerline of block located opposite L1

Run No.	Accel. (g)	Peak Strain Data (Microstrain) RAL4(right)	LAL4(left)	Shoulder Harness Tension (lb.)	Spinal Mode	Remarks
145	4.5	580	380	126	hyperext.	
146	8.0	1150	1000	220	"	
147	13.2	1880	2000	480	"	
148	18.0	3400	3320	660	"	
149	24.5	3600	2720	840	"	
150	24.0	1960	1400	500	"	(See note.)

Note: There was no fracture after Run No. 149. System malfunction during Run No. 150 resulted in an extremely low rate of onset and an acceleration that failed to reach 30g. There was also no fracture after this run.

TABLE 14

Summary of Data on Cadaver 127

Hyperextension Device: Block No. 2 (2-1/4"×4"×6"), centerline of block located opposite L1

Run No.	Accel. (g)	Peak Strain Data (Microstrain) AL4	Shoulder Harness Tension (lb.)	Spinal Mode	Remarks
151	4.0	760	108	hyperext.	
152	7.0	1440	300	"	
153	12.0	*	500	"	compression fracture of T8
154†	17.2	3200	610	"	
155†	21.6	3840	750	"	

*indicates data not acquired due to amplifier malfunction

†data from these runs are discarded, when x-rays revealed fracture during Run No. 153

solely in the hyperextended mode. There is no radiological evidence of damage to the posterior structures of the vertebrae that were run in the hyperextended mode.

4. Analysis of Data

(a) Acceleration levels and spinal modes at fracture:

Of the four cadavers run exclusively in the hyperextended mode, there were 2 hyperextension fractures at 18 and 20g, one compression fracture at 12g and one which did not fracture at 24.5g. Since the hyperextension fractures are possibly due to the disruption of the anterior ligament by strain gages, it would be a safe estimate to take the average of these four acceleration values as the fracture level in the hyperextended mode for comparison with that in the other modes. This average is 18.6g. The average g-level in the erect mode is 10.4g for 5 cadavers. In the flexed mode, the average of three fracture levels is 9.0g. Table 15 is a summary of the accelerations at fracture in the 3 modes.

A student's t-test was performed for the fracture levels between the various spinal modes. The result is given in Table 16. The difference in g-level between the hyperextended mode and the other two modes were found to be statistically significant ($P < 5.0\%$). It should be noted that the null hypothesis was rejected despite conservative estimates made for the fracture level in the hyperextended mode. The average age of the cadavers in the hyperextended mode group was 61.5 years, while in the erect and flexed mode groups,

TABLE 15

Fracture Levels in the 3 Spinal Modes

Mode	Fracture Level (g)	No. of Cadavers	Average Age (years)
Hyperextended	18.6	4	61.5
Erect	11.6	4	61.0
Flexed	9.0	3	54.3

TABLE 16

Student's t-Test of Fracture g-Levels Between the Various Spinal Modes

Modes	n	s	t	P(%)
Hyperextended & Erect	7	4.46	2.75	2.6
Hyperextended & Flexed	5	4.21	2.99	3.2
Erect & Flexed	6	3.33	0.48	> 50

it was 61 and 54.3 years respectively. There is thus no significant difference in age among the groups to confuse the data. Furthermore, when a cadaver was run in all or two of the spinal modes, fracture always occurred in the mode in which the cause could be attributed to forward bending of the vertebral column. The order of testing was randomized so as not to bias the data toward any particular mode. The result confirms the proposition that the cause of fracture is a combination of axial compression and bending, resulting in the common occurrence of anterior fractures in pilots who eject.

(b) Reduction in strain:

The effectiveness of the hyperextension device can be further demonstrated by the calculation of the percentage reduction in compressive strain as a result of its use. There were 32 runs on 8 cadavers in which strain data for the erect and hyperextended modes at the same g-level were available. Table 17 is a listing of the percentage reduction in strain for the various vertebra that were gaged anteriorly. The overall percentage reduction was 44.4% with a range of 20.1% for AT11 to 65.6% for AL3.

In order to assess the statistical significance of this reduction, a t-test was carried out for each vertebra. The difference in strain between the erect and hyperextended mode was computed, from which the value of t and the probability, P, that the null hypothesis holds, were obtained for each g-level. Table 18 lists this information for all six

TABLE 17

Summary of Percentage Reduction in Strain Between the Erect and Hyperextended Mode for Anterior Gages

Run No.	AT11	AT12	AL1	AL2	AL3	AL4	Accel. (g)
81-82	-	74.5	-	72.4	-	51.6	4.5
83-84	-	45.3	-	69.6	-	42.9	7.5
85-86	-	54.0	-	50.0	-	29.6	11.0
94-95	-	12.0	-	55.4	-	14.1	4.9
96-97	-	-	31.6	62.6	-	30.4	7.5
98-99	-	11.5	20.0	37.2	-	26.3	11.3
102-103	55.0	62.5	75.0	87.3	-	72.0	5.5
105-106	41.0	32.7	53.1	32.6	75.0	52.3	4.0
109-110	3.9	-5.5	19.9	50.0	75.4	31.9	4.6
112-113	34.4	38.8	50.0	25.6	73.0	63.0	7.6
116-117	6.4	19.5	10.6	29.7	13.3	37.2	4.5
119-120	10.9	37.0	26.3	55.0	69.5	69.5	9.0
125-126	1.3	11.5	48.5	72.5	55.0	-	4.6
127-128	5.5	14.7	20.0	44.0	41.7	-	9.0
131-132	32.3	66.5	81.7	89.5	90.2	-	4.5
133-134	10.7	16.7	50.0	100.0	97.6	-	9.0
Average	20.1	32.3	40.6	62.7	65.6	43.4	

Overall average reduction of anterior gages: 44.4%

TABLE 18

Student's t-Test of Strain Data

(anterior gages)

(g)	Vertebra																	
	T11			T12			L1			L2			L3			L4		
	n	t	P(%)	n	t	P(%)	n	t	P(%)	n	t	P(%)	n	t	P(%)	n	t	P(%)
4.5	13	3.85	0.2326	17	5.027	0.0124	13	5.4[illegible]	0.0145	17	6.18	0.0013	13	5.045	0.0287	9	5.23	0.0792
[illegible].5	5	3.69	2.10	6	4.21	0.84	6	3.59	1.56	7	2.39	5.40	5	2.67	5.94	4	4.95	1.58
9.0	5	1.507	20.6	6	3.33	2.07	6	3.669	1.44	5	9.982	0.0172	5	3.067	3.73	4	3.316	4.518

vertebrae. The number of observations at each acceleration was limited due to fracture at relatively low g-levels and to the different gaging patterns used on two of the cadavers. The t-test was carried out only when there are 3 or more pairs of data. In general, the differences were significant for the lumbar vertebra ($P < 5\%$). For T12, the reduction in strain is still acceptable since $P \leq 6\%$. However, the observed differences for T11 indicate that the hyperextension device may be beneficial in only 4 out of 5 cases.

There was also a consistent reduction in strain in the lateral gages averaging 24.7% for 17 sets of data from 6 pairs of runs in the erect and hyperextended mode. A reduction of 7.9% occurred for a pair of posterior gages placed on L2 in Cadaver 1615.

A limited comparison could also be made for runs in the flexed and hyperextended mode and those in the flexed and erect mode. Tables 19 and 20 list the percentage reduction in strain in the anterior gages for these combinations. The overall reduction between the flexed and hyperextended mode was 58.7% while that between the flexed and erect mode was 33.1%.

5. Discussion and Conclusions

The principal purpose of the experimental study was the verification of the mechanism of vertebral fracture due to caudocephalad acceleration. The existence of significant bending stresses was first noted by King and Vulcan [8] and

TABLE 19

Summary of Percentage Reduction in Strain Between the Flexed and Hyperextended Mode for Anterior Gages

Run No.	AT11	AT12	AL1	AL2	AL3	AL4	Accel. (g)
104-106	65.0	62.9	80.9	93.6	91.2	85.4	4.0
108-110	35.5	30.4	47.7	71.3	81.0	54.3	4.6
111-113	37.1	35.8	48.5	36.2	74.5	63.5	7.6
117-118	28.0	37.2	57.0	75.4	-	-	4.5
Average	41.4	41.6	58.5	69.1	82.2	67.7	

Overall average reduction of anterior gages: 58.7%

TABLE 20

Summary of Percentage Reduction in Strain Between the Flexed and Erect Mode for Anterior Gages

Run No.	AT11	AT12	AL1	AL2	AL3	AL4	Accel. (g)
104-105	39.5	44.1	59.1	63.8	65.1	69.2	4.0
108-109	33.0	33.6	33.3	42.5	22.6	31.4	4.0
111-112	4.1	-4.9	-3.4	14.7	6.4	1.4	7.6
116-118	33.2	21.9	51.8	55.0	-	-	4.5
Average	77.5	23.7	35.2	46.5	31.4	34.0	

Overall average reduction of anterior gages: 33.1%

was reported in detail by Vulcan [21]. By altering the spinal configuration, with a hyperextension device it was possible to reduce vertebral body strain and raise the fracture g-level. The results reported were found to be statistically significant despite the large biological variation in the strength of cadaver vertebrae and in the degree of curvature of the column.

When the fracture g-levels in the various modes were analyzed, it was not possible to use paired sets of data and the appropriate values of t were obtained from the equation for unpaired data with unequal samples. In particular, for hyperextended mode, the 4 fracture levels were obtained under slightly different conditions. The fact that in two of the cases the anterior ligament was left intact while it was disrupted in the other two is objectionable from the statistical viewpoint. However, physical arguments can be used to overcome such objections. Hyperextension fractures associated with a disrupted anterior ligament imply that the g-level for compressive failure can only be higher than that used in the computations, especially when one of these fractures took place during deceleration of the sled. Similarly, when the abdominal cavity was not eviscerated, the fracture level could be lowered somewhat. Therefore, the actual difference and the probability that it did not occur by chance can only be higher than that given in this report.

The significant reduction in strain along the anterior aspect of the vertebral bodies is further evidence of the role of bending as a cause for vertebral fracture and of the effectiveness of the hyperextension device. It is unfortunate that the t-test can only be carried out to 9g and that the number of observations at each acceleration was small. However, in spite of this small sample size, it was still possible to reject the null hypothesis for five of the six vertebrae under study.

This series of experiments indicates that the reduction in strains and hence the increase in acceleration level at fracture as a result of the use of a hyperextension device, cannot be attributed to any one factor. The initial pretension induced along the anterior aspects of the vertebral bodies due to hyperextension of the spine causes the vertebral bodies to act as prestressed materials, hence raising the compression level for fracture. However, this would not decrease the anterior strains as found in the experiments. If bending only was the cause of fracture, by changing the eccentricity of torso, we would expect a redistribution of the compressive load on the vertebral bodies, hence reducing the anterior strain which is a combination of pure compressive strain and pure bending strain. However, this redistribution should not affect the lateral strains on the vertebral bodies, as they would be a function of pure axial load only. The fact, that a significant reduction of the lateral strains was found due to hyperextension, suggests a decrease in the net axial compressive load on the vertebral body. This decrease in the axial load has to be transmitted to another structure. One possibility is the transmission of the load to the seat frame via the hyperextension device used. An evaluation of this was made by making successive runs, one in the erect and one in the extended mode, on the same cadaver at the same acceleration level, using the seat pan load cell measurement in the erect mode as a control. Results of these runs showed a peak load cell value of 599 lbs. for the erect mode and 592 lbs. for the hyperextended mode. This indicates that the hyperextension device does not support appreciable vertical loads and that the decreased portion of the vertebral body axial load has to be transmitted through a structure in the spine itself. This structure is the lamina via the articular facets.

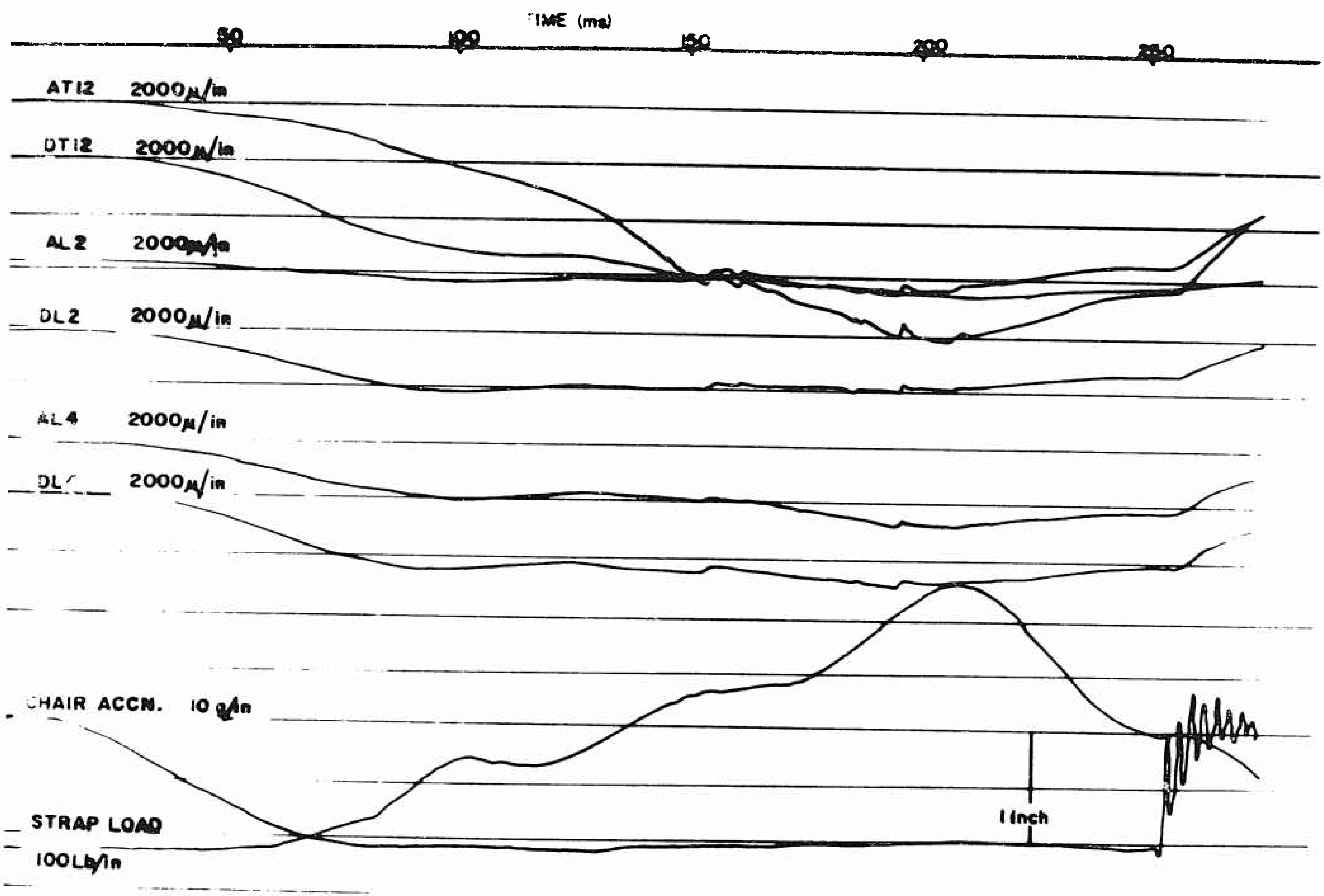

Fig. 3.1. Oscillograph Record of Run 85, Cadaver 1584, Hyperextended Mode

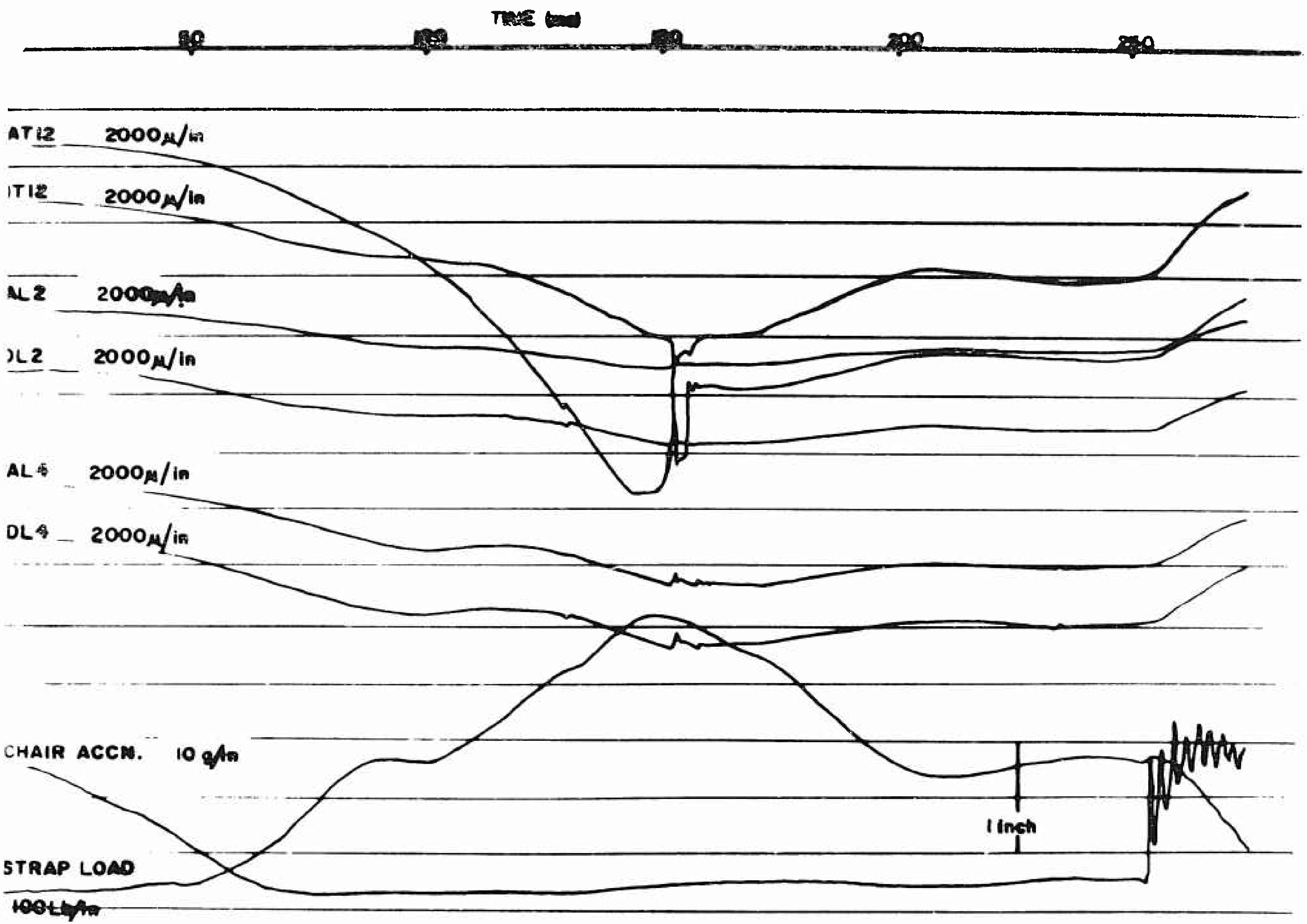

Fig. 3.2. Oscillograph Record of Run 86, Cadaver 1584, Erect Mode

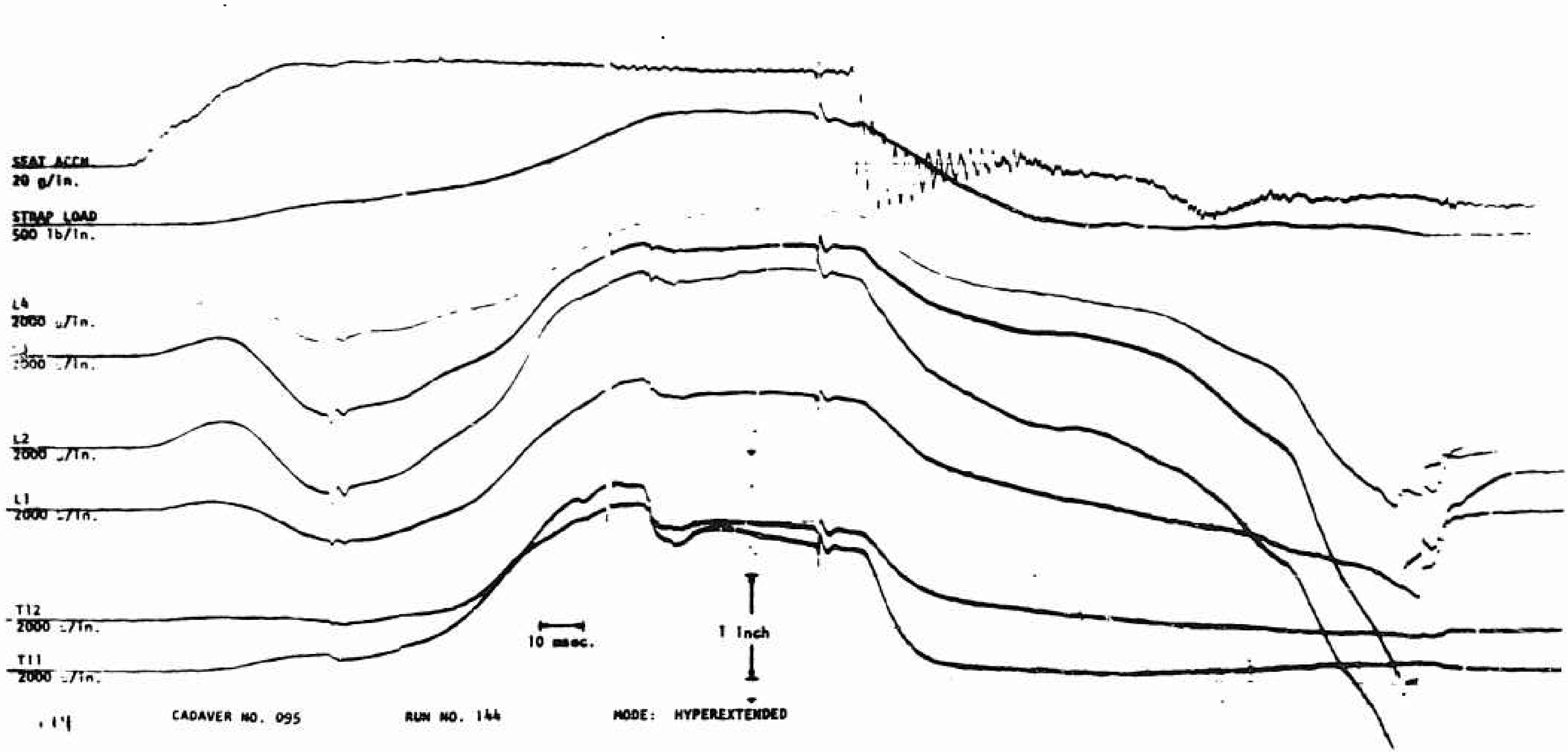

Fig. 3.3. Oscillograph Record of Run 144, Cadaver 095, Hyperextended Mode

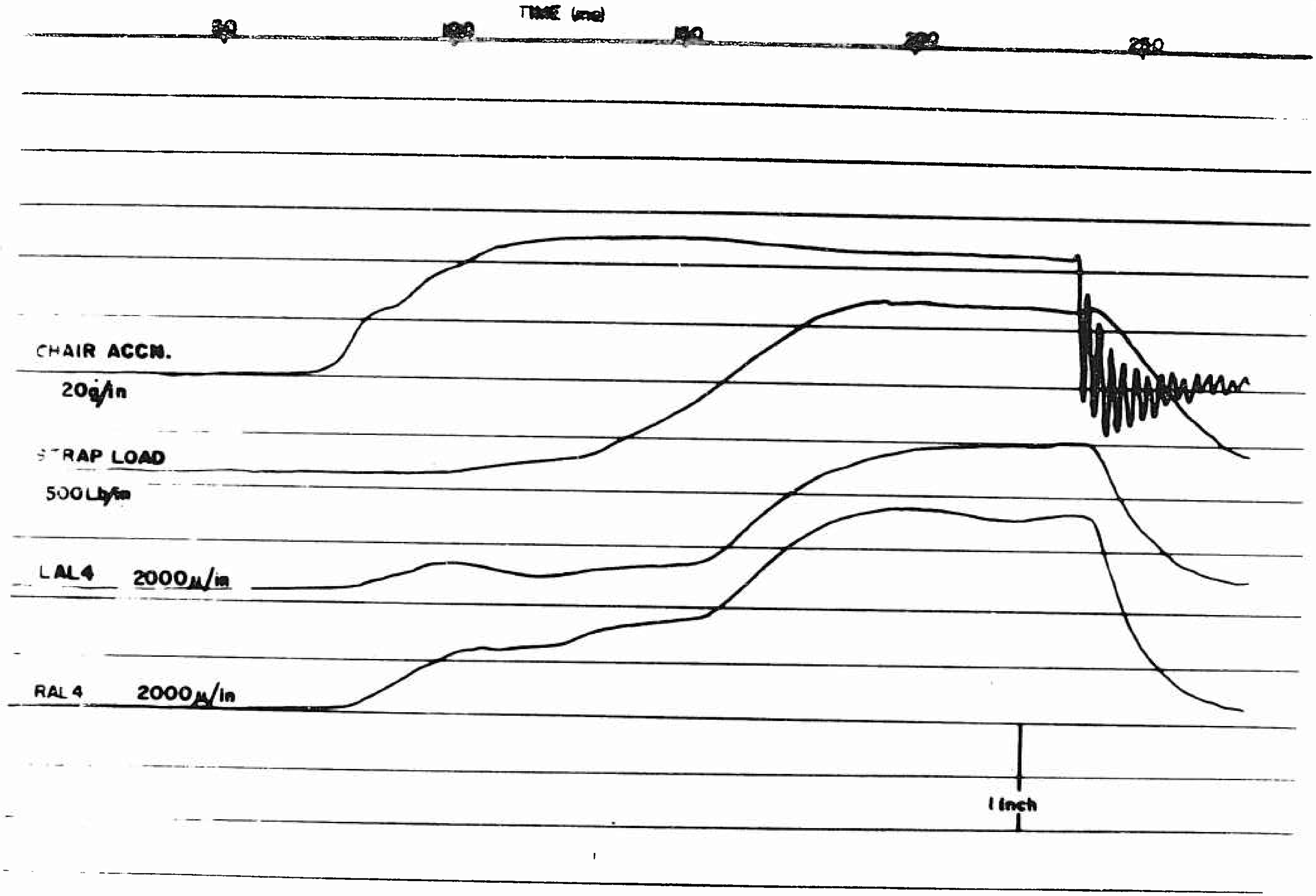

Fig. 3.4. Oscillograph Record of Run 149, Cadaver 125, Hyperextended Mode

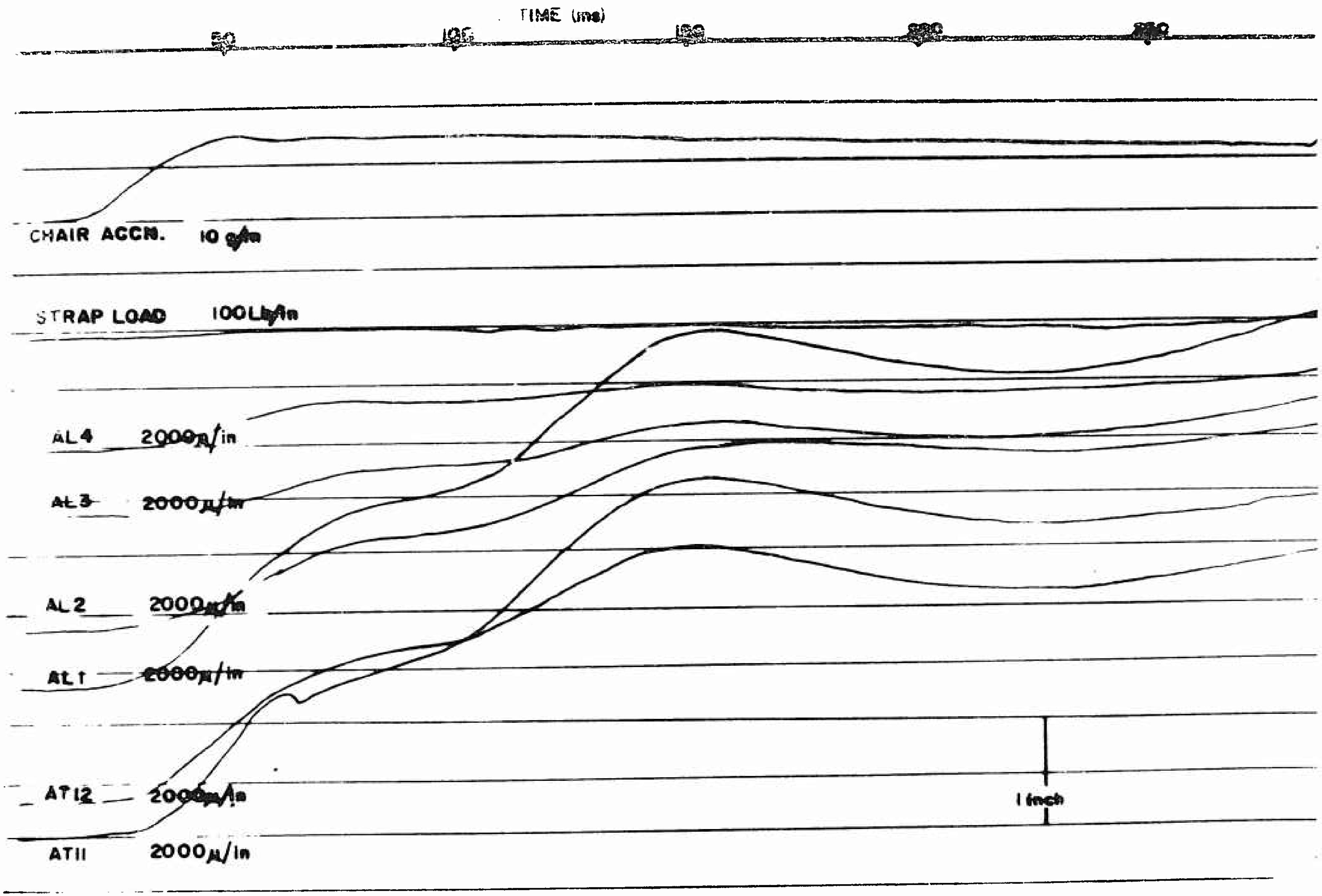

Fig. 3.5. Oscillograph Record of Run 111, Cadaver 930, Flexed Mode

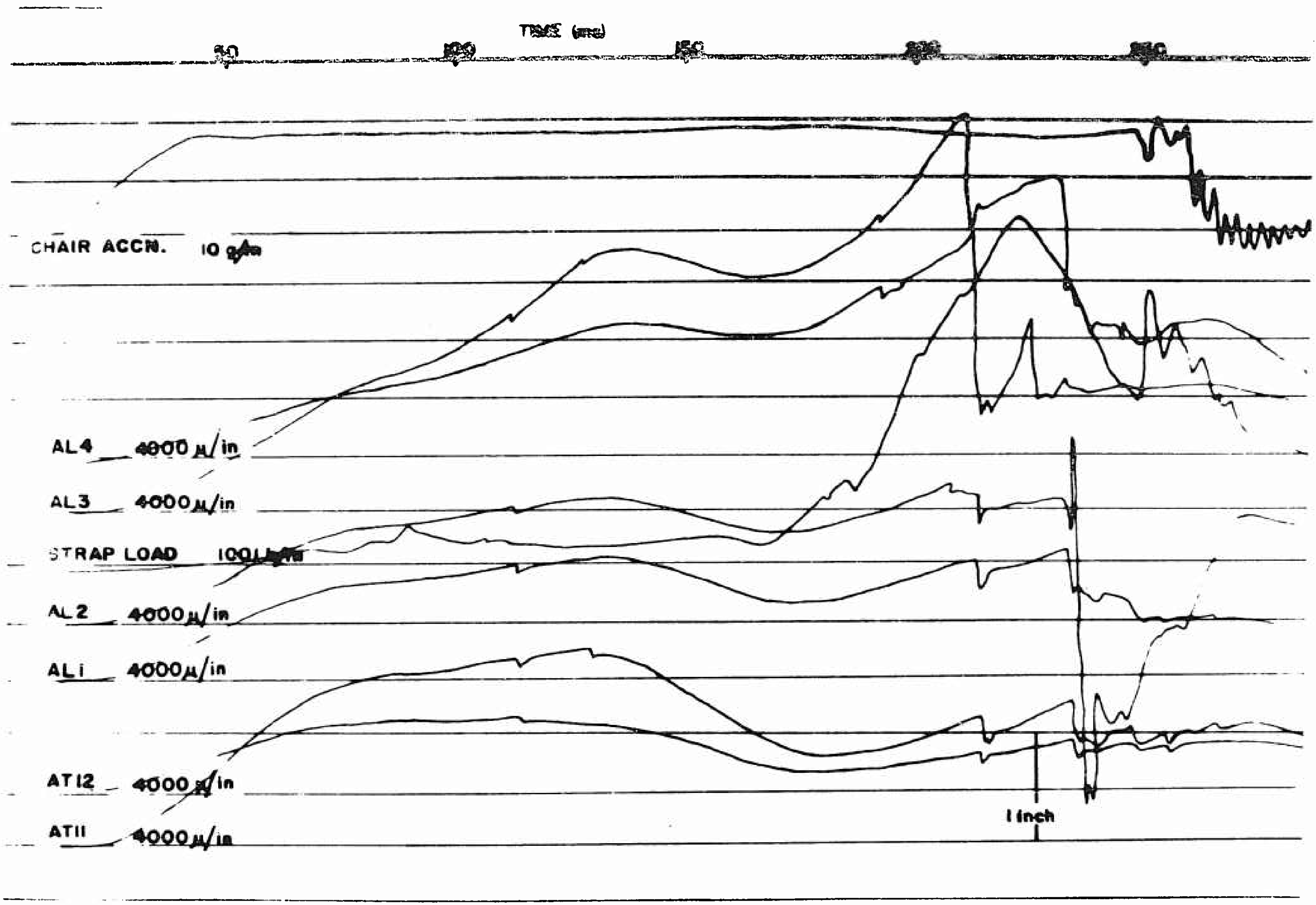

Fig. 3.6. Oscillograph Record of Run 121, Cadaver 017, Flexed Mode

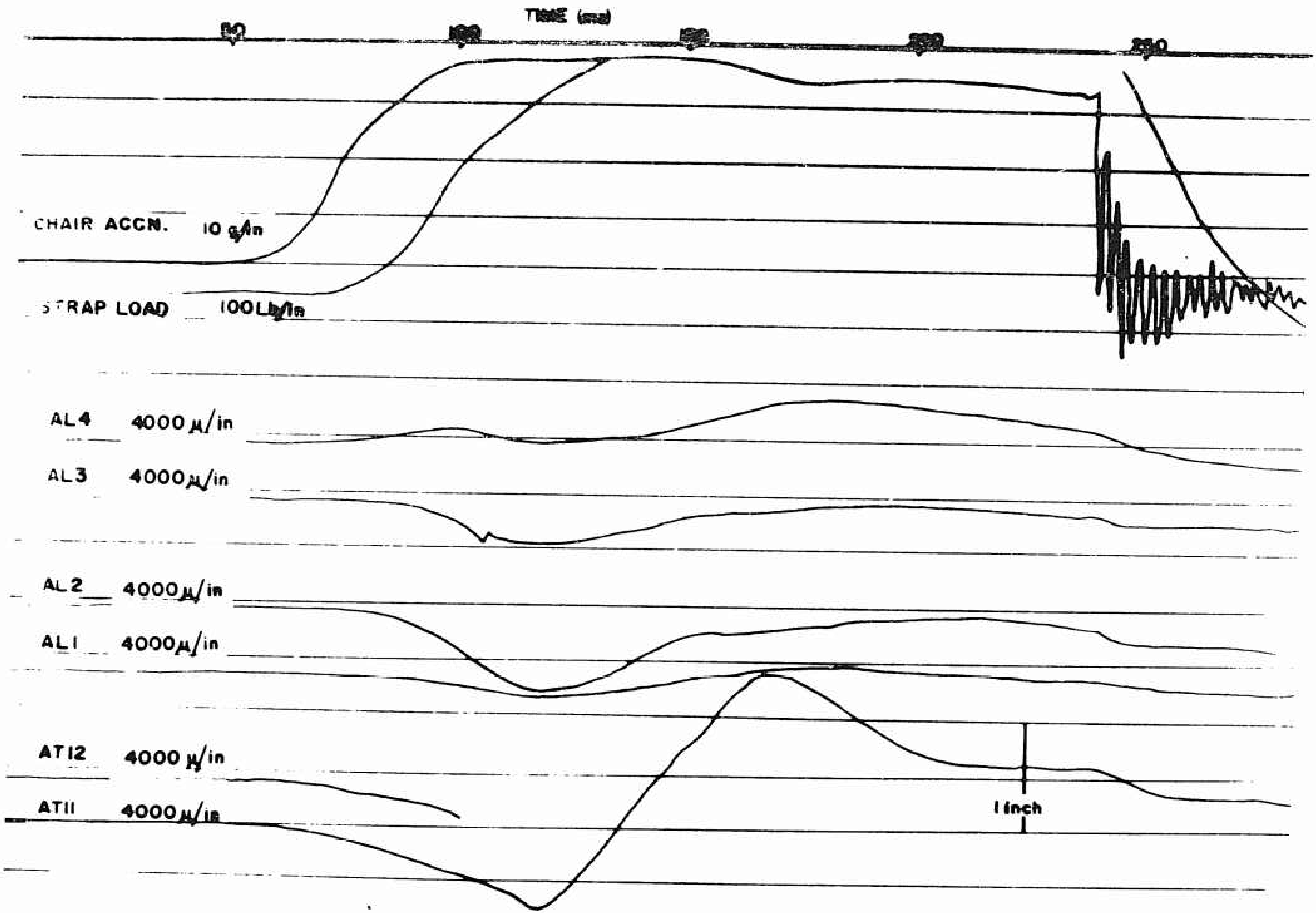

Fig. 3.7. Oscillograph Record of Run 140, Cadaver 062, Hyperextended Mode

930

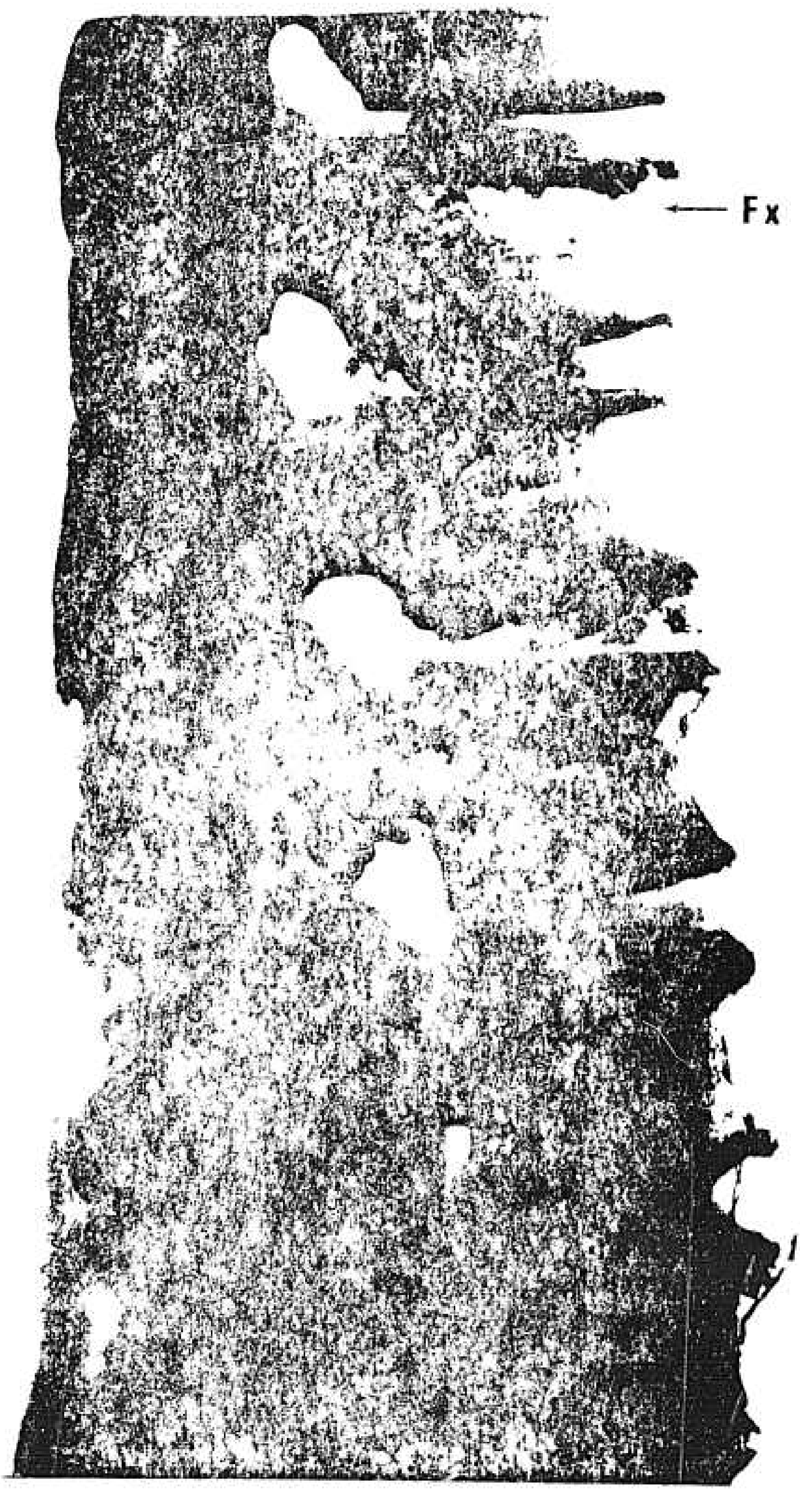

Fig. 3 [illegible] Fracture of T11

...acture of L2 and

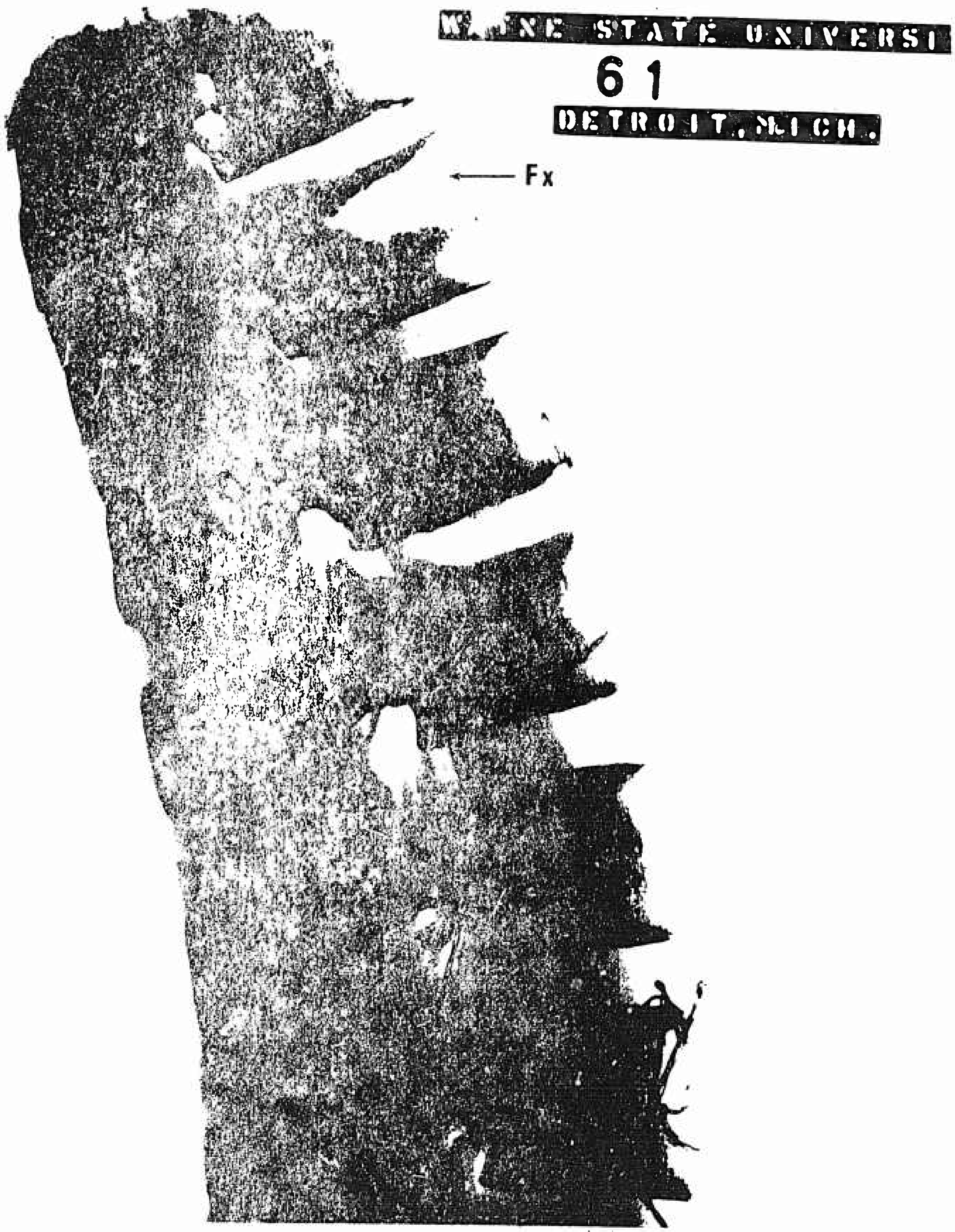

Fig. [illegible] X-Ray [illegible] [illegible]terior [illegible]pression Fracture

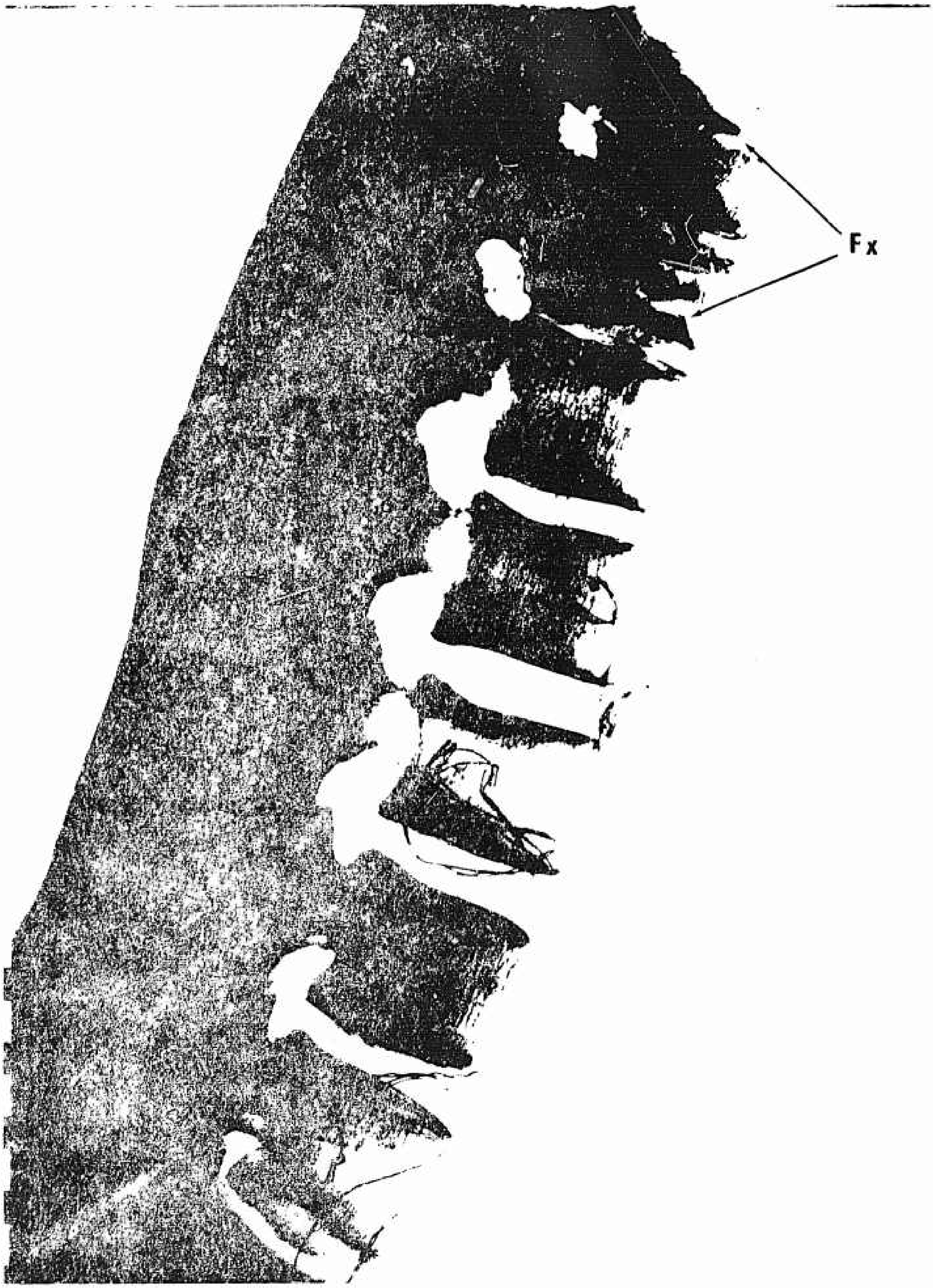

Fig. [illegible] X-Ray Showing [illegible] Anterior Wedge Fracture of T9 [illegible]

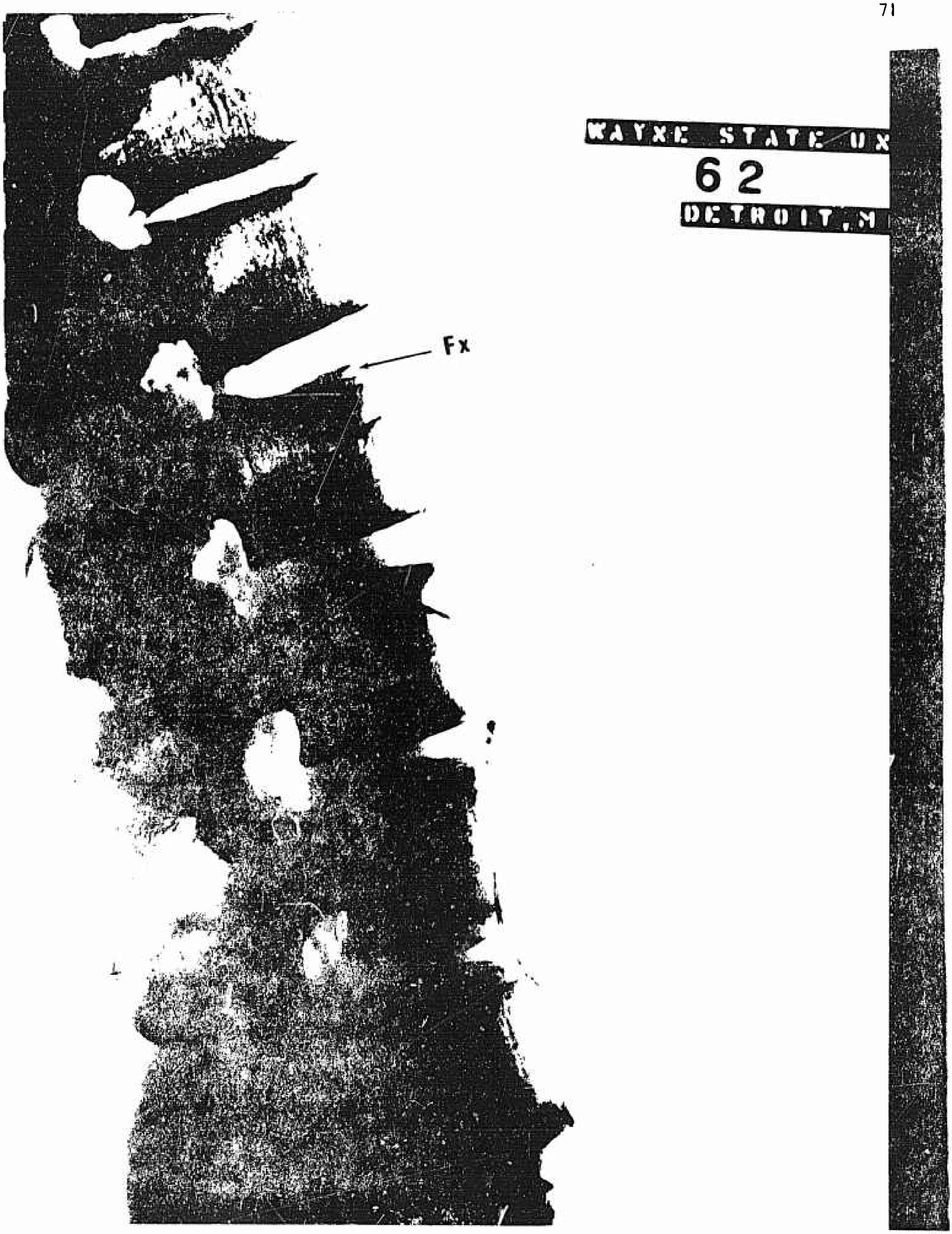

Fig. 4.12. X-Ray Showing the Hyperextension Fracture of Cadaver 062

CHAPTER IV

THE ROLE OF ARTICULAR FACETS DURING + G_z ACCELERATION

1. Introduction

In a typical vertebra, the articular facets or processes are located near the junction of the pedicles with the lamina. The pair of superior facets spring upward from the pedicles and face in the general posterior direction while the two inferior facets project downward from the lamina and face anteriorly. A view of a typical vertebra is shown in Figure 4.1. The articular surfaces are lined with hyaline cartilage and form a plane synovial joint.

It is obvious from this anatomical arrangement that the overlapping facets perform the important function of limiting rotation and of preventing one vertebra from sliding with respect to its adjacent vertebrae. The question of whether they are capable of transmitting compressive loads in the longitudinal direction of the vertebral column has never really been answered. In most texts of anatomy, the vertebral body is considered to be the weight-bearing structure of the column [3,7]. These references exemplify opinions expressed in 1948 and 1970 respectively. The facets have been said to carry no load at all [2,6]. On the other hand, Strasser [18] and Nachemson [13] have indicated that the facets can support a portion of the load borne by the spine. However, in a later paper, Nachemson [14] retracted his earlier statement and declared that the facets carry no load. His studies were based on the measurement of intradiscal pressures in isolated spinal segments which were subjected to axial loads while the disc was tilted up to 5°.

Ewing et al. [5] proposed a hypothesis for the mechanism of vertebral fracture during + G_z impact acceleration. The facets act as motion limiters preventing the posterior structures of the vertebra from being displaced as much as the vertebral body is in front. In addition, the vertebral column is subjected to eccentric loading and sustains a significant amount of bending [20]. Hence, the head and torso tend to flex forward, resulting in the anterior wedge fractures commonly noted among pilots who eject from disabled aircraft. It was shown in Chapter 3 that the level of fracture can be substantially increased from 10 to 18g in embalmed human cadavers by moderately hyperextending the vertebral column. A 2 in. thick block, 6 in. high was placed on the seat back with the centerline of the block opposite L1 to effect the hyperextension.

There was a concomitant decrease in strain along the anterior aspects of the lower thoracic and the lumbar vertebrae but the seat-pan load was not altered as a result of this hyperextension. These results point to the load-bearing capability of the motion limiters, namely, the facets. In this chapter, experimental evidence of the existence of a dual load path along the spine is documented. These findings provide a better understanding of the mechanism of injury which is also delineated.

2. Experimental Methods and Equipment

Several techniques were used to deduce the load-bearing capability of the articular facets, since direct measurement of force in a limited space environment is still beyond the state of the art.

Strain gages were an effective means of providing a qualitative indication of facet load. They were mounted on the pedicles and lamina. Methods of installing them on vertebral surfaces were developed to allow the measurement of strain just about anywhere on the external surface of a vertebra. A detailed description of the techniques used to install strain gages in vertebral bodies has been given by King and Vulcan [9]. The same methods are employed for installing them on the pedicles, for which an anterior approach is used. To mount them on the posterior surface of a lamina, a posterior approach is taken but the basic techniques remain unchanged.

Quantitative measures of facet load were obtained by means of an intervertebral load cell (IVLC) designed to fit under a disc or a vertebral body. It can measure both axial force and the eccentricity of that force with respect to its geometric center. Figure 4.2 shows the first model of an IVLC. It was almost 1 in. thick and is believed to be the first transducer capable of actually measuring the load carried by a vertebral body in an intact vertebral column. A thinner version is shown in Figure 4.3. This load cell was designed to fit above a lumbar disc, replacing the inferior segment of a vertebral body. A double-bladed rotary saw was constructed to cut slots of a precise width across the spine to accommodate the IVLC without damaging the neural arch. The lip shown in Figures 4.2 and 4.3 enables a strap to hold the IVLC in place during the experimental run. Figure 4.4 shows the IVLC in position in the lumbar spine of a cadaver. A properly installed IVLC will not result in a change in length of the vertebral column and, if the thinner model is used, the mobility of the column is also not affected. When an IVLC is used, strain gages are installed on both the anterior and posterior (lamina) aspects of the vertebrae adjacent to it to obtain correlation of facet load with strain.

Other instrumentation consists of load cells on the seat pan and back, and for the shoulder harness. Two sets of mutually perpendicular pairs of uniaxial accelerometers were mounted on the head during some of the runs to study the dynamics of head motion during $+G_z$ acceleration. The sled acceleration was also monitored.

The fully instrumented cadaver was placed in the seat of a vertical accelerator for testing. This facility is housed in an 8-story elevator shaft of the School of Medicine at Wayne State University. The sled is accelerated over a stroke of 8 feet and then gradually brought to rest by air brakes over some 30 to 40 feet. The acceleration pulse is approximately trapezoidal in shape, the rate of onset and the magnitude of the plateau being variable. Details of the accelerator have been described by Patrick [16].

The restraint system consisted of an automotive lap belt under a regular U.S.A.F. lap belt and shoulder harness combination and leg straps. The wrists were tied together and anchored to the seat pan by means of a single rope going through an eye bolt on the seat pan and looping around the lap belt. This was done to prevent flailing of the arms and to keep the lap belt in position on the pelvis during pretensioning of the shoulder harness. The head was unrestrained.

Electronic instrumentation consisted of 12 channels of bridge balance and carrier amplifier units (Heiland), a 14-channel tape recorder (Ampex), and a 24-channel light-beam recorder (Visicorder).

This chapter covers the results of approximately 82 runs made on six different cadavers. Only strain data were acquired from the first cadaver, while both IVLC and strain data were obtained from the other five. Table 1 lists the pertinent information on the cadavers used, the test conditions and the location of strain gages and the IVLC. The ability to vary the seat-back angle from 0° to 20° rearward is a recent modification to the vertical accelerator. This feature was used for the first two cadavers and provided additional evidence of the load-bearing capability of the facets. The hyperextension block was used to change the spinal curvature and thus the role of the facets, if they were indeed able to carry the load. In subsequent discussions, the hyperextended and erect spinal modes refer to runs made with and without the hyperextension block respectively. The notation for

TABLE 1

SUMMARY OF CADAVER EXPERIMENTS

Cadaver No.	Age (years)	Cause of Death	Body Weight lb.	Strain Anterior	Gage Pedicle	Locations Lamina	IVLC 1st Model	Location 2nd Model	Seat-Back Angle* (deg. rearward)
2067	62	Hemorrhage from Duodenal Ulcer	126	T8-L3	L1 (shear)	-	-	-	0-20
2062	46	Tuberculosis	100	T8-L3 T9-L3 T10,T11, L3	-	L2 T10,T11,L2 T10,T11,L3	-	- - L3-L4	0-20 0-20 0
2093	55	Arteriosclerotic Heart Disease	121	L1,L2, L4	-	L2,L3,L4	-	L3-L4	0
2231	55	Arteriosclerotic Heart Disease	161	L1	-	L3,L4	-	Below L3	0
2209	51	Arteriosclerotic Coronary Disease	145	L1	-	T12,L1	-	Below L3	0
2413	45	Arteriosclerotic Heart Disease	164	L1	-	T12,L1	-	Below L3	0

*In 5° increments from vertical position (0°).

strain gages used on the oscillograph records are as follows: A denotes an anterior gage, P a posterior gage, and D any gage on the lateral aspects of the vertebral body or on the neural arch.

3. Vertebral Strain Data

An exploratory study of facet load was made on Cadaver 2067. A strain gage was placed on the lateral surface of the neural arch of L1, near the body. Its sensitive axis was inclined at approximately 45° with respect to the longitudinal axis of the body. In this configuration, it measures shear strain on the arch and is an indicator of any shift in load from the body to the facets or vice versa. The cadaver was subjected to a 6-g pulse at various seat-back angles with the spine in the hyperextended as well as in the erect modes. Figure 4.5 shows the strain data for a run (No. 250) made with the seat back vertical (0°) and in the erect mode. The shear gage on L1 (DL1) indicated a slight compressive strain initially and then a large tensile strain during the pulse. The peak tension coincides in time with the peak compression along the anterior aspect of L1 (AL1). The results for a similar run made in the hyperextended mode are shown in Figure 4.6 (Run 249). In this case there is a slight compression at AL1 and a significant compressive strain at DL1, suggesting a shift in load from the vertebral body to the lamina and the facets.

The data for a hyperextended and an erect mode run, made at a seat-back angle of 20° rearward, are shown in Figures 4.7

(Run 243) and 4.8 (Run 244) respectively. In both cases DL1 was in compression throughout the entire acceleration pulse. However, in the erect mode the peak strain was 200μ while it was 800μ in the hyperextended mode. Further evidence of transfer of load to the posterior vertebral structures is given by the absence of a second peak in the anterior strains which were evident in runs made with the seat back vertical.

The rearward inclination of the seat back and the use of the hyperextended block have the same effect as far as the facets are concerned. In each case, there is a decrease in anterior strain and a change in sign of the shear gage output compared to that for a run made at 0° seat-back angle and in the erect mode.

To document this phenomenon more fully, the results of runs made at a seat-back angle of 10° are discussed. As shown in Figure 4.9 (Run 247), hyperextension of the spine causes DL1 to stay in compression throughout the run and the anterior gages do not show a second peak. However, in the erect mode, DL1 changes sign from compression to tension during the run with a concomitant appearance of a second peak for the anterior gages, as shown in Figure 4.10 (Run 248). Peak compression of AL1 coincides again with peak tension of DL1. At a seat-back angle of 5°, the same phenomena are repeated.

To investigate further the role of the facets, they were removed by dissection above and below L1. The lamina and spinous process of L1 were also removed. A pair of 6-g runs were made in the erect and hyperextended mode before the dissection was carried out and another pair was made with the same input acceleration after the posterior structures were removed. The seat back was vertical for all runs. Figures 4.11 (Run 253) and 4.12 (Run 257) give data for runs made in the erect mode, with and without facets respectively. The anterior strains at T12, L1 and L2 show a marked increase after the removal of the facets. In fact, for AL1, there was a 121% increase in compressive strain. Moreover, the strain pattern for the shear gage (DL1) was changed drastically. Its output dropped to nearly zero from a peak tensile strain of 1240μ when the spine was intact.

A comparison of the effect of facet removal in the hyper-extended mode can be made from Figures 4.13 (Run 254) and 4.14 (Run 258). Run 254 was made with the spine intact. The increase in AL1 strain was 90%, as a result of facet removal. There are, however, two inconsistencies in the data. The decrease in shear strain was only 18% whereas it was again expected to drop to almost zero. AL2 showed an 11% decrease in strain instead of an increase. A possible explanation of these effects is the impingement of the vertebrae against the hyperextension block, the centerline of which was located opposite L1.

These results led to a more direct approach to the problem. If the posterior structures constitute a load path, a strain gage on the lamina should provide considerable clarification of the situation. A single gage on the lamina of L2 of Cadaver 2062 constituted an initial feasibility study of acquiring useful data from this location. There were again anterior gages from T8 through L3 and the experimental plan was to make runs at various seat-back angles in the erect and hyperextended mode. It was found that the output of this gage was less than 600μ for a 6-g run. However, interesting trends could be picked out. In the hyperextended mode, the strain was generally compressive or remained compressive longer than in the erect mode. In this mode, strains that were initially compressive frequently became tensile during the latter half of the pulse.

A more extensive study of laminar strain was carried out on this cadaver by installing additional gages on the lamina of T10 and T11. The series of runs was repeated using these 3 posterior gages and anterior gages from T9 through L3. The input acceleration level was raised to 8-g. Data for the erect and hyperextended mode are shown in Figures 4.15 (Run 283) and 4.16 (Run 282) respectively. The seat back was vertical. The difference in response of the posterior gages is quite obvious. In the erect mode (Figure 4.15) PT10 and PT11 remained in tension throughout the pulse while PL2 was initially in compression and went into tension at about 50 msec after the onset of acceleration. As a result of hyperextension, PL2 remained in compression for the entire duration of the pulse, while PT10 and PT11 underwent a change in sign from compression to tension, as shown in Figure 4.16. A marked reduction in anterior strain is also quite evident.

Rearward rotation of the seat back did not alter the posterior strain pattern which was predominantly dependent upon the curvature of the spine. The response of the P-gages at 20° was the same as that at 0° in terms of the strain-time history and the reversal in sign. The difference in response between the thoracic and lumbar gages is due to the location of the vertebrae on different curves of the column. However, the qualitative evidence from these data point to a transfer of load from the facets to the vertebral body as the head and torso rotate forward.

4. Intervertebral Load Cell Data

The purpose of the IVLC was to measure the load carried by the vertebral body and to compare it with that borne by the column, the total spine load. The latter was taken to be proportional to the measured seat pan load. The ratio used was the weight of the torso above the IVLC to the total body weight. Any difference between the spine load and the IVLC output is the load carried by the articular facets, the facet load. Justifications for the validity of this method of deducing facet load are provided in the discussion section of the paper.

IVLC data were obtained from five different cadavers. The initial thicker version was used in the first two cadavers while the second thinner model was employed during runs made on the third. A typical oscillograph record of IVLC output is shown in Figure 4.17 (Run 304). This was a 10-g run made on Cadaver 2062 in the erect mode. The IVLC replaced the inferior portion of the L3-L4 disc and the superior segment of L4. The neural arch of L4 was left intact. Figure 4.18 shows the computed spine load and facet force which is the difference between the spine load and the intervertebral body force (Run 304). The facets were in compression for the first 125 msec of the pulse. However, as the head and torso rotated forward, the facets unloaded and went into tension, resulting in an intervertebral body force larger than the total spine load. The facet load and PL3 strain also show good correlation, with the zero crossover point of both traces occurring almost simultaneously. To minimize the number of figures, description of subsequent IVLC runs will be accompanied by plots of spine, facet, and intervertebral body loads and oscillograph records will be omitted. Figure 4.19 (Run 303) shows force and strain data for a 10-g run made in the hyperextended mode. The compressive facet load was larger in magnitude and longer in duration than that for the erect mode (Figure 4.18, Run 304).

The IVLC (1st model) was used again in Cadaver 2093. It was located between L3 and L4. The inferior segment of L3 and the superior portion of the L3-L4 disc was removed to accommodate the IVLC. A 2.5-g run was made in the erect mode to study spinal response near the 1-g environment. The data are shown in Figure 4.20 (Run 323). The facets were taking about 50% of the total spine, but they did not unload and go into tension. The strain pattern of PL3 again followed that of the facet load very closely. At 9 g, the proportion of spine load carried by the facets was about 35%, as shown in Figure 4.21 (Run 324). The spine was in the erect mode. The facets and PL3 were in compression throughout the pulse, indicating that unloading never took place. The location and thickness of the IVLC may have decreased the mobility of the vertebrae and the unloading phenomenon may also be dependent on the curvature of the spine.

A series of runs was carried out on three cadavers using the thinner model of the IVLC. Its overall thickness was 0.4 in. and it was placed above the L3-L4 disc by replacing the inferior segment of L3. The disc was virtually intact. These cadaver runs were used to validate mathematical models of the spine, described in Chapter V, hence the results of all the runs made are not shown in this chapter. Each cadaver was run at 6.8 and 10 g's acceleration in the erect and the hyperextended modes.

Figure 4.22 (Run 378) shows an 8-g run made in the erect mode on Cadaver 2231. The facets unloaded rather early in the acceleration pulse (at about 60 msec), but there was confirmation from PL3 strain. For an identical run made in the hyperextended mode, the facets remained in compression for the entire pulse, as shown in Figure 4.23 (Run 377). PL3 and PL4 strains were also in compression throughout the pulse. The total spine load was the same in these two runs, but the intervertebral body force decreased by about 400 lb. as a result of hyperextension. The results of the runs made at 6 and 10 g's on this cadaver were essentially the same.

The results obtained from Cadavers 2209 and 2413 were essentially the same as those obtained from Cadaver 2231. The results of all the eighteen runs made on the above three cadavers are shown in the chapter on the experimental verification of the mathematical model.

5. Discussions and Conclusions

Experimental results have been presented to document the role of the articular facets during $+G_z$ impact. Qualitative evidence in the form of strain data from the anterior and posterior aspects of both thoracic and lumbar vertebrae indicate the existence of a dual load path along the vertebral column. This led to the development of an IVLC which was used to obtain quantitative data supporting the claim that both tensile and compressive loads can be transmitted via the facets or the posterior structures of the lumbar vertebrae.

The complexity of the posterior structures and the limitation of space in and around the joints of the facets precluded a direct measurement of facet load. The load-bearing capability was deduced by comparing the total spine load with that obtained from the IVLC. The spine load was taken to be proportional to the seat pan load. That is, the dynamic response of the torso above the IVLC was assumed to be the same as that below it. Since the IVLC was placed between L3 and L4, it can be argued that there should be very little dynamic overshoot from the lower torso and legs and that the spine load should be the difference between the seat pan load and the product of sled acceleration and mass of the lower torso and legs. However, the dynamic overshoot of the seat pan load is 10% or less so that the spine load computed by either method does not differ significantly. Furthermore, during a major portion of the pulse, the seat pan load cell response is almost flat. Consequently, the facet load has been estimated fairly accurately by means of the IVLC and the seat pan load cell.

The use of the hyperextension block and the variation of the seat-back angle provided additional data confirming the role of the facets and aided in the understanding of the mechanism of injury. On the basis of the data obtained, it is now possible to assemble the research results on spinal injury and propose an injury mechanism which fully explains the commonly observed anterior wedge fractures sustained by pilots during emergency egress. Previous work by Vulcan and King [20] established the fact that during caudo-cephalad ($+ G_z$) acceleration the spine is subjected to both axial compression and bending. The bending effects are due to the eccentricity of the torso with respect to the spine and are enhanced by the forward rotation of the head and torso. Subsequent work described in Chapter III showed that fracture levels could be raised significantly by placing a 2-in. thick hyperextension block opposite L1 on the seat back. The curvature of spine was altered by the block but there was insufficient movement to decrease the eccentricity of the torso and hence the bending moment on the spine. Nevertheless, the average level of fracture was raised from 10 to 18 g and the decrease in anterior strains was generally significant at the 95% confidence level. The hypothesis that the facets act as motion limiters led to this documentation of their role during $+G_z$ acceleration. In the erect spinal mode, the facets tend to unload and go into tension, causing the vertebral bodies to sustain more compressive load than the total spine load. This occurs when the head and torso undergo maximum forward flexion. The anterior wedge fractures are therefore the result of eccentric compression coupled with the unloading of the facets. In the hyperextended mode, the facets relieve the vertebral bodies of some of the compressive load and thus it was possible to raise the fracture level by such a considerable margin.

In summary, the following conclusions can be made:

1. The articular facets are capable of bearing compressive and tensile loads.
2. Strain gages were employed to provide qualitative evidence of facet load.
3. Intervertebral body force was measured in an intact spine during impact acceleration by means of a specially designed intervertebral load cell (IVLC).
4. From the IVLC and seat pan load cell output, a facet load history was computed.
5. A better understanding of the injury mechanism of the spine has been achieved.

6. Hyperextension of the spine transfers more load to the facets.

7. The proportion of the load carried by the facets appear to increase with the decreasing g-levels, suggesting that they may also carry a portion of the static body weight when the body assumes a normal erect posture.

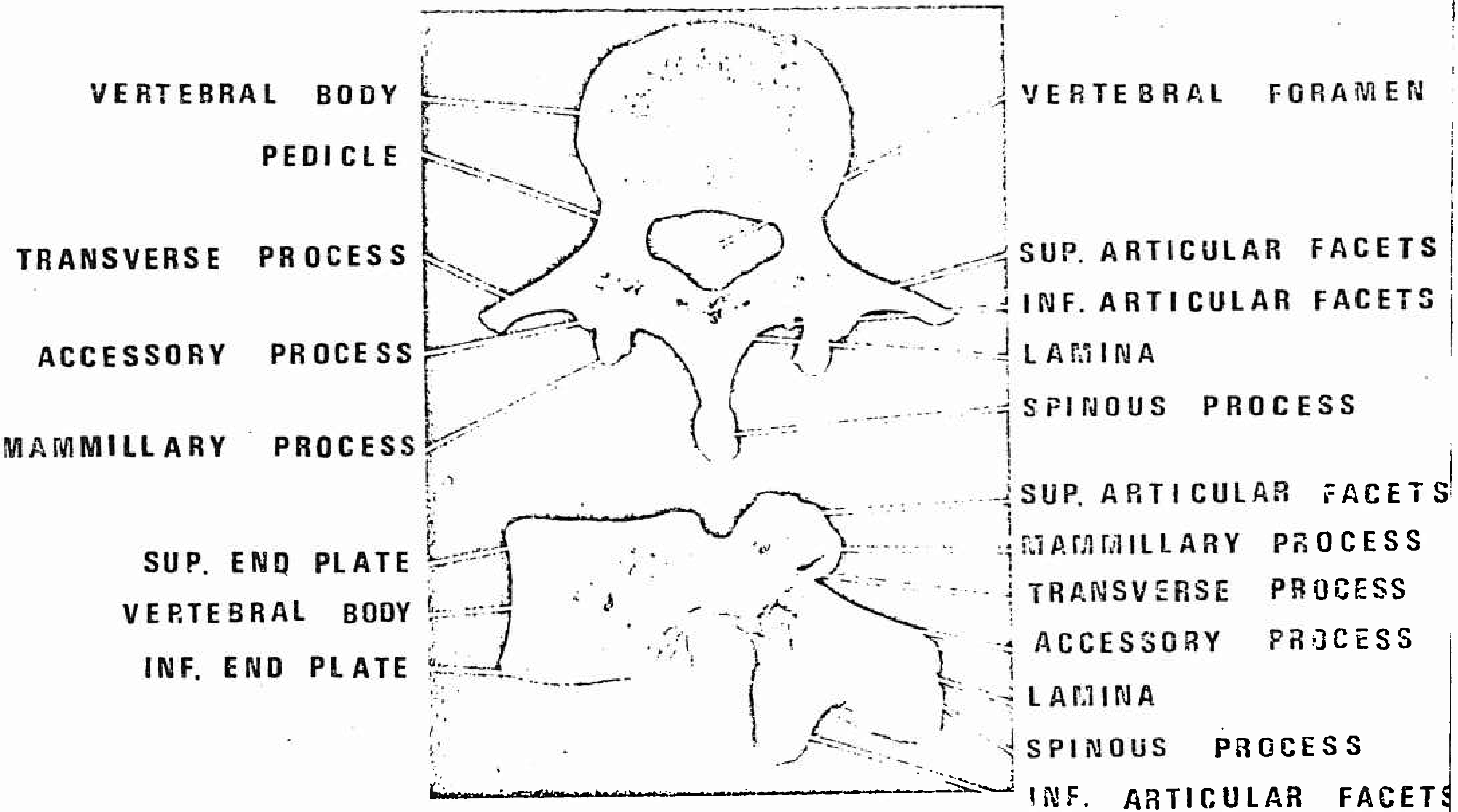

Fig. 4.1. Top and Side View of a Typical Vertebra

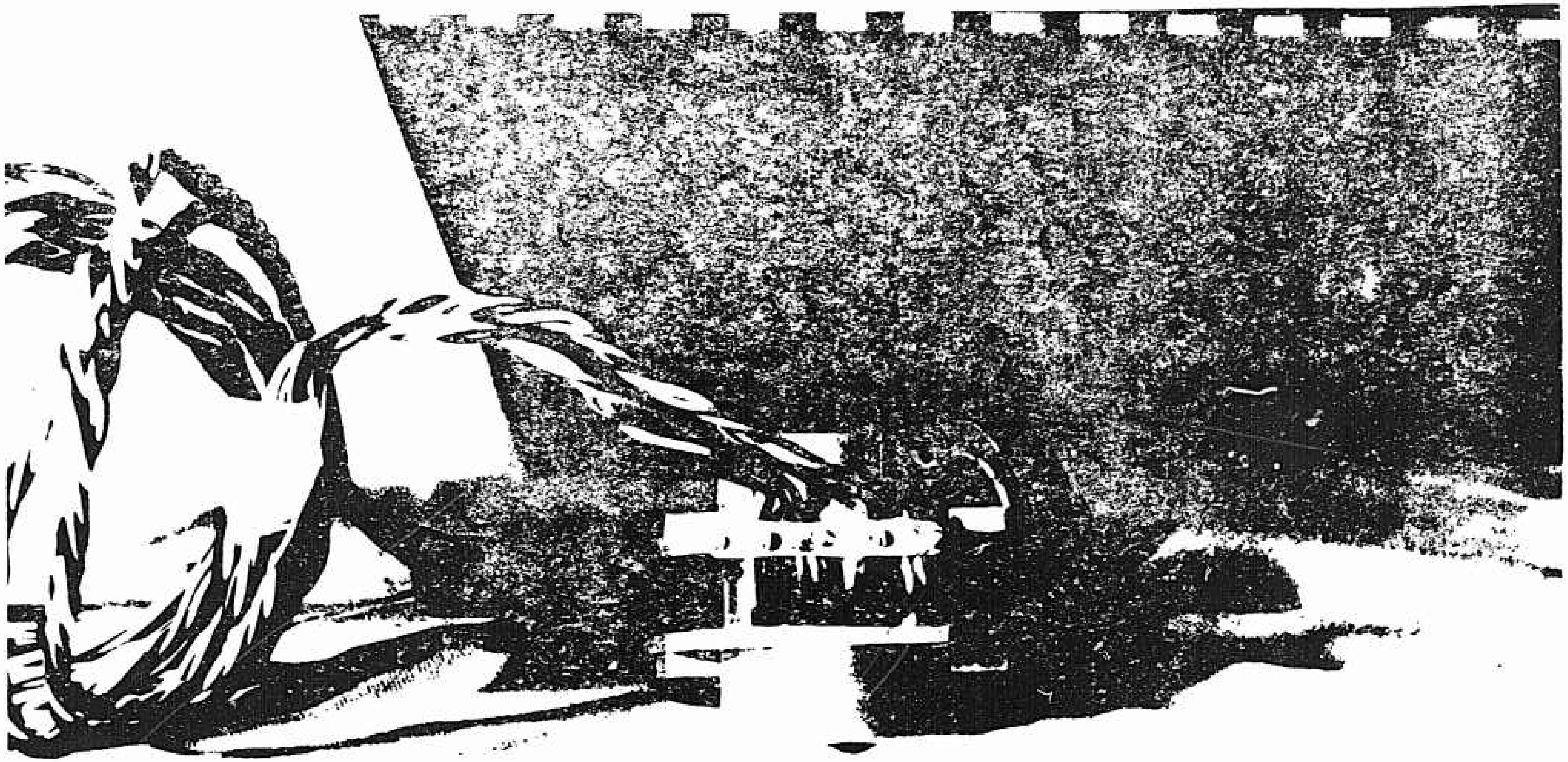

Fig. 4.2 Photograph of the First Model of an Intervertebral Load Cell (0.8 In. thick)

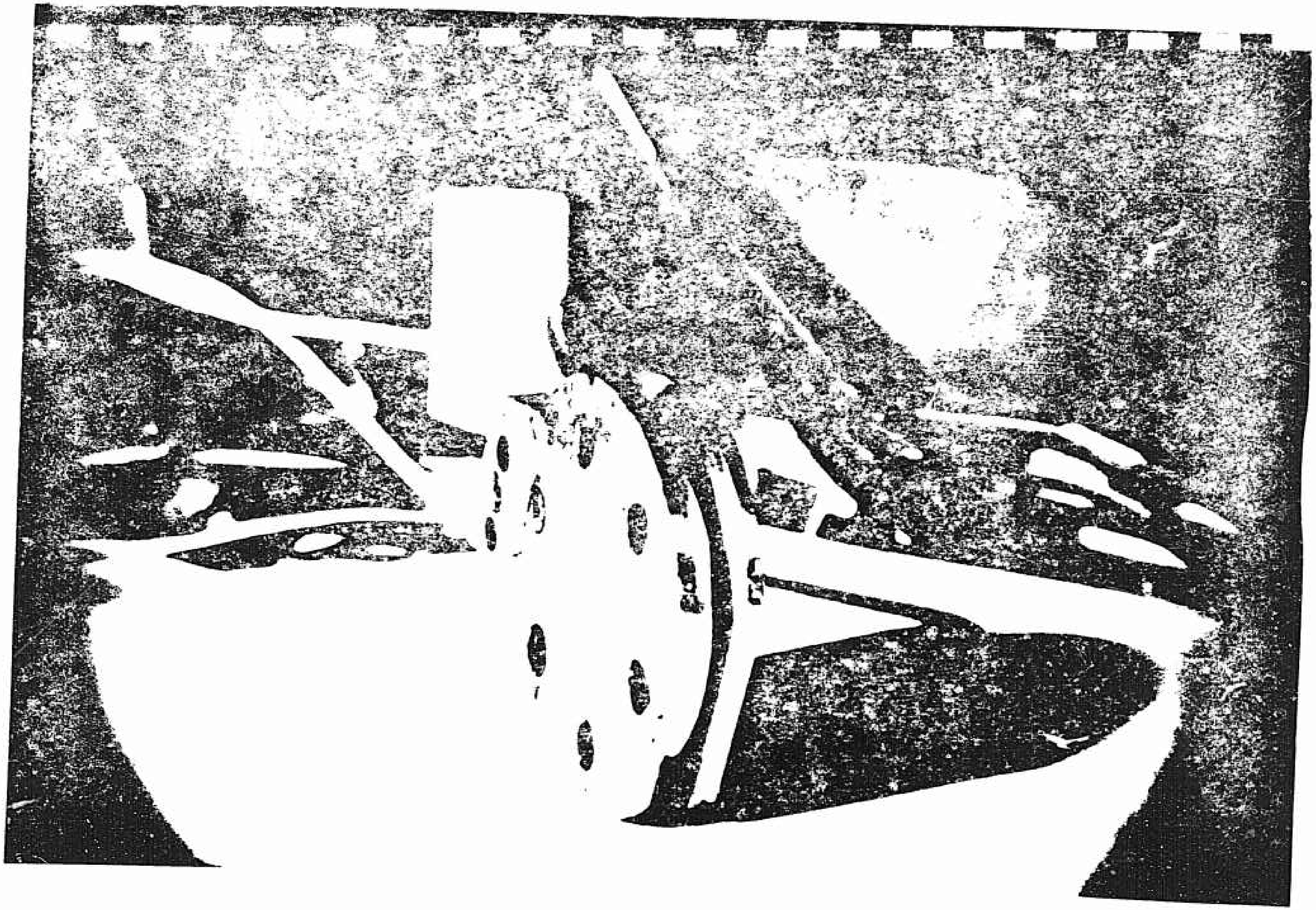

Fig. 4.3 Photograph of the Second Model of an Intervertebral Load Cell (0.4 in thick)

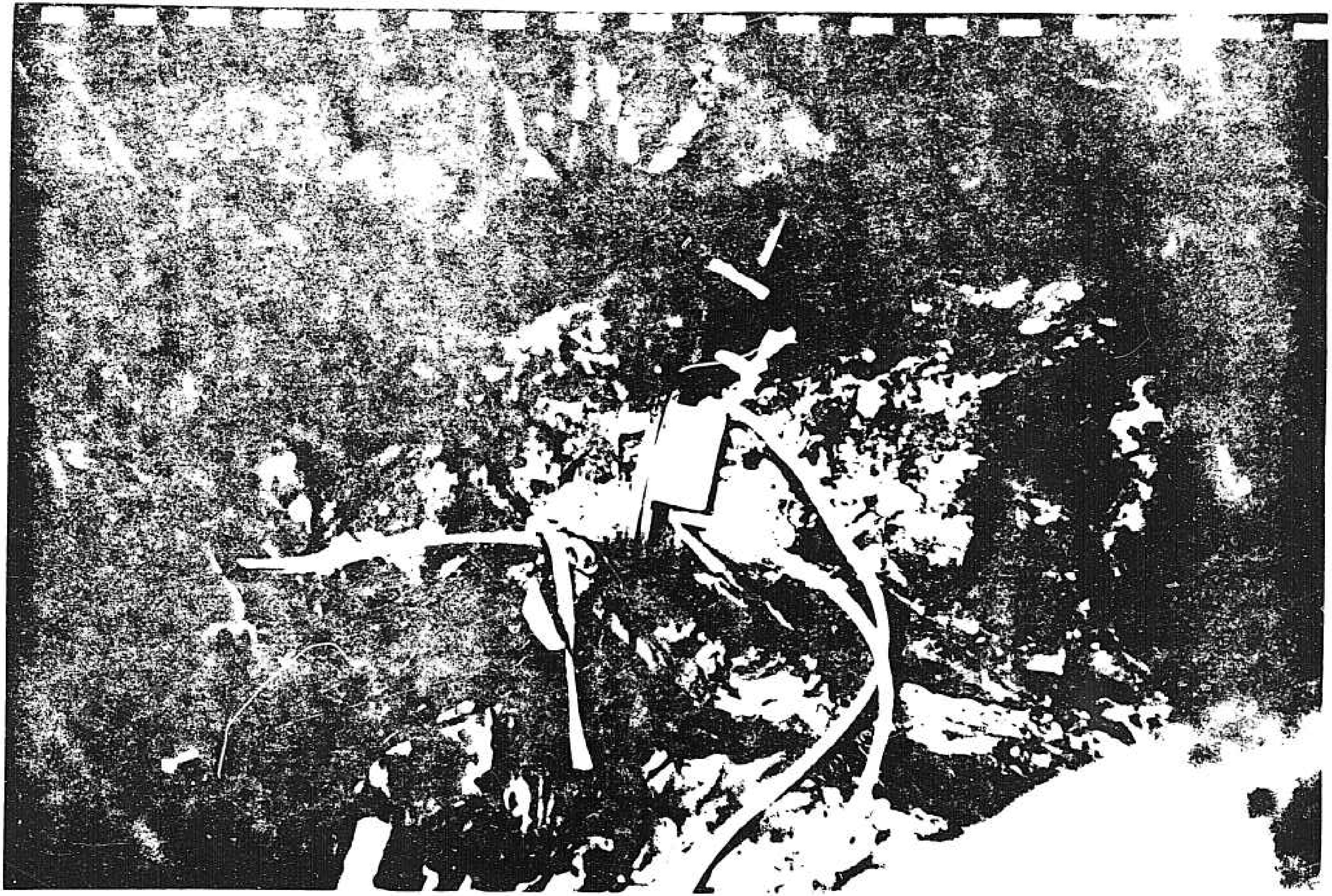

Fig. 4.4 An Intervertebral Load Cell In Place in a Lumbar Spine

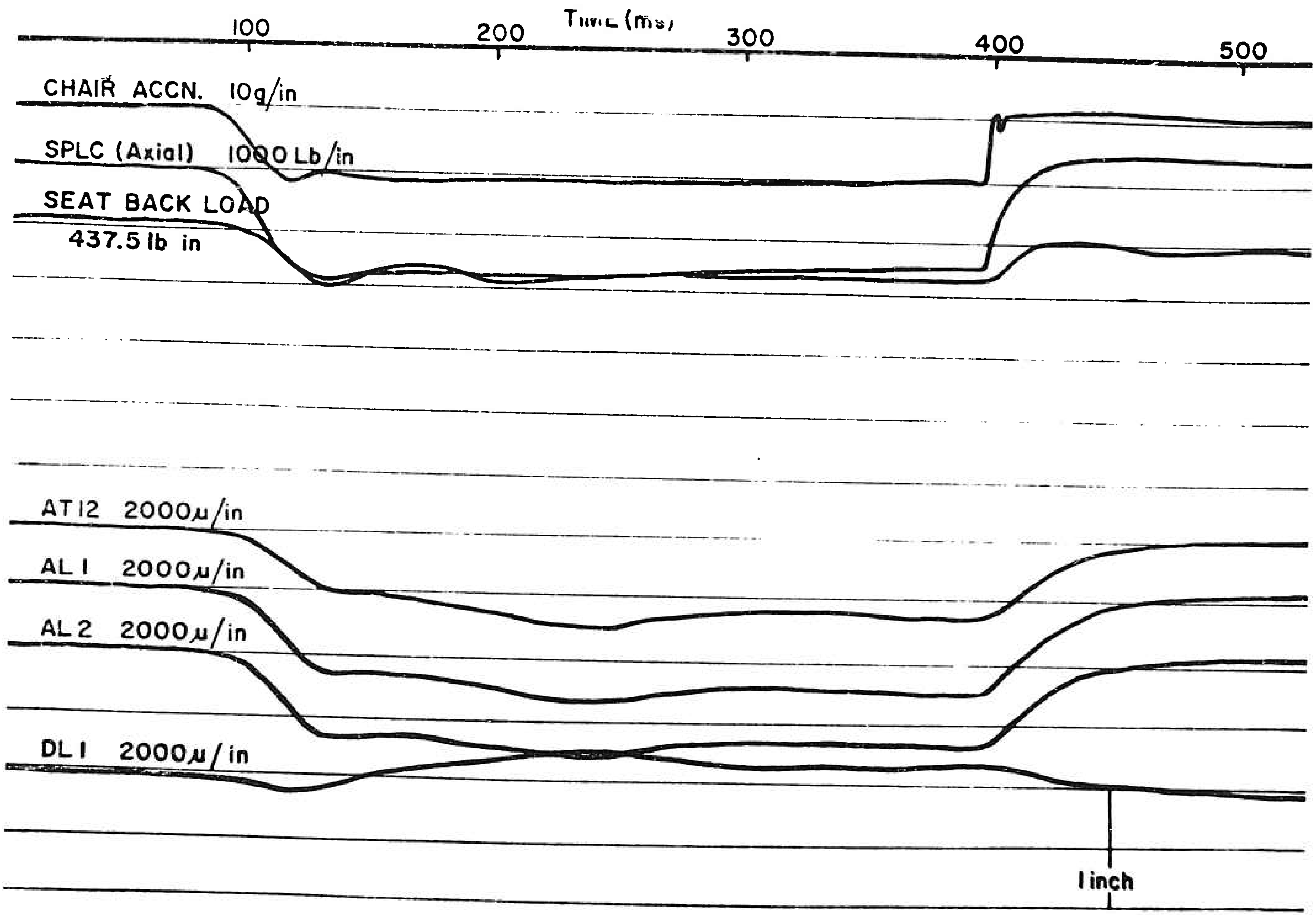

Fig. 4.5. Oscillograph Record of Run 250, Cadaver 2067 - Seat-back Angle 0°,

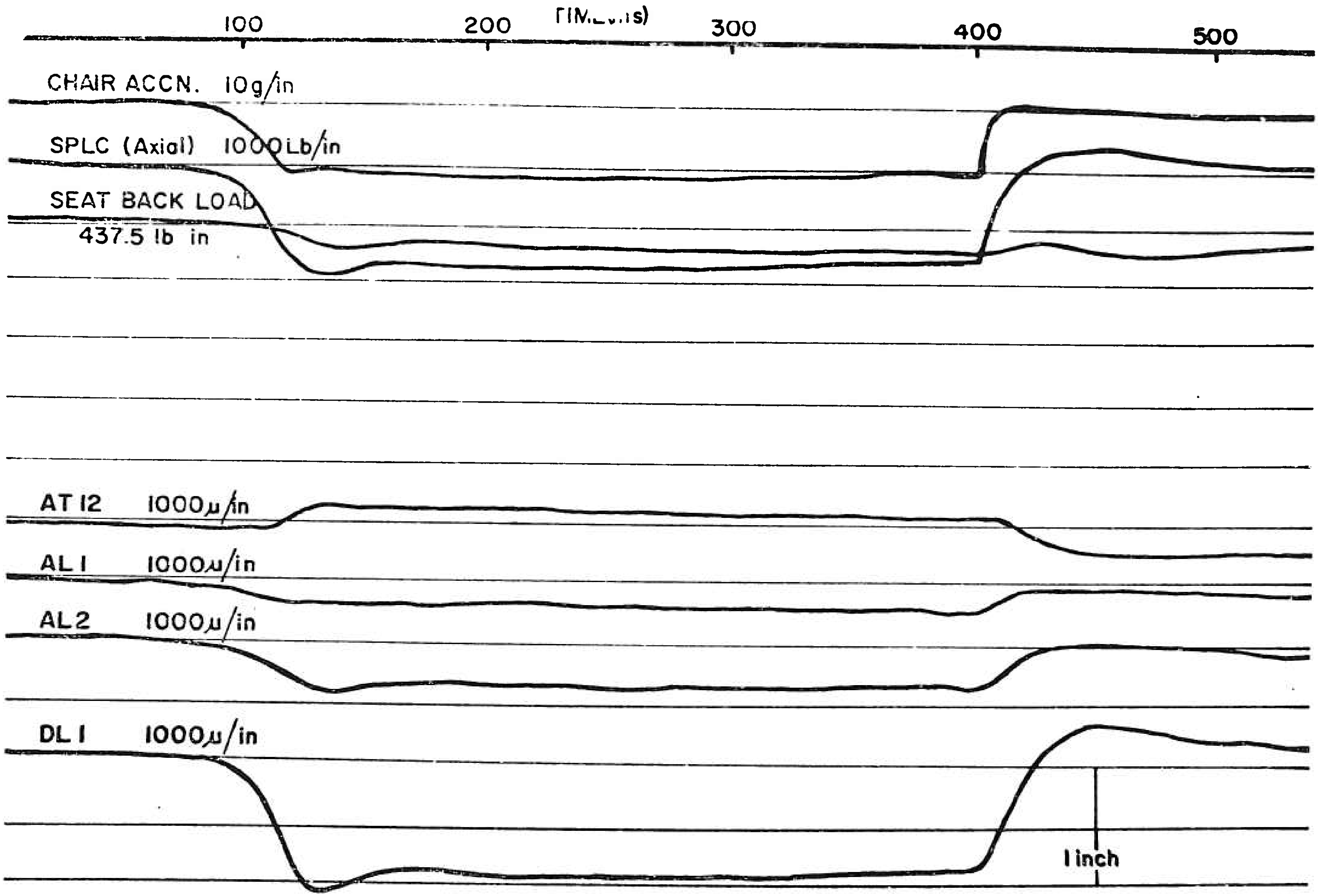

Fig. 4.6. Oscillograph Record of Run 249, Cadaver 2067 - Seat-back Angle 0°,

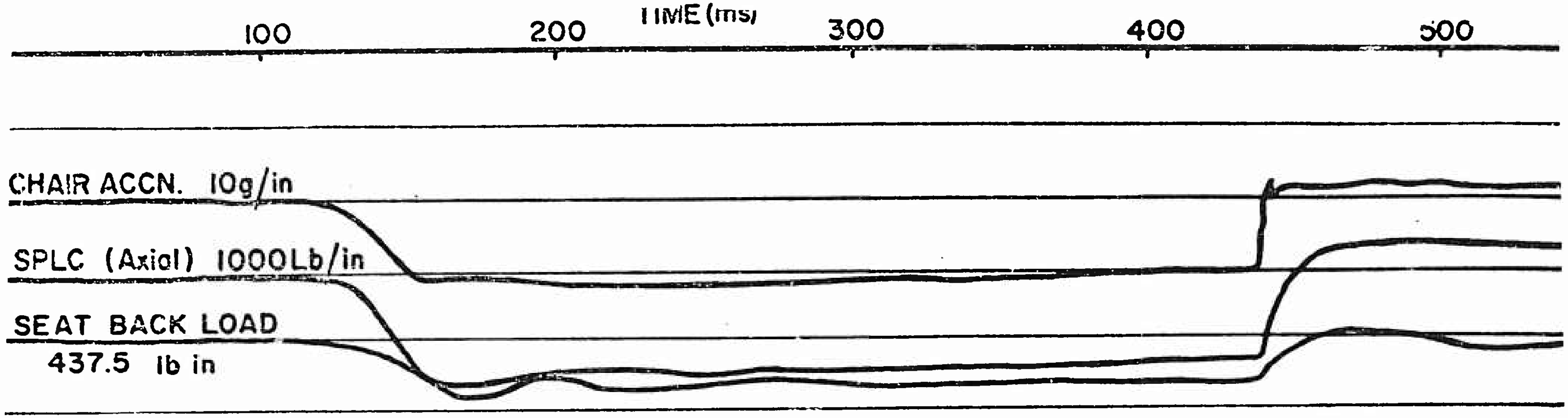

Fig. 4.7. Oscillograph Record of Run 243, Cadaver 2067 - Seat-back Angle 20°, Hyperextended Mode

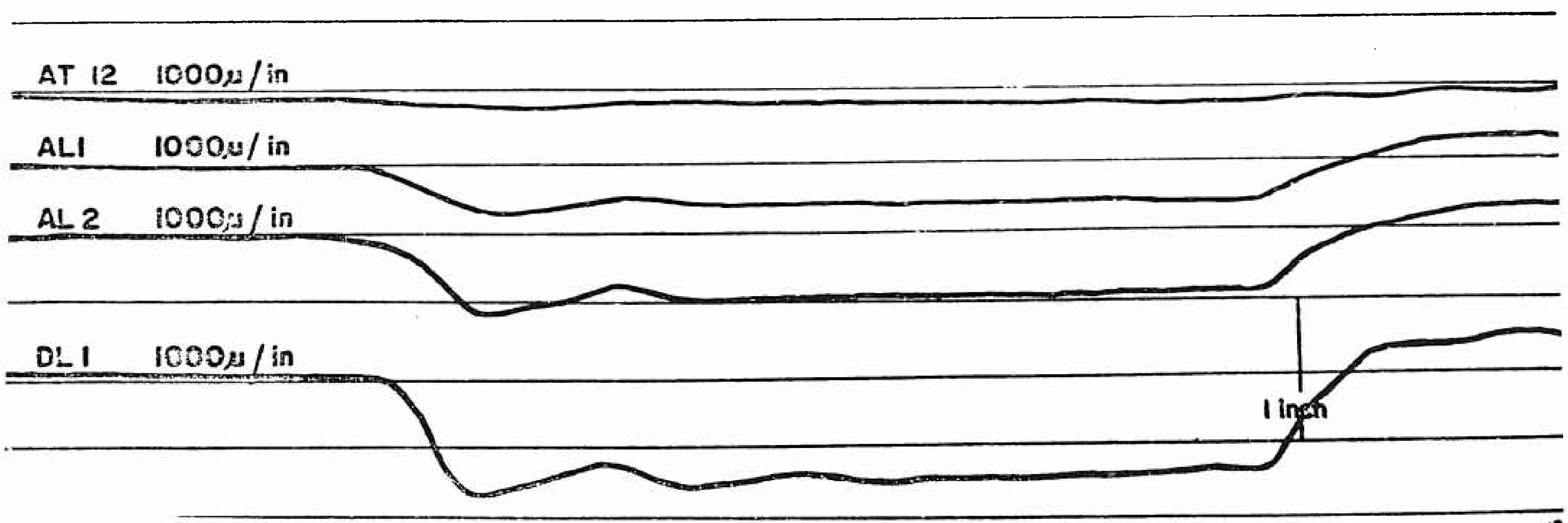

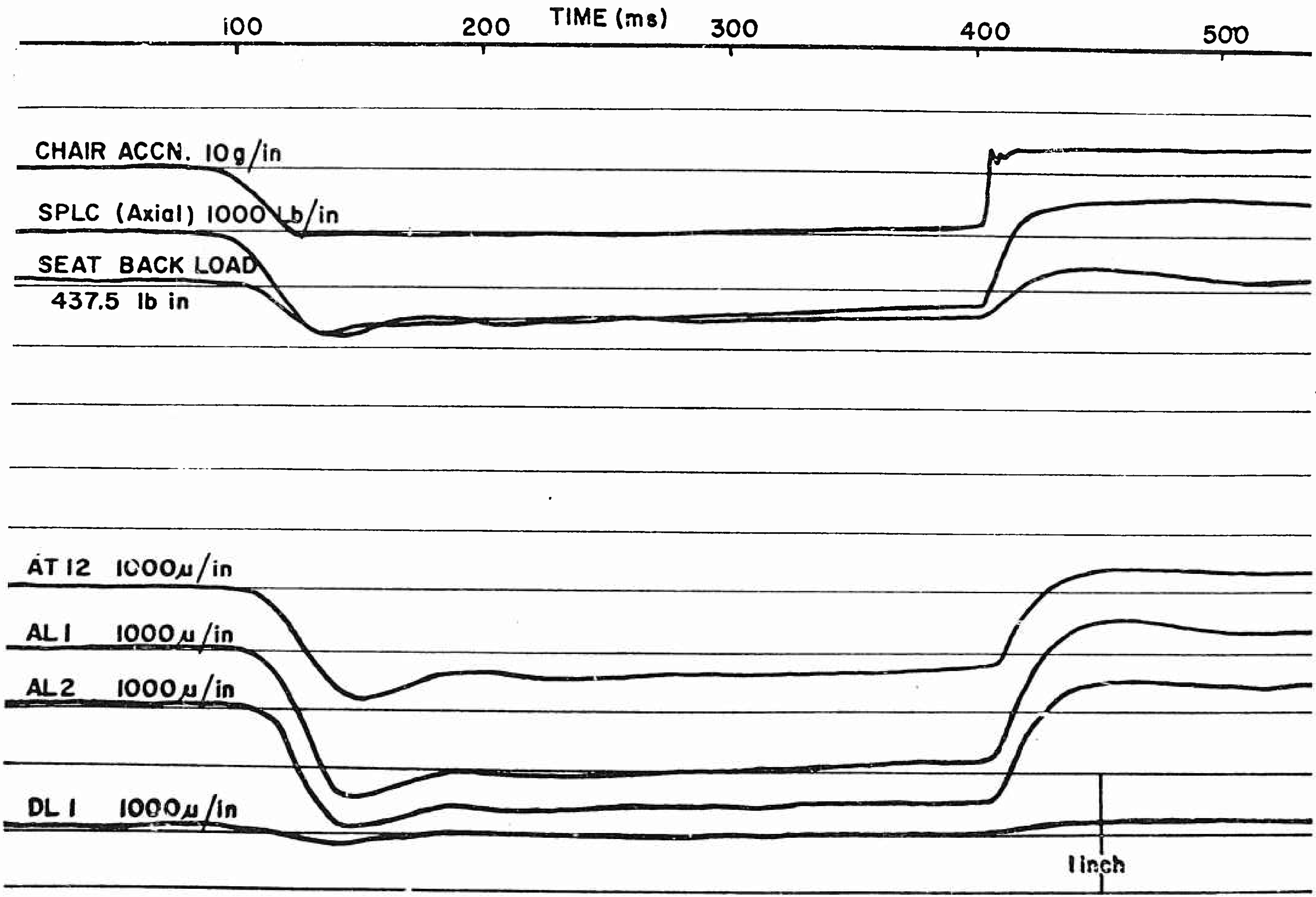

Fig. 4.8. Oscillograph Record of Run 244, Cadaver 2067 - Seat-back Angle 20°,

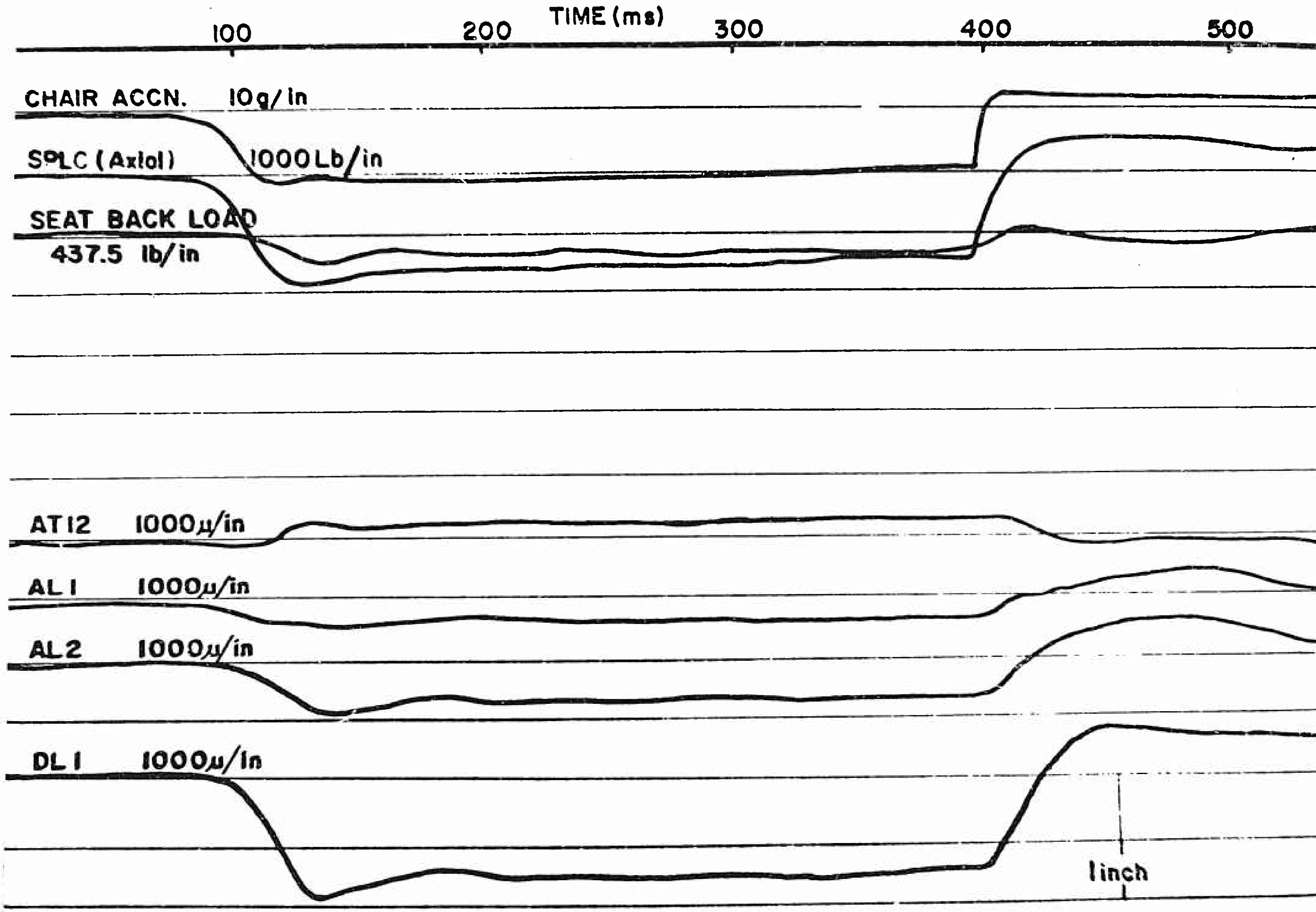

Fig. 4.9. Oscillograph Record of Run 248, Cadaver 2067 - Seat-back Angle 10°,

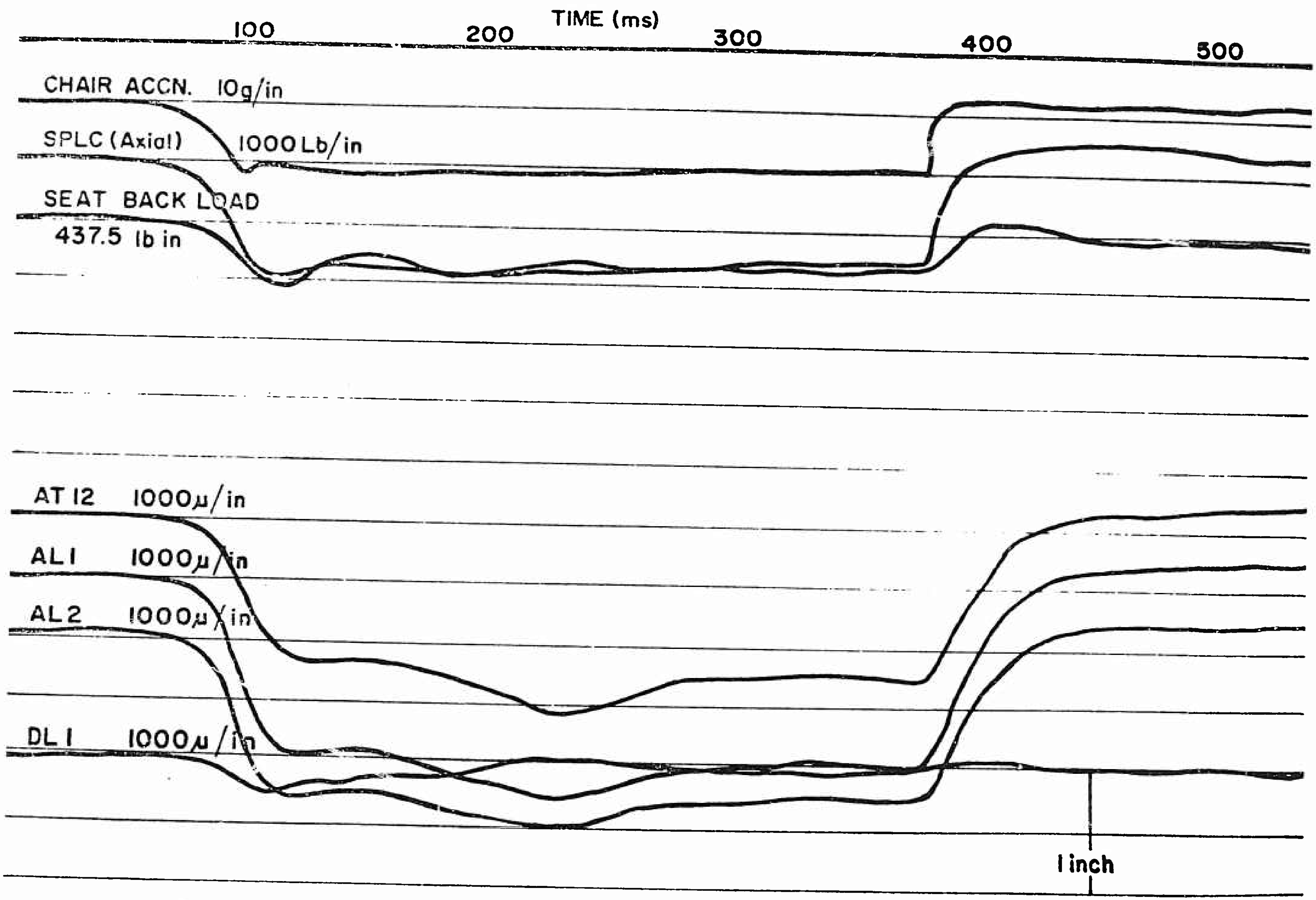

Fig. 4.10. Oscillograph Record of Run 247, Cadaver 2067 - Seat-back Angle 10°,

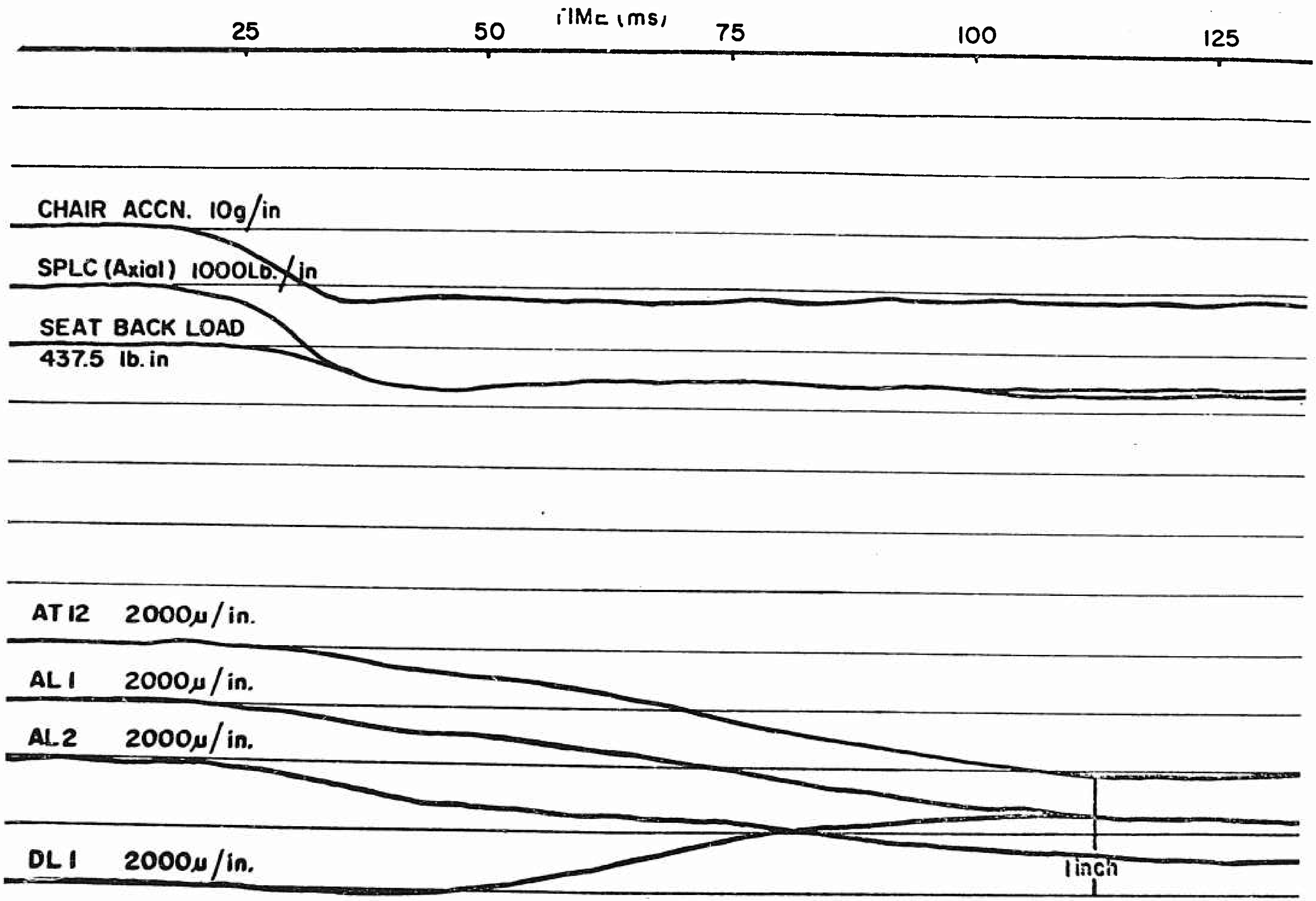

Fig. 4.11. Oscillograph Record of Run 253, Cadaver 2067 - Facets Intact.

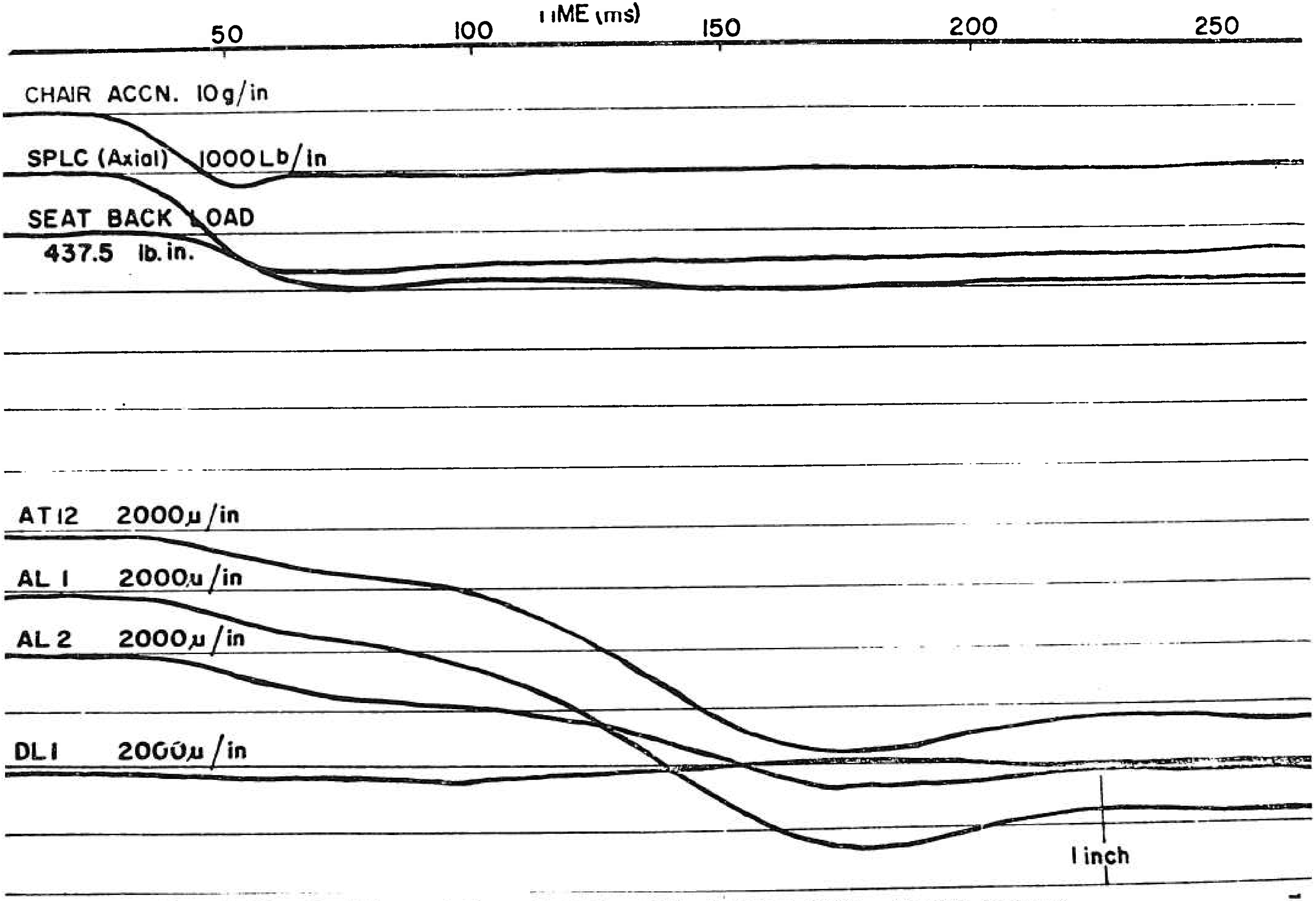

Fig. 4.12. Oscillograph Record of Run 257, Cadaver 2067 - Facets Removed, Erect Mode

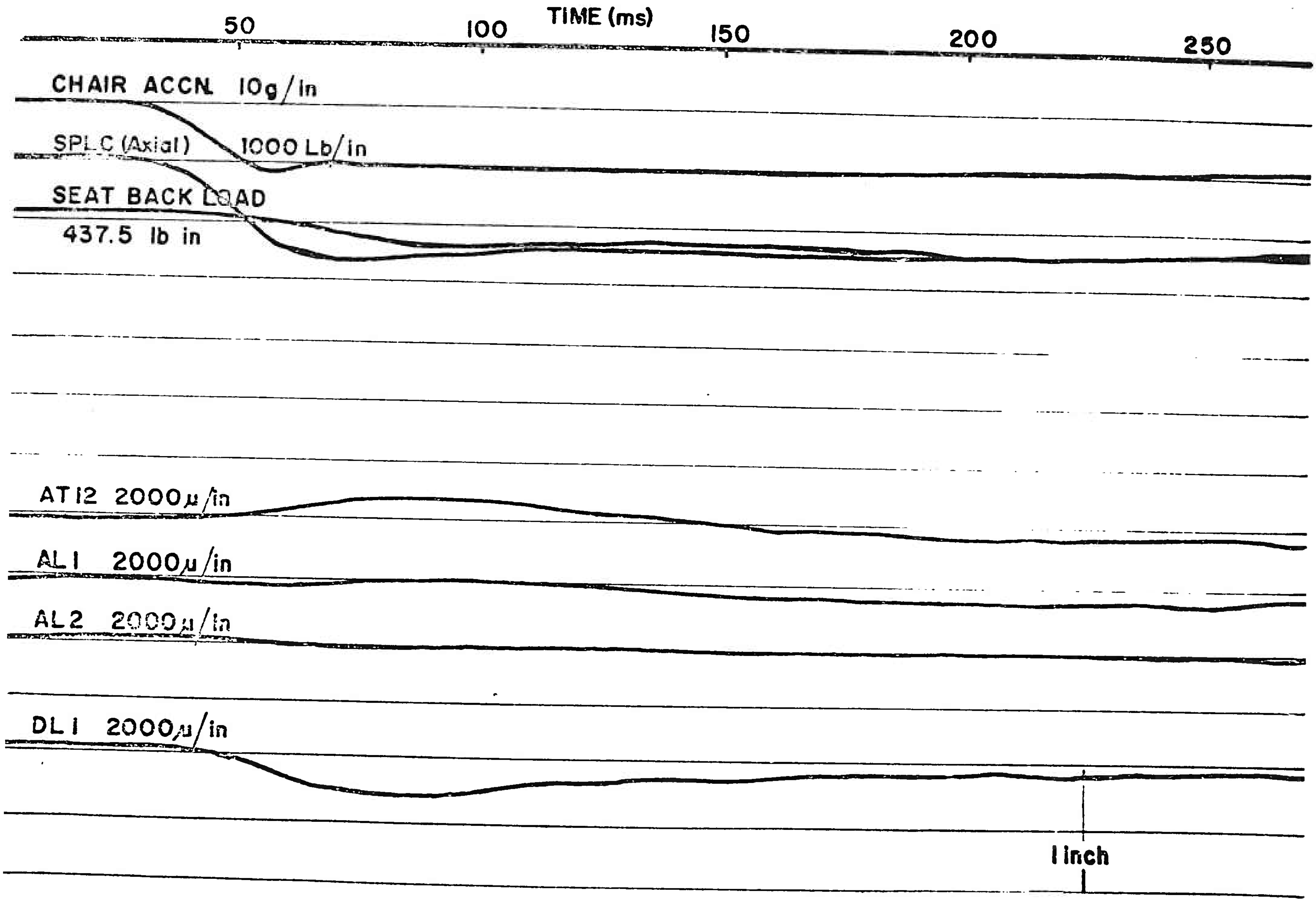

Fig. 4.13. Oscillograph Record of Run 254, Cadaver 2067 - Facets Intact, Hyperextended Mode

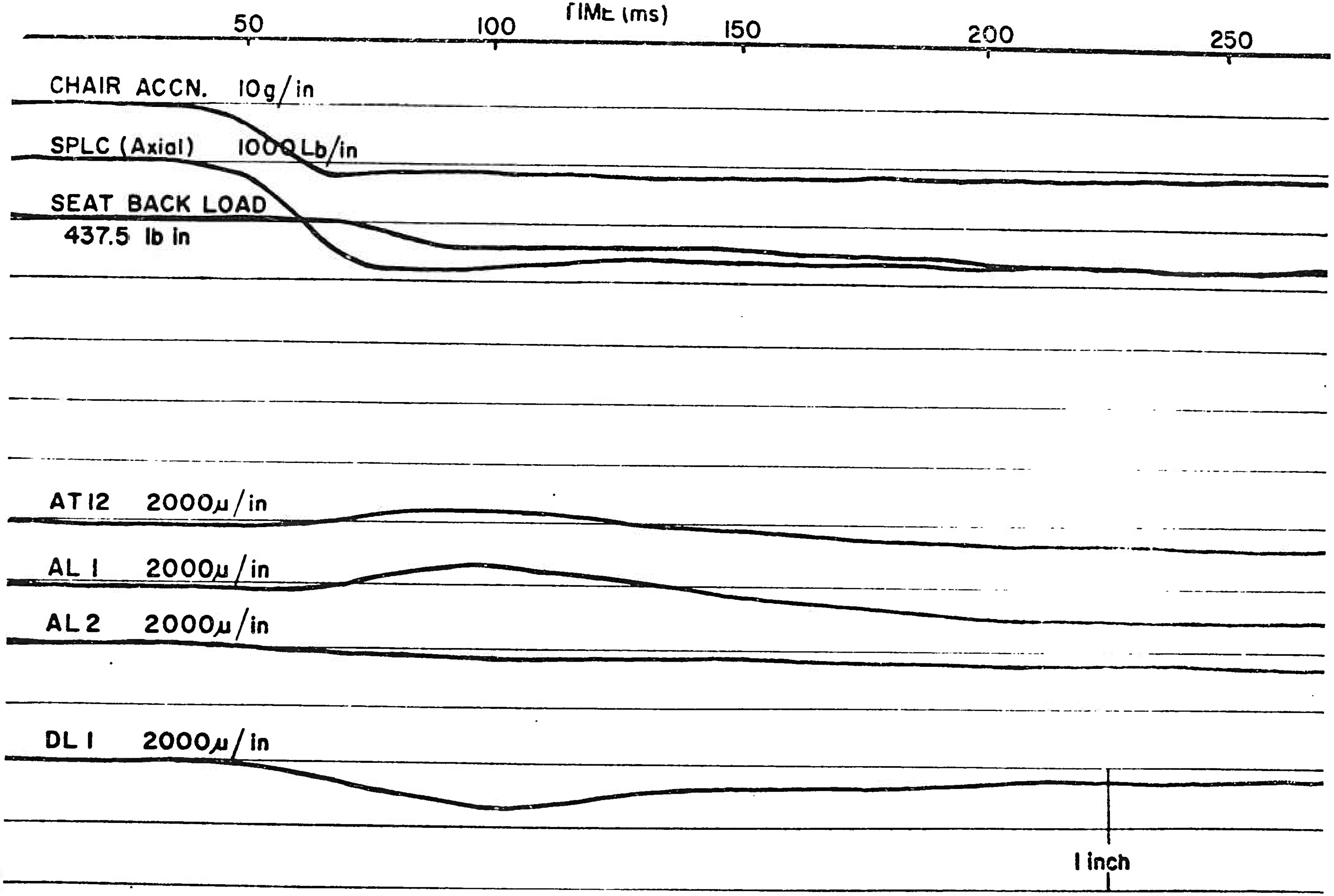

Fig. 4.14. Oscillograph Record of Run 258, Cadaver 2067 - Facets Removed, Hyperextended Mode

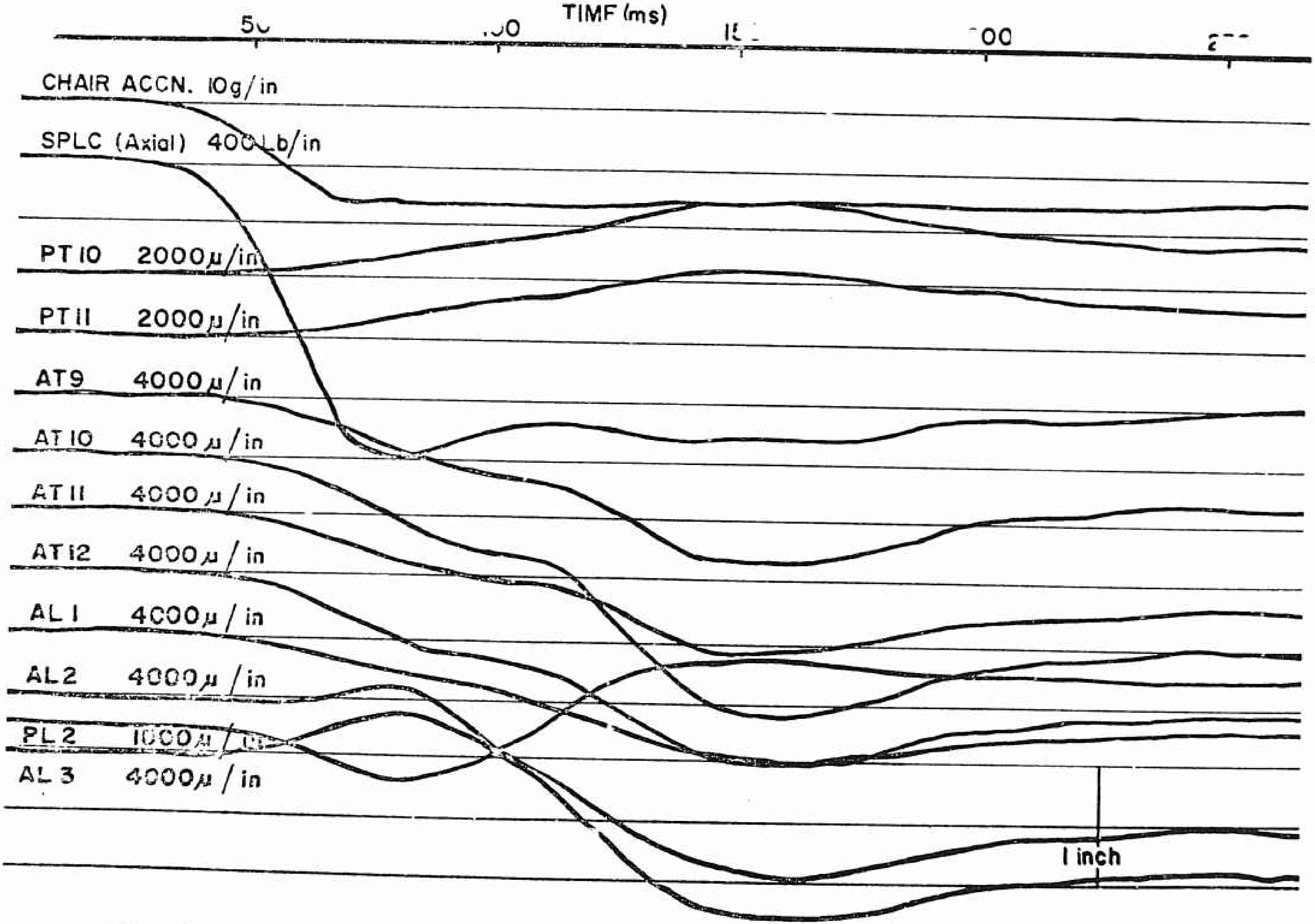

Fig. 4.15. Oscillograph Record of Run 283, Cadaver 2062, Seat-back Angle 0°,

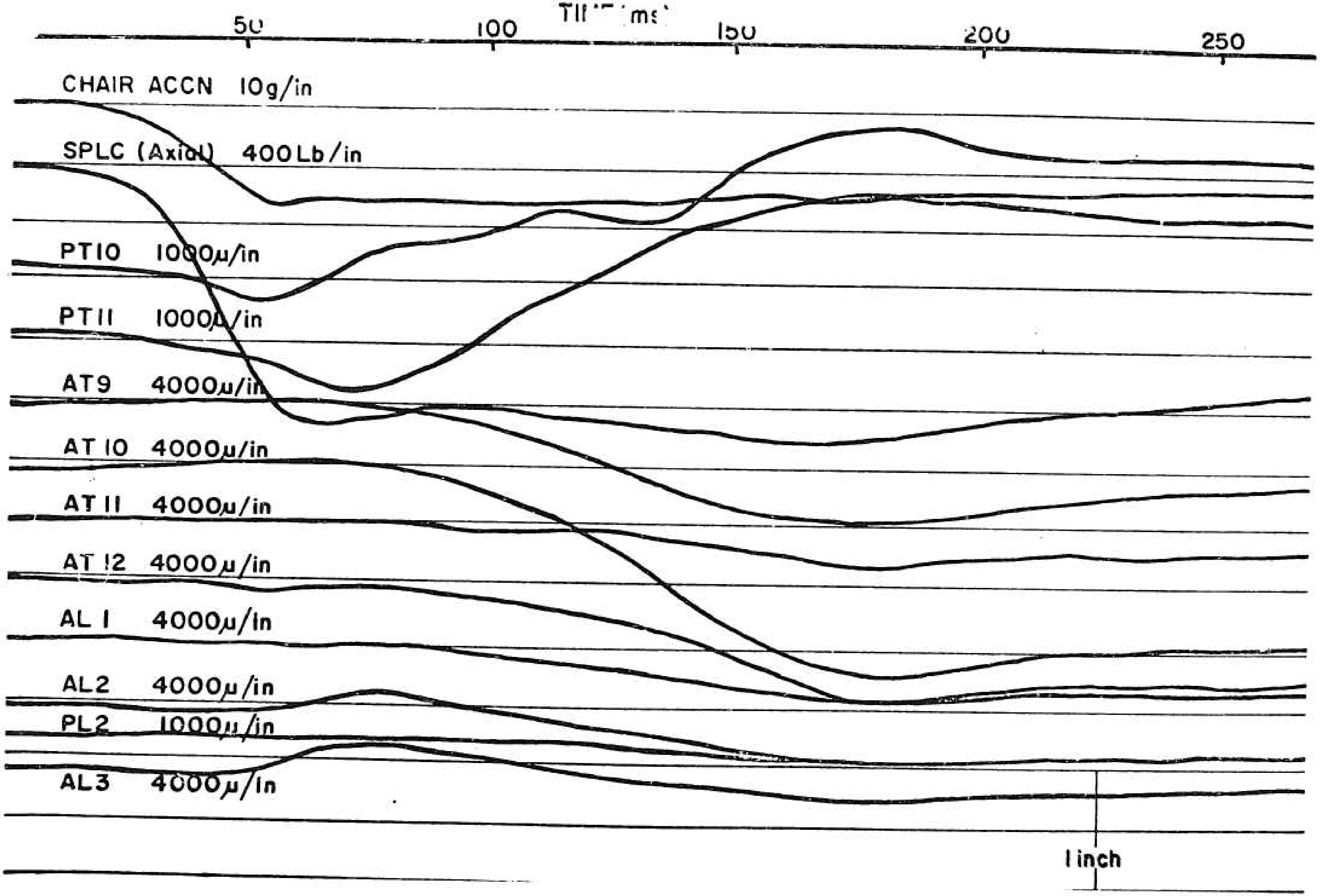

Fig. 4.16. Oscillograph Record of Run 282, Cadaver 2062, Seat-back Angle 0°, Hyperextended Mode

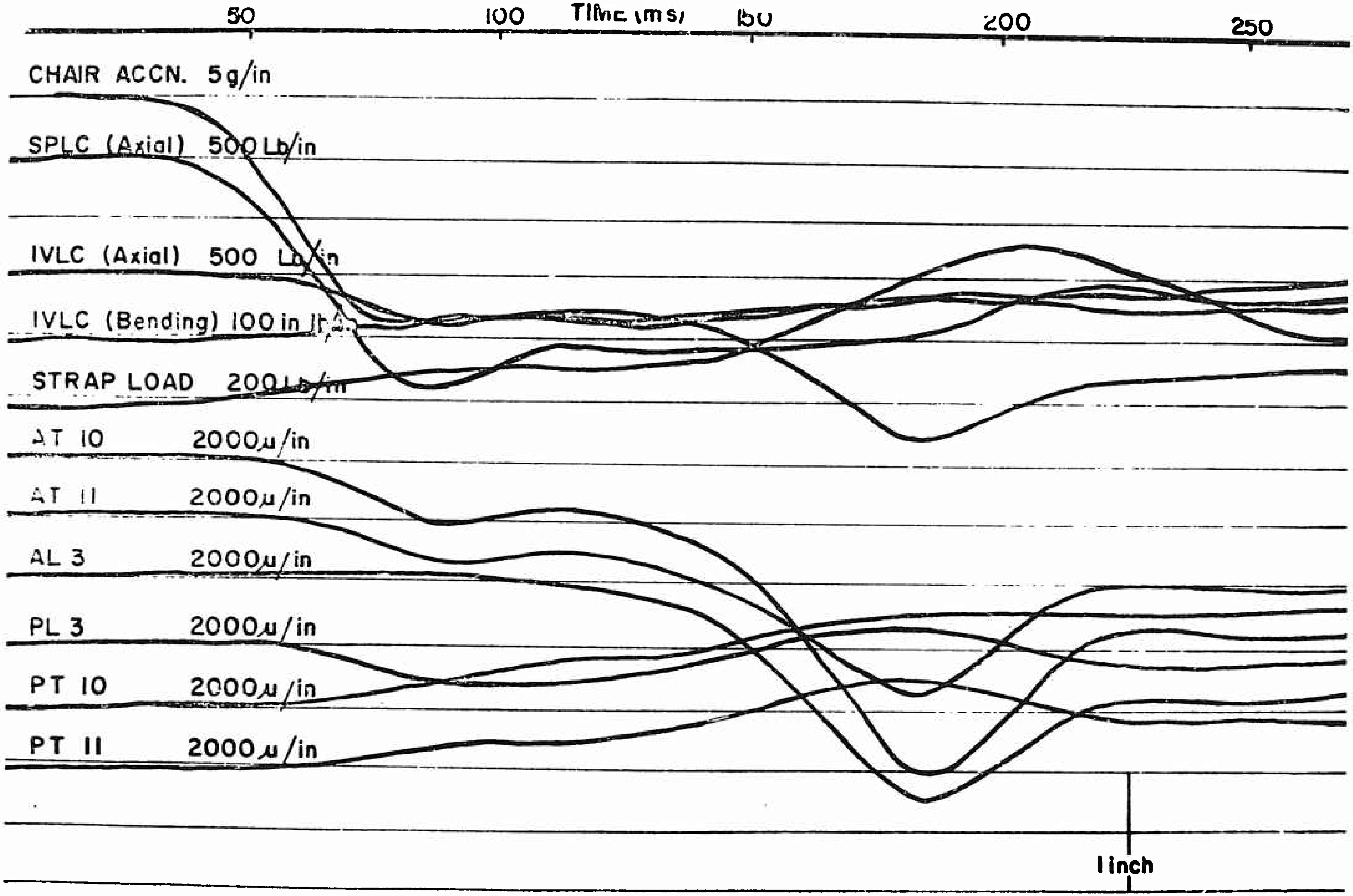

Fig. 4.17. Oscillograph Record of Run 304, Cadaver 2062, Seat-back Angle 0°, Erect Mode

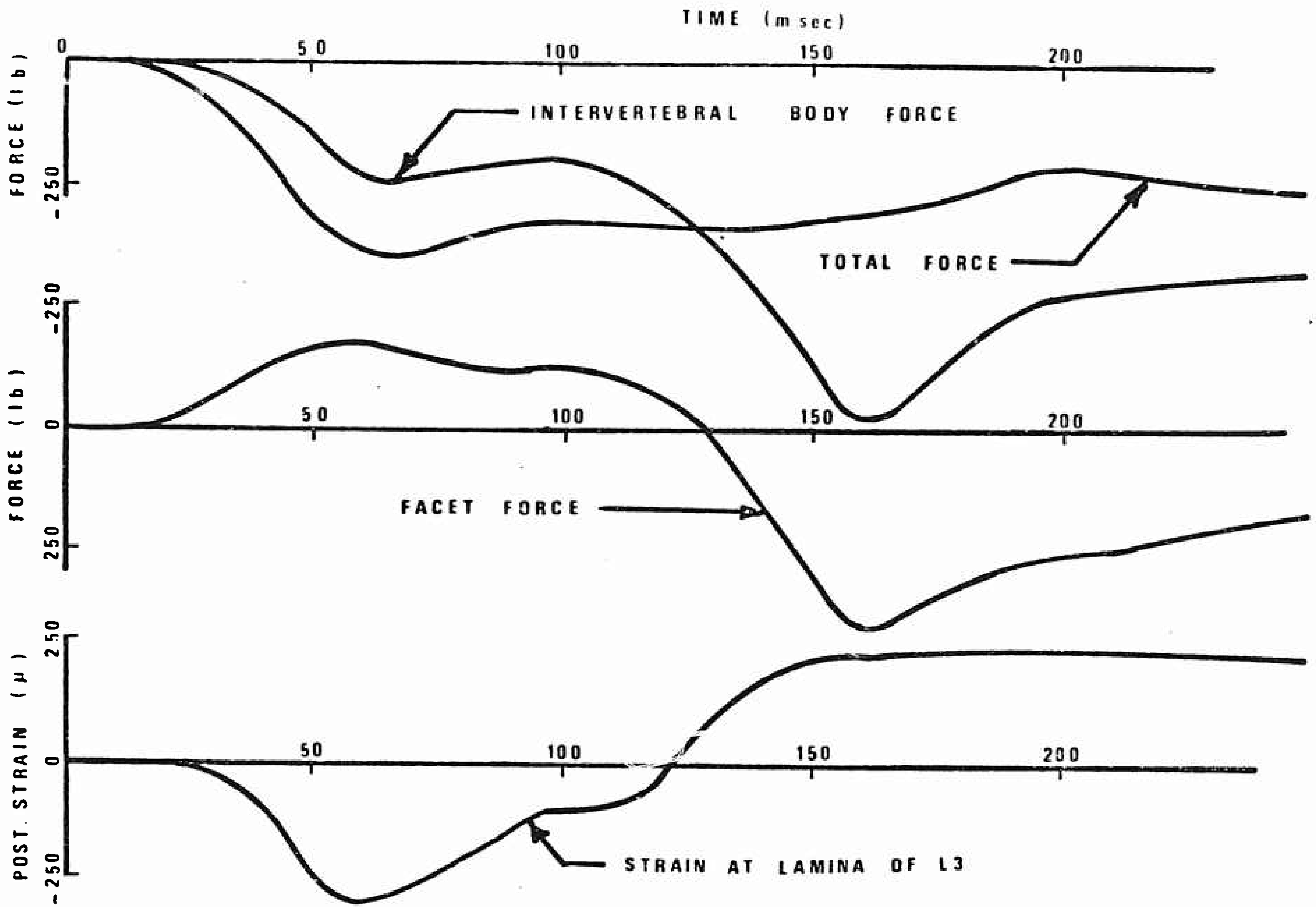

Fig. 4.18. Force, Strain, and Acceleration Data for Run 304, Cadaver 2062, Erect Mode

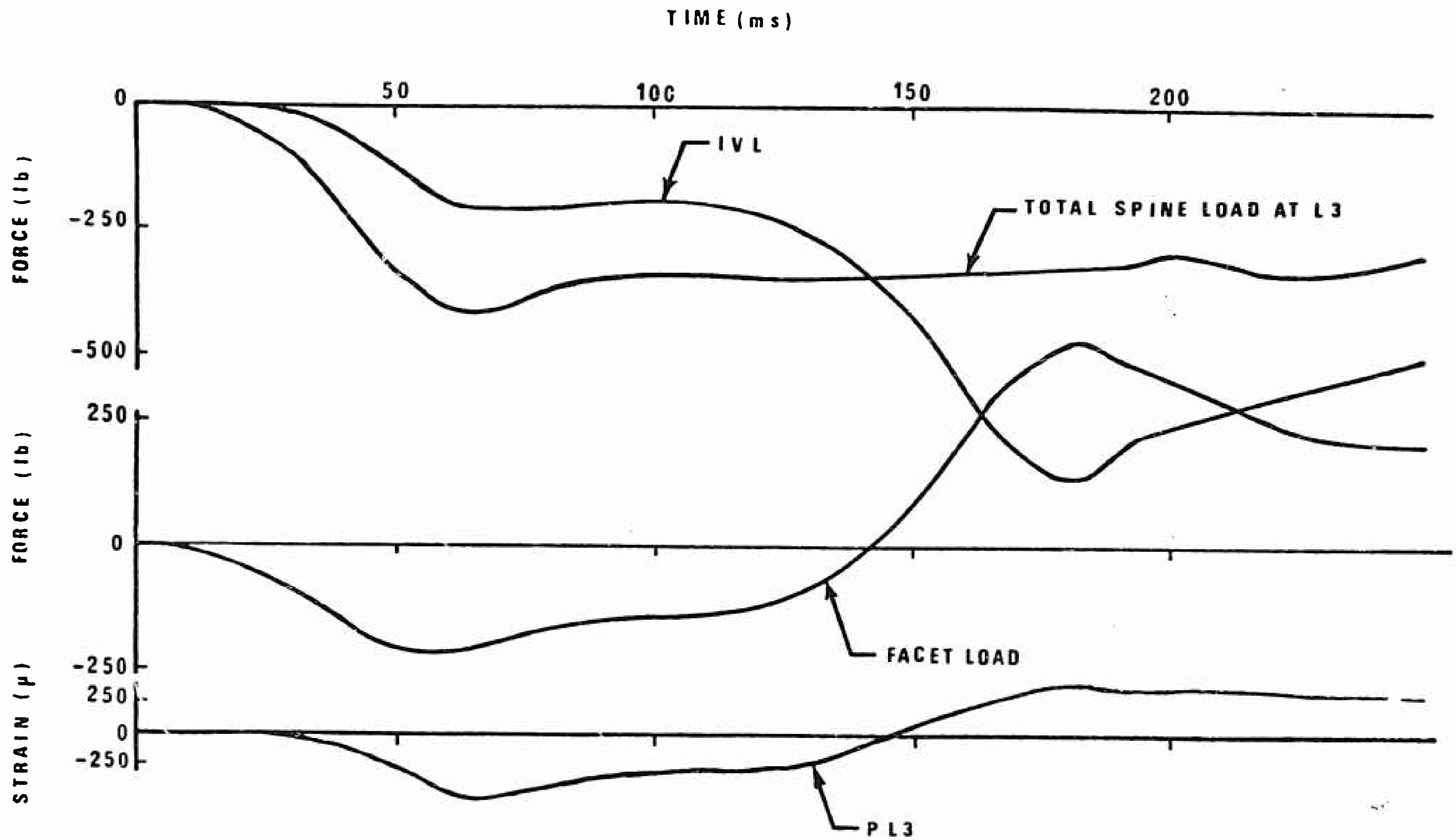

Fig: 4.19. Force, Strain, and Acceleration Data for Run 303, Cadaver 2062, Hyperextended Mode

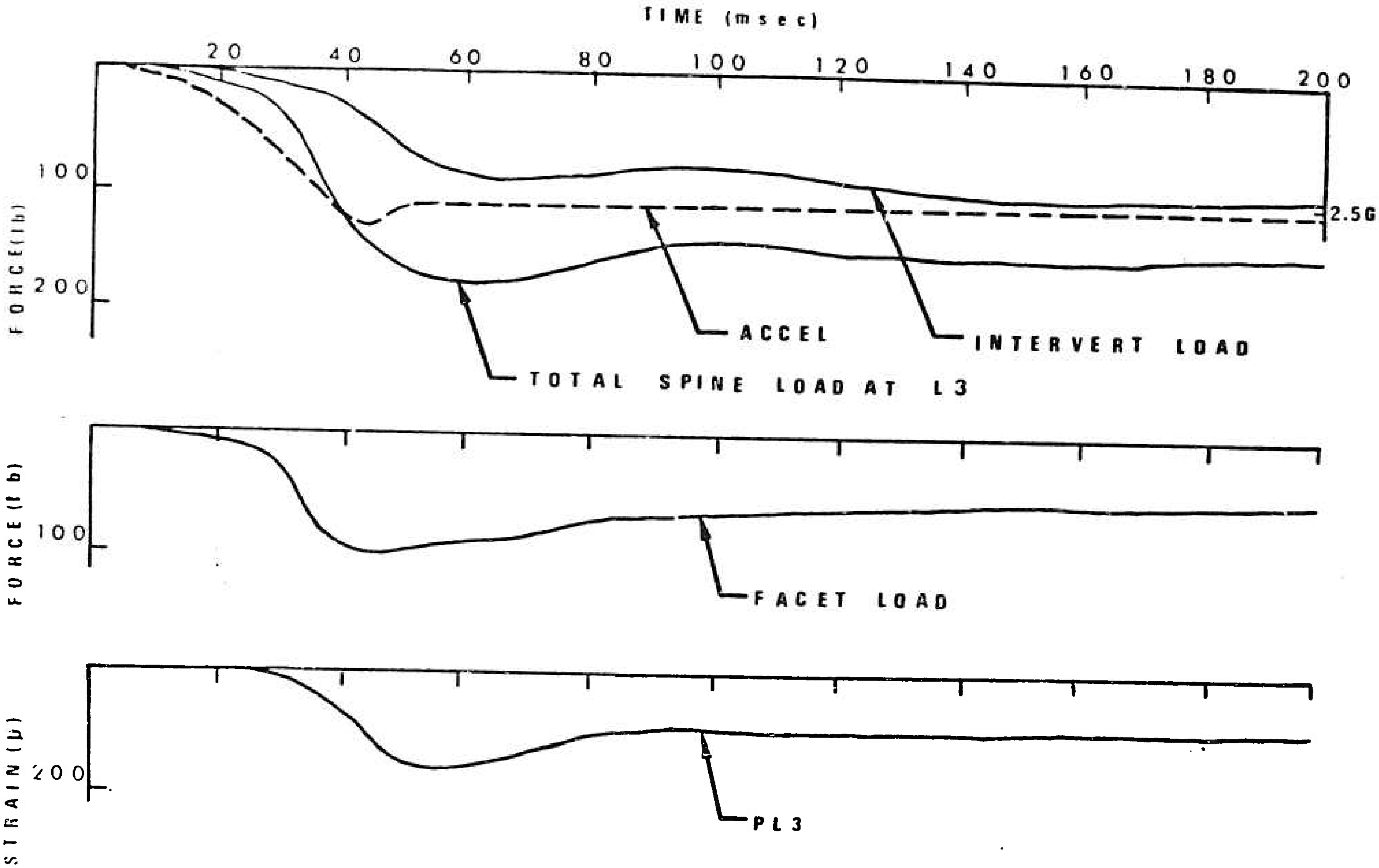

Fig. 4.20. Force, Strain, and Acceleration Data for Run 323, Cadaver 2093, Erect Mode

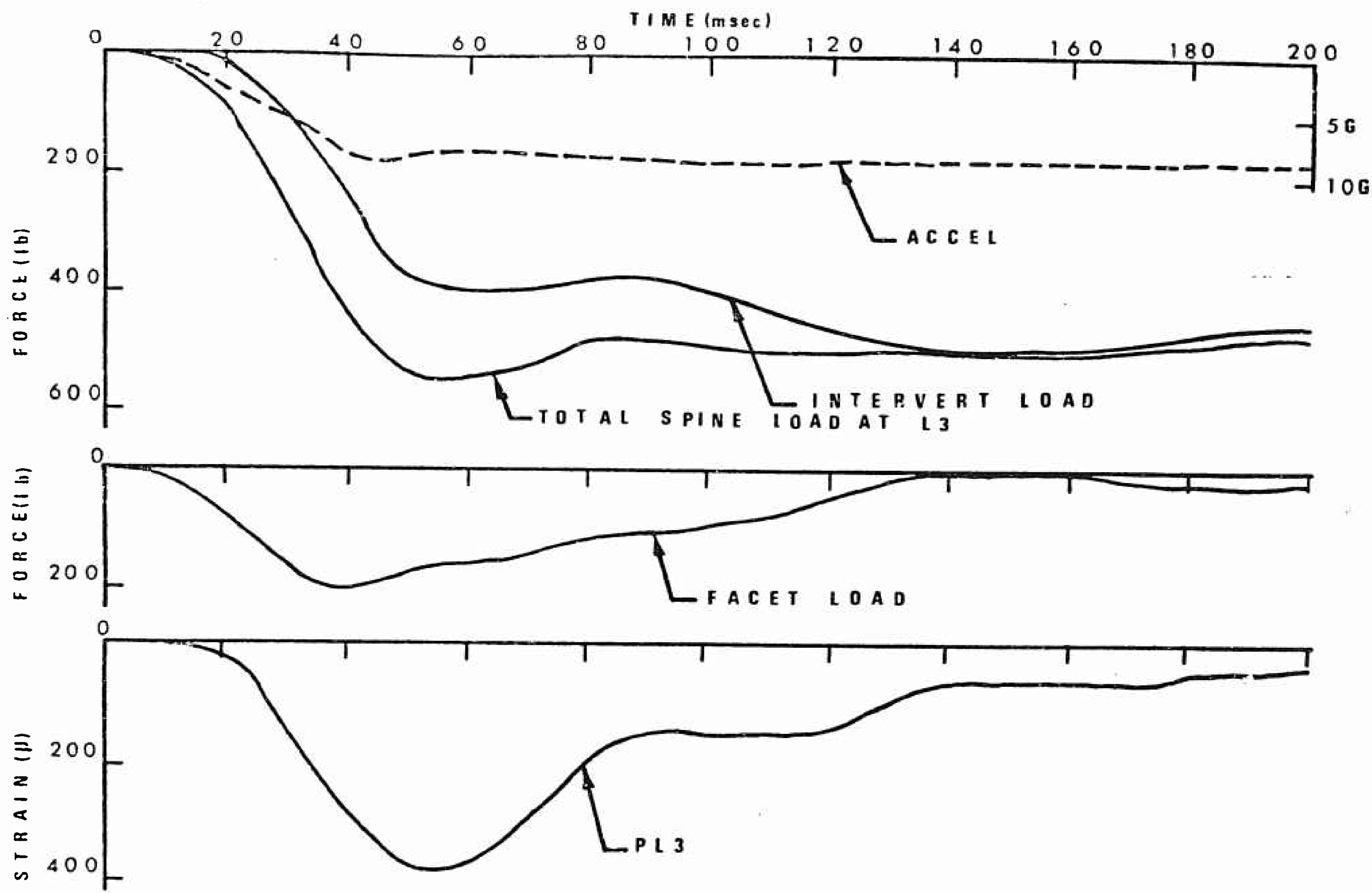

Fig. 4.21. Force, Strain, and Acceleration Data for Run 324, Cadaver 2093, Erect Mode

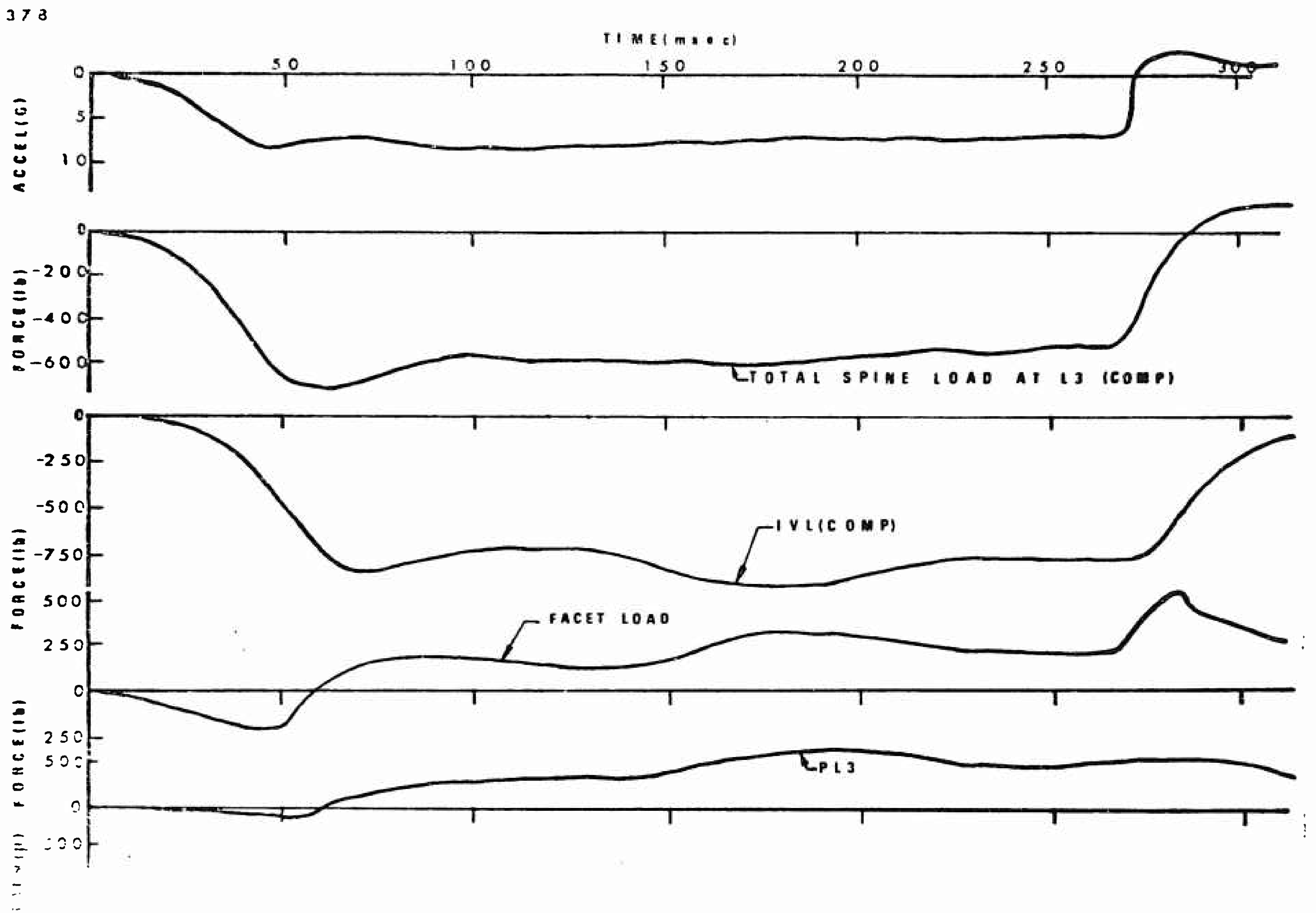

Fig. 4.22. Force, Strain, and Acceleration Data for Run 378, Cadaver 2231, Erect Mode

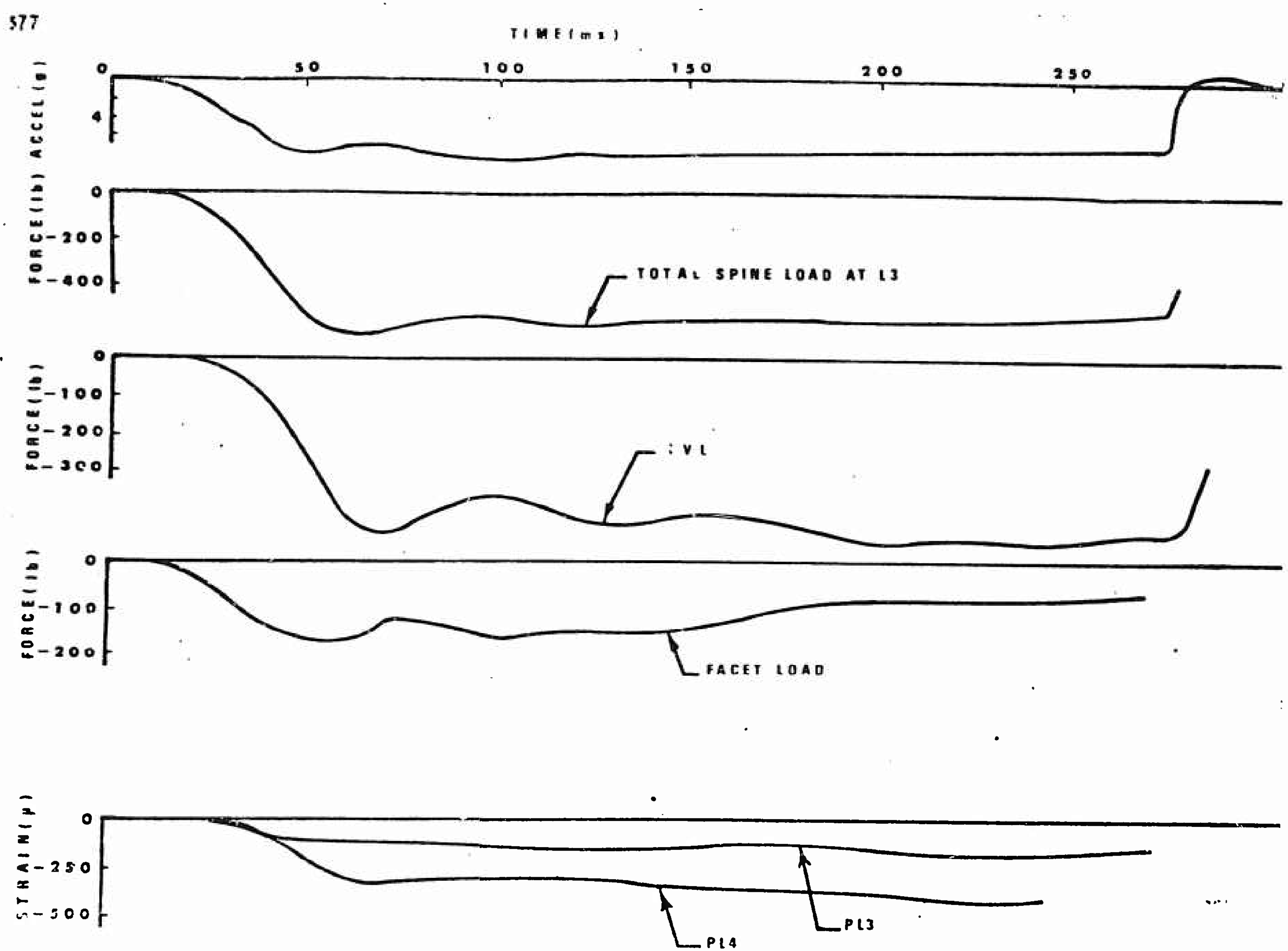

Fig. 4.23. Force, Strain, and Acceleration Data for Run 377, Cadaver 2231, Hyperextended Mode

CHAPTER V

A MATHEMATICAL MODEL FOR THE SPINE

1. Introduction

In an effort to explain vertebral body fractures due to $+ G_z$ acceleration, several mathematical models have been formulated. In recent years two models by Vulcan [21] and Orne [15] have rendered a better understanding of the mechanisms of failure of the human spine. Vulcan considered the effects of forward flexion of the upper torso, the head and neck, the curvature of the spine, and the effects of the restraint system on the spine during $+ G_z$ acceleration. He established the presence of high bending moments in the spine due to the forward eccentricity of the upper torso center of gravity with respect to the centerline of the spine. The bending effect is greatest when the chin contacts the chest and the upper torso reaches the maximum flexion allowed by the restraint systems. An important fact brought out by his experiments and model is the role played by the whipping of the head during the acceleration pulse. In his mathematical model he considers the head and half the neck as one rigid body connected by springs and dampers to another rigid body representing the torso from T1 to L4. The acceleration pulse is applied to L5. This resulted in a four degree-of-freedom model.

Orne proposed a discrete-parameter model consisting of alternately rigid and deformable bodies simulating the behavior of the vertebrae and discs, respectively, the bodies being arranged in such a fashion as to describe the natural curvatures of the spine. The mass of the system is assumed to be concentrated in the rigid bodies, which are capable of three degrees-of-freedom in the sagittal plane of the body. This resulted in a 54 degree-of-freedom model. This model renders the study of stresses at different levels of the spine in greater detail than the Vulcan model. However, the head and the neck are represented by only one rigid link ignoring the whipping effect mentioned above. Another serious shortcoming of this model is the exclusion of any restraint forces, such as the shoulder strap and seat back reaction forces. The resulting response is totally different from that observed experimentally on cadavers or during ejections from aircraft. In his model, although there is flexion of the vertebral column, it is accompanied by a rearward movement of the upper torso, resulting in rearward bending moments at the lumbar vertebrae rather than forward bending moments observed experimentally.

In view of the fact that there exist two load paths in the spine, one through the vertebral body and the other through the lamina via the articular facets, it was decided that the above two models were inadequate to simulate the response of the vertebral column due to $+G_z$ acceleration. Hence, a two dimensional discrete-parameter mathematical model of the spine was formulated with the following requirements:

(i) The model should predict the amount of forward flexion of the spine.

(ii) It should account for the natural curvatures of the spine.

(iii) It should account for the eccentric inertial loading on the spine.

(iv) It should predict head and neck motions and their effects on the forces and moments in the spine.

(v) The load transmission at each vertebral level has to take place through the vertebral body and the articular facets, thus incorporating a parallel load path with the vertebral body - a factor not considered in any of the existing mathematical models.

(vi) The effects of the restraint and support systems must be incorporated to properly simulate the ejection problem.

(vii) The model should be able to simulate off-axis impacts in the mid-sagittal plane and predict the response due to any input pulse.

2. Development of the Model

Considering the requirements of the model stated in the preceding section, the following assumptions were made in the mathematical development:

(i) The 24 vertebral bodies, the head and the pelvis are rigid bodies constrained to move in the mid-sagittal plane.

(ii) Each rigid body has three degrees-of-freedom in the mid-sagittal plane, two translational and one rotational.

(iii) The intervertebral discs are massless and deformation of the spine takes place at the discs.

(iv) The discs are replaced by a system of springs and dampers - one spring and damper for axial forces, one spring and damper for shear forces and another spring and damper arrangement for restoring torques due to relative angular motion between adjacent vertebral bodies.

(v) The facets and laminae are springs connected to the vertebral body by a massless rigid rod.

(vi) Each rigid body is assumed to carry a portion of the torso weight which is eccentric with respect to the centerline of the spine.

(vii) The rigid bodies are arranged to simulate the spinal curvatures as closely as possible.

3. Kinematic Preliminaries

Figure 5.1 shows the initial configuration of two successive links (the vertebrae) and a deformable link (the disc). It has been assumed that the axis of any disc is coincident with the axis of the vertebra immediately below it in the initial configuration for the erect mode as shown in Figure 5.1. Also it is assumed that the disc is of uniform thickness, which is not necessarily true. The two vertebrae are shown as trapezoids to simulate the change of curvature of the spine. This is a valid assumption because it has been observed that in the lumbar region the vertebral bodies are wedged posteriorly, whereas in the thoracic level they are wedged anteriorly. The position in the mid-sagittal plane of the center of the i^{th} rigid link (vertebral body) is determined by the three generalized coordinates u_i, w_i and θ_i as shown in Figure 5.1.

At time t (t > 0), the configuration of two successive rigid links is shown in Figure 5.2. The links have undergone translations and rotations causing axial, shear and rotational deformations of the discs. The chord length AB_i of the disc is determined by the generalized coordinates u_i, w_i, and θ_i of the centers of the rigid links. The calculations necessary for computing the deformation of the discs follows in the order used in the computer program.

Deformation of the disc:

From Figure 5.2

$$x_1 = (u_i + d_i \sin \theta_i) - (u_{i-1} - d_{i-1} \sin \theta_{i-1}) \qquad (1)$$

$$x_2 = (w_i - d_i \cos \theta_i) - (w_{i-1} + d_{i-1} \cos \theta_{i-1}) \qquad (2)$$

$$AB_i = \overline{x_1^2 + x_2^2} \qquad (3)$$

and $$\alpha_i = \tan^{-1} x_2/x_1 \qquad (4)$$

$$AC_i = AB_i \sin(\alpha_i - \theta_{i-1}) \tag{5}$$

and

$$BC_i = AB_i \cos(\alpha_i - \theta_{i-1}) \tag{6}$$

The lengths AC and BC will be used as the criterion for the development of forces on the vertebral bodies. Hence, at time t = 0, AC will be denoted by AC_o and BC by BC_o.

The time rate of change of AC and BC have to be found to generate viscous forces. For this, we have to first compute the rate of change of AB and the angle α. The time derivatives will be referred to by $\dot{AB}$, $\dot{\alpha}$, $\dot{AC}$, and $\dot{BC}$, etc.

Differentiating Equation (3) with respect to time, we get

$$\begin{aligned} \dot{AB}_i &= \frac{1}{2} \cdot \frac{1}{\sqrt{x_1^{\,2} + x_2^{\,2}}} \cdot (2x_1 \dot{x}_1 + 2x_2 \dot{x}_2) \\ &= \dot{x}_1 \cos \alpha_i + \dot{x}_2 \sin \alpha_i \end{aligned} \tag{7}$$

where $\dot{x}_1$ and $\dot{x}_2$, obtained by differentiating equations (1) and (2), are

$$\dot{x}_1 = (\dot{u}_i + d_i \dot{\theta}_i \cos \theta_i) - (\dot{u}_{i-1} - d_{i-1} \dot{\theta}_{i-1} \cos \theta_{i-1})$$

and

$$\dot{x}_2 = (\dot{w}_i + d_i \dot{\theta}_i \sin \theta_i) - (\dot{w}_{i-1} - d_{i-1} \dot{\theta}_{i-1} \sin \theta_{i-1})$$

$\dot{\alpha}_i$ can be obtained by differentiating (4), but a simpler equation is obtained if we consider Figure 5.3.

In this figure if v_{at} denotes the tangential velocity of BA,

$$v_{at} = AB_i \dot{\alpha}_i$$

but,

$$v_{at} = \dot{x}_2 \cos \alpha_i - \dot{x}_1 \sin \alpha_i$$

$$\dot{\alpha}_i = (\dot{x}_2 \cos \alpha_i - \dot{x}_1 \sin \alpha_i)/AB_i \tag{8}$$

Differentiating (5) and (6) we get

$$\dot{AC}_i = \dot{AB}_i \sin (\alpha_i - \theta_{i-1}) + AB_i \cos (\alpha_i - \theta_{i-1})(\dot{\alpha}_i - \dot{\theta}_{i-1})$$

and

$$\dot{BC}_i = \dot{AB}_i \cos (\alpha_i - \theta_{i-1}) - AB_i \sin (\alpha_i - \theta_{i-1})(\dot{\alpha}_i - \dot{\theta}_{i-1}) \tag{9}$$

<u>Geometry of the facets</u>:

From Figure 5.2

$$y_1 = (u_i - h_i \cos \theta_i) - (u_{i-1} - h_{i-1} \cos \theta_{i-1})$$

$$y_2 = (w_i - h_i \sin \theta_i) - (w_{i-1} - h_{i-1} \sin \theta_{i-1})$$

$$A'B'_i = \sqrt{y_1^2 + y_2^2} \tag{10}$$

and

$$\phi_i = \tan^{-1} y_2/y_1 \tag{11}$$

$$A_1A_{2i} = A'B'_i \sin (\phi_i - \theta_{i-1}) \tag{12}$$

$$A_2A_{3i} = A'B'_i \cos (\phi_i - \theta_{i-1}) \tag{13}$$

4. Forces Developed in the Disc

The initial configuration of the disc is shown in Figure 5.4 where AB is the centerline of the disc. After deformation the neutral axis AB takes the shape shown in Figure 5.5. The forces and restoring torque developed on the disc are assumed to be functions of the change in lengths AC, BC and angular deformation. The forces acting on the $i^{\underline{th}}$ disc are shown in Figure 5.6. The axial force, $T7Y_i$, is given by

$$T7Y_i = XK_i(AC_i - AC_{oi}) + C_i \, \dot{AC}_i \tag{14}$$

The shear force, $T7X_i$, is given by

$$T7X_i = XK_{si}(BC_i - BC_{oi}) + C_{si} \, \dot{BC}_i \tag{15}$$

The restoring torque B_i, is given by

$$B_i = XKT_i \{(\theta_i - \theta_{oi}) - (\theta_{i-1} - \theta_{oi-1})\} + C_{ti}(\dot{\theta}_i - \dot{\theta}_{i-1}) \tag{16}$$

where

XK_i = stiffness of the axial spring

XK_{si} = stiffness of the shear spring

C_i = damping in axial loading

C_{si} = damping in shear loading

XKT_i = stiffness of restoring torque spring

C_{ti} = damping of restoring torque spring

We have to note that the disc has not been modelled as a beam although the above method is very close to one. The disc has been replaced by a system of springs that behave in the above manner.

The reaction of the $i^{\underline{th}}$ and the $i + i^{\underline{th}}$ discs on the $i^{\underline{th}}$ vertebral body are shown in Figure 5.7 where $T6Y_i$, $T6X_i$ and B_{i+1} are the reactions of the $i + i^{\underline{th}}$ disc on the $i^{\underline{th}}$ vertebral body and $T7X_i$, $T7Y_i$ and B_i are the reactions of the $i^{\underline{th}}$ disc on the $i^{\underline{th}}$ vertebral body. Mathematically they are given by the following equations:

$$T6Y_i = XK_{i+1}(AC_{i+1} - AC_{oi+1}) + C_{i+1}\dot{AC}_{i+1} \tag{17}$$

$$T6X_i = XK_{si+1}(BC_{i+1} - BC_{oi+1}) + C_{si+1}\dot{BC}_{i+1} \tag{18}$$

$$B_{i+1} = XKT_{i+1}\{(\theta_{i+1} - \theta_{oi+1}) - (\theta_i - \theta_{oi})\} + C_{ti+1}(\dot{\theta}_{i+1} - \dot{\theta}_i) \tag{19}$$

and $T7Y_i$, $T7X_i$ and B_i are from Equations (14) - (16).

5. Forces Developed at the Facets

The articular facets have been modelled by two springs, one limiting rotation and the other limiting the sliding of one vertebra over the adjacent ones.

The force resisting relative rotation between the $i^{\underline{th}}$ and the $i\text{-}1^{\underline{th}}$ vertebrae in the erect mode is given by

$$T = XKh_i \times h_i \times \sin\{(\theta_{i-1} - \theta_{oi-1}) - (\theta_i - \theta_{oi})\} \tag{20}$$

acting at a distance h_i from the center of the vertebral body in a direction parallel to the longitudinal axis of the vertebral body, where

h_i = the distance of the articular facets from the center of the vertebral body

XKh_i = stiffness of the spring resisting the relative rotation

In the hyperextended mode, due to the forced change in curvature of the spine, it is assumed that the facets have "bottomed out" and hence the lamina acts as another beam parallel to the disc. The change in length A_1A_2 is used as the measure of axial deformation of this beam, and the force developed is given by

$$T_{51} = XKh_i \times (A_1A_{2i} - A_1A_{20i}) \qquad (20a)$$

where

A_1A_2 = length at time $t > 0$

and A_1A_{20} = length at time $t = 0$

The force resisting sliding motion at the facets between the i^{th} and the $i\text{-}1^{th}$ vertebrae is given by

$$F_{x1} = XKh_i \times (A_2A_{3i} - A_2A_{30i}) \qquad (21)$$

Due to the overlapping nature of the articular facets it is difficult to define the point of application of the above force. However, in the model, it has been assumed that this force acts perpendicular to the longitudinal axis of the vertebral body at a point ($d_i + AC_i/2$) below the center of the vertebral body. The reaction of this force on the vertebra immediately below acts at a distance d_{i-1} above the center of the $i-1^{\underline{th}}$ vertebra. This assumption is justified because the superior articular facets are shorter than the lamina and the inferior articular facets.

With the above forces developed in the spine we can now draw a free body diagram of the $i^{\underline{th}}$ vertebra, (Fig. 5.8). This diagram does not include the seat back reaction force, shoulder strap or lap belt forces and the chin-chest contact force because these forces act only on selected vertebrae and are described in the section on auxiliary equations.

6. Auxiliary Equations

(i) Shoulder strap force:

The exact model of the shoulder strap is not possible since no data is available regarding the distribution of this force via the rib cage to the spine. The model has the capability of distributing this force to various levels of the spine, however in the present study, the development of the shoulder strap force is based on the movement of T1 and the entire force is transmitted to that vertebra. The shoulder strap force in the model is also assumed to exert a restoring moment on T1 to restrict its rotation. This is a valid assumption due to the friction generated between the belt and the shoulders. The shoulder strap is considered to have a soft spring for the first three inches of deformation, after which the stiffness of the spring increases six times. This allows for the initial compression of soft tissues and also for an initial "hunching" described by Vulcan [21] and observed in high speed movies of the experiments.

The forces developed in the shoulder strap are given by the following equations:

The initial length of the shoulder strap is given by

$$\ell_{io} = u_{oi}$$

where u_{oi} is the distance of the center of T_1 from the seat back.

The length of the strap at time $t > 0$ is given by

$$\ell_i = \sqrt{(w_{oi} - w_i)^2 + u_i^2}$$

where w_{oi} = initial height of T1 from the seat pan

and w_i = height of T1 from the seat pan at $t > 0$.

The force generated in the strap is now given by

$$T4 = XKS_i(\ell_i - \ell_{oi}) \tag{22}$$

This force is set to zero if $\ell_i < \ell_{oi}$ or if $u_i < u_{oi}$ signifying that T1 has moved towards the seat back.

(ii) Lap belt force:

The lap belt force is generated when the pelvis, the first rigid link in the model, moves away from the seat back. One end of the lap belt is assumed to be fixed at the intersection of the seat back and the seat pan while the other end is attached to the center of the first link. Hence, the lap belt generates a vertical and horizontal force at the pelvis given by

$$\text{strapu} = XKS_1 \times \left(\sqrt{u_1^2 + w_1^2} - \sqrt{u_{1o}^2 + w_{1o}^2}\right) \times \cos(\tan^{-1} w_1/u_1) \tag{23}$$

where

strapu = horizontal component of lap belt force

XKS_1 = stiffness of lap belt

u_1 = distance of the center of pelvis from seat back

w_1 = distance of the center of pelvis from seat pan

u_{1o} = distance of the center of pelvis from seat back at $t = 0$

w_{1o} = distance of the center of pelvis from seat pan at $t = 0$

and

$$\text{strapw} = XKS_1 \times \left(\sqrt{u_1^2 + w_1^2} - \sqrt{u_{1o}^2 + w_{1o}^2}\right) \times \sin(\tan^{-1} w_1/u_1)$$

where strapw = vertical component of lap belt force.

(iii) Seat back reaction:

The seat back reaction force is generated when any link makes contact with the seat back. From the x-rays taken before the experimental runs we can determine the vertebrae that are in contact with the seat back. Hence, if during the run, these vertebrae tend to move towards the seat back, a reaction force is generated on the vertebrae involved. For the vertebrae not in contact with the seat back initially, distances are specified for motion towards the seat back without any seat back reaction. If the movement of a vertebra is beyond the distance specified, a seat back reaction force is generated to stop the vertebra. Hence,

$$\begin{aligned} XSF &= XKSB \times (h_i + F\ell p - u_i) \qquad && u_i < h_i + F\ell p \\ &= 0 && u_i > h_i + F\ell p \end{aligned} \tag{24}$$

where

XSF = seat back reaction force on the i^{th} vertebra

h_i = distance of articular facet from the center of the vertebra

$F\ell p$ = distance allowed to move before contacting the seat back

XKSB = stiffness of the seat back

(iv) Chin-chest contact force:

The rotation of the head relative to the torso is impeded when the chin contacts the chest. A chin-chest contact force is generated to stop further rotation of the head relative to the torso. The relative angle between the head and the torso for the chin-chest contact varies from one spine to another and is determined from movies. In the model, the criterion for chin-chest contact was chosen to be relative angle between T1 and the head. Hence, if θ_{T1} is the angle moved by T1 and θ_h is the angle moved by the head, the relative angular movement of the head and T1 is given by

$$Rdisp = \theta_h - \theta_{T1}$$

and the chin-chest contact force is given by

$$HC = Ch_1 \times (Rdisp - OCH1) \qquad (25)$$

where Ch_1 = spring constant lbs/rad

and OCh_1 = relative angular movement between head and chest without contact

Ch_1 is considered to be constant for .2 radians and is increased three times for relative rotation greater than .2 radians. Hence, essentially we have a bilinear spring, the initial part being soft to simulate the soft tissue compression. It should be mentioned here that no experimental determination of the chin-chest contact force has been made, hence the constant Ch_1 is selected arbitrarily to stop the head in the model based on the observed angular rotations by Vulcan [21].

The reaction force, HC, is assumed to act at a distance 1.5" from the center of gravity of the head parallel to the S-I axis of the head. An equal and opposite reaction force is exerted on T1.

(v) Reaction from the hyperextension block:

The hyperextension block is placed opposite L1 and covers T12 and L2. Hence in the hyperextension mode a seat back reaction is generated at T12, L1 and L2 similar to that given in section (iii). The stiffness of the block has been assumed to be the same as that of the seat back.

7. Equations of Motion

A free body diagram of the $i^{\underline{th}}$ vertebrae is shown in Figure 5.8. For the sake of clarity, the auxiliary forces described in section 6 have been omitted but they have been utilized in the computer program.

Resolving the forces on the $i^{\underline{th}}$ vertebra parallel to u_i and w_i axis, we get:

$$\begin{aligned} \Sigma F_{ui} = {} & (T6X_i+FX2-FX1)\cos\theta_i - (T6Y_i+T52-T51)\sin\theta_i \\ & - T7X_i \cos\{\theta_i - (\theta_{oi}-\theta_{oi-1})\} \\ & + T7Y_i \sin\{\theta_i - (\theta_{oi}-\theta_{oi-1})\} \end{aligned} \tag{26}$$

$$\Sigma F_{wi} = (T6Y_i + T52 - T51) \cos \theta_i + (T6X_i + FX2 - FX1) \sin \theta_i$$
$$- T7Y_i \cos\{\theta_i - (\theta_{oi} - \theta_{oi-1})\}$$
$$- T7X_i \sin\{\theta_i - (\theta_{oi} - \theta_{oi-1})\} \qquad (27)$$

Taking the sum of moments about the center of gravity,

$$\Sigma M_{Gi} = T7Y_i \cos\{\theta_{oi} - \theta_{oi-1}\}\, e_i + B_{i+1} - T6Y_i \cdot e_i$$
$$- T6X_i \cdot d_i - T7Y_i \sin(\theta_{oi} - \theta_{oi-1})\, d_i$$
$$- T7X_i \cos\{\theta_{oi} - \theta_{oi-1}\}\, d_i$$
$$- T7X_i \sin\{\theta_{oi} - \theta_{oi-1}\}\, e_i - B_i$$
$$+ (T51 - T52)(e_i + h_i) - FX2 \cdot d_i$$
$$- FX1(d_i + AC_i/2) \qquad (28)$$

The auxiliary forces and moments are added to the above if applicable to the vertebra in consideration.

Now, acceleration of the center of gravity is given by

$$\underset{\sim}{a}_g = \ddot{X}\, \underset{\sim}{I} + \ddot{Y}\, \underset{\sim}{J} + \ddot{u}_i\, \underset{\sim}{I} + \ddot{w}_i\, \underset{\sim}{J} + e_i\, \ddot{\theta}_i \cos \theta_i\, \underset{\sim}{J}$$
$$- e_i\, \dot{\theta}_i^2 \cos \theta_i\, \underset{\sim}{I} - e_i\, \ddot{\theta}_i \sin \theta_i\, \underset{\sim}{I}$$
$$- e_i\, \dot{\theta}_i^2 \sin \theta_i\, \underset{\sim}{J}$$
$$= \{\ddot{X} + \ddot{u}_i - e_i\, \dot{\theta}_i^2 \cos \theta_i - e_i\, \ddot{\theta}_i \sin \theta_i\}\, \underset{\sim}{I}$$
$$+ \{\ddot{Y} + \ddot{w}_i + e_i\, \ddot{\theta}_i \cos \theta_i - e_i\, \dot{\theta}_i^2 \sin \theta_i\}\, \underset{\sim}{J} \qquad (29)$$

where $\underset{\sim}{I}$ and $\underset{\sim}{J}$ are unit vectors parallel to the u_i and w_i axes, and $\ddot{X}$ and $\ddot{Y}$ are the horizontal and vertical acceleration of the sled.

Using Newton's laws of motion:

$$\Sigma F_{ui} = m_i\{\ddot{X} + \ddot{u}_i - e_i\,\dot{\theta}_i^{\,2}\cos\theta_i - e_i\,\ddot{\theta}_i\sin\theta_i\} \qquad (30)$$

$$\Sigma F_{wi} = m_i\{\ddot{Y} + \ddot{w}_i + e_i\,\ddot{\theta}_i\cos\theta_i - e_i\,\dot{\theta}_i^{\,2}\sin\theta_i\} \qquad (31)$$

$$\Sigma M_{Gi} = I_G\,\ddot{\theta}_i \qquad (32)$$

where m_i is the mass supported by the $i^{\underline{th}}$ body and I_G is the polar moment of inertia about the center of gravity.

8. Solution of the Equations of Motion

Equations 30-32 are non-linear, second order differential equations. For each body we have three such equations, hence there are a total of 78 equations to be solved simultaneously for i = 1-26. This is achieved by using an IBM supplied numerical technique on an IBM 360 digital computer. The method used is known as Hamming's Predictor Corrector method. To use the above routine, we have to reduce each second order differential equation to two first order differential equations. Hence, we now have a total of 156 first order differential equations to be solved simultaneously with given initial conditions, i.e., u_{oi}, w_{oi}, θ_{oi}, $\dot{u}_{oi}$, $\dot{w}_{oi}$, $\dot{\theta}_{oi}$. The accelerations $\ddot{x}$ and $\ddot{y}$ are input parameters corresponding to the sled acceleration in the x and y directions.

To integrate numerically using the above method, we have to have the highest order derivative on the left hand side of the equation. Hence, we have from Equations (30-32)

$$\ddot{\theta}_i = \Sigma M_{Gi}/I_{Gi} \tag{33}$$

$$\ddot{u}_i = \frac{\Sigma F_{ui}}{m_i} + e_i \dot{\theta}_i^2 \cos \theta_i + e_i \ddot{\theta}_i \sin \theta_i - \ddot{X} \tag{34}$$

$$\ddot{w}_i = \frac{\Sigma F_{wi}}{m_i} + e_i \dot{\theta}_i^2 \sin \theta_i - e_i \ddot{\theta}_i \cos \theta_i - \ddot{Y} \tag{35}$$

9. Choice of Parameters

(i) Geometry of the spine:

The model requires the initial coordinates of the center of each vertebral body, the length, the angle the longitudinal axis of the vertebra makes with the vertical, the distance of the articular facets from the center of the vertebral body and the thickness of the disc coincident with each vertebral body. These measurements were made with the help of x-rays taken before each run with the cadaver placed in the accelerator. It should be noted that the trapezoidal shape of the vertebral bodies is an idealization in the model, since in many spines the intervertebral discs are wedge shaped, especially at L5. However, the curvature of the spine has been simulated by making the rigid links trapezoidal.

(ii) Mass and moment of inertia of each rigid link:

The model requires the distribution of the mass of the whole body to the rigid links. Liu et al. [10] have estimated the mass distribution of segmented cadaveric trunks. The mass distribution used in the model is consistent with their data. The three different cadavers used were weighed before the experiment. After the experiments the torso was cut at the level of L3 and the two halves were weighed again to give the total mass above L3. Three further segments were made of the upper torso - the first consisting of L3 to T8, the second from T8 to C7 and the third from C7 to the head. The three segments were weighed again, their centers of gravity were determined using a load platform which utilizes three load-cells at fixed distances from one another. A trifilar pendulum was used to determine the moment of inertia of these segments. Based on the above measured data the mass and moment of inertia at the various vertebral levels were estimated. The mass of the arms were assumed to be distributed to the first five thoracic vertebrae.

(iii) Physical constants:

Each rigid link in the model is associated with a disc requiring three spring constants and facets requiring two spring constants. Hence, a total of 130 spring constants are required for the model. Theoretically all 130 constants can be different and in an ideal situation they have to be experimentally determined for each specimen. Very little data is available in the literature, and in the case of the articular facets nothing is available. Vulcan [21] has measured the stiffness in compression of the lumbar and the lower thoracic vertebrae. Markolf [11] has measured the axial stiffness of discs from L4 to T8 and has found values ranging from 7000 lbs/in in the lumbar region to 19000 lbs/in in the thoracic region. No data is available for the upper thoracic level. Markolf also gives the rotational stiffness of discs from 700 in-lb/rad to 2400 in-lb/rad. However, these measurements were made with no pre-load and at very small deflections. Most biological materials possess a sigmoidal load-deflection characteristic - i.e., the stiffness increases with increasing loads. Hence, the above values for rotational stiffness of the discs appear to be much too low for our application. Hence, in the lumbar region a rotational stiffness of 6000 in-lb/rad was assumed. In the thoracic region the rib cage imparts more rigidity to the spine, hence a rotational stiffness of 12000 in-lb/rad was assumed. In the cervical region a rotational stiffness of 2400 in-lb/rad was assumed based on the values given by Vulcan.

The constants used in the model are shown in the Appendix on input data to the model.

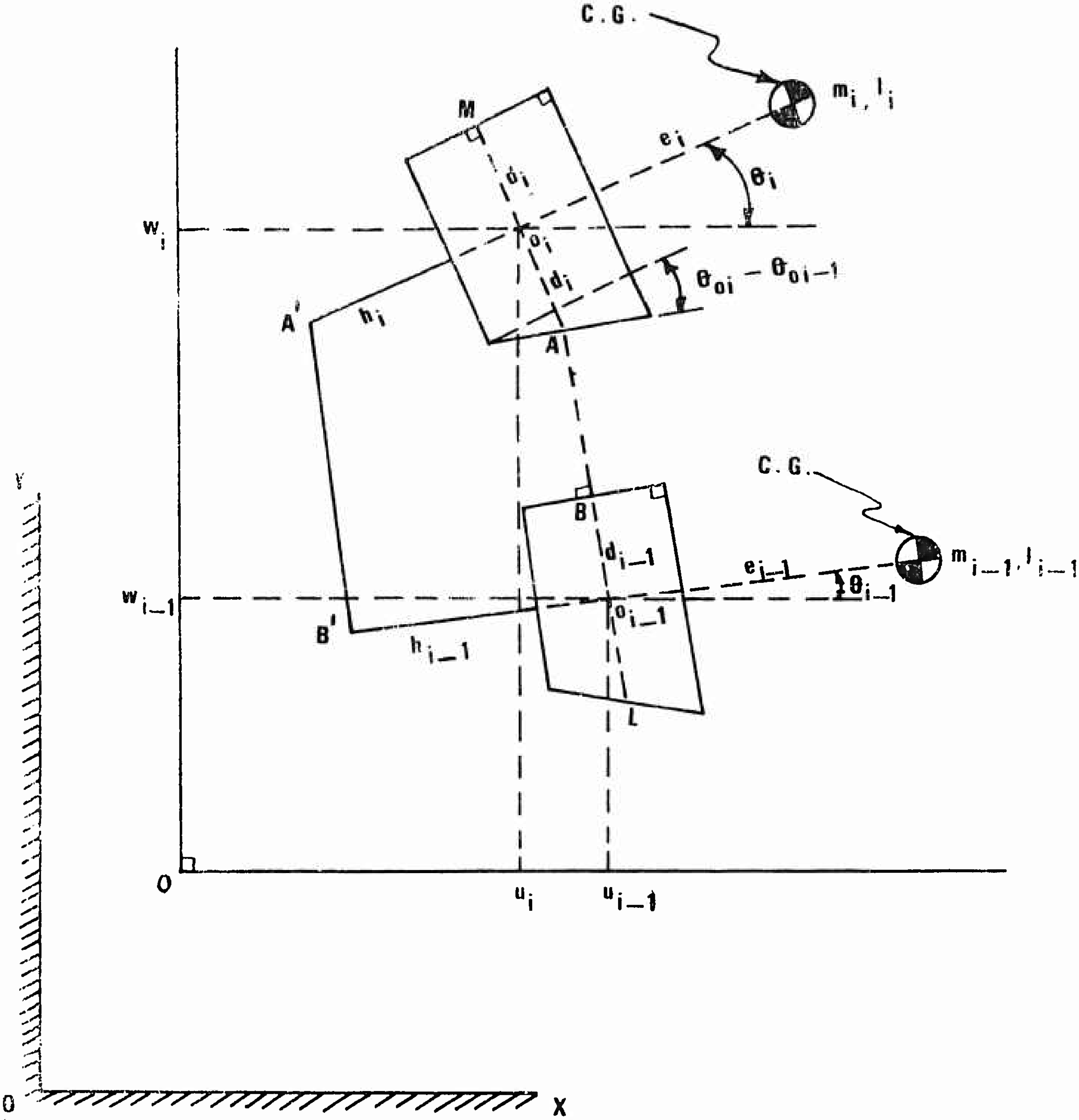

Fig. 5.1. Initial Configuration of Two Successive Vertebrae and Intervertebral Disc

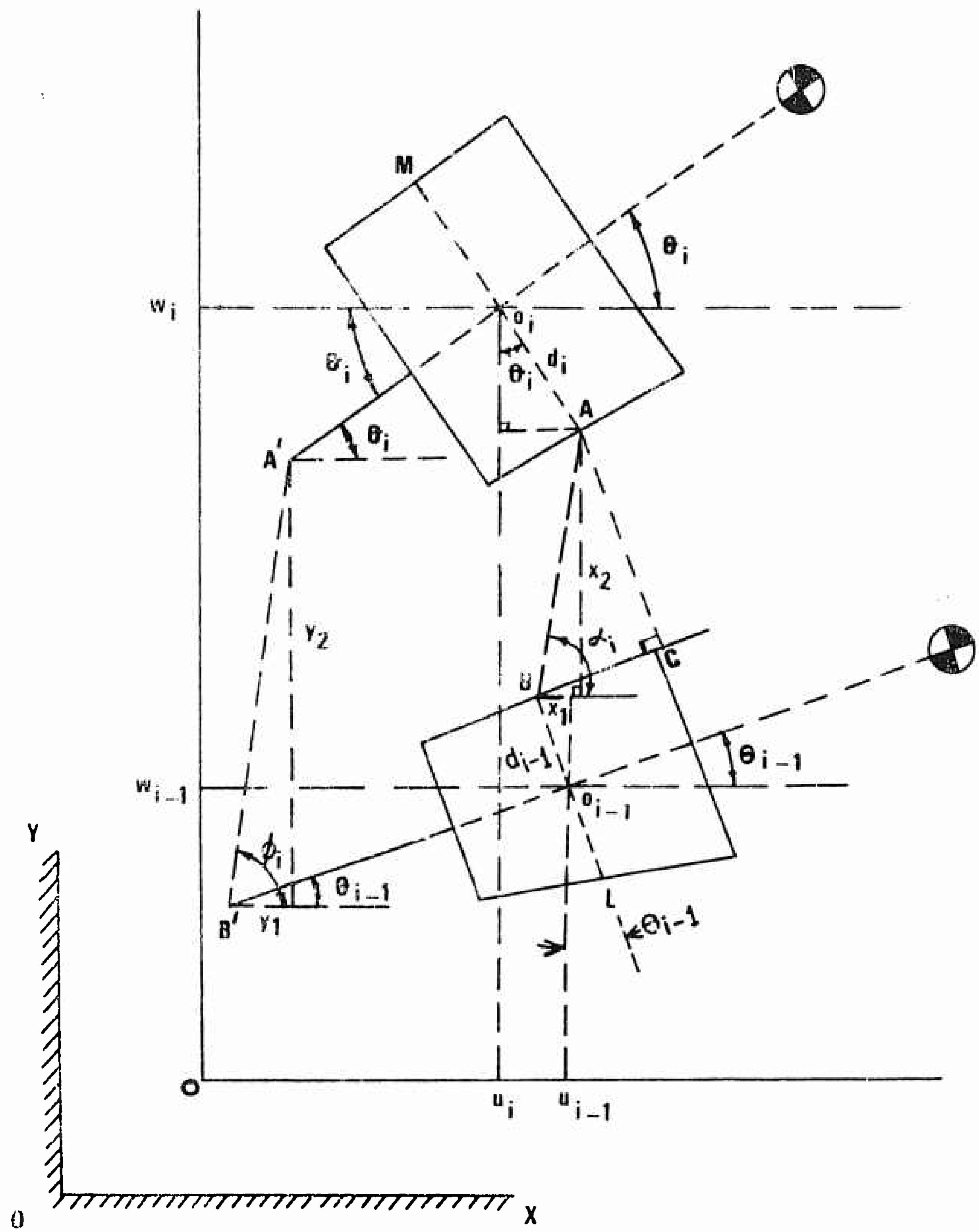

Fig. 5.2. Configuration of Two Successive Vertebrae after Deformation of Disc

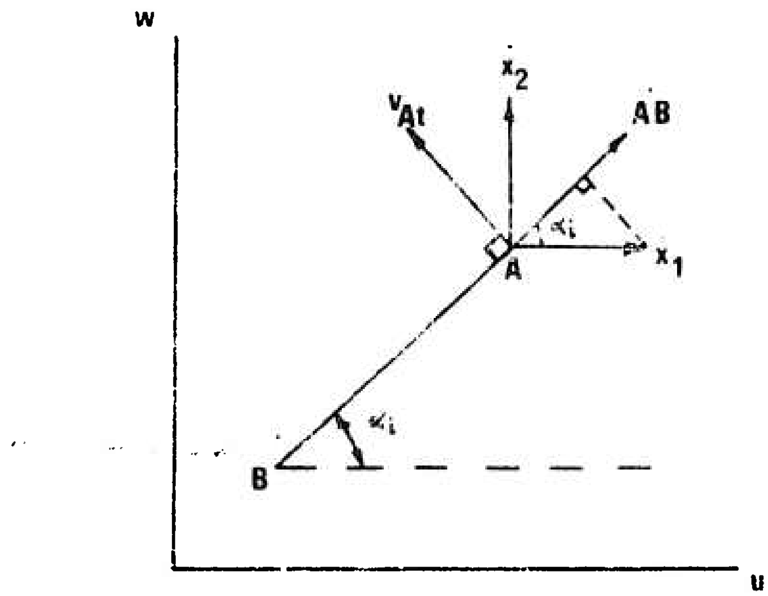

Fig. 5.3. Vector Diagram Showing Velocity of A with Respect to B

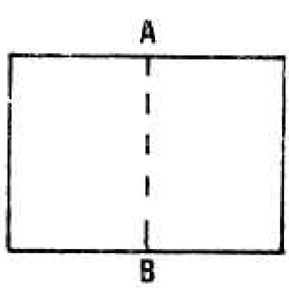

Fig. 5.4. Initial Shape of the Disc

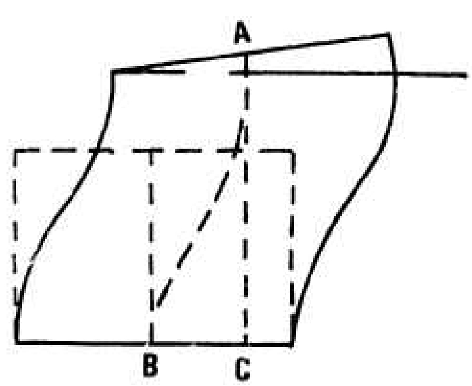

Fig. 5.5. Shape of the Disc after Deformation

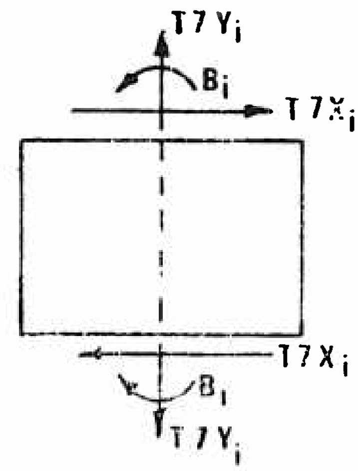

Fig. 5.6. Forces and Moments Developed in the Disc

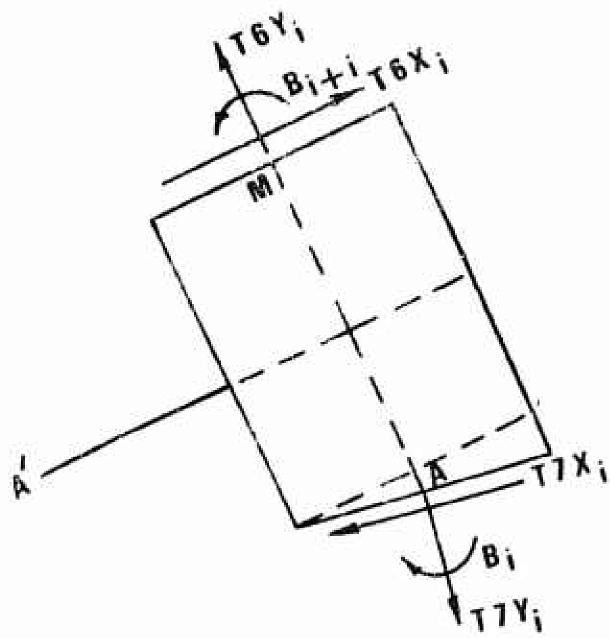

Fig. 5.7. Reaction of the i+1$^{\underline{th}}$ and the i$^{\underline{th}}$ Disc on the i$^{\underline{th}}$ Vertebral Body

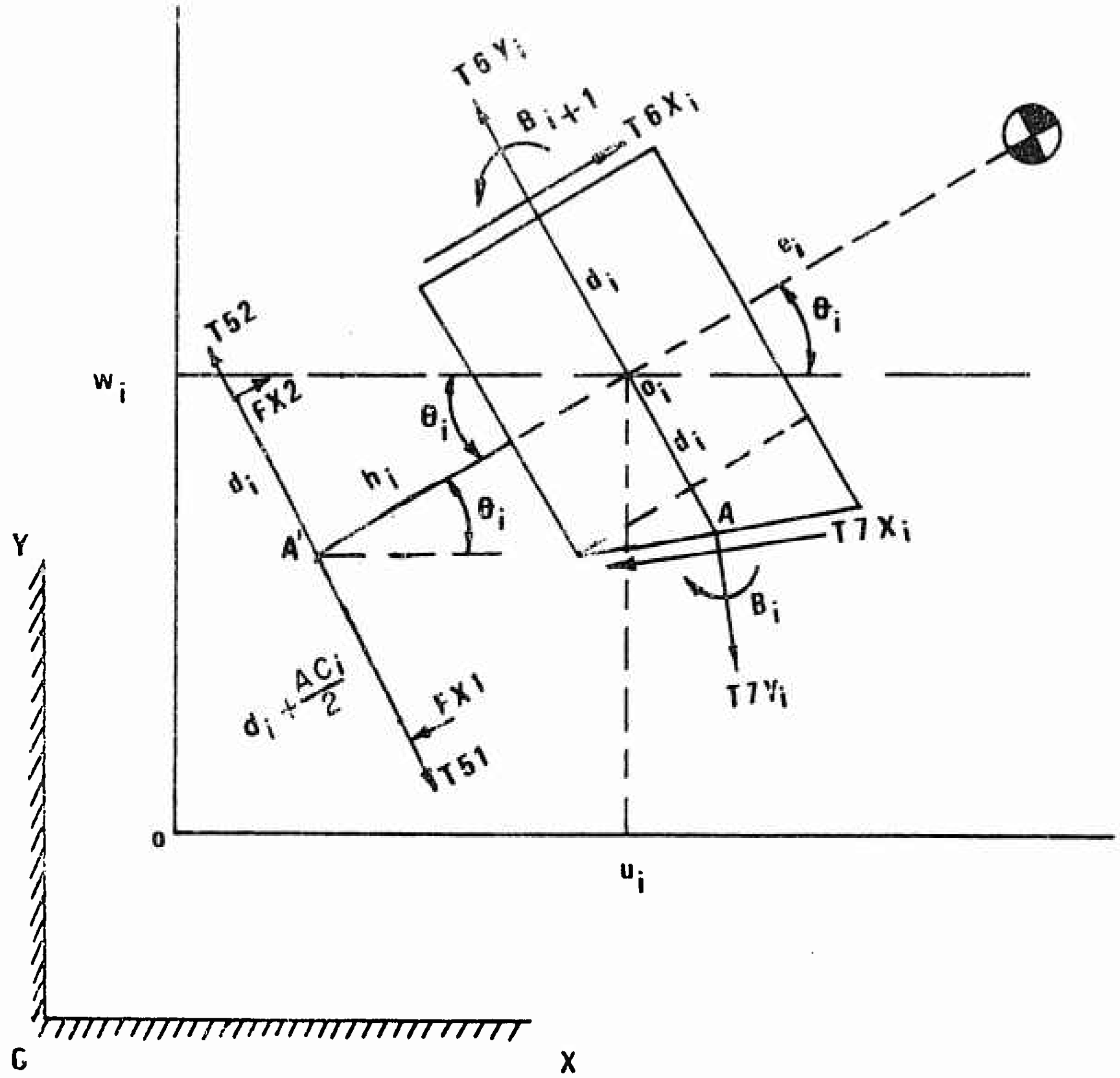

Fig. 5.8. Free Body Diagram of the $i^{\underline{th}}$ Vertebral Body

CHAPTER VI

RESULTS OF THE MATHEMATICAL MODEL AND COMPARISON WITH EXPERIMENTAL RESULTS

Three cadavers were used to experimentally verify the mathematical model. Each cadaver was run at 6, 8 and 10 g's in the erect and hyperextended modes. Figures 6.1 through 6.3 show the results of the experimental and model runs on Cadaver No. 2209 in the erect mode. The model predicts the first and second peaks of the intervertebral axial force at L3 at 6 g's. At 8 and 10 g's the first peak in the axial force is lower than that measured experimentally. In the experiments we can see that a considerable amount of tensile force is generated at the facets at the time of the first peak. However, in the model enough relative rotation between L3 and L4 has not taken place to generate tension at the facets at the time of the first peak. Hence, the model predicts a lower first peak in the intervertebral load at L3. It should be noted here that no attempt was made to curve-fit the experimental data with the model at the three acceleration levels.

Figures 6.4 through 6.6 show a comparison of the experimental results and the model results at 6, 8 and 10 g's in the hyperextended mode for Cadaver No. 2209. Both the model and the experiments indicate a reduction of the intervertebral load at L3 due to the facets carrying compressive loads for a longer duration when compared with the erect mode. There is a good correlation between the experiments and the model results. The second peak in the model appears earlier than that in the experiment. This indicates that the stiffness constants chosen in the model resulted in a higher frequency content when compared with the cadaver used.

Figures 6.7 through 6.9 show a comparison of the model results with the experimental results in the erect mode of runs made on Cadaver No. 2231. The results are similar to those obtained on Cadaver No. 2209. The correlation between the experimental and the model results is very good in this cadaver. An interesting point to note is the increase of only 25 lbs. in the peak intervertebral load measured when changing the acceleration level from 8 g's to 10 g's whereas the change from 6 g's to 8 g's is 260 lbs. The model predicts a change of 252 lbs. from 6 to 8 g's and a change of only 75 lbs. from 8 to 10 g's. Hence, it can be said that the model has simulated the three runs very accurately.

The experimental and the theoretical results of the runs made in the hyperextended mode are shown in Figures 6.10 through 6.12. There is good correlation between the model and the experimental intervertebral force, but the facet load predicted by the model at the first peak is higher than the experimental facet force. This is because the model has a larger dynamic overshoot at the first peak when compared with the cadaver.

The experimental and model results for Cadaver No. 2413 are shown in Figures 6.13 through 6.18. There is a good correlation for the 6.5 and 8 g runs between the model and the experiments. However, during the 10 g experimental runs in the erect and hyperextended modes, the head of the cadaver hit the rails on the sled, as a result of which the 2nd peak in the axial force did not build up as predicted by the model. In the hyperextended mode the model has a higher frequency content than the observed results.

Conclusions:

Over the range of measurements made, there is a good correlation between the experimental and the theoretical results. Due to the lack of instrumentation for the experiments, attempts were not made to verify the model at different vertebral levels. However, the in-vivo measurement of axial force has been made for the first time. With more refinements in the experimental techniques, measurements at various vertebral levels can be made to verify the mathematical model further. Due to a lack of data on the various stiffness values needed by the model, a perfect match between the observed and the predicted time history of the axial force has not been achieved. However, the model is general enough to take any constants if the data is available. Some optimization techniques are available for curve fitting and "hunting" for constants. These techniques if used in conjunction with the model may lead to better understanding of the physical constants involved.

The model does bring out the importance of the initial curvatures of the spine as can be seen by the difference in the response of the spine between the erect and the hyper-extended modes.

The effect of the seat back, restraint system and the chin-chest contact force can be studied with the help of the model. The results of the variation of the above parameters have not been included in this study because the above parameters were not varied in the experiments, but in simulation runs made with the model these parameters do alter the response of the spine. Hence in future experimental work, the above parameters should also be studied.

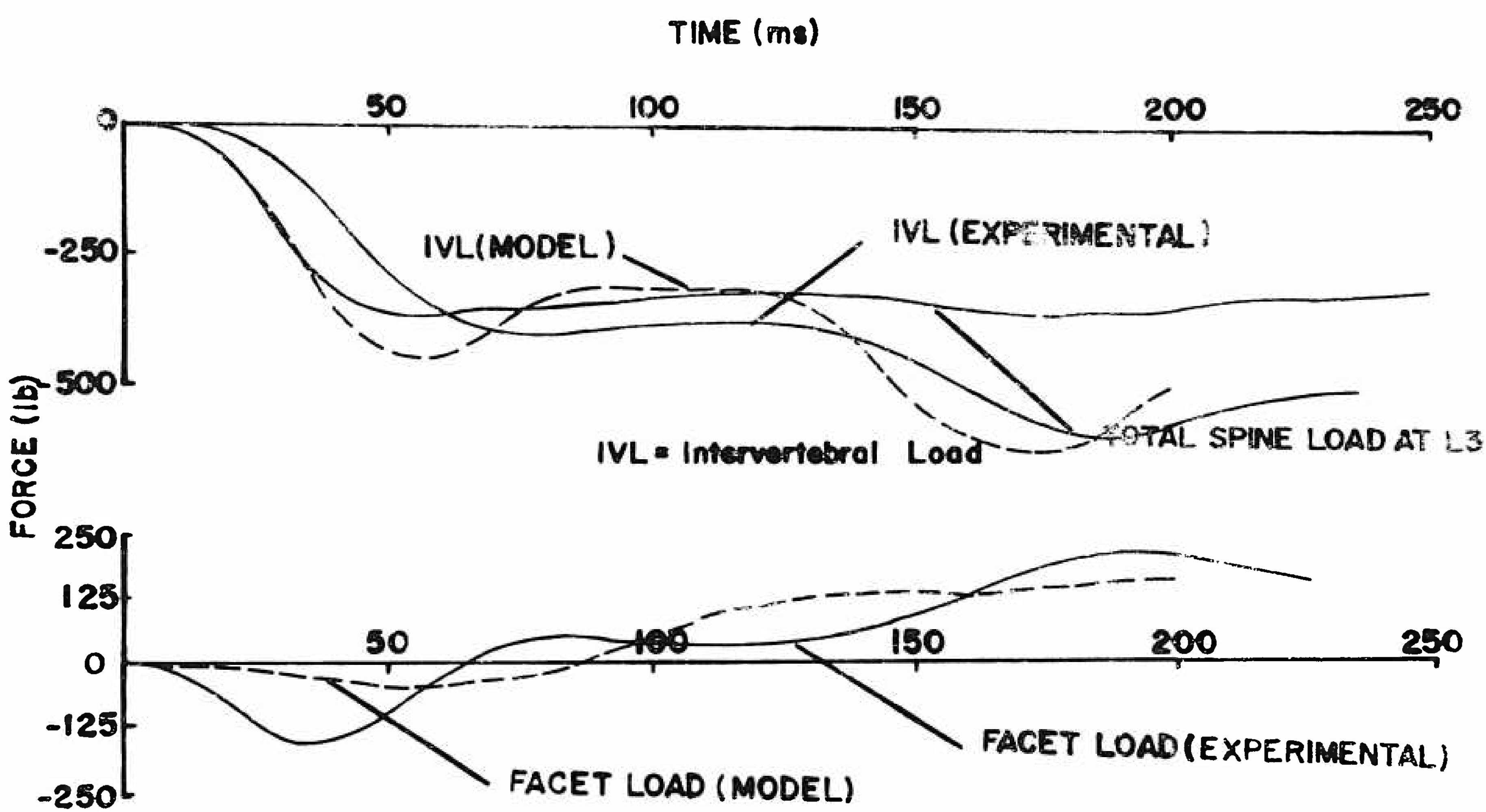

Fig. 6.1. Comparison of the Model and the Experimental Results of 6g Run on Cadaver 2209 in the Erect Mode

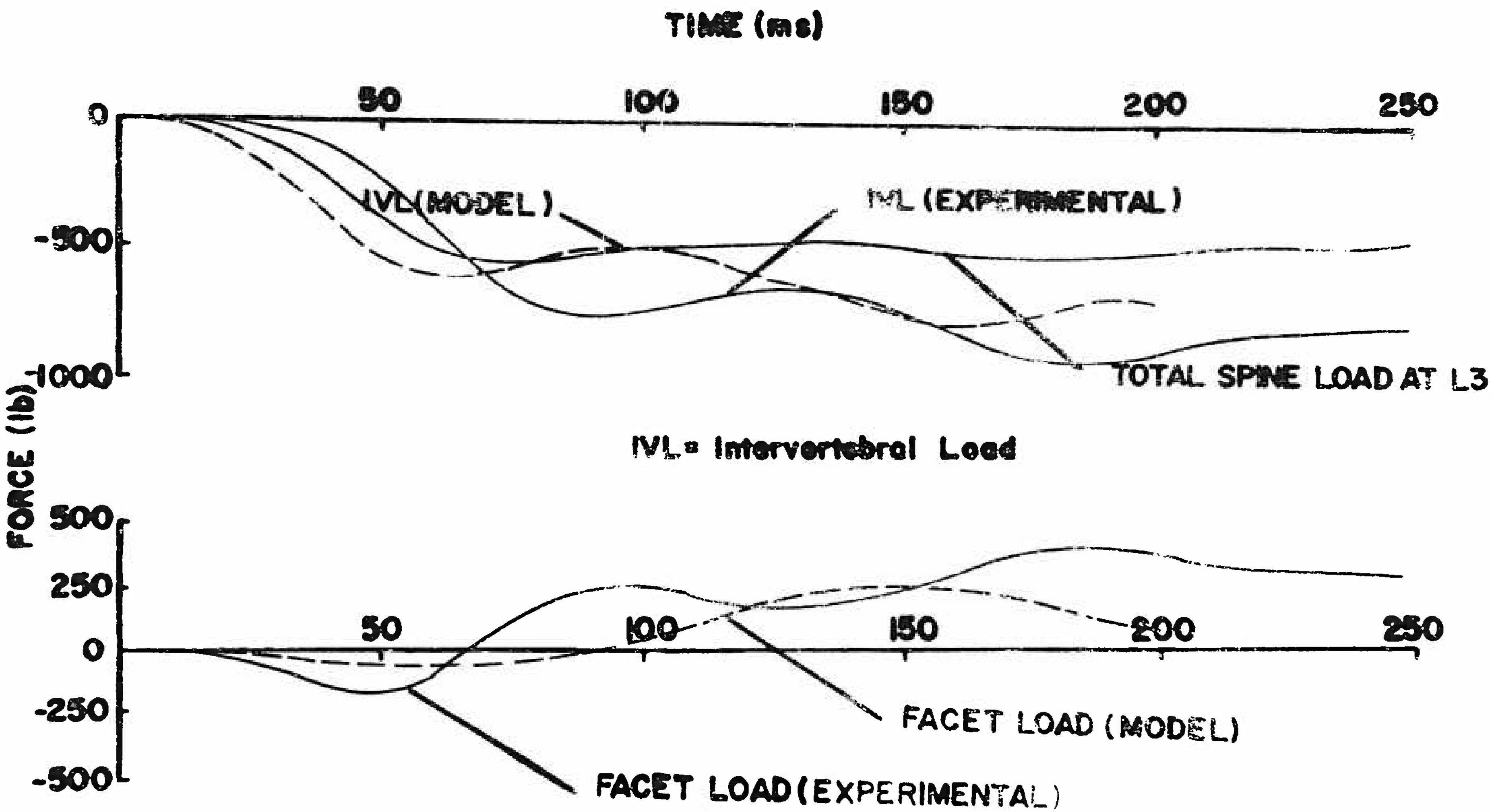

Fig. 6.2. Comparison of the Model and the Experimental Results of 8g Run on Cadaver 2209 in the Erect Mode

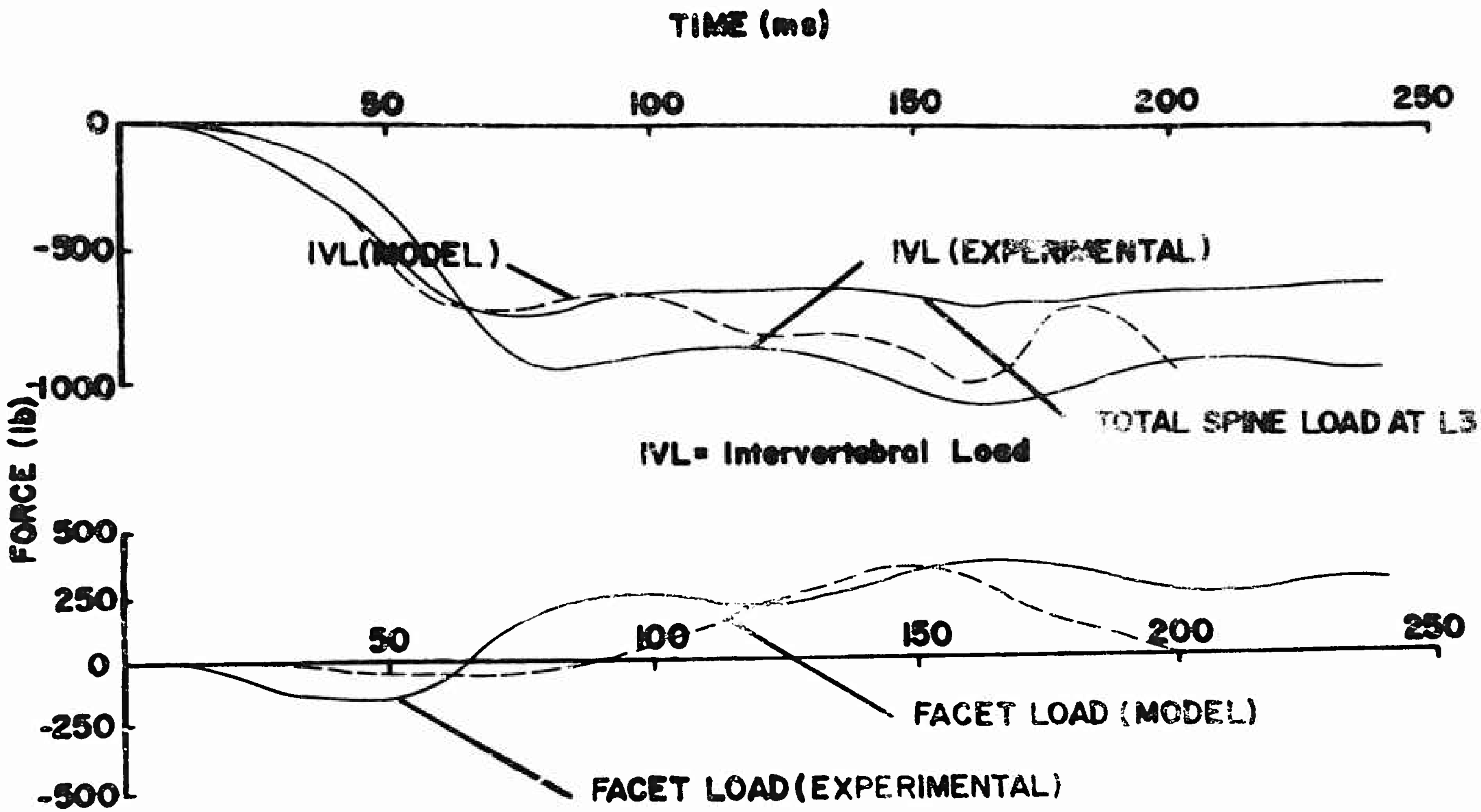

Fig. 6.3. Comparison of the Model and the Experimental Results of 10g Run on Cadaver 2209 in the Erect Mode

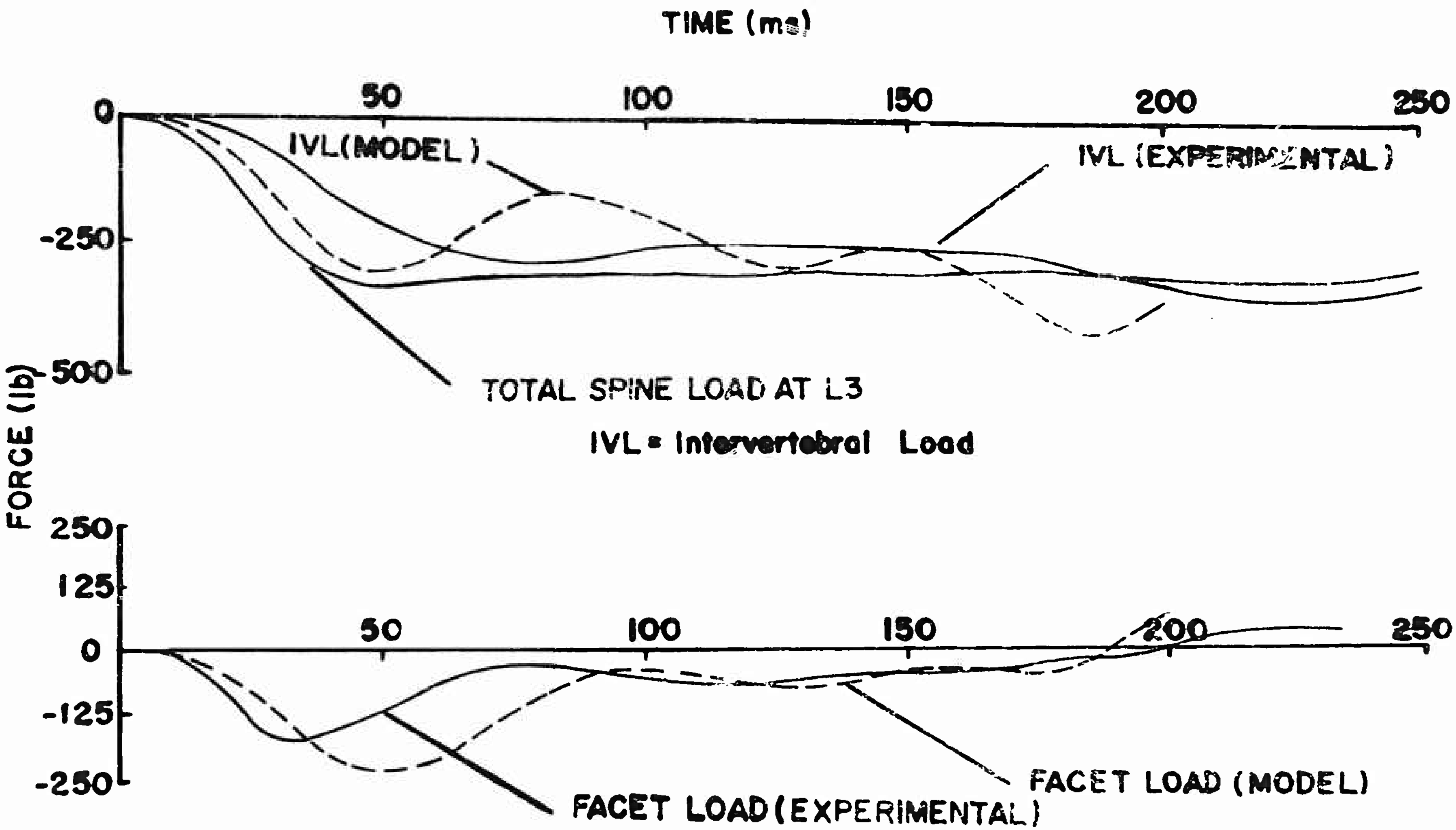

Fig. 6.4. Comparison of the Model and the Experimental Results of 6g Run on Cadaver 2209 in the Hyperextended Mode

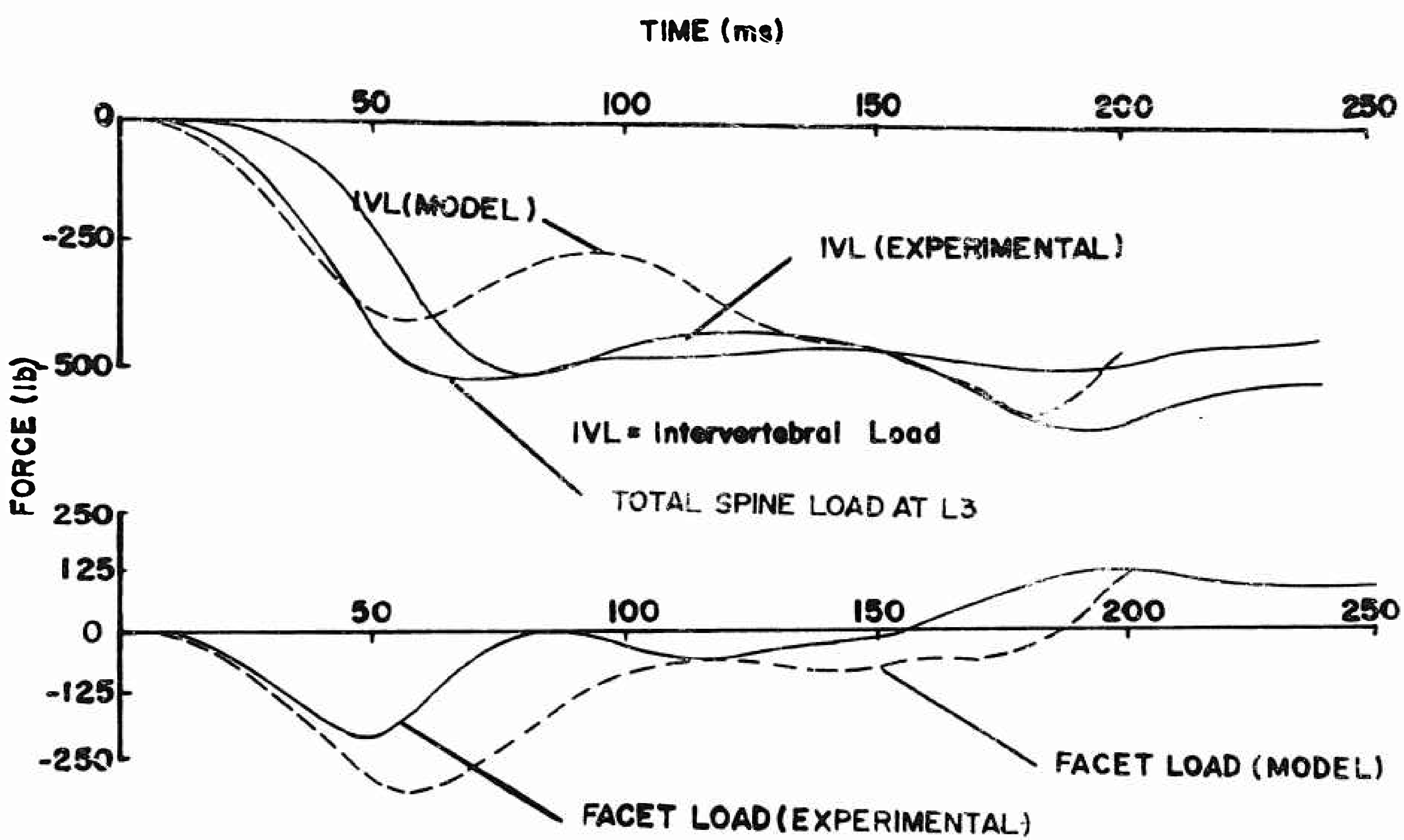

Fig. 6.5. Comparison of the Model and the Experimental Results of 6g Run on Cadaver 2009 in the Hyperextended Mode

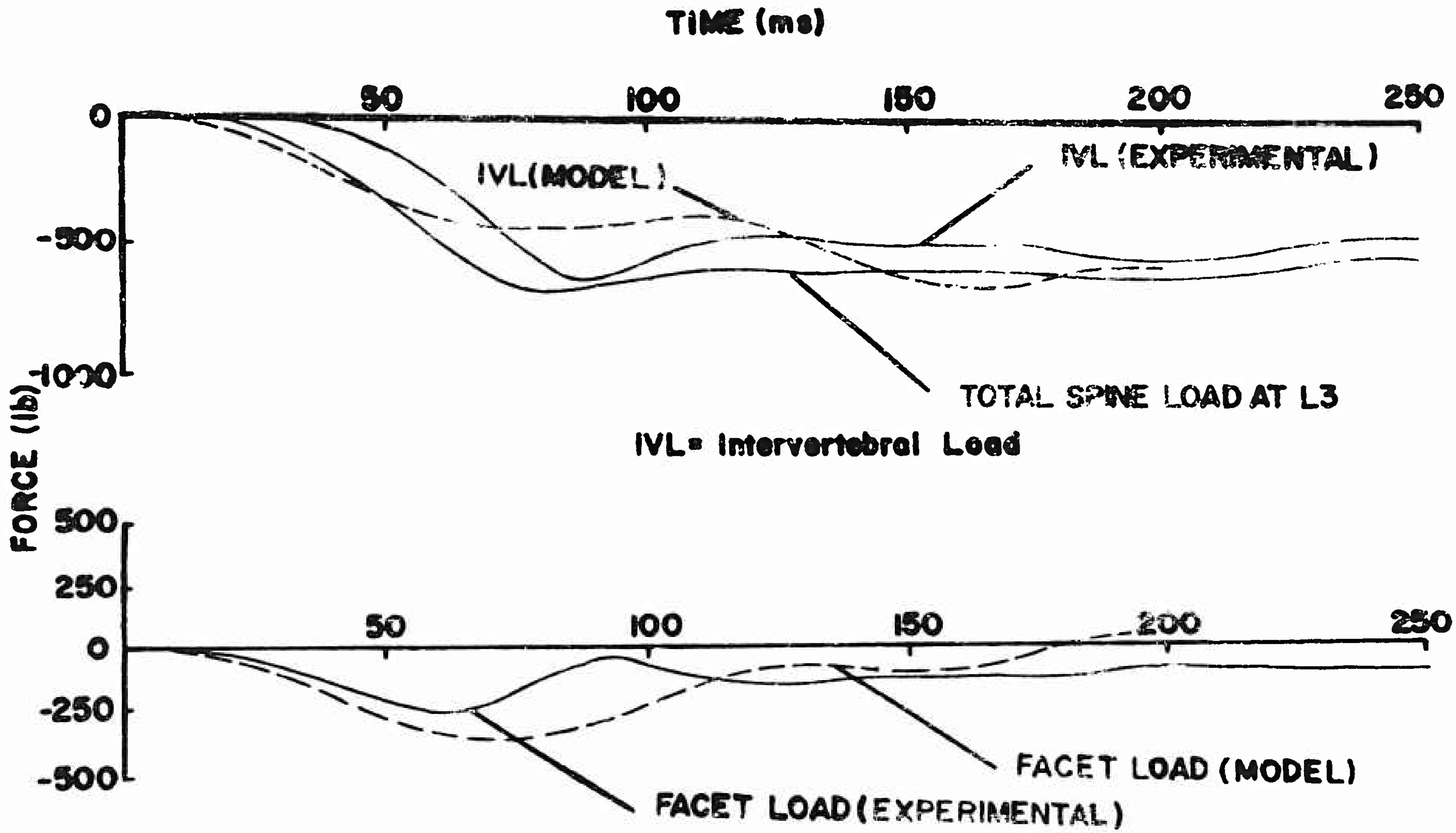

Fig. 6.6. Comparison of the Model and the Experimental Results of 10g [illegible]
Cadaver 2209 in the Hyperextended Mode

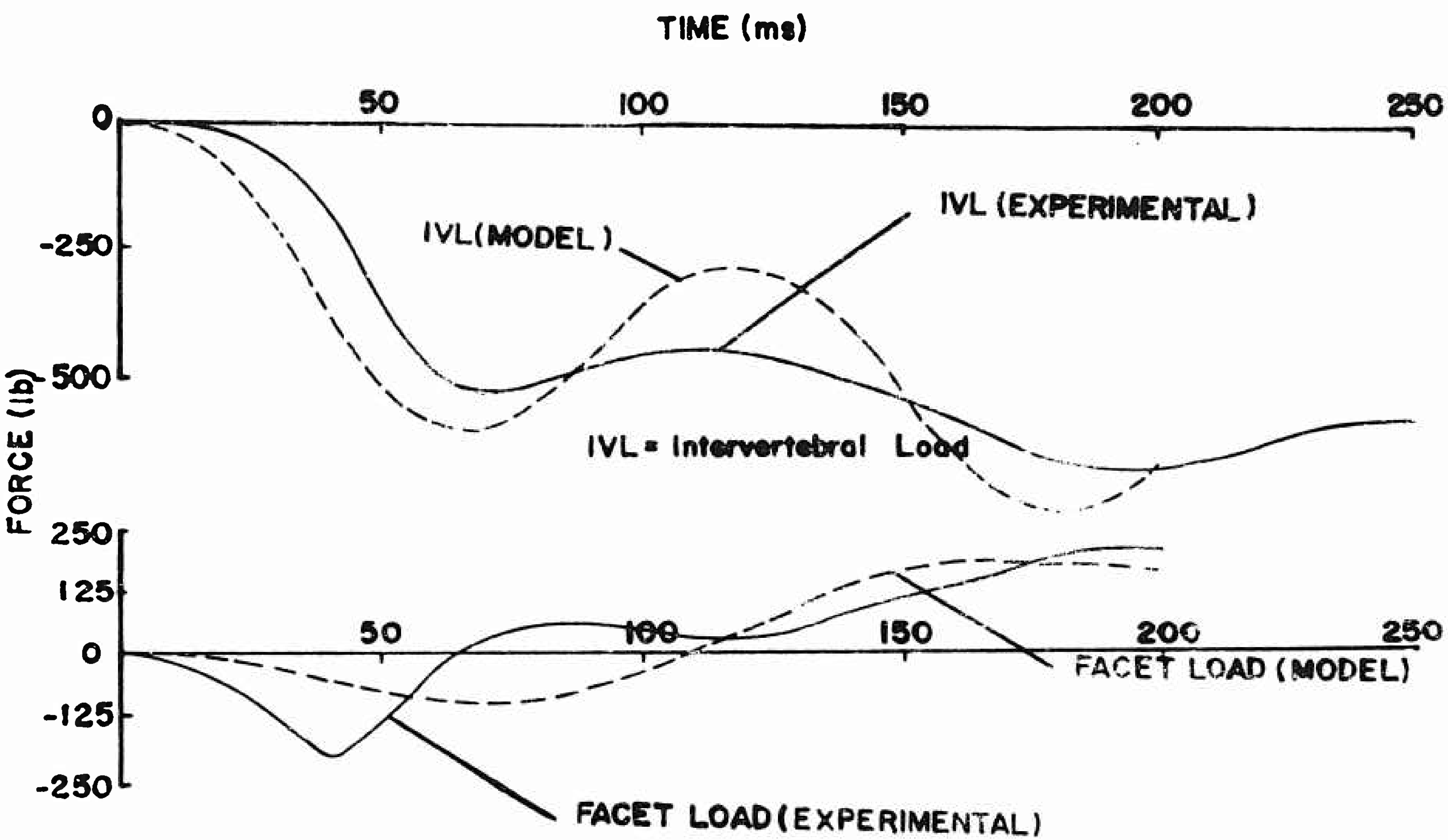

Fig. [illegible] Comparison of the Model and the Experimental Results of 6g Run [illegible] [illegible] the Facet Load

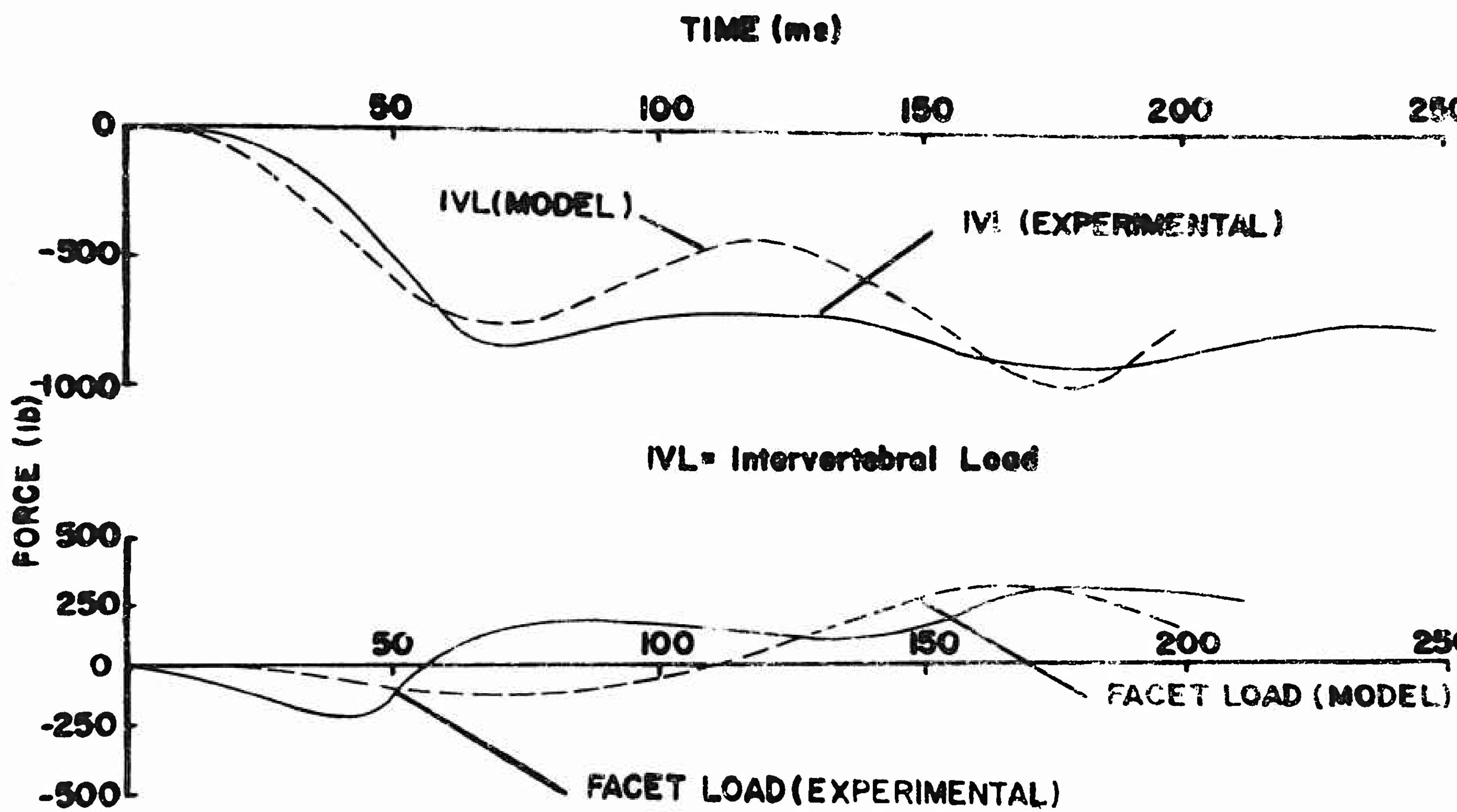

Fig. 6.8. Comparison of the Model and the Experimental Results of 8g Run on Cadaver 2[illegible]1 in the Erect Mode

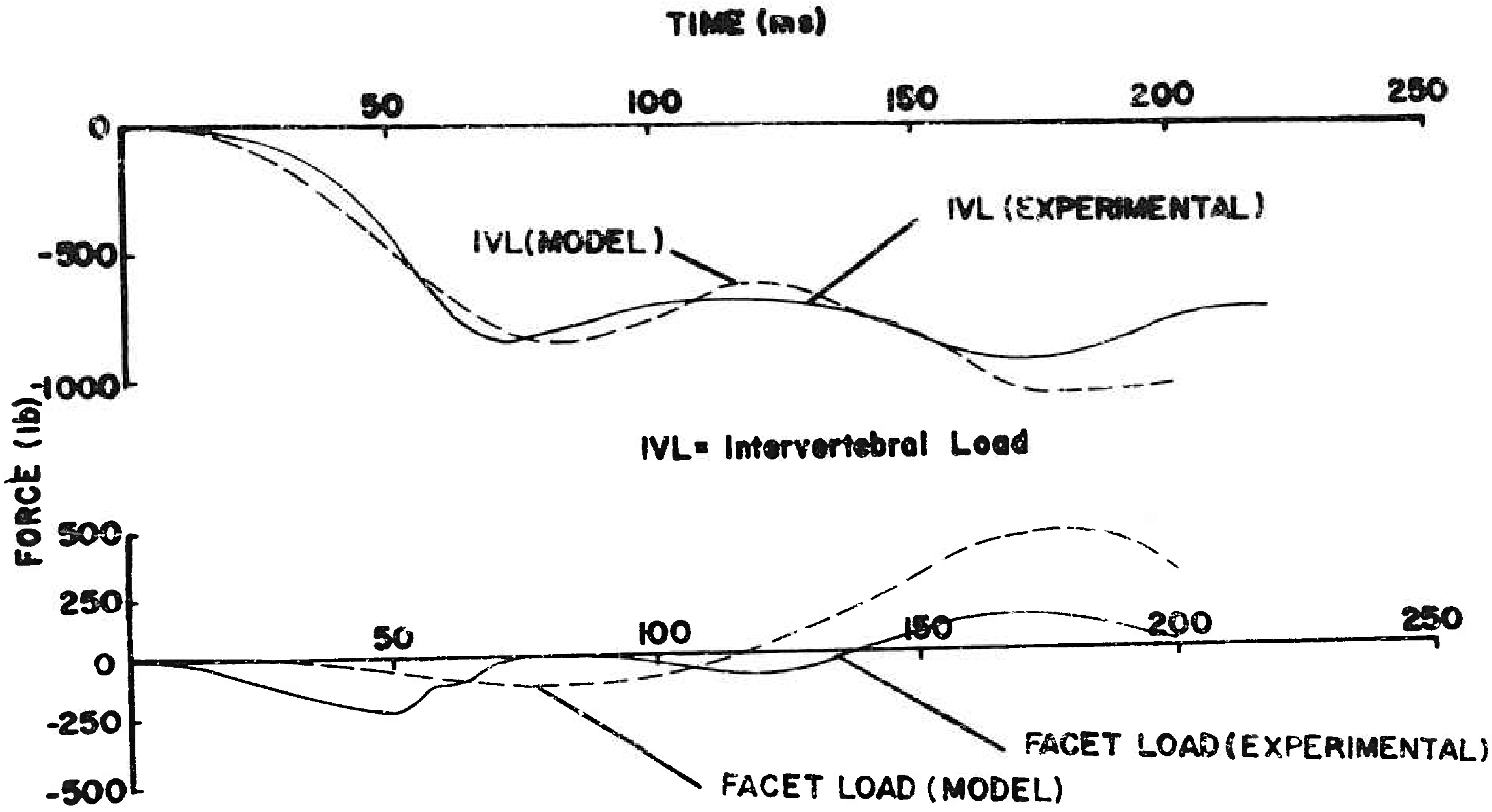

Fig. 6.9. Comparison of the Model and the Experimental Results of 10g Run on Cadaver 2231 in the Erect Mode

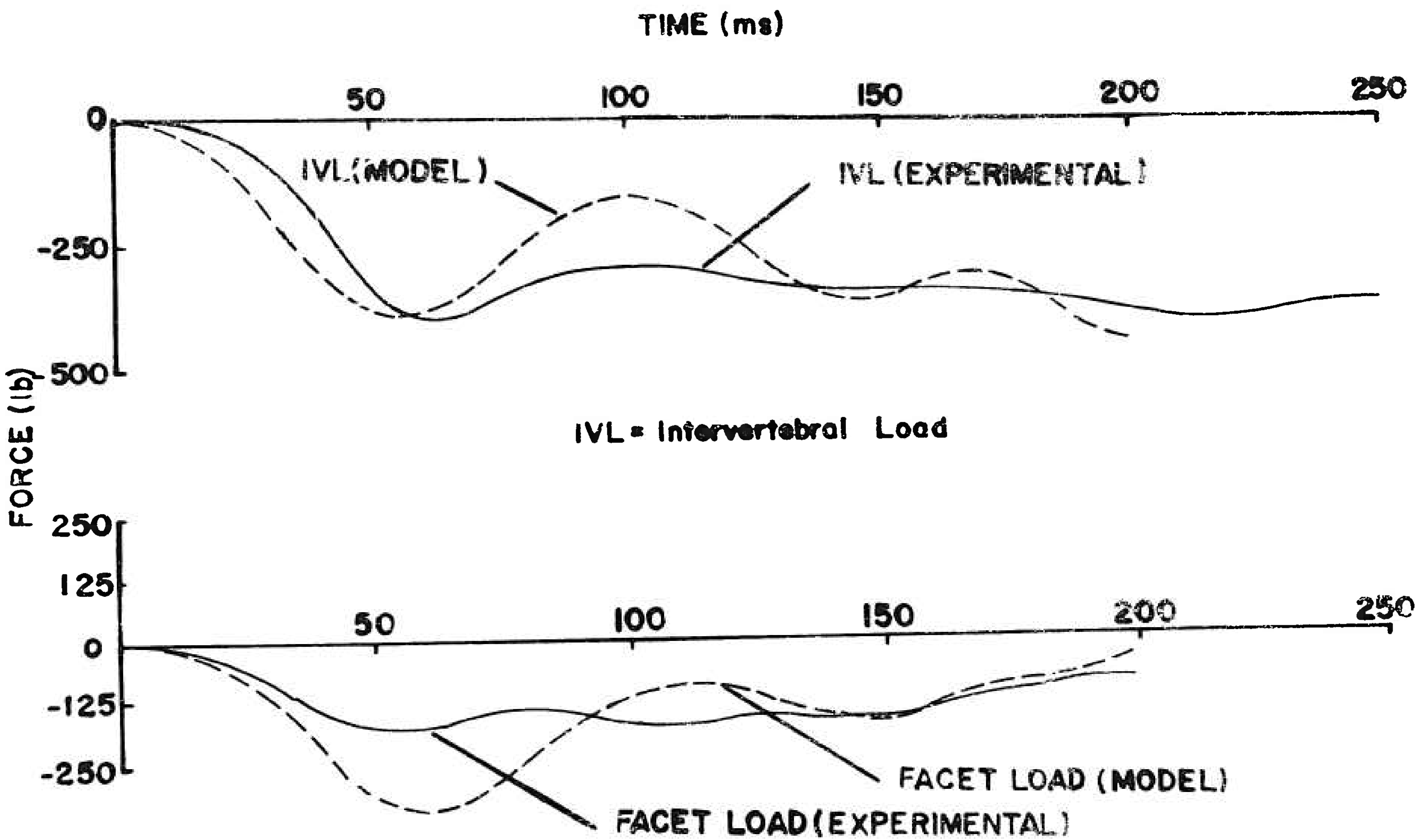

Fig. 6.10. Comparison of the Model and the Experimental Results of 6g Run on Cadaver 2231 in the Hyperextended Mode

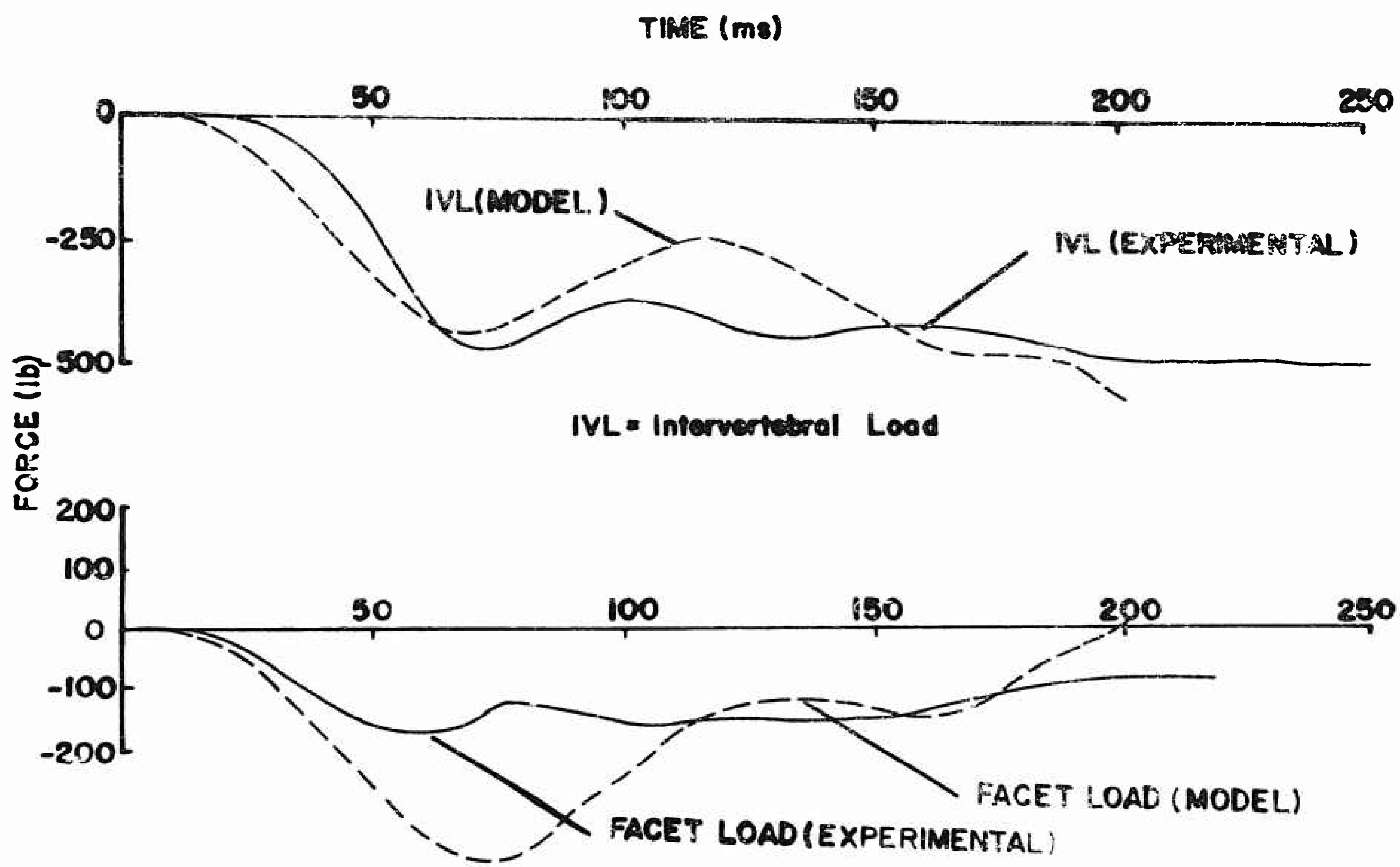

Fig. 6.11. Comparison of the Model and the Experimental Results of 8g Run on Cadaver 2231 in the Hyperextended Mode

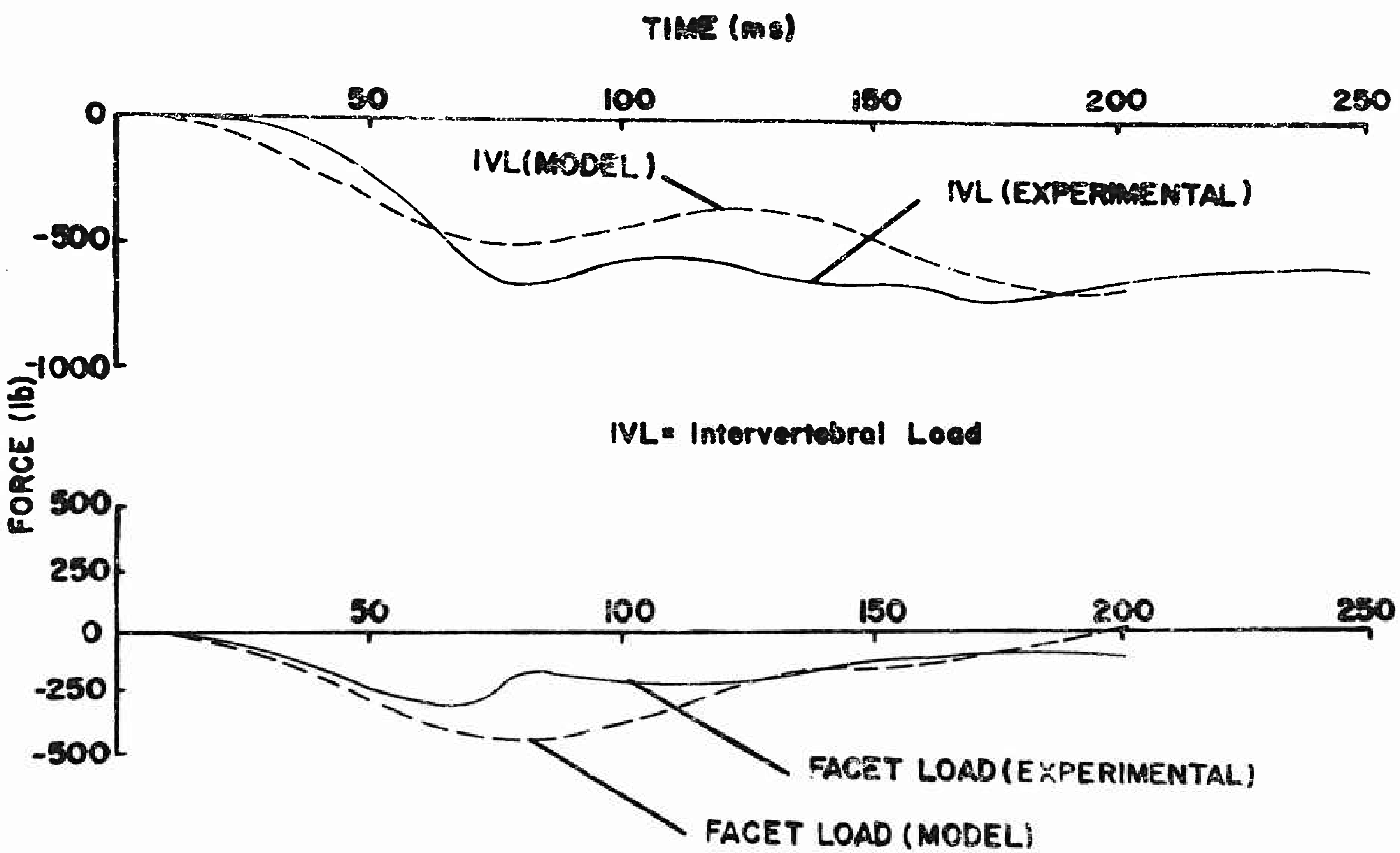

Fig. 6.12. Comparison of the Model and the Experimental Results of 10g Run on Cadaver 2231 in the Hyperextended Mode

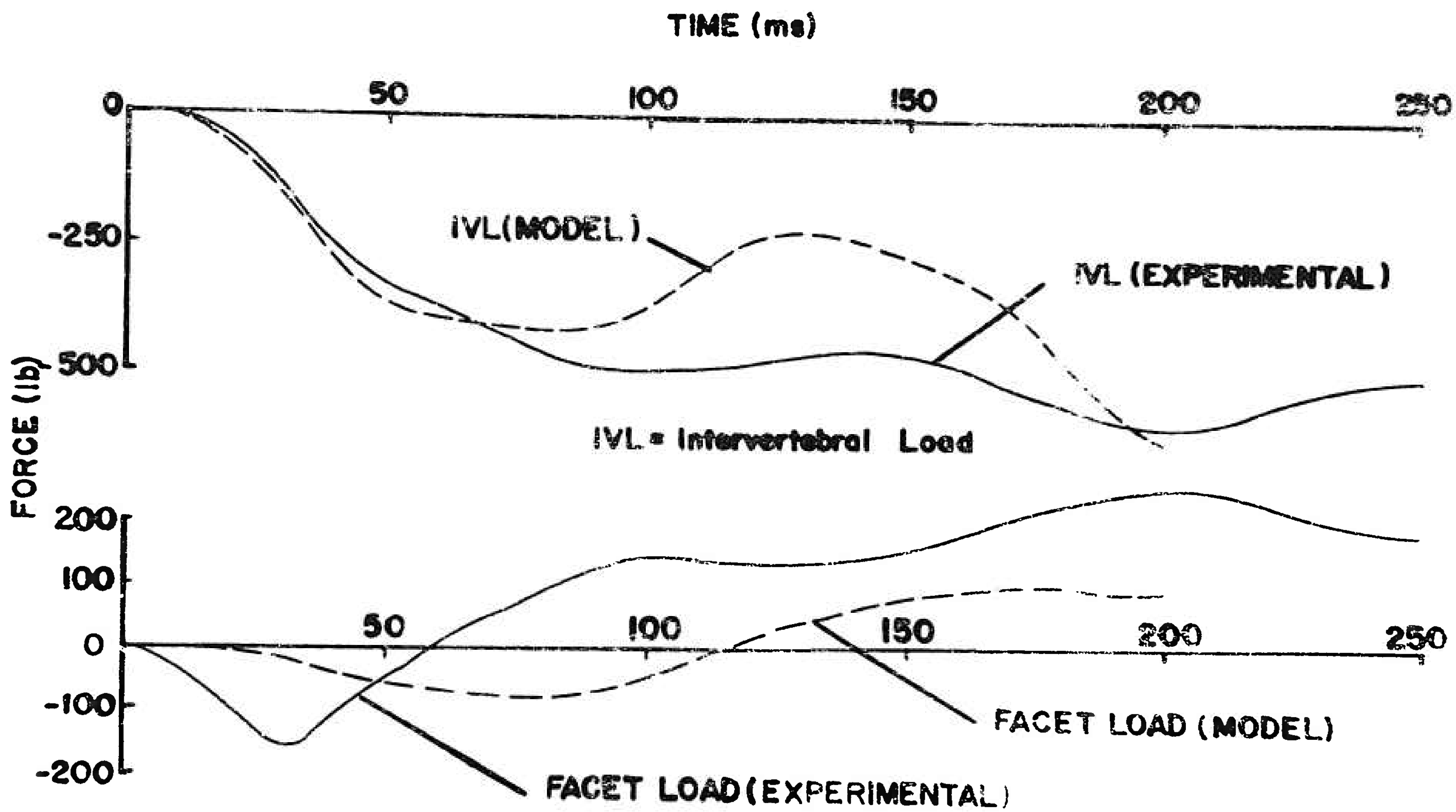

Fig. 6.13. Comparison of the Model and the Experimental Results of 6g Run on Cadaver 2413 in the Erect Mode

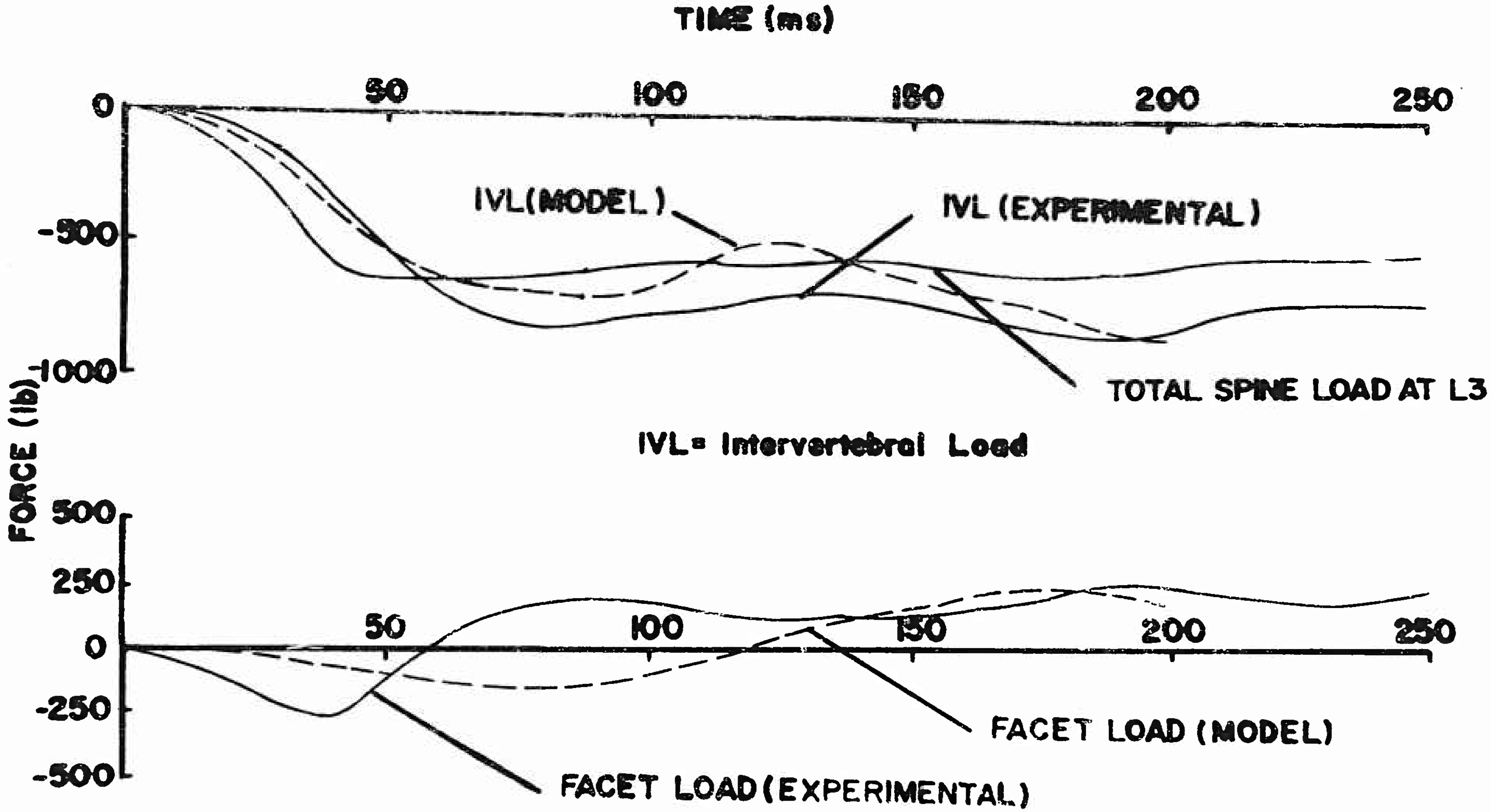

Fig. 6.14. Comparison of the Model and the Experimental Results of 8g Run on Cadaver 2413 in the Erect Mode

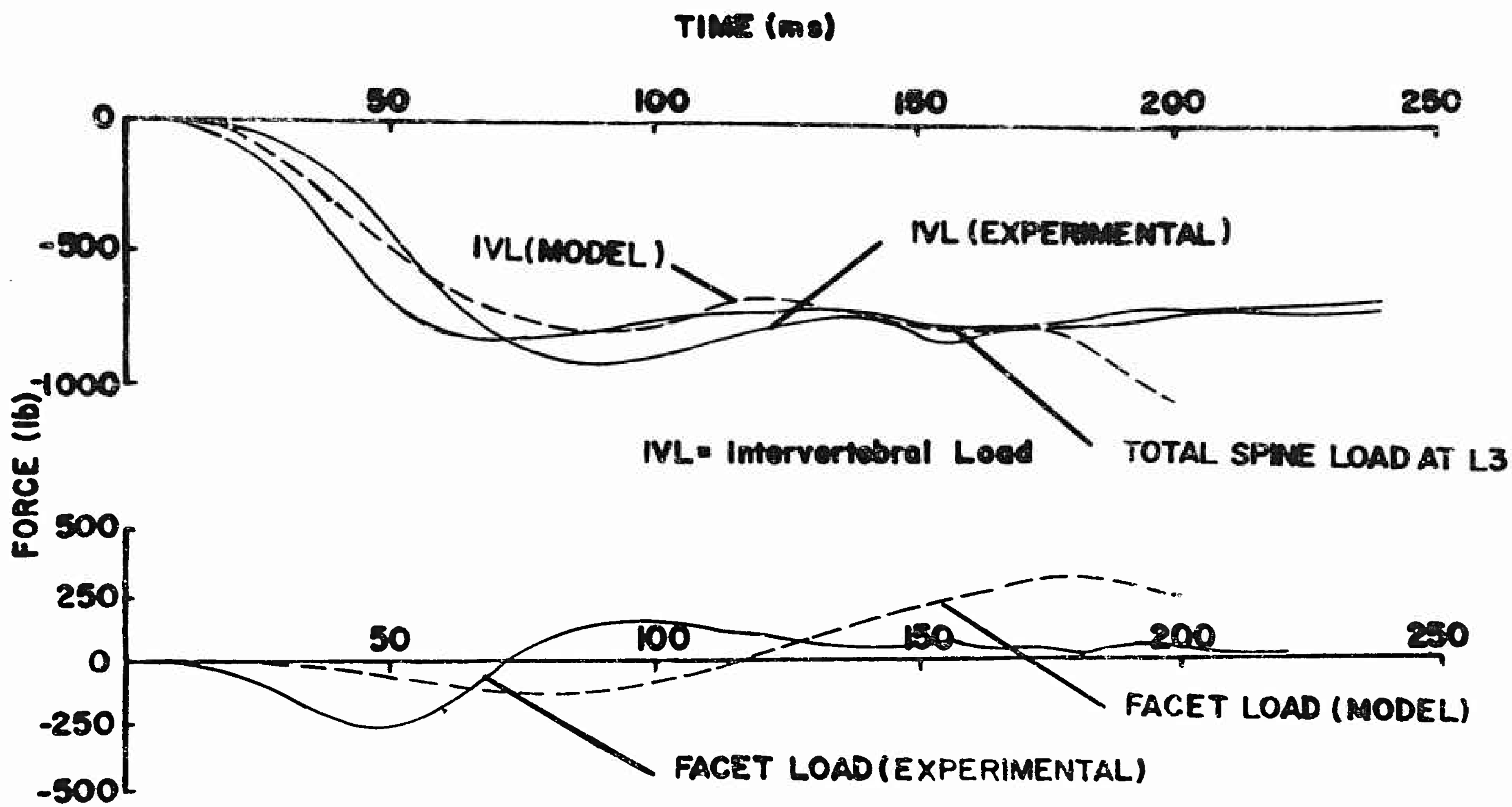

Fig. 6.15. Comparison of the Model and the Experimental Results of 10g Run on Cadaver 2413 in the Erect Mode

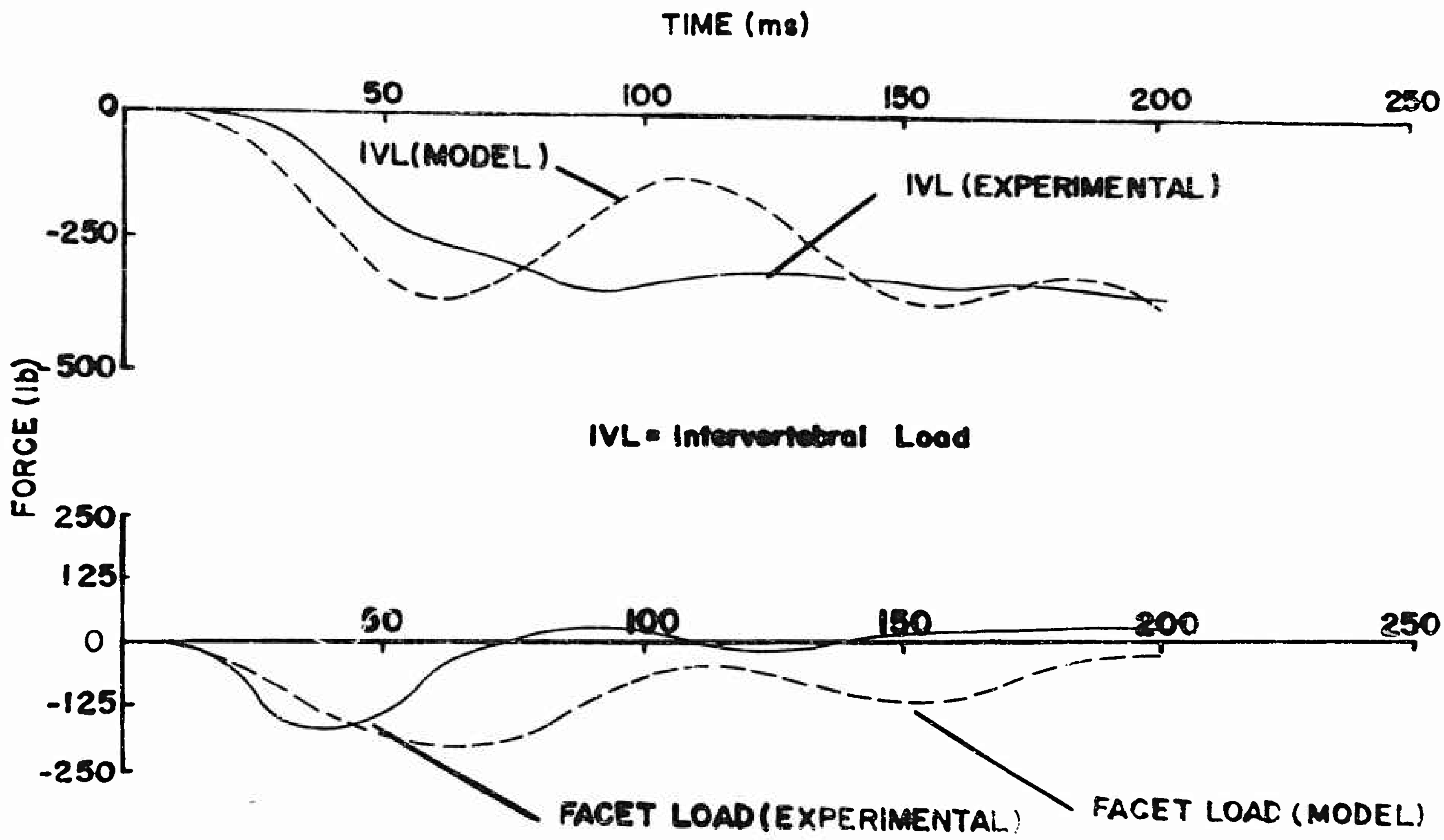

Fig. 6.16. Comparison of the Model and the Experimental Results of 6g Run on Cadaver 2413 in the Hyperextended Mode

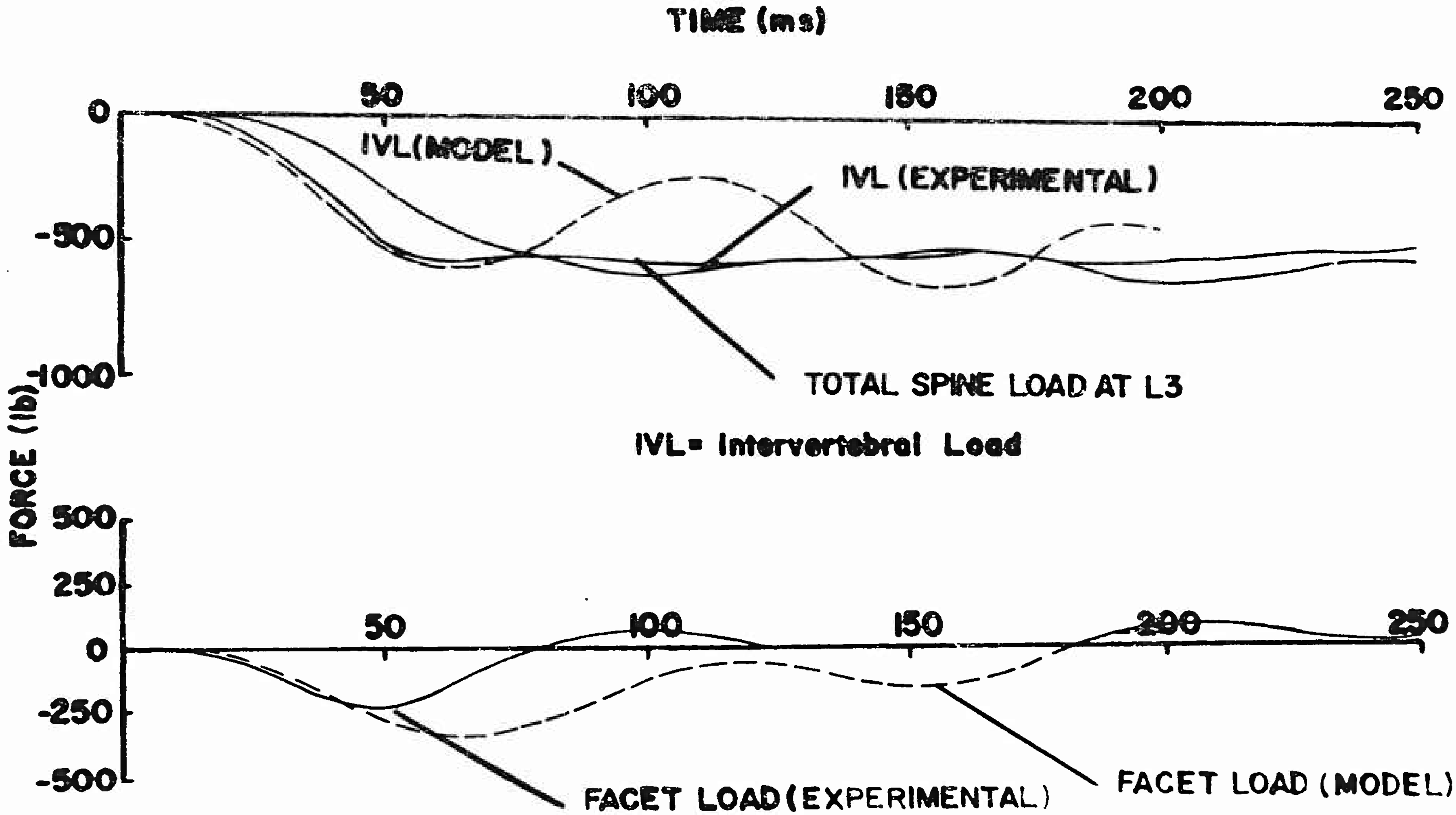

Fig. 6.17. Comparison of the Model and the Experimental Results of 8g Run on Cadaver 2413 in the Hyperextended Mode

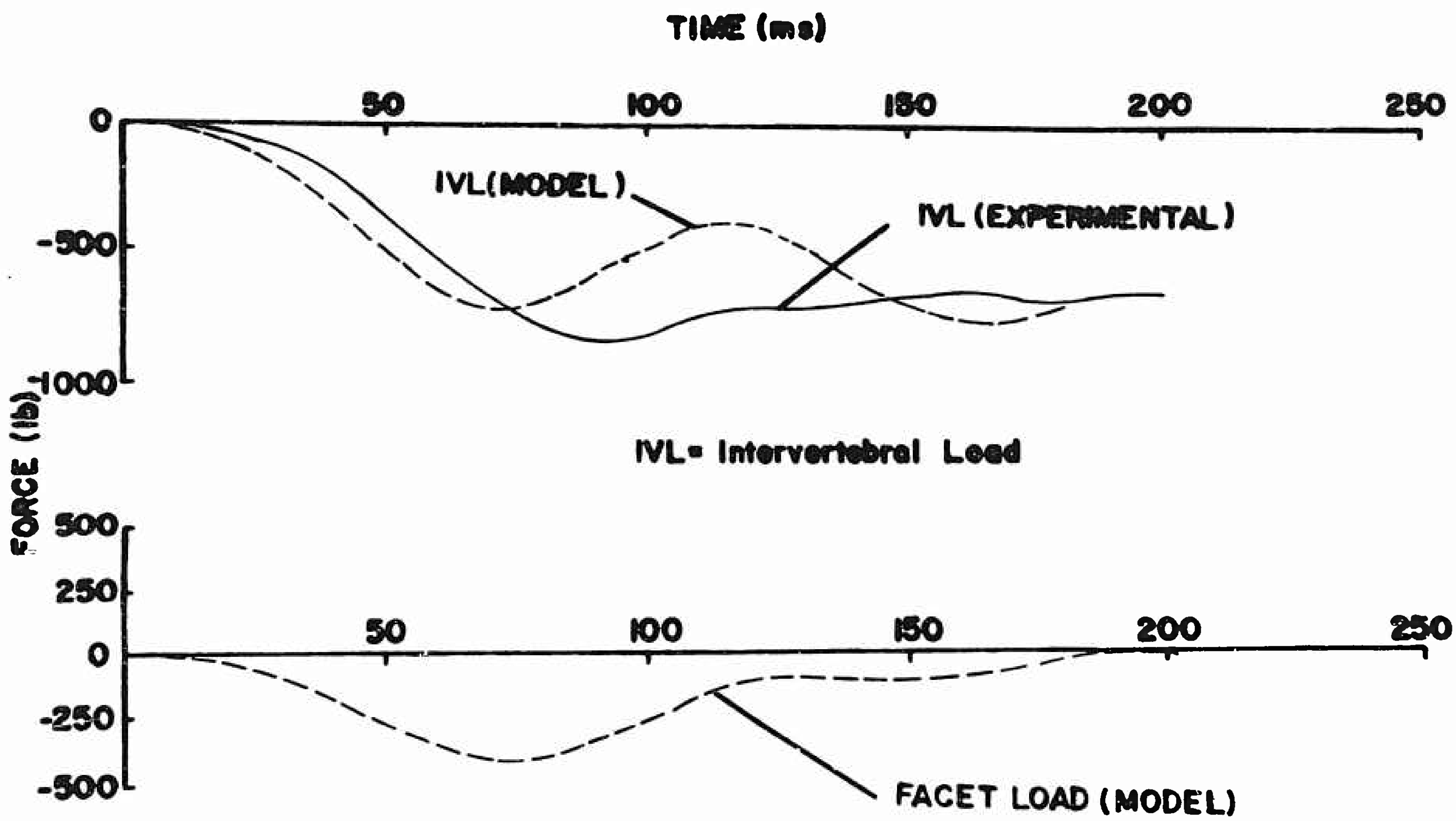

Fig. 6.18. Comparison of the Model and the Experimental Results of 10g Run on Cadaver 2413 in the Hyperextended Mode

CHAPTER VII

CONCLUSIONS AND RECOMMENDATIONS FOR FUTURE RESEARCH

On the basis of experimental and theoretical data it is now possible to explain the mechanism of anterior wedging fracture of the vertebral bodies during + G_z acceleration. A combination of bending and transference of load from the articular facets to the vertebral body results in high compressive strains at the anterior surface of the vertebral body resulting in fracture when the structural limits are exceeded.

Qualitative and quantitative evidence has been presented to document the load bearing capabilities of the articular facets. This is the first time that such a study has been done. The discovery of a load path through the articular facets has led to the fabrication of a device to increase the threshold of fracture of the spine during + G_z acceleration. This is of practical interest because a recent report on injuries sustained by pilots during the Viet Nam war states that almost one-third of the pow's sustained injuries involving fractures of the spine during emergency ejections from aircraft.

A mathematical model has been formulated and experimentally verified to predict the response of the vertebral column during + G_z acceleration. This is the most comprehensive, experimentally verified 2-dimensional mathematical model of the spine at the present time.

Future work in this area should involve the determination of the material properties of the intervertebral discs and vertebral bodies and the failure limits under a state of combined axial, shear and bending loads. The properties of the lamina and articular facets should be determined. There is no work available regarding the relative movement of the laminae, i.e., when and under what conditions do they "bottom out".

The transference of the shoulder strap load to the spine via the rib cage should be investigated. In the present mathematical model, all the strap load is transmitted to T1, but this may not be the case because the rib cage would transmit part of the load to various vertebral levels.

In the present study the effect of the generation of intra-abdominal pressure has not been studied. It has been hypothesized by Bartelink [1] and Morris et al. [12] that this pressure can reduce the reaction upon the vertebral end plate at the S1 and L5 junction. However, in the present study, the abdomen was eviscerated in all the cadavers used, hence there was no question of any intra-abdominal pressure build up. But in the case of living human subjects in an impact situation, there might be a build up of pressure, hence opening up a new load path. The question that has to be answered is whether in an impact lasting 200 msecs. any pressure will be generated and if so, how much? The force generated will tend to counteract the forward flexion of the spine.

REFERENCES

1. Bartelink, D. L.: The Role of Abdominal Pressure in Relieving Pressure on the Lumbar Intervertebral Discs. J. Bone Joint Surg., 39B: 718-725, 1957.

2. Basmajian, J. V.: Grant's Method of Anatomy, 8th Ed. The Williams and Wilkins Co., Baltimore, p. 18, 1971.

3. Basmajian, J. V.: Primary Anatomy, 6th Ed. The Williams and Wilkins Co., Baltimore, p. 27, 1970.

4. Ewing, C. L.: Non-Fatal Ejection Vertebral Fracture, U. S. Navy, Fiscal Years 1959 through 1965. Costs. Aerospace Med., to be published.

5. Ewing, C. L., A. I. King and P. Prasad: Structural Consideration of the Human Vertebral Column under + G_z Impact Acceleration. J. of Aircraft, 9(1): 84-90, 1972.

6. Fick, R.: Handbuch der Anatomie und Mechanik der Gelenke. Ver lag Gustav Fischer, Jena, 1904.

7. Gray, H.: Anatomy of the Human Body. Ed. by C. M. Goss, 25th Ed. Lea and Febiger, Philadelphia, pp. 75-76, 1948.

8. King, A. I., A. P. Vulcan and L. K. Cheng: Effects of Bending on the Vertebral Column of the Seated Human during Caudo-cephalad Acceleration. Proc. of the 21st Annual Conf. on Eng'g. in Med. and Biol., Nov., 1968.

9. King, A. I. and A. P. Vulcan: Elastic Deformation Characteristics of the Spine. J. Biomechanics, 4: 413-429, 1971.

10. Liu, Y. K. and J. K. Wickstrom, M. D.: Estimation of the Inertial Property Distribution of the Human Torso from Segmented Cadaveric Data. To be published.

11. Markolf, K. L.: Stiffness and Damping Characteristics of the Thoracolumbar Spine. Proc. of Workshop on Bio-engineering Approaches to Problems of the Spine, held on Sept. 12, 1970. Sponsored by: The Surgery Study Sections, Division of Research Grants, N. I. H., Bethesda, Md.

12. Morris, J. M., D. B. Lucas and M. S. Breslu: Role of the Trunk in the Stability of the Spine. J. Bone Joint Surg., 43A: 327-351, 1961.

13. Nachemson, A.: Lumbar Intradiscal Pressure. Acta Orthop. Scandinav. Supp., 43: 1, 1960.

14. Nachemson, A.: The Influence of Spinal Movements on the Lumbar Intradiscal Pressure and on the Tensile Stress in the Annulus Fibrosus. Acta Orthop. Scandinav., 33: 183, 1963.

15. Orne, D.: A Mathematical Model of Spinal Response to Impact. J. of Biomechanics, 4(1): 49-71, 1971.

16. Patrick, L. M.: Caudo-cephalad Static and Dynamic Injuries. Proc. of the Fifth Stapp Automotive Crash and Field Demonstration Conf., Univ. of Minnesota, 1962.

17. Perrey, O.: Fracture of the Vertebral End Plate in the Lumbar Spine. Acta Ortho. Scand., Suppl. 25, 1957.

18. Strasser, H.: Lehrbuch der Muskel und Gelenkmechanik. J. Springer, Berlin, 1913.

19. Vulcan, A. P., A. I. King and G. S. Nakamura: Effects of Bending on the Vertebral Column during + G_z Acceleration. Aerospace Med., 41(3): 294-300, 1970.

20. Vulcan, A. P. and A. I. King: Forces and Moments Sustained by the Lower Vertebral Column of a Seated Human during Seat-to-Head Acceleration. Dynamic Response of Biomechanical Systems. Ed. by N. Perrone. ASME, New York, pp. 84-100, 1971.

21. Vulcan, A. P.: Response of the Lower Vertebral Column to Caudo-cephalad Acceleration. Ph.D. Dissertation, Wayne State Univ., 1969.

APPENDIX I
MATHEMATICAL MODEL OF SPINE

```
$L SPINE
      C CALCULATE INITIAL LENGTHS
            IMPLICIT REAL*8 (A-H,O-Z)
            DIMENSION UO(26),WO(26),OO(26),D(26),H(26),E(26),XKH(26),XKT(26)
           1CT(26),C(26),XK(26),ABO(26),ALPHAO(26),ABDO(26),PHIO(26)
            DIMENSION U(26),W(26),O(26),XM(26),XI(26),XKS(26),XO1(26),XO2(2
            DIMENSION X(156),DX(156),PRMT(5),AUX(16,156),UDT(26),WDT(26),
           @ODT(26),UDDT(26),WDDT(26),ODDT(26),ALDT(26),ACO(26),BCO(26)
            DIMENSION DSOO(26),DCCO(26),HSOO(26),HCOO(26)
            DIMENSION A1A20(26),A2A30(26)
            DIMENSION AA(2),SF(26)
            EQUIVALENCE (X(1),U(1)),(X(27),UDT(1)),(X(53),W(1)),(X(79),WDT
           @(1)),(X(105),O(1)),(X(131),ODT(1))
            CALL PLTXMX(85.0)
            NAMELIST/ONE/U
            NAMELIST/TWO/W
            NAMELIST/THREE/O
            NAMELIST/FOUR/D,H,E,XM,XI
            NAMELIST/FIVE/XKH,XKT,CT,C,XK,XKS
            NAMELIST/SIX/PACC,SCH1,SCH2,SCH3,AA,TT1,TT2,IC1,MODE
      C       MODE=1 SIGNIFIES ERECT MODE
            NAMELIST/SEVEN/OCH1,OCH2,CH1,CH2,XKSB,SF
            EXTERNAL DERIV,OUTP
            COMMON/CDIST/D,H,E,ABC,ABDO,ALPHAO,PHIO,OO,UO,WO,XO1,XO2,ACO,BC
            COMMON/CONST/XKH,XKT,CT,C,XKS,XK,XM,XI
            COMMON/FACET/A1A20,A2A30
            COMMON KOUNT,LL
            COMMON/PEL1/ABSBO
            COMMON/PULSE/PACC,SCH1,SCH2,SCH3,AA,TT1,TT2,IC1,MODE
            COMMON/HEAD/OCH1,OCH2,CH1,CH2,XKSB,SF
            READ(5,ONE)
            READ(5,TWO)
            READ(5,THREE)
            READ(5,FOUR)
            READ(5,FIVE)
            READ(5,SIX)
            READ(5,SEVEN)
            LL=0
            KOUNT=0
            PI=3.14159265
            DO 117 I=1,18
            C(I)=.8*DSQRT(XK(I)*XM(I))
            CT(I)=.08*DSQRT(XKT(I)*XI(I))
        117 CONTINUE
            DO 2 I=1,26
            O(I)=(PI/180.)*O(I)
            OO(I)=O(I)
            UO(I)=U(I)
          2 WO(I)=W(I)
            DO 111 I=1,26
            UDT(I)=0.
            WDT(I)=0.
            ODT(I)=0.
        111 CONTINUE
            DATA PRMT/0.00,0.20,0.0001,.001/
            DO 112 I=1,156
        112 DX(I)=1./156.
            DO 110 I=1,26
            SOO=DSIN(OO(I))
```

```
            COO=DCOS(OO(I))
            DSOO(I)=D(I)*SOO
            DCOO(I)=D(I)*COO
            HSOO(I)=H(I)*SOO
            HCOO(I)=H(I)*COO
  110       CONTINUE
            ABO(1)=WO(1)-D(1)
            ALPHAO(1)=PI/2.
            ABDO(1)=0.
            PHIO(1)=0.
            XO1(1)=0.
            XO2(1)=ABO(1)
            ACO(1)=ABO(1)
            BCO(1)=0.
            A1A2O(1)=0.
            A2A3O(1)=0.
            ABSBO=DSQRT(UO(1)*UO(1)+WO(1)*WO(1))
            DO 1 I=2,26
            XO1(I)=-(UO(I-1)-DSOO(I-1))+(UO(I)+DSOO(I))
            XO2(I)=(WO(I)-D(I)*DCOS(OO(I)))-(WO(I-1)+DCOO(I-1))
            ABO(I)=DSQRT(XO1(I)*XO1(I)+XO2(I)*XO2(I))
            ALPHAO(I)=DATAN2(XO2(I),XO1(I))
     13     YO1=-(UO(I)-HCOO(I))+(UO(I-1)-HCOO(I-1))
            YO2=(WO(I)-HSOO(I))-(WO(I-1)-HSOO(I-1))
            ABDO(I)=DSQRT(YO1*YO1+YO2*YO2)
            PHIO(I)=DATAN2(YO2,-YO1)
            A1A2O(I)=ABDO(I)*DSIN(PHIO(I)-OO(I-1))
            A2A3O(I)=ABDO(I)*DCOS(PHIO(I)-OO(I-1))
     14     ACO(I)=ABO(I)*DSIN(ALPHAO(I)-OO(I-1))
            BCO(I)=ABO(I)*DCOS(ALPHAO(I)-OO(I-1))
      1     CONTINUE
            CALL DHPCG(PRMT,X,DX,156,IHLF,DERIV,OUTP,AUX)
            PRINT 120,IHLF
  120       FORMAT(' END OF SIMULATION. IHLF= ',I3)
            CALL PLOT(0,0,999)
            STOP
            END
            SUBROUTINE DERIV(T,X,DX)
            IMPLICIT REAL*8(A-H,O-Z)
            DIMENSION X(156),DX(156),X1(26),X2(26),ALDT(26),AC(26),BC(26),
           @ACDT(26),BCDT(26)
            DIMENSION DELU(26)
  C   CALCULATE R.H.S. (SUB.DERIV)
            DIMENSION UDT(26),WDT(26),ODT(26),UDDT(26),WDDT(26),ODDT(26),
           @ABDT(26),AB(26),ALPHA(26),PHI(26),ABD(26),RHS(26,2)
           @,U(26),W(26),O(26),RX(26),RY(26),X1DT(26),X2DT(26),SIGFU(26)
            DIMENSION SO(26),CO(26),DSO(26),DCO(26),HSO(26),HCO(26),IC(26)
            DIMENSION A1A2(26),A2A3(26)
            DIMENSION BETA(26),SHTRO(26),SHTP(26),SHRAP(26)
            COMMON/CDIST/D(26),H(26),E(26),ABO(26),ABDO(26),ALPHAO(26),
           @PHIO(26),OO(26),UO(26),WO(26),XO1(26),XO2(26),ACO(26),BCO(26)
            COMMON/CONST/XKH(26),XKT(26),CT(26),C(26),XKS(26),XK(26),
           @XM(26),XI(26)
            COMMON/DIST/AB,ABD,ABDT,ALPHA,PHI,X1,X2,X1DT,X2DT,ALDT,AC,BC,
           @ACDT,BCDT,SIGFU
            COMMON/FACET/A1A2O(26),A2A3O(26)
            COMMON/FACETV/A1A2,A2A3
            COMMON/PEL1/ABSBO
            COMMON/PELVIS/STRAP
            COMMON/SHOL/SHRAP
```

```
      COMMON/HEAD/OCH1,OCH2,CH1,CH2,XKSB,SF(26)
      DO 101 I=1,26
      U(I)=X(I)
      UDT(I)=X(I+26)
      DX(I)=UDT(I)
      W(I)=X(I+52)
      WDT(I)=X(I+78)
      DX(I+52)=WDT(I)
      O(I)=X(I+104)
      ODT(I)=X(I+130)
  101 DX(I+104)=ODT(I)
      IF(T.EQ.0.)GO TO 1001
      GO TO 1003
 1001 DO 1002 I=1,156
      DX(I)=0.
 1002 CONTINUE
      RETURN
 1003 PI=3.14159265
      DO 110 I=1,26
      SO(I)=DSIN(O(I))
      CO(I)=DCOS(O(I))
      DSO(I)=D(I)*SO(I)
      DCO(I)=D(I)*CO(I)
      HSO(I)=H(I)*SO(I)
      HCO(I)=H(I)*CO(I)
  110 CONTINUE
      A1A2(1)=0.
      A2A3(1)=0.
      AB(1)=W(1)-D(1)
      ALPHA(1)=PI/2.
      ABD(1)=0.
      PHI(1)=PI/2.
      X1DT(1)=0.
      X2DT(1)=+WDT(1)
      ABDT(1)=+WDT(1)
      AC(1)=AB(1)
      BC(1)=0.
      ALDT(1)=0.
      ACDT(1)=WDT(1)
      BCDT(1)=0.
      X1(1)=0.
      X2(1)=AB(1)
      ABSB=DSQRT(U(1)*U(1)+W(1)*W(1))
      SANG=DATAN2(W(1),U(1))
      ABST=(W(1)*WDT(1)+U(1)*UDT(1))/ABSB
      STRAP=0.
      IF(ABSB.LE.ABSBO)STRAP=0.
      STRAPU=-STRAP*DCOS(SANG)
      STRAPW=-STRAP*DSIN(SANG)
      DO 2 I=2,26
      X1(I)=-(U(I-1)-DSO(I-1))+(U(I)+DSO(I))
      X2(I)=(W(I)-DCO(I))-(W(I-1)+DCO(I-1))
      AB(I)=DSQRT(X1(I)*X1(I)+X2(I)*X2(I))
      BETA(I)=DATAN2((WO(I)-W(I)),U(I))
      SHTRO(I)=DSQRT(UO(I)*UO(I))
      SHTR(I)=DSQRT((WO(I)-W(I))*(WO(I)-W(I))+U(I)*U(I))
      SHDT=(U(I)*UDT(I)-W(I)*WDT(I))/SHTR(I)
      SHRAP(I)=XKS(I)*(SHTR(I)-SHTRO(I))
      IF(SHTR(I)-SHTRO(I).GE.2.)SHRAP(I)=XKS(I)*2.+6.*XKS(I)
     @*(SHTR(I)-SHTRO(I)-2.)
```

```
          IF(SHRAP(I).LE.0.)SHRAP(I)=0.
           IF (U(I).LE.JO(I))SHRAP(I)=0.
          IF(SHTR(I).LE.SHTRO(I))SHRAP(I)=0.
          ALPHA(I)=DATAN2(X2(I),X1(I))
       22 Y1=(U(I-1)-HCO(I-1))-(U(I)-HCO(I))
          Y2=(W(I)-HSO(I))-(W(I-1)-HSO(I-1))
          PHI(I)=DATAN2(Y2,-Y1)
          ABD(I)=DSQRT(Y1*Y1+Y2*Y2)
C         RATE OF CHANGE OF AB
       24 X1DT(I)=-(UDT(I-1)-D(I-1)*ODT(I-1)*CO(I-1))+(UDT(I)+D(I)
         @*ODT(I)*CO(I))
          X2DT(I)=+(WDT(I)+D(I)*ODT(I)*SO(I))-(WDT(I-1)-D(I-1)*ODT(I-1)
         1*SO(I-1))
          ABDT(I)=+DCOS(ALPHA(I))*X1DT(I)+DSIN(ALPHA(I))*X2DT(I)
          AC(I)=AB(I)*DSIN(ALPHA(I)-O(I-1))
          BC(I)=AB(I)*DCOS(ALPHA(I)-O(I-1))
          ALDT(I)=(DCOS(ALPHA(I))*X2DT(I)-DSIN(ALPHA(I))*X1DT(I))/AB(I)
          ACDT(I)=ABDT(I)*DSIN(ALPHA(I)-O(I-1))+BC(I)*(ALDT(I)-ODT(I-1))
          BCDT(I)=ABDT(I)*DCOS(ALPHA(I)-O(I-1))-AC(I)*(ALDT(I)-ODT(I-1))
          A1A2(I)=ABD(I)*DSIN(PHI(I)-O(I-1))
          A2A3(I)=ABD(I)*DCOS(PHI(I)-O(I-1))
        2 CONTINUE
          DO 3000 I=1,26
     3000 HC(I)=0.
          TDISP=DABS(O(18)-OO(18))
          RDISP=DABS(O(26))-TDISP
          IF(RDISP.GE.OCH1)HC(26)=CH1*(RDISP-OCH1)
          IF(RDISP.GE.OCH2)HC(26)=CH1*(OCH2-OCH1)+CH2*(RDISP
         @-OCH2)
          HC(18)=HC(26)
          HC(17)=.0*HC(26)
          HC(16)=0.*HC(26)
          DO 3001 I=11,15
     3001 HC(I)=0*HC(26)
C       CALCULATION OF BENDING MOMENT
          DO 100 I=1,26
          FLP=0.
          IF(I.EQ.5)FLP=3.908149
          IF(I.EQ.6)FLP=3.764956
          IF(I.EQ.7)FLP=3.705202
          IF(I.EQ.15)FLP=4.396967
          IF(I.EQ.16)FLP=4.504419
          IF(I.EQ.1)FLP=3.
          IF(I.EQ.1)GO TO 1
          OREL1=(O(I-1)-OO(I-1))-(O(I)-OO(I))
          T1=XKT(I)*OREL1+CT(I)*(ODT(I-1)-ODT(I))
          GO TO 3
        1 T1=XKT(I)*(-O(I)+OO(I))+CT(I)*(-ODT(I))
        3 IF(I.EQ.26)GO TO 4
          OREL2=(O(I)-OO(I))-(O(I+1)-OO(I+1))
          T2=XKT(I+1)*OREL2+CT(I+1)*(ODT(I)
         @-ODT(I+1))
          GO TO 5
        4 T2=0.
        5 IF(U(I).GE.(H(I)+FLP))XSF=0.
          IF(U(I).LE.H(I)+FLP)XSF=XKSB*(H(I)+FLP-U(I))
          IF(I.GE.18)XSF=0.
          T3=0.
          XKST=XKS(I)
          IF(U(I).LE.UO(I))XKS(I)=0.
```

```
      T14=SHRAP(I)*DCOS(BETA(I))
      T141=SHRAP(I)*DSIN(BETA(I))
      T4=T14
      T41=0.
      IF(I.GT.18) T4=0.
      IF(I.GT.18) T41=0.
       IF (I.LE.8)T4=0.
       IF(I.LE.8) T41=0.
      T42=SHRAP(I)*2.5
      IF(I.GT.18) T42=0.
      IF(I.LE.8)T42=0.
C   ABOVE IS STRAP FORCE
      XKHI=XKH(I)
      T51=XKH(I)*(A1A20(I)-A1A2(I))
      IF(MODE.EQ.1)T51=-XKH(I)*H(I)*DSIN(OREL1)
      IF(I.EQ.26) GO TO 6
      T52=XKH(I+1)*(A1A20(I+1)-A1A2(I+1))
      IF(MODE.EQ.1)T52=-XKH(I+1)*H(I+1)*DSIN(OREL2)
      GO TO 7
    6 T52=0.
    7 T5=T51-T52
C   THE ABOVE IS THE REACTION AT FACETS
      IF(I.EQ.26) GO TO 8
      T6Y=XK(I+1)*(AC(I+1)-ACO(I+1))+C(I+1)*ACDT(I+1)
      T6X=SP(I+1)*(XK(I+1)*(BC(I+1)-BCO(I+1))+C(I+1)*BCDT(I+1))
      GO TO 9
    8 T6Y=0.
      T6X=0.
    9 T7YY=XK(I)*(AC(I)-ACO(I))+C(I)*ACDT(I)
      IF(I.EQ.1) GO TO 10
      T7XX=SP(I)*(XK(I)*(BC(I)-BCO(I))+C(I)*BCDT(I))
      T7Y=T7YY*DCOS(OO(I)-OO(I-1))-T7XX*DSIN(OO(I)-OO(I-1))
      T7X=T7XX*DCOS(OO(I)-OO(I-1))+T7YY*DSIN(OO(I)-OO(I-1))
      GO TO 11
   10 T7Y=T7YY*DCOS(O(I))
      IF(AC(1).GE.ACO(1))T7Y=0.
      T7X=T7YY*DSIN(O(I))
      IF(AC(1).GE.ACO(1))T7X=0.
C     THE ABOVE ARE FORCES ON VERTEBRAE DUE TO DEFORMATION
   11 SIGMG1=T1-T2-T3-T5*(H(I)+F(I))+T42
      IF(I.EQ.26)GO TO 23
      SIGMG2=-T6Y*E(I)-T6X*D(I)
      GO TO 25
   23 SIGMG2=HC(I)*1.5
   25 SIGMG3=T7Y*E(I)-T7X*D(I)
      IF(I.EQ.1)SIGMG3=0.
      FX1=XKH(I)*(A2A3(I)-A2A30(I))
      IF(I.EQ.26)GO TO 70
      FX2=XKH(I+1)*(A2A3(I+1)-A2A30(I+1))
      GO TO 71
   70 FX2=0.
   71 SIGMG4=FX1*(D(I)+AC(I)/2.)+FX2*D(I)
      SIGMG=SIGMG1+SIGMG2+SIGMG3-SIGMG4
      ODDT(I)=SIGMG/XI(I)
      IF(I.EQ.1)ODDT(I)=0.
C   SUMMATION OF FORCES IN X-DIRECTION
      FX1U=FX1*DCOS(O(I))
      IF(I.EQ.26)GO TO 31
      FX2U=FX2*DCOS(O(I))
      FX3U=+T6X*CO(I)+HC(I)*SO(18)
```

```
      GO TO 32
   31 FX2U=0.
      FX3U=0.
   32 FX4U=-T7X*CO(I)
      SIGFX=FX2U+FX3U+FX4U-FX1U
      IF(I.EQ.1) GO TO 51
      SIGMS=-T4+XSF
      GO TO 52
   51 SIGMS=STRAPU+XSF
   52 SIGFU(I)=SIGFX+SIGMS
C     SUMMATION OF FORCES IN Y-DIRECTION
      FY1=T5
      IF(I.EQ.26) GO TO 41
      FY2=T6Y
      GO TO 42
   41 FY2=HC(I)
   42 FY3=T7Y+HC(I)*DCOS(O(26))*DCOS(O(I))+HC(I)*DSIN(O(I))*DSIN(O(26))
      SIGY=FY1+FY2-FY3
      IF(I.EQ.1) T41=STRAPW
   62 SIGFY=SIGY
C     EQUATIONS OF MOTION
      UDDT(I)=(1./XM(I))*(SIGFU(I)-SIGFY*SO(I))+
     @F(I)*ODDT(I)*SO(I)+E(I)*ODT(I)*ODT(I)*
     @CO(I)-XDDT(T)
      IF(I.EQ.1) UDDT(I)=0.
 2000 WDDT(I)=(1./XM(I))*(SIGFY*CO(I)+T41+(T6X-T7X+FX2-FX1)*SO(I))+
     @F(I)*ODT(I)*ODT(I)*SO(I)-E(I)*(ODDT(I))*CO(I)
     @-YDDT(T)
      XKS(I)=XKST
      XKH(I)=XKHI
  100 CONTINUE
      DO 200 I=1,26
      DX(I+130)=ODDT(I)
      DX(I+78)=WDDT(I)
  200 DX(I+26)=UDDT(I)
      RETURN
      END
      FUNCTION YDDT(T)
      IMPLICIT REAL*8(A-H,O-Z)
      DIMENSION SC(2)
      COMMON/PULSE/PACC,SCH1,SCH2,SCH3,AA(2),T1,T2,IC1,MODE
      SC(1)=386.4*AA(1)
      SC(2)=386.4*AA(2)
      IF(IC1.EQ.1)GO TO 3
      IF(T.GE.T2)GO TO 1
      IF(T.GE.T1)GO TO 2
      YDDT=T*SC(1)/T1
      RETURN
    2 YDDT=SC(1)-(SC(1)-SC(2))*(T-T1)/(T2-T1)
      RETURN
    1 YDDT=SC(2)
      RETURN
    3 YDDT=0.
      RETURN
      END
      FUNCTION XDDT(T)
      IMPLICIT REAL*8(A-H,O-Z)
      COMMON/PULSE/PACC,SCH1,SCH2,SCH3,AA(2),T1,T2,IC1,MODE
      IF(IC1.EQ.0) GO TO 3
      IF(T.LE.SCH1) XDDT=-(PACC/SCH1)*T*386.4
```

```
      IF(T.GT.SCH1) XDDT=-PACC*386.4
      IF(T.GT.SCH2) XDDT=-(PACC-((PACC/(SCH3-SCH2))*
     @(T-SCH2)))*386.4
      RETURN
    3 XDDT=0.
      RETURN
      END
      SUBROUTINE OUTP(T,X,DX,IHLF,NDIM,PRMT)
      IMPLICIT REAL*8 (A-H,O-Z)
      DIMENSION X(156),DX(156),FY(26),SMG(26),X1(26),X2(26)
      DIMENSION FXT(26),FXB(26),FYT(26)
      DIMENSION UDT(26),WDT(26),ODT(26),UDDT(26),WDDT(26),ODDT(26),
     @ABDT(26),AB(26),ALPHA(26),PHI(26),ABD(26),RHS(26,2)
     @,U(26),W(26),O(26),RX(26),RY(26),X1DT(26),X2DT(26),SIGPI(26)
     @,PRMT(5),ALDT(26),AC(26),BC(26),ACDT(26),BCDT(26)
      COMMON/CDIST/D(26),H(26),E(26),ABO(26),ABDO(26),ALPHAO(26),
     @PHIO(26),OO(26),UO(26),WO(26),XO1(26),XO2(26),ACO(26),BCO(26)
      COMMON/CONST/XKH(26),XKT(26),CT(26),C(26),XKS(26),XK(26),
     @XM(26),XT(26)
      COMMON/DIST/AB,ABD,ABDT,ALPHA,PHI,X1,X2,X1DT,X2DT,ALDT,AC,BC,
     @ACDT,BCDT,SIGPI
      COMMON/PELVIS/PLOAD
      COMMON/FACETV/A1A2(26),A2A3(26)
      COMMON/HEAD/OCH1,OCH2,CH1,CH2,XKSB,SF(26)
      COMMON/FACET/A1A20(26),A2A30(26)
      COMMON/SHOL/SHRAP(26)
      REAL*4 XP(28),YP(28)
      DATA XP(27),XP(28),YP(27),YP(28)/3.,1.,0.,1./
      DO 101 I=1,26
      U(I)=X(I)
      UDT(I)=X(I+26)
      UDDT(I)=DX(I+26)
      W(I)=X(I+52)
      WDT(I)=X(I+78)
      WDDT(I)=DX(I+78)
      O(I)=X(I+104)
      ODT(I)=X(I+130)
      XP(I)=U(I)/3.
      YP(I)=W(I)/3.0
  101 ODDT(I)=DX(I+130)
      PI=3.14159265
      COMMON KOUNT,LL
      KOUNT=KOUNT+1
C  DETERMINE CORRECT PRINT INCREMENT
      IF(T.LE.LL*.005)RETURN
      CALL PLOT(2.0,0.0,-3)
      CALL LINE(XP,YP,26,1,1,0)
C   CALCULATE SEAT PAN LOAD
      SLC=((ABO(1)-AB(1))*XK(1)-C(1)*ABDT(1))*DSIN(ALPHA(1))
      IF(ABO(1).LE.AB(1)) SLC=0.
C   CALCULATE  SHOULDER STRAP LOAD
      STRAP=SHRAP(18)
      DO 100 I=1,26
      T7Y=XK(I)*(AC(I)-ACO(I))+C(I)*ACDT(I)
      T7X=SF(I)*(XK(I)*(BC(I)-BCO(I))+C(I)*BCDT(I))
      IF(I.EQ.26) GO TO 6
      T6Y=XK(I+1)*(AC(I+1)-ACO(I+1))+C(I+1)*ACDT(I+1)
      T6X=SF(I+1)*(XK(I+1)*(BC(I+1)-BCO(I+1))+C(I+1)*BCDT(I+1))
      GO TO 7
    6 T6Y=0.
```

```
      T6X=0.
    7 FY(I)=T7Y
      FXT(I)=T6X
      FXB(I)=T7X
      FYT(I)=T6Y
      IF(I.EQ.1)GO TO 3000
      OREL1=O(I-1)-OO(I-1)-(O(I)-OO(I))
      T1=XKT(I)*OREL1+CT(I)*(ODT(I-1)-ODT(I))
      GO TO 3001
 3000 T1=XKT(I)*(-O(I)+OO(I))+CT(I)*(-ODT(I))
 3001 SMG(I)=T1
      DIMENSION T51(26)
      T51(I)=XKH(I)*(A1A2(I)-A1A20(I))
      IF(MODE.EQ.1)T51(I)=XKH(I)*H(I)*DSIN(OREL1)
  100 CONTINUE
      PRINT 5,T,SLC,STRAP,PLOAD,O(26),KOUNT
    5 FORMAT(1X,'T=',F5.3,1X,'SEAT LOAD=',F6.1,1X,'STRAP=',F5.1,
     &1X,'LAP=',F6.1,1X,'HEAD ANGLE=',F6.3,1X,'KOUNT=',I3)
      PRINT 210
  210 FORMAT(1H0,'LINK',3X,'AXIAL',6X,'SHEAR',5X,'MOMENT',6X,'FACET')
      PRINT 215
  215 FORMAT(1X,' NO.',1X,'FORCE (LB)',2X,'FORCE (LB)',1X,'(IN-LB)',
     &4X,'FORCE (LB)')
  203 PRINT 201,(I,FY(I),FXB(I),SMG(I),T51(I),I=1,26)
  201 FORMAT(1X,I3,1X,F10.4,1X,F10.4,1X,F10.4,1X,F10.4)
      PRINT 211
  211 FORMAT(1H0,'LINK',6X,'U',9X,'UDT',8X,'UDDT',9X,'W',9X,
     &'WDT',7X,'WDDT')
      PRINT 212
  212 FORMAT(1X,' NO.',4X,'(INS)',4X,'(IN/SEC)',3X,'(IN/SEC2)',
     &5X,'(INS)',4X,'(IN/SEC)',2X,'(IN/SEC2)')
      PRINT 202,(I,U(I),UDT(I),UDDT(I),W(I),WDT(I),WDDT(I),
     &I=1,26)
  202 FORMAT(1X,I3,3X,F10.4,1X,F10.4,1X,F10.4,1X,F10.4,1X,F10.4
     &,1X,F10.4)
      PRINT 213
  213 FORMAT(1H0,'LINK',4X,'O',11X,'ODT',8X,'ODDT')
      PRINT 214
  214 FORMAT(1X,' NO.',2X,'(RAD)',6X,'(RAD/SEC)',2X,'(RAD/SEC2)')
      PRINT 204,(I,O(I),ODT(I),ODDT(I),I=1,26)
  204 FORMAT(1X,I3,F10.4,2X,F10.4,2X,F10.4)
      LL=LL+1
      KOUNT=0
      RETURN
      END
END OF FILE
```

APPENDIX II

DESCRIPTION OF THE INPUT DATA TO THE COMPUTER PROGRAM

The Input Data to the computer program is in the Namelist format. The symbols used are as follows:

u = An array of the x coordinates of the centers of the 26 links at time t = 0.

Units = inches

w = An array of the y coordinates of the centers of the 26 links at time t = 0.

Units = inches

θ = An array of the angles made with the horizontal by the 26 links at time t = 0.

Units = degrees

D = An array of the half-height of each link.

Units = inches

E = An array of the eccentricity of the center of mass of each link.

Units = inches

H = An array of the distance of the facets from the center of each link.

Units = inches

XM = An array of the mass of the 26 links.

Units = $lb\text{-}sec^2/in$

XI = An array of the Moment of Inertia about the center of gravity of each link.

Units = $lb\text{-}in\text{-}sec^2$

XK = An array of axial stiffness of the 26 discs.

Units = lb/in

XKH = An array of the stiffness of the facets.

Units = lb/in

C = Axial damping array.

Units = lb/in/sec

XKT = Rotational stiffness array of the discs.

Units = in-lb/radian

XKS = Strap stiffness array.

Units = lb/in

OCH1 = Relative angle between head and T1 at time of chin-chest contact.

Units = radians

OCH2 = Relative angle between head and T1 (see eqn.).

Units = radians

CH1 = Chin-chest contact resistance stiffness.

Units = lb/rad

CH2 = Chin-chest contact resistance stiffness.

Units = lb/rad

PACC = Horizontal Acceleration Input (see Fig. A.2.1).

SCH1, SCH2, SCH3 = Horizontal Acceleration Input (see Fig. A.2.1).

AA, TT1, TT2 = Vertical Acceleration Input (see Fig. A.2.2).

IC1 = Parameter controlling mode of Input Acceleration.

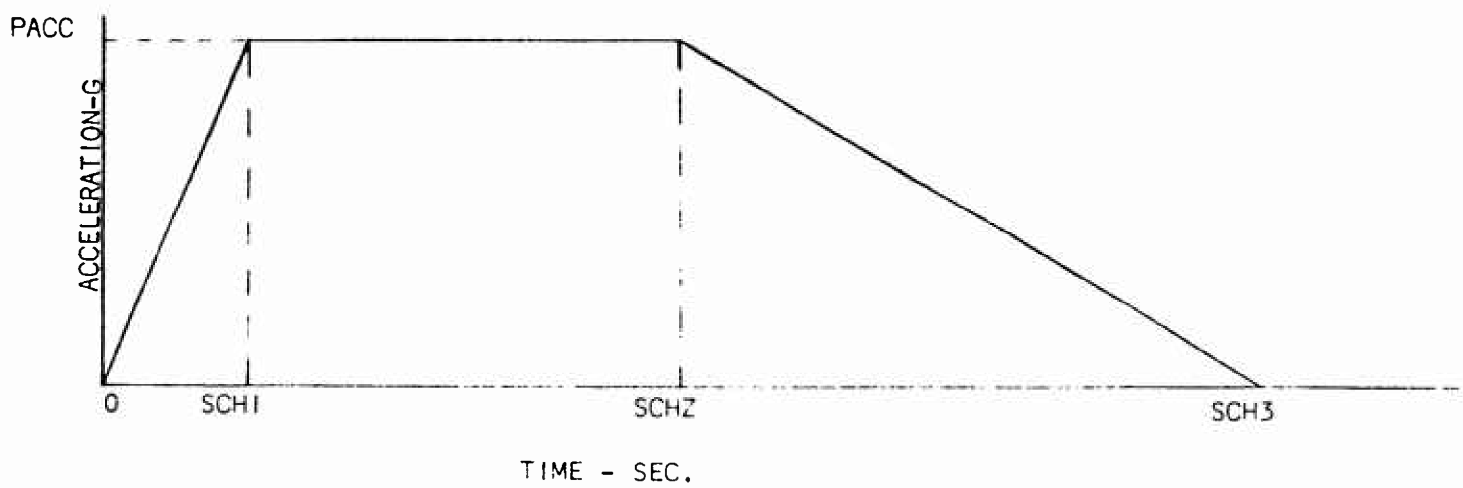

Figure A. 2. 1. Horizontal Acceleration Input

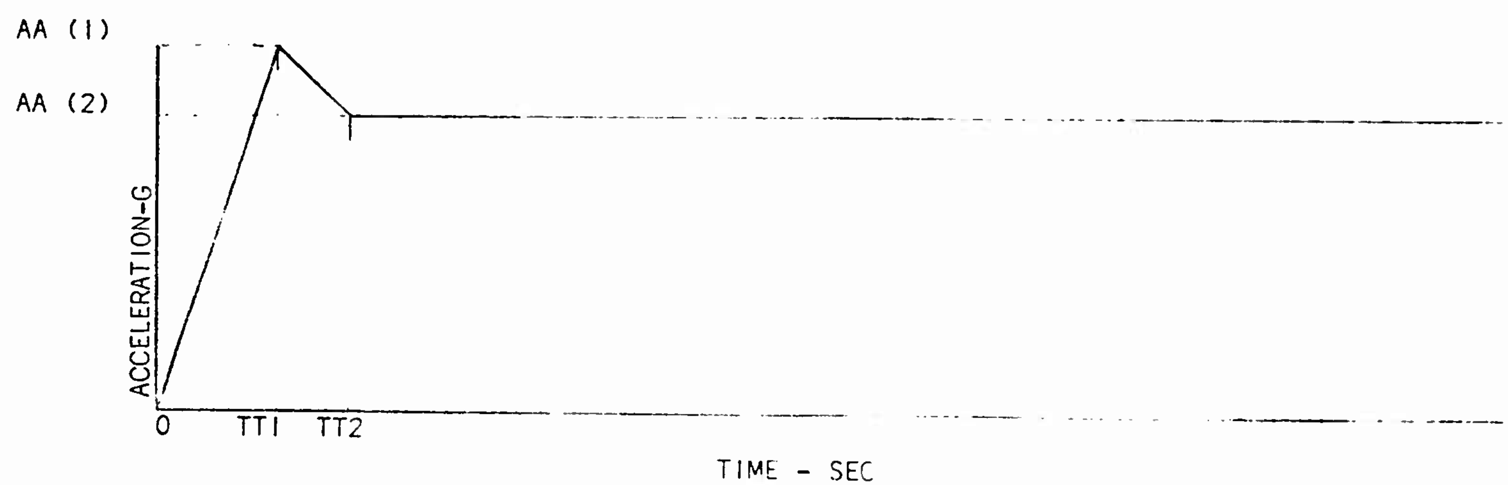

Figure A. 2. 2. Vertical Acceleration Input

INPUT DATA FOR CADAVER 2209 ERECT MODE

```
S2209
&ONE U=2.38,2.690427,2.792220,2.710238,2.57787,2.365789,2.148553,
1.960876,1.852983,1.851235,1.917455,2.030657,2.147288,2.321480,
2.601492,2.937513,3.316967,3.728339,4.127255,4.509113,4.884779,
5.240254,5.592818,5.838168,6.093318,6.713071,
&END
&TWO W=2.18,3.850049,5.391536,6.789083,8.182024,9.565668,10.847358,
12.083129,13.175178,14.175727,15.172790,16.166351,17.10907,17.989807,
18.844269,19.623856,20.327835,21.013809,21.648911,22.235291,22.765686,
23.248913,23.734238,24.252548,24.816177,26.926865,
&END
&THREE O=-12.,-7.,3.,4.,8.,10.,9.,8.,1.5,-2.,-6.5,-6.5,-8.,-16.2,-21.2
-27.2,-30.2,-32.2,-32.,-35.,-36.,-37.,-34.,-21.,-18.,-12.,
&END
&FOUR
D=.8,6*.5,.45,4*.4,3*.35,3*.3,2*.25,5*.2,1.8,
E=0.,2*1.,1.3,1.4,1.7,1.8,1.9,2*2.,.9,4*1.,4*1.,7*0.,
H=2*1.,3*1.1,3*1.2,3*1.1,1.05,.84,.94,.9,.97,.9,.8,.75,.72,.5,
3*.5,.4,.35,
XM=.17686,2*.0125,.0037537,.0035088,.0034175,.00293022,.0066479,
.0056099,.0058787,3*.0057327,.014847,.01515,.016359,.017266,.01787,
3*.0024182,4*.00151138,.028325,
XI=.454,2*.07,4*.01563,.0625,.0534,.0546,.0491,.0476,.0392,.0340,
.0278,.0255,.0184,.0066,.004,.003,.003,.0025,.0016,.0013,
.0013,.2816,
&END
&FIVE
XK=100000.,5*10000.,4*12000.,8*14000.,3*1894.,4*5424.,22190.,
XKH=0.,17*6000.,7*1200.,1200.,
C=240,7*10.,3*15.,2*20.,5*25.,3*2.6,4*1.3,6.34,
XKT=10000.,7*6000.,10*12000.,8*2400.,
CT=20.,7*10.,10*20.,7*1.,2.,
XKS=1000.,7*0.,6*0.,2*0.,0.,20.,8*0.,
&END
&SIX
PACC=9.,SCH1=.01,SCH2=.06,SCH3=.2,AA=6.,5.,TT1=.03,TT2=.04,IC1=0,
MODE=1
&END
&SEVEN
OCH1=1.,OCH2=1.2,,CH1=500.,CH2=1500.,XKSB=500.,
SP=7*.5,19*1.,
&END
ND OF FILE
```

INPUT DATA FOR CADAVER 2209 HYPEREXTENDED MODE

```
T  S2209H
        &ONE U=2.1,2.733448,3.012689,3.109282,3.050843,2.957538,2.852097,
        2.722313,2.626441,2.549727,2.492163,2.439826,2.390106,2.367430,
        2.407533,2.507562,2.656758,2.833289,3.014729,3.196686,3.390055,
        3.578775,3.764130,3.919375,4.044083,4.332906,
        &END
        &TWO W=1.7,3.842850,5.366177,6.759296,8.157768,9.554643,10.849936,
        12.093080,13.188893,14.185863,15.184196,16.182816,17.131500,18.030685,
        18.929260,19.772598,20.558441,21.338577,22.066284,22.741989,23.362518,
        23.932037,24.502487,25.081848,25.668549,27.849045,
        &END
        &THREE O=-17.,-12.,-7.,1.5,4.,3.5,6.5,5.,5.,3.5,3.,3.,3.,-1.,-5.,-10.,
        -12.,-14.,-14.,-17.,-18.,-19.,-16.,-13.,-10.,-7.,
        &END
        &FOUR
        D=1.34,6*.5,.45,4*.4,3*.35,3*.3,2*.25,5*.2,1.8,
        F=0.,2*1.,1.3,1.4,1.7,1.8,1.9,2*2.,.9,4*1.,4*1.,7*0.,
        H=2*1.,3*1.1,3*1.2,3*1.1,1.05,.84,.94,.9,.97,.9,.8,.75,.72,.5,
        3*.5,.4,.35,
        XM=.17686,2*.0125,.0037537,.0035088,.0034175,.00293022,.0066479,
        .0056099,.0053787,3*.0057327,.014847,.01515,.016359,.017266,.01737,
        3*.0024182,4*.0015113B,.028325,
        XI=.454,2*.07,4*.01563,.0625,.0534,.0546,.0491,.0476,.0392,.0340,
        .0278,.0255,.0184,.0066,.004,.003,.003,.0025,.0016,.0013,
        .0013,.2816,
        &END
        &FIVE
        XK=100000.,8*8000.,4*10000.,5*14000.,3*1894.,4*5424.,22390.,
        XKH=0.,5*6000.,12*2000.,7*1200.,1200.,
        C=240,7*10.,3*15.,2*20.,5*25.,3*2.6,4*1.3,6.34,
        XKT=10000.,7*6000.,10*12000.,8*2400.,
        CT=20.,7*10.,10*20.,7*1.,2.,
        XKS=1000.,7*0.,6*0.,2*0.,0.,20.,8*0.,
        &END
        &SIX
        PACC=9.,SCH1=.01,SCH2=.06,SCH3=.2,AA=8.,7.5,TT1=.048,TT2=.058,IC1=0,
        MODE=0
        &END
        &SEVEN
        OCH1=1.,OCH2=1.2,CH1=500.,CH2=1500.,XKSB=150.,
        SF=7*.5,19*1.,
        &END
..D OF FILE
```

INPUT DATA FOR CADAVER #2231 ERECT MODE

```
L  2231
&ONE Z=4.2,5.361970,5.434295,5.364548,5.173203,4.951617,4.811328,
4.659310,4.54405,4.469265,4.421728,4.434802,4.520178,4.696826,4.975723,
5.297739,5.600764,5.856194,6.102103,6.403275,6.821037,7.228933,
7.640957,8.075334,8.472024,9.516200,
&END
&TWO W=3.6,5.905665,8.451958,10.049521,11.6366,13.169313,14.662684,
16.154938,17.524887,18.747589,19.846283,20.895416,21.931312,
22.873199,23.83316,24.811508,25.717148,26.48053,27.215469,27.355555,
28.42717,28.995987,29.561584,30.110458,30.682907,32.732208,
&END
&THREE O=-20.,-5.,1.,5.,10.,5.,6.,5.5,2*3.5,1.,-3.5,-7.,-15.,-18.,4*-18.
-37.,-36.,-35.,-38.,-39.,-27.,-27.,
&END
&FOUR
D=2.36,.55,3*.6,3*.55,.475,2*.45,4*.4,.45,.325,.3,.275,6*.25,1.8,
F=0.,2*1.,1.3,1.4,1.7,1.8,1.9,2*2.,.9,4*1.,4*1.,7*0.,
H=2*1.,3*1.1,3*1.2,3*1.1,1.05,.84,.94,.9,.97,.9,.8,.75,.72,.5,
3*.5,.4,.35,
XM=.19722,.0125,.0125,6*.0044086,4*.01031,5*.0165625,3*.002537,
4*.0015959,.02991,
XI=.454,2*.07,4*.01563,.0625,.0534,.0546,.0491,.0476,.0392,.0340,
.0278,.0255,.0184,.0066,.004,.003,.003,.0025,.0016,.0013,
.0013,.2816,
&END
&FIVE
XK=100000.,2*8000.,6*8000.,4*10310.,5*16562.,3*2537.,4*1595.,39991.,
XKH=0.,5*6000.,12*2000.,7*1200.,1200.,
C=240,7*10.,3*15.,2*20.,5*25.,3*2.6,4*1.3,6.34,
XKT=0.,7*6000.,10*12000.,8*2400.,
CT=20.,7*10.,10*20.,7*1.,2.,
XKS=1000.,7*0.,6*0.,2*0.,0.,20.,8*0.,
&END
&SIX
PACC=9.,SCH1=.01,SCH2=.06,SCH3=.2,AA=6.4,6.,TT1=.03,TT2=.04,IC1=0,
MODE=1
&END
&SEVEN
OCH1=1.2,OCH2=1.4,CH1=300.,CH2=100.,XKSB=150.,
SF=7*.5,19*1.,
&END
ND OF FILE
```

INPUT DATA FOR CADAVER #2231 HYPEREXTENDED MODE

```
EL S2231H
&ONE U=4.2,5.375862,5.502109,5.519561,5.477707,5.388755,5.326816,
5.210068,5.026078,4.786098,4.567543,4.492618,4.457726,4.435055,4.497805,
4.643146,4.838540,4.999030,5.153540,5.376998,5.766094,6.181767,
6.537599,5.350544,7.110828,7.821566,
&END
&TWO W=3.6,6.890363,8.433189,10.033036,11.631574,13.178802,14.677468,
16.172058,17.534485,18.733978,19.808456,20.854826,21.853973,22.852600,
23.850021,24.367798,25.803604,26.592438,27.351868,28.031601,28.611588,
29.173294,29.775635,30.401337,31.050186,33.237610,
&END
&THREE O=-22.,-7.,-1.,0.,4.,2.,3.,7.,9.,15.3,6.,1.,3.5,-2.,-5.,-11.5,
-11.5,-11.5,-11.5,-31.,-39.,-32.,-28.,-24.,-18.,-18.,
&END
&FOUR
D=2.36,.55,3*.6,3*.55,.475,2*.45,4*.4,.45,.325,.3,.275,6*.25,1.8,
E=0.,2*1.,1.3,1.4,1.7,1.8,1.9,2*2.,.9,4*1.,4*1.,7*0.,
H=2*1.,3*1.1,3*1.2,3*1.1,1.05,.84,.94,.9,.97,.9,.8,.75,.72,.5,
3*.5,.4,.35,
XM=.19722,.0125,.0125,6*.0044086,4*.01031,5*.0165625,3*.002537,
4*.0015959,.02991,
XI=.454,2*.07,4*.01563,.0625,.0534,.0546,.0491,.0476,.0392,.0340,
.0273,.0255,.0184,.0066,.004,.003,.003,.0025,.0016,.0013,
.0013,.2816,
&END
&FIVE
XK=100000.,2*8000.,6*8000.,4*10310.,5*16562.,3*2537.,4*1595.,29991.,
XKH=0.,5*5000.,12*2000.,7*1200.,1200.,
C=240,7*10.,3*15.,2*20.,5*25.,3*2.6,4*1.3,6.34,
XKT=0.,7*6000.,10*12000.,8*2400.,
CT=20.,7*10.,10*20.,7*1.,2.,
XKS=1000.,7*0.,6*0.,2*0.,0.,20.,8*0.,
&END
&SIX
PACC=9.,SCH1=.01,SCH2=.06,SCH3=.2,AA=10.,10.,TT1=.065,TT2=.065,IC1=0
PACC=9.,SCH1=.01,SCH2=.06,SCH3=.2,AA=6.4,6.,TT1=.03,TT2=.04,IC1=0,
MODE=0
&SEVEN
OCH1=1.2,OCH2=1.4,CH1=300.,CH2=900.,XKSB=150.,
SF=7*.5,19*1.,
&END
END OF FILE
```

INPUT DATA FOR CADAVER #2413 ERECT MODE

```
I 2413
&ONE H=4.2,4.657293,4.719193,4.644216,4.439836,4.137877,3.871481,
3.725181,3.716866,3.826682,3.995487,4.320004,4.758177,5.211830,5.657092,
6.130437,6.595435,6.994955,7.275577,7.479338,7.647783,7.780452,
7.876976,7.937099,7.960649,7.960649,
&END
&TWO W=3.6,7.179608,8.876950,10.574315,12.250443,13.882444,15.408269,
16.850235,18.195732,19.451920,20.555740,21.625565,22.655151,23.585388,
24.423615,25.224091,26.029480,26.784180,27.478714,28.148148,28.827332,
29.514404,30.207489,30.904663,31.604034,33.904022,
&END
&THREE O=-8.,-4.,1.,5.,10.,11.5,7.,3.5,-5.,-5.,-14.,-21.,-25.,-26.,
-31.,-30.,-30.,-24.,-18.,-15.,-12.,-9.,-6.,-3.,0.,0.,
&END
&FOUR
D=2.36,4*.65,.6,.55,2*.5,4*.46,4*.375,.3,7*.25,1.8,
E=0.,2*0.,6*0.,.9,.7,.65,.5,.2,4*0.,7*.5,1.,
H=2*1.,3*1.1,3*1.2,3*1.1,1.05,.84,.94,.9,.97,.9,.8,.75,.72,.7,
3*.7,.7,.7,
XM=.2147,.0125,.0125,5*.004933,5*.007764,5*.01736,2*.0021,2*.0025,
.0016,2*.0013,.02611,
XI=.454,2*.07,4*.01563,.0625,.0534,.0546,.0491,.0476,.0392,.0340,
.0278,.0255,.0184,.0066,.004,.003,.003,.0025,.0016,.0013,
.0013,.2816,
&END
&FIVE
XK=100000.,2*8000.,5*8000.,5*7764.,5*17360.,2*2100.,2*2500.,1600.,
2*1300.,26110.,
XKH=0.,5*4000.,12*2000.,7*2000.,2000.,
C=240,7*10.,3*15.,2*20.,5*25.,3*2.6,4*1.3,6.34,
XKT=0.,7*4000.,10*10000.,8*2400.,
CT=20.,7*10.,10*20.,7*1.,2.,
XKS=1000.,7*0.,6*0.,2*0.,0.,20.,8*0.,
&END
&SIX
PACE=9.,SCH1=.01,SCH2=.06,SCH3=.2,AA=10.,10.,TT1=.05,TT2=.05,IC1=0,
MODE=1
&END
&SEVEN
OCH1=1.2,OCH2=1.4,CH1=300.,CH2=900.,XKSB=250.,
SF=7*.5,19*1.,
&END
END OF FILE
```

INPUT DATA FOR CADAVER #2413 HYPEREXTENDED MODE

```
SI S2413H
        &ONE
        H=4.2,4.731940,4.908710,4.970212,5.008149,4.964955,4.905202,4.816681,
        4.756063,4.742100,4.782191,4.935352,5.207064,5.509657,5.818257,
        6.160552,6.493831,6.770370,6.938837,7.039748,7.116378,7.173037,
        7.217510,7.241061,7.241061,7.241061,
        &END
        &TWO
        W=3.6,7.161468,8.855491,10.554238,12.252575,13.902007,15.450533,16.8979
        18.245246,19.506104,20.624329,21.731750,22.817215,23.806976,24.704529,
        25.569183,26.437393,27.245285,27.975159,28.557740,29.363410,30.061081,
        30.759628,31.459000,32.158997,34.458984,
        &END
        &THREE
        O=-10.,-5.,-1.5,-3.,1.5,1.5,3.5,3.5,1.,0.,-5.,-12.,-17.,-17.,-22.,
        -21.,-21.,-15.,-9.,-7.,-5.,-4.,-3.,3*0.,
        &END
        &FOUR
        D=2.36,4*.65,.6,.55,2*.5,4*.46,4*.375,.3,7*.25,1.8,
        F=0.,2*0.,6*0.,.9,.7,.65,.5,.2,4*0.,7*.5,1.,
        U=2*1.,3*1.1,3*1.2,3*1.1,1.05,.84,.94,.9,.97,.9,.8,.75,.72,.7,
        3*.7,.7,.7,
        XM=.2147,.0125,.0125,5*.004933,5*.007764,5*.01736,2*.0021,2*.0025,
        .0016,2*.0013,.02611,
        YI=.454,2*.07,4*.01563,.0625,.0534,.0546,.0491,.0476,.0392,.0340,
        .0278,.0255,.0184,.0066,.004,.003,.003,.0025,.0015,.0013,
        .0013,.2816,
        &END
        &FIVE
        XK=100000.,2*8000.,5*3000.,5*7764.,5*17360.,2*2100.,2*2500.,1600.,
        2*1300.,26110.,
        XKH=0.,5*4000.,12*2000.,7*2000.,2000.,
        C=240,7*10.,3*15.,2*20.,5*25.,3*2.6,4*1.3,6.34,
        XKT=0.,7*4000.,10*10000.,8*2400.,
        CT=20.,7*10.,10*20.,7*1.,2.,
        XKS=1000.,7*0.,6*0.,2*0.,0.,20.,8*0.,
        &END
        &SIX
        PACC=3.,SCH1=.01,SCH2=.06,SCH3=.2,AA=5.5,5.,TT1=.035,TT2=.04,IC1=0,
        MODE=0
        &END
        &SEVEN
        OCH1=1.2,OCH2=1.4,CH1=300.,CH2=900.,XKSB=50.,
        SF=7*.5,19*1.,
        &END
END OF FILE
```

OUTPUT DATA FOR CADAVER #2413 HYPEREXTENDED MODE
FOR INPUT DATA SHOWN ON P. 182

PLOT DESCRIPTION GENERATION BEGINS
T=0.000 SEAT LOAD= 0.0 STRAP= 0.0 LAP= 0.0 HEAD ANGLE= 0.0 KOUNT= 2

LINK NO.	AXIAL FORCE (LB)	SHEAR FORCE (LB)	MOMENT (IN-LB)	FACET FORCE (LB)
1	-0.0089	0.0	-0.0	0.0
2	-0.0000	0.0000	0.0000	0.0000
3	0.0000	-0.0000	-0.0000	-0.0000
4	-0.0000	-0.0000	0.0000	-0.0000
5	-0.0000	-0.0000	-0.0000	-0.0000
6	-0.0000	-0.0000	0.0000	0.0
7	-0.0000	-0.0000	-0.0000	0.0
8	-0.0000	-0.0000	0.0000	-0.0000
9	-0.0000	-0.0000	-0.0000	0.0
10	0.0000	0.0000	-0.0000	0.0
11	0.0000	0.0000	-0.0000	0.0
12	-0.0000	-0.0000	-0.0000	0.0
13	-0.0000	-0.0000	-0.0000	0.0
14	-0.0000	-0.0000	-0.0000	0.0
15	-0.0000	-0.0000	0.0000	0.0
16	-0.0000	-0.0000	0.0000	0.0
17	-0.0000	-0.0000	0.0000	0.0
18	-0.0000	-0.0000	0.0000	0.0
19	0.0	0.0	0.0	0.0
20	0.0	0.0	0.0	0.0
21	0.0	0.0	0.0	0.0
22	0.0	0.0	0.0	0.0
23	0.0	0.0	0.0	0.0
24	0.0	0.0	0.0	0.0
25	0.0	0.0	0.0	0.0
26	0.0	0.0	0.0	0.0

LINK NO.	U (INS)	UDT (IN/SEC)	UDDT (IN/SEC2)	W (INS)	WDT (IN/SEC)	WDDT (IN/SEC2)
1	4.2000	0.0	0.0	3.6000	-0.0001	-2.9944
2	4.7319	-0.0000	0.0000	7.1615	-0.0001	-3.0356
3	4.9087	0.0000	-0.0000	8.8555	-0.0001	-3.0360
4	4.9702	0.0000	0.0000	10.5542	-0.0001	-3.0360
5	5.0081	0.0000	0.0000	12.2526	-0.0001	-3.0360
6	4.9650	-0.0000	0.0000	13.9020	-0.0001	-3.0360
7	4.9952	-0.0000	0.0000	15.4506	-0.0001	-3.0360
8	4.8167	0.0000	-0.0000	16.8979	-0.0001	-3.0360
9	4.7561	-0.0000	0.0000	18.2462	-0.0001	-3.0360
10	4.7421	-0.0000	-0.0000	19.5061	-0.0001	-3.0360
11	4.7822	0.0000	-0.0000	20.6243	-0.0001	-3.0360
12	4.9354	0.0000	0.0000	21.7317	-0.0001	-3.0360
13	5.2071	0.0000	0.0000	22.8172	-0.0001	-3.0360
14	5.5097	0.0000	0.0000	23.8070	-0.0001	-3.0360
15	5.8183	0.0000	0.0000	24.7045	-0.0001	-3.0360
16	6.1506	0.0000	0.0000	25.5692	-0.0001	-3.0360
17	6.4938	0.0000	0.0000	26.4374	-0.0001	-3.0360
18	6.7704	0.0	0.0000	27.2453	-0.0001	-3.0360
19	6.9389	0.0	-0.0	27.9752	-0.0001	-3.0360
20	7.0397	0.0	-0.0	28.6677	-0.0001	-3.0360
21	7.1164	0.0	-0.0	29.3634	-0.0001	-3.0360

22	7.1730	0.0	-0.0	30.0611	-0.0001	-3.0360
23	7.2175	0.0	-0.0	30.7596	-0.0001	-3.0360
24	7.2411	0.0	-0.0	31.4590	-0.0001	-3.0360
25	7.2411	0.0	-0.0	32.1590	-0.0001	-3.0360
26	7.2411	0.0	-0.0	34.4590	-0.0001	-3.0360

LINK NO.	Q (RAD)	QDT (RAD/SEC)	QDDT (RAD/SEC2)
1	-0.1745	0.0	0.0
2	-0.1047	-0.0000	-0.0000
3	-0.0262	-0.0000	-0.0000
4	-0.0524	-0.0000	-0.0000
5	0.0262	0.0000	0.0000
6	0.0262	0.0000	0.0000
7	0.0611	0.0000	0.0000
8	0.0611	-0.0000	-0.0000
9	0.0175	-0.0000	-0.0000
10	-0.0000	0.0000	0.0000
11	-0.0873	-0.0000	0.0000
12	-0.2094	-0.0000	-0.0000
13	-0.2967	-0.0000	-0.0000
14	-0.2967	0.0000	0.0000
15	-0.3840	0.0000	0.0000
16	-0.3665	0.0000	0.0000
17	-0.3665	0.0000	0.0000
18	-0.2618	0.0	0.0000
19	-0.1571	0.0	0.0
20	-0.1222	0.0	0.0
21	-0.0873	0.0	0.0
22	-0.0698	0.0	0.0
23	-0.0524	0.0	0.0
24	0.0	0.0	0.0
25	0.0	0.0	0.0
26	0.0	0.0	0.0

T=0.005 SEAT LOAD= 69.4 STRAP= 0.0 LAP= 0.0 HEAD ANGLE=-0.000 KOUNT= 52

LINK NO.	AXIAL FORCE (LB)	SHEAR FORCE (LB)	MOMENT (IN-LB)	FACET FORCE (LB)
1	-69.3538	0.0	-0.0	0.0
2	-4.3245	0.3790	0.0934	-1.4372
3	-2.6305	0.0375	-0.0631	-0.8384
4	-1.1193	-0.0671	-0.0076	-0.3684
5	-0.6894	-0.0349	-0.0139	-0.2257
6	-0.4056	-0.0413	0.0012	-0.1171
7	-0.2405	-0.0248	-0.0058	-0.0359
8	-0.1223	-0.0173	0.0003	-0.0157
9	-0.0631	-0.0087	0.0003	-0.0069
10	-0.0230	-0.0027	0.0008	-0.0022
11	-0.0081	-0.0012	-0.0006	-0.0009
12	-0.0027	-0.0004	-0.0002	-0.0003
13	-0.0009	-0.0001	-0.0001	-0.0001
14	-0.0004	-0.0000	-0.0000	-0.0000
15	-0.0001	-0.0000	-0.0000	-0.0000
16	-0.0000	-0.0000	-0.0000	-0.0000
17	-0.0000	-0.0000	-0.0000	-0.0000
18	-0.0000	-0.0000	-0.0000	-0.0000
19	-0.0000	0.0000	0.0000	0.0000
20	-0.0000	0.0000	0.0000	0.0000
21	0.0000	0.0000	0.0000	0.0000
22	-0.0000	0.0000	-0.0000	-0.0000

23	-0.0000	0.0000	-0.0000	-0.0000
24	-0.0000	0.0000	-0.0000	-0.0000
25	-0.0000	-0.0000	0.0000	-0.0000
26	0.0000	0.0000	-0.0000	-0.0000

LINK NO.	U (INS)	UDT (IN/SEC)	UDDT (IN/SEC2)	W (INS)	WDT (IN/SEC)	WDDT (IN/SEC2)
1	4.2000	0.0	0.0	3.5995	-0.1812	-9.8374
2	4.7819	0.0032	-0.9588	7.1606	-0.4096	-81.6862
3	4.9087	0.0139	9.3976	8.8544	-0.5508	-141.7276
4	4.9702	0.0115	10.5546	10.5531	-0.6296	-187.6244
5	5.0082	0.0084	8.5493	12.2514	-0.6823	-224.7842
6	4.9650	0.0043	5.1978	13.9008	-0.7162	-253.5163
7	4.9052	0.0018	2.6653	15.4494	-0.7379	-275.5524
8	4.8167	0.0007	1.1402	16.8967	-0.7497	-289.7239
9	4.7561	0.0002	0.4115	18.2450	-0.7556	-297.7739
10	4.7421	0.0001	0.1412	19.5048	-0.7578	-301.2958
11	4.7822	0.0001	0.1092	20.6231	-0.7586	-302.7544
12	4.9354	0.0000	0.0585	21.7305	-0.7589	-303.3195
13	5.2071	0.0000	0.0192	22.8160	-0.7590	-303.5303
14	5.5097	0.0000	0.0069	23.8057	-0.7590	-303.5808
15	5.8183	0.0000	0.0021	24.7033	-0.7590	-303.5950
16	6.1505	0.0000	0.0005	25.5679	-0.7590	-303.5987
17	6.4938	0.0000	0.0001	26.4361	-0.7590	-303.5996
18	6.7704	0.0000	0.0000	27.2440	-0.7590	-303.5998
19	6.9389	-0.0000	0.0000	27.9739	-0.7590	-303.5999
20	7.0397	-0.0000	-0.0000	28.6665	-0.7590	-303.5999
21	7.1164	-0.0000	-0.0000	29.3621	-0.7590	-303.5999
22	7.1730	-0.0000	-0.0000	30.0598	-0.7590	-303.5999
23	7.2175	-0.0000	-0.0000	30.7584	-0.7590	-303.5999
24	7.2411	-0.0000	-0.0000	31.4577	-0.7590	-303.5999
25	7.2411	-0.0000	0.0000	32.1577	-0.7590	-303.5999
26	7.2411	0.0000	-0.0000	34.4577	-0.7590	-303.5999

LINK NO.	O (RAD)	ODT (RAD/SEC)	ODDT (RAD/SEC2)
1	-0.1745	0.0	0.0
2	-0.1047	-0.0166	-10.9579
3	-0.0262	-0.0062	-5.4367
4	-0.0524	-0.0041	-2.8704
5	0.0262	-0.0010	-0.6882
6	0.0262	-0.0016	-1.7471
7	0.0611	0.0001	0.2856
8	0.0611	0.0000	0.0721
9	0.0175	-0.0000	-0.0116
10	-0.0000	-0.0001	-0.2368
11	-0.0873	-0.0000	-0.0968
12	-0.2094	-0.0000	-0.0334
13	-0.2967	-0.0000	-0.0088
14	-0.2967	-0.0000	-0.0022
15	-0.3840	-0.0000	-0.0002
16	-0.3665	-0.0000	-0.0000
17	-0.3665	0.0000	0.0000
18	-0.2618	0.0000	-0.0000
19	-0.1571	0.0000	-0.0000
20	-0.1222	-0.0000	-0.0000
21	-0.0873	-0.0000	-0.0000
22	-0.0698	-0.0000	-0.0000
23	-0.0524	-0.0000	-0.0000
24	-0.0000	-0.0000	-0.0000

25	-0.0000	0.0000	-0.0000
26	-0.0000	-0.0000	0.0000

T=0.010 STAT LOAD= 158.7 STRAP= 0.0 LAP= 0.0 HEAD ANGLE= 0.000 KOUNT= [illegible]

LINK NO.	AXIAL FORCE (LB)	SHEAR FORCE (LB)	MOMENT (IN-LB)	FACET FORCE (LB)
1	-158.6685	0.0	-0.0	0.0
2	-21.2163	0.9150	1.1665	-7.6494
3	-15.1601	0.2270	-0.4590	-6.6071
4	-10.2655	-0.3738	-0.3981	-4.7633
5	-8.6628	-0.2655	-0.2691	-3.9026
6	-7.4140	-0.6226	0.1565	-2.[illegible]473
7	-6.7328	-0.5331	-0.2869	-1.5947
8	-5.4699	-0.6990	0.0787	-1.0219
9	-4.3231	-0.5801	0.1613	-0.7581
10	-2.9300	-0.3777	0.3071	-0.4522
11	-1.8713	-0.2857	-0.0785	-0.3294
12	-1.2055	-0.1608	-0.0995	-0.2112
13	-0.8023	-0.0721	-0.0702	-0.1334
14	-0.6473	-0.0396	-0.0389	-0.0497
15	-0.3391	-0.0363	-0.0197	-0.0247
16	-0.1673	-0.0085	-0.0048	-0.0111
17	-0.0764	-0.0057	-0.0009	-0.0046
18	-0.0249	-0.0022	-0.0005	-0.0018
19	-0.0025	-0.0005	0.0004	-0.0007
20	-0.0012	-0.0004	-0.0000	-0.0004
21	-0.0006	-0.0003	-0.0001	-0.0002
22	-0.0002	-0.0001	-0.0000	-0.0001
23	-0.0001	-0.0000	-0.0000	-0.0000
24	-0.0000	-0.0000	-0.0000	-0.0000
25	-0.0000	-0.0000	-0.0000	-0.0000
26	-0.0000	-0.0000	-0.0000	-0.0000

LINK NO.	U (INS)	UDT (IN/SEC)	UDDT (IN/SEC2)	W (INS)	WDT (IN/SEC)	WDDT (IN/SEC2)
1	4.2000	0.0	0.0	3.5986	-0.1761	-2.4774
2	4.7813	-0.0056	3.2428	7.1579	-0.6416	-35.5436
3	4.9099	0.0899	18.9372	8.8503	-1.0183	-70.7552
4	4.9706	0.1469	37.5969	10.5480	-1.3283	-107.8425
5	5.0085	0.1410	42.9223	12.2454	-1.6148	-148.4792
6	4.9652	0.1086	36.8625	13.8941	-1.8872	-195.8347
7	4.9053	0.0772	26.4347	15.4421	-2.1610	-255.4678
8	4.8168	0.0396	12.6438	16.8888	-2.4068	-320.1218
9	4.7561	0.0175	4.4458	18.2367	-2.6117	-385.5251
10	4.7421	0.0104	3.1699	19.4963	-2.7639	-446.2326
11	4.7822	0.0150	7.1473	20.6144	-2.8697	-497.1308
12	4.9354	0.0150	9.0698	21.7217	-2.9436	-539.3882
13	5.2071	0.0092	6.7605	22.8071	-2.9959	-574.0739
14	5.5097	0.0058	6.0060	23.7969	-3.0156	-538.4894
15	5.8183	0.0041	4.1022	24.6944	-3.0262	-597.2217
16	6.1606	0.0021	2.3375	25.5591	-3.0315	-602.1079
17	6.4338	0.0010	1.2229	26.4273	-3.0339	-604.6239
18	6.7704	0.0005	0.6770	27.2352	-3.0349	-605.7092
19	6.9389	0.0002	0.2958	27.9650	-3.0355	-606.4221
20	7.0397	0.0001	0.1531	28.6576	-3.0357	-606.8035
21	7.1164	0.0001	0.0897	29.3533	-3.0359	-606.9965
22	7.1730	0.0000	0.0470	30.0510	-3.0359	-607.1062
23	7.2175	0.0000	0.0263	30.7495	-3.0360	-607.1552
24	7.2411	0.0000	0.0128	31.4489	-3.0360	-607.1805
25	7.2411	0.0000	0.0020	32.1489	-3.0360	-607.1966

26	7.2411	0.0000	0.0008	34.4489	-3.0360	-607.1938

LINK NO.	O (RAD)	ODT (RAD/SEC)	ODDT (RAD/SEC2)
1	-0.1745	0.0	0.0
2	-0.1050	-0.0784	-7.2563
3	-0.0263	-0.0595	-10.9915
4	-0.0524	-0.0207	-4.8382
5	0.0262	0.0049	2.5905
6	0.0261	-0.0085	2.9888
7	0.0611	0.0196	9.3183
8	0.0611	0.0102	5.9471
9	0.0175	-0.0006	-0.2913
10	-0.0000	-0.0190	-8.8938
11	-0.0873	-0.0165	-10.0114
12	-0.2095	-0.0106	-7.6129
13	-0.2967	-0.0057	-4.8740
14	-0.2967	-0.0024	-2.2625
15	-0.3840	-0.0006	-0.6934
16	-0.3665	-0.0001	-0.1262
17	-0.3665	0.0000	0.0124
18	-0.2618	0.0001	0.0753
19	-0.1571	-0.0001	-0.0820
20	-0.1222	-0.0001	-0.0824
21	-0.0873	-0.0000	-0.0555
22	-0.0698	-0.0000	-0.0349
23	-0.0524	-0.0000	-0.0167
24	-0.0000	-0.0000	-0.0062
25	-0.0000	-0.0000	-0.0011
26	0.0000	0.0000	0.0000

T=0.015 SEAT LOAD= 256.2 STRAP= 0.0 LAP= 0.0 HEAD ANGLE= 0.000 KOUNT= 50

LINK NO.	AXIAL FORCE (LB)	SHEAR FORCE (LB)	MOMENT (IN-LB)	FACET FORCE (LB)
1	-256.1528	0.0	-0.0	0.0
2	-44.9629	2.0937	3.0077	-16.8478
3	-35.1158	0.9415	-0.6987	-16.0900
4	-27.3425	-0.3632	-1.2266	-13.7035
5	-24.8138	-0.1494	-1.1285	-12.4644
6	-23.4140	-1.4688	0.2362	-10.2284
7	-24.1573	-1.4764	-1.3147	-6.1495
8	-22.4561	-2.5629	0.4442	-4.7036
9	-20.3051	-2.5013	1.8062	-4.0402
10	-17.2881	-1.8758	2.4448	-3.1733
11	-14.1631	-1.7004	0.5857	-2.8398
12	-11.8095	-1.0248	-0.2396	-2.4601
13	-10.0919	-0.3364	-0.5175	-2.1026
14	-9.6655	-0.0036	-0.9336	-1.0206
15	-7.0230	-0.4185	-0.6579	-0.7118
16	-4.8212	-0.1227	-0.3571	-0.4694
17	-3.0452	-0.2076	-0.1465	-0.2737
18	-1.5853	-0.1360	-0.0710	-0.1380
19	-0.2424	-0.0580	0.0313	-0.1100
20	-0.1563	-0.0544	0.0060	-0.0760
21	-0.1054	-0.0441	-0.0034	-0.0486
22	-0.0563	-0.0287	-0.0055	-0.0343
23	-0.0265	-0.0158	-0.0078	-0.0228
24	-0.0166	-0.0108	-0.0057	-0.0157
25	-0.0132	-0.0092	-0.0019	-0.0111
26	-0.0211	-0.0143	-0.0005	-0.0015

LINK NO.	U (INS)	UDT (IN/SEC)	UDDT (IN/SEC2)	W (INS)	WDT (IN/SEC)	WDDT (IN/SEC2)
1	4.2000	0.0	0.0	3.5977	-0.2032	-5.7342
2	4.7820	0.0257	2.9705	7.1541	-0.8735	-55.0492
3	4.9096	0.1771	12.8290	8.8442	-1.4505	-100.3174
4	4.9717	0.2940	17.1571	10.5399	-1.9601	-146.8375
5	5.0097	0.3363	23.2673	12.2354	-2.4402	-190.7900
6	4.9662	0.3011	26.2250	13.8822	-2.9152	-233.6778
7	4.9961	0.2089	19.1195	15.4281	-3.4453	-283.9289
8	4.8171	0.0725	-1.1170	16.8729	-3.9802	-339.2724
9	4.7562	-0.0153	-20.2944	18.2190	-4.4991	-399.2519
10	4.7421	-0.0415	-31.9394	19.4770	-4.9830	-463.3211
11	4.7323	-0.0147	-32.9665	20.5937	-5.4234	-533.7131
12	4.9355	0.0277	-20.4886	21.6999	-5.8308	-609.9673
13	5.2072	0.0582	1.8596	22.7844	-6.2108	-691.1235
14	5.5099	0.0990	27.2260	23.7737	-6.3922	-735.6436
15	5.8184	0.1020	39.1943	24.6709	-6.5277	-774.1833
16	6.1607	0.0864	41.0406	25.5354	-6.6230	-805.0691
17	6.4333	0.0674	37.5344	26.4035	-6.6837	-826.7579
18	6.7704	0.0528	32.7380	27.2113	-6.7155	-839.2273
19	6.9389	0.0317	21.6996	27.9411	-6.7535	-859.0843
20	7.0398	0.0206	14.9533	28.6336	-6.7804	-874.6895
21	7.1164	0.0148	11.1498	29.3293	-6.7977	-885.5727
22	7.1730	0.0106	8.4451	30.0269	-6.8102	-893.9357
23	7.2175	0.0074	6.0438	30.7255	-6.8185	-900.1527
24	7.2411	0.0041	3.4648	31.4249	-6.8245	-905.0673
25	7.2411	0.0010	0.9161	32.1248	-6.8296	-909.4159
26	7.2411	0.0006	0.6002	34.4248	-6.8302	-909.9491

LINK NO.	O (RAD)	ODT (RAD/SEC)	ODDT (RAD/SEC2)
1	-0.1745	0.0	0.0
2	-0.1054	-0.1030	-7.1704
3	-0.0267	-0.0897	-3.2778
4	-0.0526	-0.0522	-4.3664
5	0.0262	0.0007	-2.5202
6	0.0261	0.0064	-0.5838
7	0.0614	0.0847	12.1309
8	0.0613	0.0631	14.0516
9	0.0175	0.0119	7.1126
10	-0.0062	-0.0498	2.9585
11	-0.0875	-0.0876	-12.2401
12	-0.2097	-0.1020	-27.4462
13	-0.2369	-0.0979	-35.2306
14	-0.2968	-0.0620	-27.2707
15	-0.3840	-0.0325	-17.5318
16	-0.3665	-0.0127	-8.5570
17	-0.3665	-0.0029	-2.7734
18	-0.2618	0.0023	0.5856
19	-0.1571	-0.0038	-1.5999
20	-0.1222	-0.0054	-2.6832
21	-0.0873	-0.0050	-2.7469
22	-0.0698	-0.0038	-2.2004
23	-0.0524	-0.0019	-1.0164
24	-0.0000	-0.0005	-0.1297
25	-0.0000	-0.0001	-0.0455
26	0.0000	0.0000	0.0149

T=0.020 SEAT LOAD= 368.3 STRAP= 0.0 LAP= 0.0 HEAD ANGLE=-0.000 KOUNT= [illegible]

LINK	AXIAL	SHEAR	MOMENT	FACET

NO.	FORCE (LB)	FORCE (LB)	(IN-LB)	FORCE (LB)
1	-358.3431	0.0	-0.0	0.0
2	-73.7756	3.8118	5.5239	-30.1014
3	-64.3979	2.1058	-1.2085	-30.2877
4	-53.3015	-0.3473	-2.1014	-27.2247
5	-50.1273	0.1807	-2.2860	-25.7949
6	-48.7199	-2.5249	0.2210	-22.2436
7	-52.3260	-2.6198	-3.4578	-14.1055
8	-50.7681	-5.2956	0.5248	-11.3324
9	-48.0782	-5.5623	4.4600	-10.1274
10	-44.0833	-4.3503	6.5294	-8.6972
11	-39.6226	-4.2644	4.7227	-8.0366
12	-35.3978	-2.3305	3.3005	-7.4792
13	-32.5056	0.1727	1.1793	-7.1269
14	-32.4749	1.7149	-3.1690	-3.8360
15	-26.1441	-0.2407	-3.4106	-3.1732
16	-19.3613	0.1742	-2.9309	-2.5232
17	-14.2153	-0.8077	-1.9535	-1.7285
18	-8.5784	-0.8788	-1.2218	-1.0224
19	-2.0233	-0.5037	0.0521	-1.3288
20	-1.6228	-0.5156	0.0328	-1.0427
21	-1.3435	-0.4580	-0.0133	-0.7678
22	-0.3264	-0.3414	-0.0483	-0.6324
23	-0.5627	-0.2179	-0.0805	-0.5591
24	-0.4345	-0.1779	-0.0383	-0.4647
25	-0.4003	-0.1788	0.0493	-0.3818
26	-0.6394	-0.3151	-0.0076	-0.0502

LINK NO.	U (INS)	UDT (IN/SEC)	UDDT (IN/SEC2)	W (INS)	WDT (IN/SEC)	WDDT (IN/SEC2)
1	4.2000	0.0	0.0	3.5366	-1.2325	-6.5647
2	4.7821	0.0130	-2.1273	7.1490	-1.1743	-66.4893
3	4.3106	0.2114	2.0394	8.8356	-2.0066	-123.3755
4	4.9733	0.3402	3.2433	10.5281	-2.7732	-180.4688
5	5.0115	0.3699	-3.0429	12.2206	-3.5110	-237.0658
6	4.9676	0.3158	-12.8976	13.8644	-4.2514	-295.3914
7	4.9072	0.2040	-23.6449	15.4070	-5.0792	-361.2489
8	4.8173	-0.0162	-45.8182	16.8483	-5.9182	-426.1704
9	4.7557	-0.2228	-73.3331	18.1911	-6.7536	-491.4874
10	4.7413	-0.3552	-98.1235	19.4459	-7.5523	-553.6431
11	4.7815	-0.3691	-117.1207	20.5596	-8.3208	-614.6724
12	4.9351	-0.2692	-93.7994	21.6628	-9.0725	-675.5332
13	5.2073	-0.0763	-55.4425	22.7444	-9.8168	-738.3854
14	5.5106	0.1795	-0.1337	23.7322	-10.2157	-779.0969
15	5.8136	0.3534	54.1446	24.6283	-10.5456	-816.6136
16	6.1619	0.4488	99.5602	25.4919	-10.8043	-849.0234
17	6.4351	0.4856	131.9242	26.3594	-10.9841	-873.6306
18	6.7715	0.4831	148.6395	27.1669	-11.0913	-890.6601
19	6.9397	0.3842	136.6217	27.8961	-11.2986	-933.1855
20	7.0404	0.3006	116.7656	28.5882	-11.4818	-976.0797
21	7.1169	0.2379	95.6976	29.2835	-11.6256	-1014.0234
22	7.1734	0.1849	74.3324	29.9809	-11.7497	-1050.7753
23	7.2178	0.1307	51.1796	30.6792	-11.8670	-1092.7176
24	7.2412	0.0754	29.3489	31.3783	-11.9777	-1136.7167
25	7.2411	0.0279	13.0503	32.0781	-12.0848	-1130.3031
26	7.2411	0.0247	13.2232	34.3781	-12.0969	-1185.5164

LINK NO.	O (RAD)	ODT (RAD/SEC)	ODDT (RAD/SEC2)
1	-0.1745	0.0	0.0

2	-0.1061	-0.1410	-4.5175
3	-0.1272	-0.1086	-2.9670
4	-0.0529	-0.0546	1.1959
5	0.0262	0.0095	4.8952
6	0.0262	0.0020	2.6342
7	0.0611	0.1326	13.5318
8	0.0618	0.1457	19.5073
9	0.1177	0.0950	18.8646
10	-0.0094	-0.0064	8.6943
11	-0.0881	-0.1327	-11.4028
12	-0.2106	-0.2592	-35.3015
13	-0.2979	-0.3375	-56.4387
14	-0.2976	-0.2980	-63.7421
15	-0.3846	-0.2247	-59.7516
16	-0.3668	-0.1414	-47.2580
17	-0.3667	-0.0726	-31.5554
18	-0.2618	-0.0233	-17.1822
19	-0.1571	-0.0082	-0.2904
20	-0.1222	-0.0046	8.0627
21	-0.0873	-0.0007	12.7457
22	-0.0698	0.0056	15.0320
23	-0.0524	0.0132	13.7951
24	0.0000	0.0129	8.6836
25	-0.0000	-0.0015	-0.8869
26	-0.0000	-0.0004	-0.5578

T=0.025 SEAT LOAD= 498.0 STRAP= 0.2 LAP= 0.0 HEAD ANGLE=-0.000 KOUNT= 50

LINK NO.	AXIAL FORCE (LB)	SHEAR FORCE (LB)	MOMENT (IN-LB)	FACET FORCE (LB)
1	-497.9787	0.0	-0.0	0.0
2	-124.7026	6.1921	8.4700	-48.7643
3	-105.2420	3.6905	-1.9416	-50.3412
4	-91.5102	-0.3064	-3.2961	-46.6441
5	-86.4836	0.6765	-3.8439	-45.0526
6	-85.2211	-3.9956	0.2770	-39.7364
7	-92.3688	-4.1352	-6.7437	-25.8630
8	-91.4626	-9.0895	0.2188	-21.3105
9	-88.0129	-10.0441	7.9690	-19.1861
10	-82.6187	-8.2887	13.5005	-16.6658
11	-76.4956	-8.4642	13.6630	-15.2402
12	-70.3469	-8.5624	12.5042	-14.2878
13	-64.7390	1.0047	7.6918	-14.0523
14	-65.1672	4.9855	-3.9322	-7.5888
15	-53.1864	1.5006	-6.9685	-6.7709
16	-41.3606	2.1044	-8.1151	-5.8885
17	-30.6023	-0.6187	-7.1813	-4.4662
18	-20.2720	-1.6215	-5.7498	-3.0270
19	-6.9912	-1.2892	-1.1132	-5.3146
20	-5.4781	-1.4442	-0.6920	-4.5096
21	-5.1532	-1.4091	-0.5195	-3.6057
22	-4.2318	-1.1873	-0.3214	-3.1722
23	-3.0553	-0.8510	-0.0069	-3.1414
24	-2.6159	-0.7463	0.3887	-2.9294
25	-2.5322	-0.8033	0.8429	-2.5803
26	-4.5276	-1.4723	0.0190	-0.3229

LINK NO.	U (INS)	UDT (IN/SEC)	UDDT (IN/SEC2)	W (INS)	WDT (IN/SEC)	WDDT (IN/SEC2)
1	4.2000	0.0	0.0	3.5953	-0.2697	-7.7229
2	4.7822	0.0120	-2.0461	7.1423	-1.5263	-68.5754

3	4.9117	0.2047	-4.1136	8.8240	-2.6588	-125.8265
4	4.9750	0.3184	-12.9571	10.5119	-3.7120	-178.5396
5	5.0133	0.3069	-31.5008	12.2000	-4.7237	-228.0604
6	4.9692	0.1666	-62.3267	13.8394	-5.7371	-277.4472
7	4.9077	-0.0888	-105.8897	15.3770	-6.8750	-334.8293
8	4.8162	-0.4946	-151.8477	16.8134	-8.0319	-395.3503
9	4.7532	-0.8530	-181.5591	18.1511	-9.1846	-456.1401
10	4.7379	-1.0629	-185.6897	19.4012	-10.2792	-512.9648
11	4.7781	-1.0562	-165.6727	20.5103	-11.3295	-566.2834
12	4.9324	-0.8345	-127.4020	21.6091	-12.3651	-621.9371
13	5.2061	-0.4169	-73.5935	22.6862	-13.4123	-683.7598
14	5.5115	0.1413	-7.8746	23.6715	-14.0172	-727.5835
15	5.8220	0.6286	59.9938	24.5655	-14.5460	-772.7781
16	6.1655	1.0283	131.1100	25.4273	-14.9980	-820.1852
17	6.4995	1.3349	201.8731	26.2935	-15.3421	-863.6829
18	6.7763	1.5232	258.8966	27.1002	-15.5715	-897.2145
19	6.9440	1.4555	282.9024	27.8279	-16.0082	-949.1336
20	7.0440	1.3002	278.0688	28.5185	-16.4149	-995.6361
21	7.1199	1.0972	248.6213	29.2126	-16.7653	-1038.2985
22	7.1757	0.8570	199.9542	29.9088	-17.1087	-1085.1449
23	7.2194	0.5874	139.5419	30.6058	-17.5187	-1152.7161
24	7.2421	0.3415	84.7804	31.3037	-17.9619	-1232.8446
25	7.2415	0.1695	48.7466	32.0022	-18.4085	-1316.1495
26	7.2415	0.1910	59.3234	34.3020	-18.4549	-1324.3804

LINK NO.	O (RAD)	ODT (RAD/SEC)	ODDT (RAD/SEC2)
1	-0.1745	0.0	0.0
2	-0.1068	-0.1501	-1.6365
3	-0.0278	-0.1081	2.4433
4	-0.0531	-0.0433	7.5084
5	0.0263	0.0503	15.5638
6	0.0263	0.0575	19.9955
7	0.0628	0.2517	30.5041
8	0.0628	0.2590	23.5013
9	0.0184	0.1576	5.6032
10	-0.0004	-0.0253	-17.4174
11	-0.0890	-0.2481	-36.4073
12	-0.2124	-0.4769	-53.6660
13	-0.3004	-0.6476	-68.7228
14	-0.3000	-0.6546	-77.6885
15	-0.3866	-0.5946	-84.9861
16	-0.3683	-0.4840	-86.0767
17	-0.3676	-0.3540	-78.4367
18	-0.2623	-0.2227	-61.8166
19	-0.1572	-0.0497	-21.8007
20	-0.1221	0.0725	14.4399
21	-0.0870	0.1601	43.0025
22	-0.0694	0.2035	57.4469
23	-0.0520	0.1832	51.0747
24	0.0003	0.1101	30.0211
25	-0.0000	-0.0087	-0.7894
26	-0.0000	-0.0170	-7.8478

T=0.139 SEAT LOAD= 645.2 STRAP= 0.4 LAP= 0.0 HEAD ANGLE=-0.000 KOUNT= 50

LINK NO.	AXIAL FORCE (LB)	SHEAR FORCE (LB)	MOMENT (IN-LB)	FACET FORCE (LB)
1	-645.1743	0.0	-0.0	0.0
2	-181.6565	9.1812	11.5813	-73.0342
3	-156.3956	5.6668	-3.1540	-76.3534

4	-138.9697	-0.1956	-5.1943	-71.8737
5	-132.2420	1.2831	-6.1960	-70.0834
6	-131.2292	-5.9855	0.0781	-62.4316
7	-144.5634	-6.5246	-10.8335	-40.9311
8	-143.4835	-14.7302	0.7056	-33.7352
9	-139.1724	-16.6016	15.4678	-30.3395
10	-132.1247	-13.8805	25.8232	-26.3303
11	-123.6410	-14.1247	27.6186	-24.0562
12	-115.5012	-7.5792	26.2750	-22.7031
13	-106.2246	1.9595	18.1808	-22.6865
14	-107.6462	9.2564	-2.4562	-12.0276
15	-89.1814	4.3576	-9.0515	-11.1049
16	-70.5981	6.1118	-13.5376	-10.1532
17	-53.9741	1.5829	-14.6872	-8.3489
18	-37.7804	-0.9552	-14.4234	-6.3496
19	-12.7215	-2.0721	-4.4813	-13.0299
20	-11.9302	-2.5976	-3.4060	-11.5565
21	-11.8673	-2.8328	-2.6438	-9.6491
22	-10.6233	-2.7481	-1.5044	-8.6678
23	-8.2732	-2.2408	0.2909	-8.9496
24	-7.3754	-2.0779	1.9335	-8.6103
25	-7.3022	-2.2941	3.4230	-7.7022
26	-13.5433	-4.8003	0.6456	-0.7146

LINK NO.	U (INS)	UDT (IN/SEC)	UDDT (IN/SEC2)	W (INS)	WDT (IN/SEC)	WDDT (IN/SEC2)
1	4.2000	0.0	0.0	3.5939	-0.3014	-4.5222
2	4.7822	-0.0046	-3.9260	7.1339	-1.8029	-39.7227
3	4.9126	0.1671	-14.4042	8.8093	-3.1606	-71.0424
4	4.9763	0.1839	-48.0917	10.4914	-4.4126	-98.4808
5	5.0141	-0.0377	-111.5655	12.1739	-5.6261	-129.7620
6	4.9687	-0.4420	-184.0737	13.8077	-6.8658	-170.5219
7	4.9053	-0.9587	-244.3063	15.3389	-8.2717	-220.3725
8	4.8114	-1.5637	-275.8524	16.7688	-9.7134	-273.3419
9	4.7462	-2.0117	-278.5476	18.1000	-11.1523	-326.3274
10	4.7299	-2.1886	-261.5065	19.3439	-12.5268	-380.1139
11	4.7705	-2.0284	-224.0336	20.4471	-13.8532	-437.0988
12	4.9265	-1.5511	-163.0368	21.5490	-15.1862	-501.1297
13	5.2031	-0.3018	-82.6951	22.6110	-16.5741	-576.2230
14	5.5121	0.1384	7.9253	23.5927	-17.4265	-632.0043
15	5.8260	1.0057	94.7768	24.4834	-18.2115	-688.4396
16	6.1725	1.7924	177.8212	25.3423	-18.9317	-745.6037
17	6.5089	2.4734	254.5724	26.2062	-19.5214	-796.2220
18	6.7875	2.9771	314.5982	27.0113	-19.9406	-834.8456
19	6.9552	3.0449	337.2768	27.7361	-20.6825	-901.1872
20	7.0544	2.8999	341.0965	28.4240	-21.3531	-958.8840
21	7.1289	2.5900	327.1756	29.1158	-21.9304	-1006.4168
22	7.1830	2.1341	294.0371	29.8097	-22.5017	-1049.9446
23	7.2245	1.5578	240.6671	30.5039	-23.2250	-1105.4852
24	7.2453	1.0014	181.5615	31.1985	-24.0448	-1172.1502
25	7.2433	0.5998	134.6778	31.8938	-24.8962	-1245.9324
26	7.2436	0.7306	169.7643	34.1933	-24.9835	-1253.5983

LINK NO.	O (RAD)	ODT (RAD/SEC)	ODDT (RAD/SEC2)
1	-0.1745	0.0	0.0
2	-0.1076	-0.1577	1.5647
3	-0.0283	-0.0770	13.6912
4	-0.0532	0.0557	31.8235
5	0.0269	0.1957	41.3067

6	0.0[illegible]69	0.2003	36.4670
7	0.0645	0.3972	26.6775
8	0.0643	0.3371	4.6550
9	0.0192	0.1478	-10.6845
10	-0.0008	-0.1500	-30.0536
11	-0.0908	-0.4823	-54.0811
12	-0.2155	-0.8028	-76.9298
13	-0.3046	-1.0495	-95.1112
14	-0.3043	-1.0980	-102.5937
15	-0.3907	-1.0684	-104.3770
16	-0.3719	-0.9558	-98.3337
17	-0.3704	-0.7828	-85.6975
18	-0.2643	-0.5688	-68.4338
19	-0.1579	-0.2204	-39.7830
20	-0.1217	0.0729	-12.1813
21	-0.0857	0.3120	14.5011
22	-0.0677	0.4554	35.7873
23	-0.0504	0.4369	41.3529
24	0.0012	0.2749	28.2946
25	-0.0001	-0.0088	-2.8988
26	-0.0003	-0.0912	-21.9745

T=0.035 SEAT LOAD= 802.2 STRAP= 0.9 LAP= 0.0 HEAD ANGLE=-0.001 KOUNT= 50

LINK NO.	AXIAL FORCE (LB)	SHEAR FORCE (LB)	MOMENT (IN-LB)	FACET FORCE (LB)
1	-802.2196	0.0	-0.0	0.0
2	-244.8142	12.5948	14.2723	-101.2495
3	-213.1604	3.0578	-5.6260	-107.0071
4	-192.1477	0.0553	-8.6316	-101.8446
5	-184.3474	1.6749	-9.3435	-99.3886
6	-184.6921	-8.8508	0.3408	-88.4564
7	-205.2713	-10.0001	-14.1051	-57.8697
8	-205.3493	-22.3609	3.3787	-47.4136
9	-199.3032	-24.9277	26.9849	-43.1755
10	-191.5949	-20.8167	43.1038	-37.5379
11	-181.0033	-21.0496	47.4506	-34.2958
12	-170.3479	-11.1065	45.8398	-32.6140
13	-157.4399	3.5471	33.3409	-33.0984
14	-160.5263	15.2530	0.7865	-17.3327
15	-134.3174	8.8196	-10.9067	-16.5107
16	-108.3968	12.2309	-20.6293	-15.7316
17	-84.3703	5.3539	-25.4341	-13.6974
18	-61.8930	0.4965	-27.4592	-11.1606
19	-22.2583	-3.1511	-9.6389	-24.6973
20	-21.2046	-4.2262	-7.7524	-22.3248
21	-21.5039	-4.9070	-6.2499	-18.9670
22	-19.8266	-5.1541	-3.7780	-17.1078
23	-15.7734	-4.4935	0.4224	-17.8160
24	-14.2739	-4.2887	4.3117	-17.2430
25	-14.3308	-4.7910	7.7694	-15.4197
26	-27.3924	-11.4669	2.2179	-0.9166

LINK NO.	U (INS)	UDT (IN/SEC)	UDDT (IN/SEC2)	W (INS)	WDT (IN/SEC)	WDDT (IN/SEC2)
1	4.2000	0.0	0.0	3.5924	-0.3175	-2.5207
2	4.7821	-0.0369	-11.7278	7.1245	-1.9384	-17.3179
3	4.9131	-0.0046	-61.3041	8.7928	-3.3993	-30.6021
4	4.9763	-0.2599	-136.8169	10.4684	-4.7606	-49.6887
5	5.0121	-0.8518	-216.6935	12.1445	-6.1045	-72.8332
6	4.9638	-1.6329	-285.6736	13.7716	-7.5230	-104.1438

7	4.8970	-2.4453	-343.9598	15.2952	-9.1482	-141.5296
8	4.7997	-3.1871	-366.3459	16.7172	-10.8291	-182.0049
9	4.7324	-3.6033	-354.9275	18.0407	-12.4952	-220.0442
10	4.7154	-3.6531	-321.8331	19.2771	-14.1071	-260.2779
11	4.7573	-3.2753	-269.1769	20.3729	-15.6985	-306.7658
12	4.9166	-2.4545	-190.4705	21.4584	-17.3515	-366.5778
13	5.1980	-1.2376	-86.3117	22.5215	-19.1285	-442.1626
14	5.5130	0.2270	27.7890	23.4982	-20.2801	-502.8585
15	5.8324	1.5783	130.5519	24.3842	-21.3575	-560.8507
16	6.1839	2.7953	218.1974	25.2388	-22.3611	-615.4471
17	6.5247	3.8507	289.6522	26.0992	-23.1895	-659.6379
18	6.8964	4.6130	339.6976	26.9017	-23.7841	-693.7484
19	6.9746	4.7625	351.3159	27.6220	-24.8124	-733.3798
20	7.0732	4.6093	345.3429	28.3059	-25.7405	-773.5251
21	7.1460	4.2314	331.2369	28.9942	-26.5356	-809.9107
22	7.1975	3.6525	313.8555	29.6847	-27.3090	-846.1572
23	7.2356	2.8955	295.5907	30.3747	-28.2884	-893.6511
24	7.2530	2.1546	283.8412	31.0644	-29.4060	-946.8866
25	7.2485	1.6252	283.9964	31.7546	-30.5769	-1000.4598
26	7.2501	2.0332	362.1893	34.0535	-30.6970	-1005.7653

LINK NO.	O (RAD)	ODT (RAD/SEC)	ODDT (RAD/SEC2)
1	-0.1745	0.0	0.0
2	-0.1083	-0.1006	23.2549
3	-0.0284	0.0603	41.2181
4	-0.0524	0.2556	46.3663
5	0.0284	0.4190	44.5148
6	0.0284	0.3869	35.0321
7	0.0668	0.5177	20.6641
8	0.0600	0.3244	-5.6135
9	0.0197	0.0565	-23.3251
10	-0.0020	-0.3313	-43.8513
11	-0.0939	-0.7846	-69.3568
12	-0.2206	-1.2419	-97.5044
13	-0.3111	-1.5985	-119.5179
14	-0.3112	-1.6747	-123.0403
15	-0.3474	-1.6219	-114.1684
16	-0.3779	-1.4444	-96.8654
17	-0.3754	-1.1845	-76.5049
18	-0.2679	-0.8777	-57.3133
19	-0.1594	-0.3879	-26.7276
20	-0.1214	0.0182	-6.8767
21	-0.0841	0.3515	4.6807
22	-0.0551	0.5604	3.1232
23	-0.0478	0.5449	1.0978
24	0.0028	0.3197	-12.9981
25	-0.0093	-0.0894	-31.8804
26	-0.0011	-0.2344	-35.5931

T=0.040 SEAT LOAD= 852.0 STRAP= 1.6 LAP= 0.0 HEAD ANGLE=-0.003 KOUNT= 50

LINK NO.	AXIAL FORCE (LB)	SHEAR FORCE (LB)	MOMENT (IN-LB)	FACET FORCE (LB)
1	-851.9991	0.0	-0.0	0.0
2	-302.7977	15.8718	14.3484	-131.1557
3	-268.7640	10.5042	-9.6733	-139.9763
4	-247.8747	0.1389	-12.5423	-134.0112
5	-240.2687	1.7784	-12.2975	-130.6926
6	-243.1204	-12.4134	1.5449	-116.0855
7	-272.2483	-14.5559	-16.0164	-75.6709

8	-274.3516	-31.9142	8.6308	-61.4329
9	-267.4854	-34.8872	43.0409	-56.9390
10	-258.4137	-28.9369	65.7864	-49.6038
11	-246.1351	-28.9864	73.7412	-45.3228
12	-233.1316	-14.8846	72.0201	-43.4182
13	-216.1103	6.1101	53.4114	-44.8026
14	-220.9570	23.4461	4.8261	-23.4300
15	-187.0098	15.3478	-14.6581	-23.0725
16	-151.6987	20.1609	-31.5905	-22.7709
17	-120.6415	9.8929	-40.8863	-20.5218
18	-90.3236	1.6865	-45.0649	-17.2837
19	-33.3966	-4.7621	-16.5855	-39.4100
20	-32.2430	-6.4598	-13.2816	-35.8180
21	-33.1987	-7.6522	-10.5632	-30.5704
22	-31.1828	-8.2046	-6.2923	-27.5266
23	-25.0283	-7.2102	0.9331	-28.8099
24	-22.7369	-6.8780	7.5057	-27.9979
25	-22.9118	-7.6958	13.2378	-25.0807
26	-44.4907	-19.4297	4.0000	-1.1874

LINK NO.	U (INS)	UDT (IN/SEC)	UDDT (IN/SEC2)	W (INS)	WDT (IN/SEC)	WDDT (IN/SEC2)
1	4.2000	0.0	0.0	3.5915	-0.0332	13.8211
2	4.7317	-0.1440	-25.6323	7.1161	-1.3212	129.4669
3	4.9121	-0.4791	-127.0403	8.7773	-2.6021	229.3094
4	4.9729	-1.1664	-221.3561	10.4459	-3.9255	278.6133
5	5.0047	-2.1575	-300.9835	12.1151	-5.2926	319.8219
6	4.9517	-3.2712	-362.3744	13.7348	-6.7963	341.8137
7	4.8802	-4.3185	-403.8890	15.2499	-8.5431	351.1625
8	4.7789	-5.1473	-413.3043	16.6631	-10.3708	348.1959
9	4.7097	-5.4948	-392.3957	17.9778	-12.1831	337.1311
10	4.6930	-5.3434	-342.3485	19.2057	-13.9552	317.8015
11	4.7375	-4.6420	-266.6032	20.2931	-15.7337	291.3578
12	4.9020	-3.3671	-167.0737	21.3696	-17.6326	255.0954
13	5.1908	-1.6040	-56.5310	22.4230	-19.7294	204.3810
14	5.5146	0.4178	48.6356	23.3932	-21.1555	157.5109
15	5.8420	2.2638	140.2045	24.2732	-22.4935	112.8469
16	6.2106	3.9092	221.7004	25.1221	-23.7443	69.4777
17	6.5476	5.3258	295.1550	25.9778	-24.7744	32.6586
18	6.8338	6.3593	354.3978	26.7770	-25.5109	5.9000
19	7.0030	6.6026	387.9475	27.4917	-26.6777	-10.3108
20	7.1007	6.4585	405.3591	28.1706	-27.7384	-24.5008
21	7.1715	6.0536	415.6502	28.8546	-28.6635	-39.2439
22	7.2200	5.4430	423.9488	29.5409	-29.5734	-54.6076
23	7.2542	4.6673	432.7744	30.2254	-30.7401	-77.0725
24	7.2679	3.9497	447.2354	30.9090	-32.0652	-102.4077
25	7.2609	3.4982	469.7269	31.5927	-33.4364	-126.6737
26	7.2658	4.4120	592.5659	33.3910	-33.5765	-129.4464

LINK NO.	O (RAD)	ODT (RAD/SEC)	ODDT (RAD/SEC2)
1	-0.1745	0.0	0.0
2	-0.1083	0.0985	60.8112
3	-0.0275	0.3204	64.2963
4	-0.0595	0.5057	54.7756
5	0.0311	0.6324	43.6227
6	0.0307	0.5459	33.9518
7	0.0696	0.6056	13.0860
8	0.0675	0.2930	-10.0287
9	0.0197	-0.0784	-32.9635

10	-0.0043	-0.5957	-61.6318
11	-0.0983	-1.1858	-88.4381
12	-0.2281	-1.7584	-105.8808
13	-0.3206	-2.1863	-112.3105
14	-0.3211	-2.2664	-109.9441
15	-0.4069	-2.1735	-103.3979
16	-0.3863	-1.9232	-93.8982
17	-0.3823	-1.5765	-82.5101
18	-0.2731	-1.1878	-71.0229
19	-0.1617	-0.5498	-46.8785
20	-0.1215	-0.0528	-31.0763
21	-0.0823	0.3229	-23.0252
22	-0.0623	0.5315	-21.7083
23	-0.0452	0.4703	-27.9784
24	0.0041	0.1775	-38.4971
25	-0.0012	-0.3071	-51.0481
26	-0.0027	-0.4575	-54.7247

T=0.045 SEAT LOAD= 918.2 STRAP= 2.5 LAP= 0.0 HEAD ANGLE=-0.006 KOUNT= 50

LINK NO.	AXIAL FORCE (LB)	SHEAR FORCE (LB)	MOMENT (IN-LB)	FACET FORCE (LB)
1	-918.2402	0.0	-0.0	0.0
2	-345.4072	19.3587	8.7717	-158.8472
3	-312.3763	12.2553	-14.5357	-168.2407
4	-294.7183	-0.0096	-15.4985	-161.3332
5	-288.5317	1.7465	-14.1004	-157.6331
6	-295.0845	-15.9446	3.7140	-140.2141
7	-333.6172	-19.3326	-15.7334	-91.3126
8	-339.6154	-42.1119	16.4309	-73.5276
9	-332.5223	-45.3838	64.4653	-69.5023
10	-324.8608	-37.3147	94.7147	-60.7221
11	-312.1678	-36.8093	106.3236	-55.6901
12	-297.1528	-17.9951	102.6065	-54.0508
13	-275.3443	9.8334	75.4175	-56.8025
14	-282.4572	33.1691	8.4898	-29.8651
15	-240.2833	23.0968	-19.9879	-30.1518
16	-195.9242	28.9301	-44.8977	-30.4771
17	-157.3329	14.7932	-59.0915	-28.0352
18	-119.7085	2.6605	-65.4146	-24.0390
19	-44.6432	-6.6199	-24.7995	-55.4210
20	-43.5310	-8.9608	-19.6887	-50.4610
21	-45.3553	-10.7395	-15.3825	-43.1310
22	-43.2020	-11.6244	-8.9721	-38.7073
23	-34.3575	-10.2174	1.7034	-40.6342
24	-31.7257	-9.7225	11.2421	-39.5866
25	-32.0378	-10.8695	19.4240	-35.4898
26	-62.3667	-28.2217	6.1407	-1.4069

LINK NO.	U (INS)	UDT (IN/SEC)	UDDT (IN/SEC2)	W (INS)	WDT (IN/SEC)	WDDT (IN/SEC2)
1	4.2000	0.0	0.0	3.5910	-0.1653	-3.1747
2	4.7807	-0.2514	-26.2394	7.1100	-1.1936	13.6596
3	4.9080	-1.1342	-120.1636	8.7657	-2.1937	36.7385
4	4.9641	-2.3972	-244.2985	10.4285	-3.2434	65.5595
5	4.9899	-3.8255	-348.2193	12.0916	-4.3327	100.9193
6	4.9305	-5.2504	-418.0149	13.7044	-5.5693	145.1378
7	4.8534	-6.4751	-446.7175	15.2114	-7.0206	214.4424
8	4.7479	-7.2713	-419.0362	16.6159	-8.5753	298.3655
9	4.6774	-7.4152	-357.5715	17.9219	-10.1450	393.5827
10	4.6622	-6.9462	-284.4666	19.1411	-11.7533	433.3139

11	4.7111	-5.8515	-210.1940	20.2196	-13.4519	557.1301
12	4.8832	-4.0926	-124.0418	21.2863	-15.3685	607.0872
13	5.1823	-1.8071	-29.5306	22.3288	-17.5781	632.3854
14	5.5173	0.6962	56.5171	23.2914	-19.1773	620.4734
15	5.8551	2.9613	134.9506	24.1642	-20.6911	600.3174
16	6.2229	4.9891	209.1410	25.0064	-22.1256	573.0647
17	6.5779	6.7731	283.2119	25.8565	-23.3235	544.6339
18	6.8700	8.1319	352.5495	26.6517	-24.1893	520.9253
19	7.0410	8.6257	416.2290	27.3604	-25.3996	521.1011
20	7.1384	8.6799	475.1894	28.0239	-26.4764	529.2922
21	7.2075	8.4416	530.0221	28.7132	-27.4122	539.5836
22	7.2532	7.9718	578.7672	29.3949	-28.3238	553.4098
23	7.2837	7.3103	619.3254	30.0734	-29.5024	570.0763
24	7.2941	6.7017	653.8520	30.7503	-30.8499	586.0394
25	7.2852	6.3741	686.2687	31.4270	-32.2493	599.4889
26	7.2963	7.9991	847.4912	33.7246	-32.3982	598.6754

LINK NO.	O (RAD)	ODT (RAD/SEC)	ODDT (RAD/SEC 2)
1	-0.1745	0.0	0.0
2	-0.1070	0.4009	41.9628
3	-0.0250	0.6794	67.8677
4	-0.0473	0.7958	61.7348
5	0.0348	0.8468	43.7285
6	0.0339	0.7133	26.0165
7	0.0727	0.6253	-12.3279
8	0.0688	0.1691	-44.1223
9	0.0188	-0.2994	-54.9753
10	-0.0989	-0.9099	-58.8374
11	-0.1958	-1.6020	-68.2923
12	-0.2381	-2.2427	-78.2579
13	-0.3329	-2.6939	-84.4739
14	-0.3337	-2.7655	-88.0274
15	-0.4190	-2.6518	-88.7391
16	-0.3971	-2.3783	-88.3653
17	-0.3312	-2.0071	-88.1007
18	-0.2800	-1.5924	-88.1103
19	-0.1652	-0.8911	-85.9972
20	-0.1223	-0.3383	-90.5915
21	-0.0812	0.0817	-73.1695
22	-0.0601	0.3211	-64.8115
23	-0.0433	0.2643	-58.5308
24	0.0045	-0.0517	-57.2141
25	-0.0034	-0.5836	-61.5432
26	-0.0055	-0.7820	-73.9023

T=0.050 SEAT LOAD= 985.0 STRAP= 3.6 LAP= 0.0 HEAD ANGLE=-0.011 COUNT= [illegible]

LTNK NO.	AXIAL FORCE (LB)	SHEAR FORCE (LB)	MOMENT (IN-LB)	FACIT FORCE (LB)
1	-984.9834	0.0	-0.0	0.0
2	-381.5118	22.0613	-0.9888	-187.8143
3	-349.3516	12.9270	-21.5117	-195.4649
4	-334.1139	-1.3761	-18.2260	-184.4668
5	-329.1695	0.2916	-14.3460	-178.7030
6	-338.2859	-20.4736	7.7003	-157.5404
7	-382.9891	-25.0083	-11.6718	-101.5318
8	-391.3178	-52.6201	27.5425	-80.3055
9	-382.1691	-55.1546	88.5014	-77.7557
10	-375.2842	-44.6418	125.1437	-67.8204
11	-362.5952	-43.1543	140.4665	-62.2954

12	-346.3498	-20.0049	134.7616	-61.2320
13	-321.6105	13.9816	98.5327	-65.7349
14	-329.7952	42.9231	13.5033	-34.7710
15	-282.2500	31.4758	-24.6249	-36.1247
16	-231.6218	37.7462	-57.9021	-37.4029
17	-187.9650	19.8629	-77.2517	-35.0397
18	-145.1952	3.6604	-85.8108	-30.4830
19	-54.4502	-8.3674	-33.1910	-70.6605
20	-53.4566	-11.2958	-26.3676	-64.4217
21	-56.1473	-13.6967	-20.5190	-55.1213
22	-54.0142	-15.0071	-12.0038	-49.2884
23	-43.7537	-13.2567	2.1838	-51.7380
24	-39.9454	-12.6296	14.8739	-50.4122
25	-40.4910	-14.1192	25.7218	-45.1407
26	-30.3035	-38.0675	8.8327	-1.2248

LINK NO.	U (INS)	UDT (IN/SEC)	UDDT (IN/SEC2)	W (INS)	WDT (IN/SEC)	WDDT (IN/SEC2)
1	4.2000	0.0	0.0	3.5963	-0.1174	9.0572
2	4.7791	-0.3876	-14.9971	7.1046	-0.8888	90.1670
3	4.9011	-1.6119	-65.2196	8.7558	-1.6474	163.7502
4	4.9494	-3.3685	-138.8803	10.4138	-2.4341	230.6651
5	4.9667	-5.3347	-226.7260	12.0718	-3.4016	285.0505
6	4.8992	-7.1534	-301.6787	13.6788	-4.4988	324.9018
7	4.8157	-8.4965	-328.2374	15.1791	-5.7234	371.5792
8	4.7067	-9.0768	-283.1492	16.5767	-6.9745	425.5634
9	4.6364	-8.8372	-198.0574	17.8760	-8.1394	494.5146
10	4.6245	-7.9813	-112.2069	19.0883	-9.2930	570.6607
11	4.6798	-6.5503	-44.2613	20.1595	-10.5181	658.9934
12	4.8615	-4.4748	0.9044	21.2177	-11.9935	752.7964
13	5.1730	-1.8670	27.4560	22.2459	-13.8170	848.4901
14	5.5214	0.9306	47.5978	23.2046	-15.3194	887.2689
15	5.8714	3.5276	88.3556	24.0698	-16.7941	916.9838
16	6.2503	5.9180	149.0976	24.9047	-18.2541	932.6402
17	6.6152	8.0894	225.1857	25.7486	-19.5179	935.2084
18	6.8150	9.8205	303.9805	26.5392	-20.4584	930.1967
19	7.0893	10.6933	396.3030	27.2421	-21.5673	977.6390
20	7.1878	11.1040	482.3377	27.9104	-22.5162	1026.7396
21	7.2566	11.2161	568.4675	28.5852	-23.3328	1067.9445
22	7.3007	11.0900	658.2175	29.2626	-24.1161	1107.3414
23	7.3285	10.7579	751.7933	29.9356	-25.1373	1155.0397
24	7.3366	10.4539	843.1411	30.6061	-26.3158	1207.4625
25	7.3266	10.4009	925.1325	31.2761	-27.5494	1261.3796
26	7.3480	12.9241	1122.1619	33.5729	-27.6981	1262.7882

LINK NO.	O (RAD)	ODT (RAD/SEC)	ODDT (RAD/SEC2)
1	-0.1745	0.0	0.0
2	-0.1047	0.5472	30.3695
3	-0.0209	0.9349	39.2749
4	-0.0425	1.1060	51.8420
5	0.0396	1.0961	47.7632
6	0.0377	0.8375	28.9531
7	0.0756	0.5182	-20.1585
8	0.0689	-0.1233	-63.1953
9	0.0165	-0.6111	-70.4222
10	-0.0133	-1.2152	-68.8877
11	-0.1145	-1.8642	-46.9530
12	-0.2501	-2.4798	-20.8754
13	-0.3471	-2.9376	-9.2619

14	-0.3484	-3.0757	-26.4434
15	-0.4333	-3.0193	-47.9617
16	-0.4100	-2.7885	-68.6709
17	-0.4024	-2.4445	-83.6813
18	-0.2891	-2.0513	-94.4890
19	-0.1708	-1.3565	-98.4095
20	-0.1252	-0.8044	-103.1691
21	-0.0819	-0.3811	-109.6549
22	-0.0595	-0.1292	-114.5751
23	-0.0430	-0.1611	-112.9680
24	0.0033	-0.4489	-103.9681
25	-0.0072	-0.9537	-87.8304
26	-0.0107	-1.1804	-84.1060

T=0.055 SEAT LOAD=1028.5 STRAP= 4.8 LAP= 0.0 HEAD ANGLE=-0.018 KOUNT= 50

LINK NO.	AXIAL FORCE (LB)	SHEAR FORCE (LB)	MOMENT (IN-LB)	FACET FORCE (LB)
1	-1028.5016	0.0	-0.0	0.0
2	-401.2067	24.2083	-13.7348	-212.5707
3	-371.6856	13.0316	-29.4888	-217.4090
4	-360.1023	-2.8894	-21.6541	-202.1887
5	-357.8184	-1.9778	-13.8970	-193.4928
6	-370.5749	-25.7006	13.2821	-167.9458
7	-420.2506	-31.6276	-3.1981	-106.2452
8	-430.6381	-63.5667	42.6839	-81.6997
9	-417.6507	-64.1793	114.7074	-81.9438
10	-410.1989	-50.9688	154.9950	-70.9609
11	-395.5248	-48.0836	169.8498	-65.2442
12	-376.9379	-21.6457	161.1497	-64.5694
13	-348.9313	16.5596	118.6225	-70.2002
14	-357.4580	49.6156	21.5370	-36.7487
15	-305.4301	38.5089	-24.6582	-39.1011
16	-250.4663	45.5827	-65.9348	-41.4373
17	-204.2523	25.3062	-91.3086	-39.7179
18	-159.7610	5.4052	-103.0290	-35.2307
19	-60.9109	-9.4230	-40.9495	-82.1751
20	-59.4486	-12.7973	-32.6003	-75.0568
21	-63.1480	-15.7914	-25.2340	-64.3227
22	-61.5590	-17.5666	-14.7695	-57.3351
23	-50.1759	-15.5864	2.5012	-60.2185
24	-45.3761	-14.8511	17.8642	-58.7256
25	-46.7703	-16.6052	30.9033	-52.5629
26	-93.7284	-46.3374	11.1612	-0.8647

LINE NO.	U (INS)	UDT (IN/SEC)	UDDT (IN/SEC2)	W (INS)	WDT (IN/SEC)	WDDT (IN/SEC2)
1	4.2000	0.0	0.0	3.5898	-0.0751	10.2419
2	4.7771	-0.4054	-3.0092	7.1014	-0.3908	110.3503
3	4.8923	-1.8640	-36.0953	8.7498	-0.7324	203.2099
4	4.9312	-3.8722	-66.9660	10.4045	-1.1790	298.1534
5	4.9379	-6.0559	-74.0852	12.0588	-1.7251	372.4502
6	4.8607	-8.0518	-65.6392	13.6611	-2.4710	460.4176
7	4.7702	-9.4776	-50.3191	15.1562	-3.3082	559.4113
8	4.6588	-9.8834	-10.7293	16.5484	-4.1703	656.4708
9	4.5906	-9.2715	47.6947	17.9428	-4.9188	752.5583
10	4.5841	-7.9972	111.1867	19.0503	-5.6795	837.7132
11	4.6474	-6.2410	158.1111	20.1163	-6.5176	913.1702
12	4.8409	-3.9780	181.8889	21.1681	-7.6200	977.3942
13	5.1646	-1.3465	175.3329	22.1922	-9.0783	1036.9607
14	5.5270	1.3883	143.8723	23.1399	-10.4113	1067.0521

15	5.8901	3.9799	109.6215	23.9981	-11.7493	1090.3059
16	6.2814	6.4780	90.5386	24.8259	-13.1294	1105.1853
17	6.6579	8.8878	100.1708	25.6635	-14.3774	1107.4981
18	6.9673	10.9483	141.5420	26.4494	-15.3360	1104.0128
19	7.1473	12.3520	247.5590	27.1475	-16.1222	1168.6981
20	7.2451	13.3168	380.8738	27.8119	-16.7181	1246.6253
21	7.3197	14.0025	529.5257	28.4833	-17.2238	1321.7215
22	7.3645	14.4774	687.3353	29.1575	-17.6992	1401.9192
23	7.3923	14.7781	851.4181	29.8261	-18.3489	1506.9042
24	7.4001	15.0909	1006.2864	30.4916	-19.1121	1627.0150
25	7.3911	15.5790	1136.2953	31.1564	-19.9107	1752.6748
26	7.4277	19.1513	1355.3991	33.4525	-20.0475	1756.6300

LINK NO.	O (RAD)	ODT (RAD/SEC)	ODDT (RAD/SEC 2)
1	-0.1745	0.0	0.0
2	-0.1015	0.6989	21.0422
3	-0.0157	1.1023	22.8154
4	-0.0365	1.2522	9.7898
5	0.0455	1.2105	-2.7541
6	0.0422	0.9289	-3.4261
7	0.0780	0.4376	-24.6241
8	0.0676	-0.3914	-43.0919
9	0.0126	-0.9480	-49.9471
10	-0.0203	-1.5346	-42.8337
11	-0.1244	-2.0707	-22.6733
12	-0.2626	-2.5229	3.6057
13	-0.3617	-2.8641	28.9475
14	-0.3638	-3.0220	37.7827
15	-0.4486	-3.0516	27.7017
16	-0.4246	-2.9691	1.3616
17	-0.4155	-2.7628	-33.8380
18	-0.3905	-2.4856	-69.0337
19	-0.1789	-1.9128	-126.8578
20	-0.1306	-1.4381	-162.4754
21	-0.0854	-1.0769	-184.4544
22	-0.0619	-0.3637	-193.0141
23	-0.0454	-0.8796	-181.7530
24	-0.0004	-1.0872	-152.3582
25	-0.0132	-1.4457	-106.1976
26	-0.0177	-1.6152	-89.1292

T=0.060 SEAT LOAD= 1044.5 STRAP= 6.1 LAP= 0.0 HEAD ANGLE=-0.027 KOUNT= 50

LINK NO.	AXIAL FORCE (LB)	SHEAR FORCE (LB)	MOMENT (IN-LB)	FACET FORCE (LB)
1	-1044.4640	0.0	-0.0	0.0
2	-400.3588	25.2972	-28.3810	-229.6851
3	-375.5499	12.2817	-37.4073	-230.3928
4	-368.8385	-4.7037	-24.0775	-210.3263
5	-369.6333	-4.6356	-12.2804	-198.6466
6	-385.7871	-39.3870	19.2076	-169.5327
7	-438.5217	-37.8037	7.5832	-104.8776
8	-451.4648	-73.2720	59.1356	-77.6592
9	-435.1397	-71.4298	141.2337	-81.5051
10	-428.3686	-55.4713	182.4234	-70.3732
11	-412.7965	-59.9649	194.4679	-65.1695
12	-393.0701	-22.1721	181.4331	-65.3399
13	-363.3489	18.5999	133.3281	-72.1204
14	-372.3911	54.0057	28.4408	-37.4130
15	-318.5981	42.7496	-22.1553	-40.3863

16	-261.2970	50.3459	-68.0819	-43.2796
17	-212.9674	28.8938	-97.4790	-42.0026
18	-166.3126	6.9008	-112.0103	-37.6349
19	-61.2232	-9.6075	-44.9628	-87.1208
20	-60.6494	-13.1389	-36.2723	-79.6839
21	-64.6980	-16.4703	-28.2846	-68.3793
22	-63.5778	-18.6106	-16.8977	-60.7300
23	-51.9448	-16.6026	1.9982	-63.7101
24	-47.6918	-15.8349	18.8349	-62.1329
25	-48.6855	-17.6968	33.0677	-55.5661
26	-98.8017	-50.6374	12.2975	-9.4914

LINK NO.	U (INS)	UDT (IN/SEC)	UDDT (IN/SEC 2)	W (INS)	WDT (IN/SEC)	WDDT (IN/SEC 2)
1	4.2000	0.0	0.0	3.5896	-0.0150	12.4219
2	4.7750	-0.4265	2.3074	7.1009	0.1851	108.6879
3	4.8327	-1.9456	10.7931	8.7488	0.3159	194.7056
4	4.9114	-3.9550	45.3227	10.4024	0.2942	272.5126
5	4.9074	-6.0324	105.1853	12.0550	0.1537	347.4940
6	4.8205	-7.8097	185.5776	13.6545	-0.1733	427.4999
7	4.7235	-8.9344	276.2594	15.1467	-0.5192	523.3608
8	4.6107	-9.0272	348.8554	16.5358	-0.8732	625.8978
9	4.5462	-8.1963	378.4141	17.8277	-1.1313	724.7642
10	4.5465	-6.8071	366.2018	19.0325	-1.4527	816.7999
11	4.6189	-5.0292	328.6398	20.0953	-1.8959	901.3988
12	4.8228	-2.8114	282.7823	21.1425	-2.6326	987.5476
13	5.1604	-0.2930	236.4724	22.1601	-3.7333	1078.2262
14	5.5360	2.2474	185.7024	23.1016	-4.8689	1131.5605
15	5.9116	4.6353	142.4216	23.9535	-6.0309	1182.4475
16	6.3150	6.9580	102.6781	24.7746	-7.2642	1230.2623
17	6.7034	9.2822	72.4109	25.6062	-8.4210	1267.4169
18	7.0233	11.4068	66.2222	26.3873	-9.3403	1288.9883
19	7.2114	13.2181	127.0689	27.0821	-9.8691	1335.9606
20	7.3198	14.8511	251.7453	27.7444	-10.1580	1333.7107
21	7.3959	16.3955	431.3423	28.4142	-10.3419	1434.1227
22	7.4454	17.8454	649.0075	29.0870	-10.4277	1500.3770
23	7.4770	19.1666	834.2559	29.7538	-10.4851	1614.9887
24	7.4887	20.4091	1100.0012	30.4172	-10.5322	1760.4646
25	7.4839	21.6356	1269.9363	31.0799	-10.5765	1916.3166
26	7.5411	26.3177	1493.7283	33.3753	-10.6971	1917.3835

LINK NO.	O (RAD)	ODT (RAD/SEC)	ODDT (RAD/SEC 2)
1	-0.1745	0.0	0.0
2	-0.0979	0.7428	0.1778
3	-0.0101	1.1194	-15.2756
4	-0.0303	1.2156	-29.8508
5	0.0513	1.0984	-44.8934
6	0.0455	0.7854	-48.7134
7	0.0797	0.2155	-54.0607
8	0.0652	-0.5672	-26.5135
9	0.0075	-1.0424	6.4364
10	-0.0281	-1.5380	37.9931
11	-0.1347	-1.9982	52.4739
12	-0.2750	-2.3786	59.6757
13	-0.3756	-2.6495	63.2110
14	-0.3784	-2.7811	59.7305
15	-0.4634	-2.8340	57.4961
16	-0.4392	-2.8212	47.7793
17	-0.4294	-2.7623	24.8010

18	-0.3135	-2.6762	-12.2709
19	-0.1901	-2.5438	-112.8464
20	-0.1401	-2.3963	-198.1707
21	-0.0935	-2.2483	-259.1232
22	-0.0691	-2.1088	-284.2515
23	-0.0525	-2.0159	-261.2696
24	-0.0080	-1.9844	-203.7642
25	-0.0218	-2.0115	-122.8603
26	-0.0269	-2.0562	-85.2235

T=0.065 SEAT LOAD=1032.4 STRAP= 7.3 LAP= 0.0 HEAD ANGLE=-0.038 KOUNT= 50

LINK NO.	AXIAL FORCE (LB)	SHEAR FORCE (LB)	MOMENT (IN-LB)	FACET FORCE (LB)
1	-1032.4482	0.0	-0.0	0.0
2	-383.3156	25.2906	-42.8143	-237.6048
3	-363.6663	10.7581	-43.7500	-233.3049
4	-362.4040	-6.6352	-24.8272	-208.8329
5	-366.4512	-7.3045	-9.2733	-194.5125
6	-385.2959	-33.9093	25.1515	-163.1061
7	-433.3740	-42.1714	18.6090	-98.6840
8	-452.9242	-79.5127	72.9259	-70.2819
9	-433.7190	-75.3909	160.6947	-77.7031
10	-423.0293	-57.3698	202.6120	-66.6378
11	-412.9262	-52.2781	214.5403	-61.7148
12	-392.9445	-22.1885	199.0567	-62.5646
13	-362.0369	13.9153	146.5537	-70.3951
14	-370.4060	56.5607	36.1724	-36.0820
15	-315.7412	45.3415	-18.2602	-39.7239
16	-257.9051	52.0561	-66.6287	-42.9246
17	-209.3697	29.5342	-97.0633	-41.7983
18	-162.6139	6.8600	-111.7015	-37.3869
19	-58.7252	-9.1211	-43.4150	-84.9472
20	-57.9574	-12.4765	-35.2989	-77.6861
21	-61.6400	-15.6613	-27.9541	-60.6474
22	-60.3981	-17.7660	-17.4668	-59.0039
23	-48.9748	-15.8060	0.4716	-61.7214
24	-44.8312	-15.0657	16.7303	-60.1128
25	-45.8316	-16.8389	30.6076	-53.7284
26	-94.1377	-48.4151	10.8768	-0.6891

LINK NO.	U (INS)	UDT (IN/SEC)	UDDT (IN/SEC2)	W (INS)	WDT (IN/SEC)	WDDT (IN/SEC2)
1	4.2000	0.0	0.0	3.5896	0.0350	7.1886
2	4.7730	-0.3562	22.9634	7.1030	0.6006	56.9911
3	4.8734	-1.6986	92.2298	8.7524	1.0599	104.2020
4	4.8128	-3.3433	205.2495	10.4067	1.3510	156.1342
5	4.8796	-4.8754	352.1568	12.0595	1.5524	219.5687
6	4.7852	-6.0693	495.7468	13.6584	1.6375	303.1381
7	4.6837	-6.7061	599.8901	15.1501	1.7761	400.3024
8	4.5713	-6.5096	645.0834	16.5387	1.9325	501.5183
9	4.5111	-5.6282	636.3631	17.8306	2.1688	597.9381
10	4.5181	-4.3806	597.5702	19.0350	2.3368	697.5007
11	4.5986	-2.8900	531.0826	20.0967	2.3769	803.4530
12	4.8129	-1.0490	434.4827	21.1414	2.1530	920.1156
13	5.1622	1.0771	323.1019	22.1549	1.6094	1049.5435
14	5.5497	3.2319	214.3231	23.0915	0.8214	1134.5594
15	5.9365	5.3311	135.4847	23.9383	-0.0266	1206.1411
16	6.3510	7.4414	86.9944	24.7540	-0.9843	1262.4115
17	6.7507	9.6391	69.2565	25.5802	-1.9400	1297.3659
18	7.0812	11.7645	82.8588	26.3570	-2.7461	1313.5872

19	7.2792	13.9187	163.4395	27.0499	-3.0052	1367.4254
20	7.3972	16.1501	291.7367	27.7113	-3.0427	1418.3493
21	7.4832	18.5260	447.0288	28.3807	-3.0001	1460.9638
22	7.5426	20.9986	632.2331	29.0538	-2.8274	1498.2722
23	7.5338	23.4851	848.7055	29.7216	-2.4570	1555.9566
24	7.6043	25.8665	1070.6312	30.3863	-1.9330	1636.4945
25	7.6081	28.0480	1266.3251	31.0505	-1.3260	1737.3472
26	7.6915	33.8610	1494.0184	33.3453	-1.4713	1726.2439

LINK NO.	O (RAD)	ODT (RAD/SEC)	ODDT (RAD/SEC2)
1	-0.1745	0.0	0.0
2	-0.0942	0.6833	-30.2009
3	-0.0049	0.9455	-58.9359
4	-0.0248	0.9230	-82.2624
5	0.0561	0.7507	-87.9376
6	0.0498	0.4867	-68.7992
7	0.0801	-0.0223	-42.5435
8	0.0521	-0.6263	3.2327
9	0.0025	-0.9488	28.6208
10	-0.0352	-1.2764	58.0205
11	-0.1438	-1.6093	93.2952
12	-0.2859	-1.9215	120.0728
13	-0.3878	-2.1757	129.2330
14	-0.3913	-2.3604	113.1982
15	-0.4768	-2.4819	84.9199
16	-0.4526	-2.5714	48.2443
17	-0.4429	-2.6555	8.9631
18	-0.3270	-2.7493	-28.1535
19	-0.2041	-3.0405	-97.9101
20	-0.1544	-3.2616	-154.1554
21	-0.1078	-3.4024	-200.0648
22	-0.0830	-3.4266	-232.4437
23	-0.0658	-3.2965	-236.4304
24	-0.0206	-3.0388	-204.9027
25	-0.0335	-2.6763	-137.5370
26	-0.0382	-2.4653	-80.7688

T=0.070 SEAT LOAD= 1003.4 STRAP= 8.5 LAP= 0.0 HEAD ANGLE=-0.052 KOUNT= 50

LINK NO.	AXIAL FORCE (LB)	SHEAR FORCE (LB)	MOMENT (IN-LB)	FACET FORCE (LB)
1	-1003.4384	0.0	-0.0	0.0
2	-356.2541	24.4351	-53.8209	-236.7921
3	-341.8219	8.8562	-47.1780	-227.5065
4	-344.4952	-8.3601	-23.7002	-199.3953
5	-359.4319	-3.4220	-5.8455	-183.3408
6	-363.3726	-35.6598	29.3660	-151.2225
7	-420.5730	-44.4779	27.3254	-89.4131
8	-435.4755	-82.2609	82.2025	-60.7822
9	-414.1895	-76.5574	173.2943	-70.6334
10	-408.3995	-58.4558	215.1206	-59.7006
11	-394.1246	-52.1259	226.2382	-55.1170
12	-374.3774	-22.3381	219.0146	-56.3346
13	-343.6395	13.9820	157.2244	-64.6274
14	-356.8708	55.2021	47.8063	-31.9771
15	-297.1137	45.1130	-7.3751	-35.9998
16	-240.9054	51.3734	-56.1530	-39.1907
17	-193.7899	23.7517	-86.9263	-38.4064
18	-148.6733	7.6504	-102.0118	-34.3594
19	-52.5000	-7.2371	-37.4976	-76.1405

20	-51.4871	-10.2563	-30.8458	-69.7699
21	-54.5554	-13.0344	-24.9808	-59.9318
22	-53.3082	-14.9130	-16.4023	-53.0476
23	-42.8276	-13.2000	-1.1580	-55.5549
24	-38.9204	-12.5478	12.6018	-54.2144
25	-39.6544	-14.0283	24.2831	-48.6462
26	-81.9876	-38.1483	6.5126	-2.0684

LINK NO.	U (INS)	UDT (IN/SEC)	UDDT (IN/SEC2)	W (INS)	WDT (IN/SEC)	WDDT (IN/SEC2)
1	4.2000	0.0	0.0	3.5899	0.0659	6.3278
2	4.7715	-0.2064	38.9525	7.1066	0.8190	37.0346
3	4.8665	-1.0017	184.2072	8.7588	1.4773	74.1083
4	4.8794	-1.8844	370.0549	10.4152	2.0397	132.1453
5	4.8604	-2.6121	542.4069	12.0698	2.5569	196.4331
6	4.7619	-3.0739	686.7549	13.6702	3.0414	272.7493
7	4.6586	-3.1757	790.7201	15.1637	3.6359	355.3692
8	4.5477	-2.7453	841.4510	16.5544	4.2677	441.5613
9	4.4918	-1.9253	834.0789	17.8485	4.9460	521.2284
10	4.5045	-0.9008	785.4652	19.0549	5.5702	602.5338
11	4.5916	0.2259	702.1086	20.1182	6.1120	692.4380
12	4.8138	1.5252	581.0862	21.1633	6.4745	802.1537
13	5.1721	2.9758	431.6939	22.1757	6.6053	932.5612
14	5.5687	4.4592	283.5488	23.1095	6.2854	1027.7052
15	5.9549	6.0667	172.8423	23.9530	5.8152	1103.7115
16	6.3893	7.3913	106.5404	24.7645	5.1297	1156.3856
17	6.7398	10.0068	83.9954	25.5864	4.3136	1181.2615
18	7.1412	12.2333	100.3714	26.3593	3.5449	1183.5605
19	7.3511	14.8513	186.3166	27.0513	3.4299	1181.3119
20	7.4819	17.7461	320.9406	27.7131	3.5479	1184.1600
21	7.5817	20.9135	481.6440	28.3831	3.7201	1189.3645
22	7.6557	24.2645	651.2735	29.0574	4.0222	1201.3630
23	7.7118	27.7084	821.1630	29.7277	4.6115	1234.0874
24	7.7468	31.0299	975.6417	30.3959	5.4476	1282.3869
25	7.7636	34.0289	1104.3533	31.0641	6.4413	1339.9090
26	7.8789	40.9724	1330.0721	33.3580	6.2062	1314.7530

LINK NO.	Q (RAD)	QDT (RAD/SEC)	QDDT (RAD/SEC2)
1	-0.1745	0.0	0.0
2	-0.0914	0.4168	-72.5872
3	-0.0311	0.5135	-108.2599
4	-0.0213	0.4502	-104.4524
5	0.0537	0.2947	-91.6616
6	0.0514	0.1335	-68.6339
7	0.0795	-0.2406	-44.4496
8	0.0591	-0.5960	1.3709
9	-0.0019	-0.7800	34.9414
10	-0.0498	-0.9570	72.3977
11	-0.1507	-1.1023	112.1444
12	-0.2938	-1.2324	149.0200
13	-0.3968	-1.4018	167.1949
14	-0.4915	-1.6791	148.7652
15	-0.4880	-1.9941	107.5557
16	-0.4649	-2.3241	56.1822
17	-0.4562	-2.6446	6.1374
18	-0.3412	-2.9364	-34.4779
19	-0.2206	-3.5993	-119.6415
20	-0.1727	-4.0765	-173.2314
21	-0.1272	-4.3867	-199.8972

22	-0.1029	-4.4992	-203.4620
23	-0.0850	-4.3414	-185.2841
24	-0.0381	-3.9342	-153.5650
25	-0.0485	-3.3078	-112.9869
26	-0.0515	-2.8927	-91.6595

T=0.075 SEAT LOAD= 958.1 STRAP= 9.7 LAP= 0.0 HEAD ANGLE=-0.067 KOUNT= 50

LINK NO.	AXIAL FORCE (LB)	SHEAR FORCE (LB)	MOMENT (IN-LB)	FACET FORCE (LB)
1	-958.1043	0.0	-0.0	0.0
2	-322.7543	22.4479	-57.7315	-225.3142
3	-311.1278	7.0647	-47.1421	-213.2613
4	-314.9134	-9.1211	-22.6410	-184.1633
5	-321.9457	-19.7821	-3.5256	-167.1481
6	-341.3162	-35.7935	31.2714	-135.3261
7	-387.7790	-44.9482	33.5207	-77.8421
8	-402.2187	-81.5464	86.9369	-49.9468
9	-379.7150	-74.8476	177.5497	-61.3406
10	-374.7769	-57.2359	218.0654	-50.7290
11	-360.1901	-50.7640	227.9840	-46.4838
12	-341.2014	-22.9103	212.5032	-47.7604
13	-312.1043	15.4094	164.2469	-55.8239
14	-318.3351	49.2991	63.8774	-25.4787
15	-268.3926	41.2305	12.8562	-29.3764
16	-216.1416	43.4343	-33.9534	-32.1498
17	-171.7017	29.9180	-65.1297	-32.0500
18	-129.2645	10.5095	-82.6032	-28.9925
19	-45.2948	-3.8441	-26.3624	-62.4972
20	-43.4866	-6.5304	-23.1146	-57.8255
21	-45.2542	-8.7844	-20.2501	-50.0345
22	-43.5874	-10.5772	-14.8945	-44.5617
23	-34.3937	-9.5965	-3.6458	-46.8130
24	-30.9015	-9.2545	6.7113	-45.8322
25	-31.3377	-10.4235	15.5439	-41.3806
26	-65.2073	-24.2257	0.8518	-3.9810

LINK NO.	U (INS)	UDT (IN/SEC)	UDDT (IN/SEC2)	W (INS)	WDT (IN/SEC)	WDDT (IN/SEC2)
1	4.2000	0.0	0.0	3.5903	0.0998	6.5818
2	4.7711	0.0321	51.1747	7.1111	0.9865	28.1005
3	4.8640	0.0402	214.4322	8.7671	1.8242	60.6170
4	4.8749	0.1432	411.3964	10.4271	2.6660	110.2373
5	4.8546	0.3315	603.6089	12.0850	3.4951	166.9532
6	4.7556	0.6238	767.4829	13.6887	4.3472	235.7585
7	4.6531	1.0506	885.1005	15.1862	5.3248	306.8317
8	4.5450	1.7510	943.4495	16.5810	6.3400	376.6074
9	4.4932	2.5583	939.0848	17.8795	7.3760	439.7756
10	4.5103	3.3238	882.4111	19.0900	8.3617	502.4048
11	4.6020	3.9773	781.9271	20.1570	9.2911	566.8427
12	4.8299	4.6204	648.6492	21.2051	10.1161	641.0949
13	5.1127	5.3293	506.9699	22.2196	10.7946	727.7105
14	5.5950	6.1172	381.7254	23.1529	10.8908	790.6863
15	5.9978	7.1876	281.9691	23.9949	10.7604	854.5248
16	6.4304	8.6411	202.3065	24.8037	10.3295	902.5567
17	6.8510	10.5501	140.7447	25.6218	9.6497	934.7478
18	7.2036	12.7376	103.3603	26.3909	8.9131	949.2642
19	7.4274	15.6134	111.3146	27.0822	8.6951	922.5065
20	7.5742	19.0426	175.2903	27.7443	8.7137	887.3733
21	7.6917	22.9075	278.5365	28.4151	8.8061	853.3541
22	7.7344	27.0257	406.7928	29.0909	9.0645	820.6488

23	7.8598	31.2564	553.3425	29.7644	9.7026	798.9063
24	7.9132	35.3035	700.9446	30.4372	10.6616	791.4213
25	7.9466	38.9186	835.3363	31.1109	11.8249	797.2978
26	8.0995	47.0423	1088.7363	33.4033	11.4222	754.5026

LINK NO.	O (RAD)	ODT (RAD/SEC)	ODDT (RAD/SEC2)
1	-0.1745	0.0	0.0
2	-0.0903	0.0218	-79.3179
3	0.0001	-0.0523	-111.4274
4	-0.0205	-0.1013	-113.4344
5	0.0590	-0.1841	-102.3700
6	0.0512	-0.2204	-78.4452
7	0.0777	-0.4699	-49.7589
8	0.0560	-0.6138	-2.4925
9	-0.0053	-0.6092	37.0676
10	-0.0446	-0.5585	83.9085
11	-0.1547	-0.4986	121.6430
12	-0.2981	-0.4936	139.9911
13	-0.4018	-0.6251	138.9757
14	-0.4081	-0.9821	125.3506
15	-0.4966	-1.4481	107.1132
16	-0.4757	-1.9703	85.3566
17	-0.4691	-2.4916	60.1980
18	-0.3561	-2.9591	34.2200
19	-0.2400	-4.0600	-45.9802
20	-0.1951	-4.8289	-106.7132
21	-0.1516	-5.2929	-146.4843
22	-0.1278	-5.4408	-167.1899
23	-0.1090	-5.2126	-168.2318
24	-0.0596	-4.6743	-153.5479
25	-0.0664	-3.8826	-126.5076
26	-0.0672	-3.3810	-103.6693

T=0.980 SEAT LOAD= 897.9 STRAP= 10.8 LAP= 0.0 HEAD ANGLE=-0.085 KOUNT= 50

LINK NO.	AXIAL FORCE (LB)	SHEAR FORCE (LB)	MOMENT (IN-LB)	FACET FORCE (LB)
1	-897.8503	0.0	-0.0	0.0
2	-284.7744	19.8523	-54.0222	-203.2736
3	-273.1144	5.8315	-43.8175	-191.3223
4	-275.9986	-8.8990	-21.2489	-163.7020
5	-283.2793	-11.2153	-2.1850	-146.7914
6	-301.6717	-34.1747	30.8512	-116.5226
7	-342.3681	-43.3695	36.7364	-64.9326
8	-356.4091	-77.2827	86.6614	-38.7936
9	-333.8543	-70.2967	172.1433	-51.0169
10	-329.5218	-54.4323	210.1519	-41.0933
11	-316.5487	-48.7892	220.9835	-36.9769
12	-300.0648	-24.2626	210.2052	-37.8431
13	-274.2980	9.9632	170.7558	-45.2509
14	-281.0305	40.3815	82.9802	-17.6235
15	-235.3456	35.4775	37.7057	-21.3471
16	-188.5305	44.2189	-6.1608	-23.5836
17	-147.7070	29.4839	-37.0450	-24.2501
18	-105.6637	13.8895	-56.8440	-22.3646
19	-39.0042	0.1697	-10.8178	-46.4146
20	-36.0863	-2.1734	-11.8375	-43.8533
21	-36.1737	-3.6629	-13.0448	-38.4967
22	-33.6288	-5.2317	-11.9338	-34.8916
23	-25.5818	-5.1242	-5.8039	-37.0389

24	-22.3702	-5.1463	0.1641	-36.5763
25	-22.3333	-5.9614	5.3173	-33.4951
26	-46.5022	-6.8518	-6.3038	-6.5635

LINK NO.	U (INS)	UDT (IN/SEC)	UDDT (IN/SEC2)	W (INS)	WDT (IN/SEC)	WDDT (IN/SEC2)
1	4.2000	0.0	0.0	3.5909	0.1264	3.3570
2	4.7718	0.2397	29.2072	7.1163	1.0865	11.1920
3	4.8666	0.9683	147.7614	8.7768	2.0405	22.2930
4	4.8305	2.0013	319.8501	10.4415	3.0619	41.5493
5	4.8636	3.1721	518.7861	12.1042	4.1092	69.6758
6	4.7582	4.3645	709.6623	13.7130	5.2514	114.4988
7	4.6694	5.4701	856.1201	15.2162	6.5391	164.0344
8	4.5657	6.4785	918.2127	16.6169	7.8622	213.8927
9	4.5177	7.2230	901.6054	17.9212	9.1547	251.2517
10	4.5379	7.6908	846.0836	19.1373	10.3867	286.1670
11	4.6317	7.8883	771.0780	20.2096	11.5627	320.5688
12	4.8604	7.9585	681.6434	21.2626	12.6776	363.7785
13	5.2260	8.0566	583.5259	22.2815	13.7026	419.0862
14	5.6308	8.2862	485.1334	23.2160	14.0919	470.1040
15	6.0378	8.8863	393.7611	24.0581	14.2209	519.6291
16	6.4766	9.9239	305.6058	24.8653	14.0288	569.4352
17	6.9059	11.4508	217.5946	25.6804	13.5408	613.4200
18	7.2687	13.3289	138.3178	26.4462	12.9239	644.4981
19	7.5066	16.0322	71.0813	27.1360	12.5997	626.4421
20	7.6709	19.5230	40.5303	27.7978	12.4204	582.7297
21	7.8085	23.6572	49.4328	28.4685	12.2719	524.3035
22	7.9232	28.2256	99.0257	29.1450	12.2548	452.6089
23	8.0214	33.0840	192.6663	29.8210	12.6131	369.4187
24	8.0970	37.8586	319.8797	30.4982	13.3519	293.7675
25	8.1501	42.2048	461.7566	31.1776	14.3867	237.3686
26	8.3471	51.7309	770.9882	33.4673	13.7115	170.1695

LINK NO.	O (RAD)	ODT (RAD/SEC)	ODDT (RAD/SEC2)
1	-0.1745	0.0	0.0
2	-0.0311	-0.3265	-56.3540
3	-0.0015	-0.5664	-92.5503
4	-0.0224	-0.6684	-112.1835
5	0.0567	-0.7319	-114.0338
6	0.0490	-0.6643	-94.9327
7	0.0747	-0.7368	-53.9809
8	0.0530	-0.5868	10.5614
9	-0.0079	-0.3947	43.1304
10	-0.0464	-0.1611	68.8695
11	-0.1558	0.0303	84.5892
12	-0.2390	0.1069	96.4350
13	-0.4033	-0.0135	105.4691
14	-0.4116	-0.4037	109.3737
15	-0.5025	-0.9139	110.0000
16	-0.4844	-1.4848	107.9491
17	-0.4306	-2.0673	103.0282
18	-0.3702	-2.6130	94.8294
19	-0.2604	-4.0207	59.2293
20	-0.2201	-5.0751	-0.2591
21	-0.1794	-5.7817	-51.3318
22	-0.1569	-6.1192	-98.9117
23	-0.1371	-6.0007	-136.2245
24	-0.0350	-5.4741	-154.9882
25	-0.0376	-4.5961	-152.9728

26 -0.0855 -3.9502 -127.9220
T=0.085 STAT LOAD= 830.0 STRAP= 12.1 LAP= 0.0 HEAD ANGLE=-0.107 KOUNT= 52

LINK NO.	AXIAL FORCE (LB)	SHEAR FORCE (LB)	MOMENT (IN-LB)	FACET FORCE (LB)
1	-830.0106	0.0	-0.0	0.0
2	-245.7953	16.4887	-44.8564	-174.4374
3	-233.2302	4.4537	-36.9107	-163.6698
4	-233.0369	-8.3082	-18.0108	-139.1437
5	-239.9545	-19.7503	-0.7401	-123.6315
6	-255.3353	-30.7457	28.5645	-36.5729
7	-290.5966	-39.3317	36.1042	-52.3352
8	-302.5198	-69.2964	82.3961	-29.0228
9	-281.7418	-63.2912	158.9719	-40.5314
10	-278.5543	-50.2690	195.6642	-31.2191
11	-268.2454	-45.9872	209.5392	-27.0281
12	-254.9461	-25.2955	204.6447	-27.4016
13	-233.1082	4.3436	174.8939	-34.0836
14	-239.9904	31.8218	101.0084	-9.5583
15	-200.1473	29.0087	62.3043	-13.0758
16	-159.8737	39.0739	22.1928	-14.7550
17	-123.6763	28.2452	-7.4903	-16.1503
18	-89.0103	16.8528	-28.7437	-15.4219
19	-34.5678	4.0998	7.4643	-30.0519
20	-30.6558	2.0262	2.3523	-29.6643
21	-29.2326	1.4545	-3.0209	-26.7359
22	-25.7014	0.3712	-6.3929	-25.2048
23	-18.3040	-0.2553	-5.8605	-27.7016
24	-15.0014	-0.5680	-5.1486	-28.0197
25	-14.2099	-0.9776	-4.6512	-26.4757
26	-28.6447	13.5252	-14.3129	-9.9036

LINK NO.	U (INS)	UDT (IN/SEC)	UDDT (IN/SEC2)	W (INS)	WDT (IN/SEC)	WDDT (IN/SEC2)
1	4.2000	0.0	0.0	3.5915	0.1370	0.2163
2	4.7733	0.3451	16.1979	7.1218	1.0832	-14.4212
3	4.8730	1.5404	89.6420	8.7871	2.0172	-32.4724
4	4.8941	3.3287	214.1803	10.4570	3.0482	-45.3596
5	4.8853	5.4178	368.1504	12.1251	4.1524	-50.0304
6	4.7983	7.5049	521.3347	13.7400	5.4343	-40.8015
7	4.7068	9.3047	646.9706	15.2501	6.8806	-28.5875
8	4.6089	10.6355	719.5736	16.6575	8.3667	-14.4601
9	4.5646	11.3724	744.0162	17.9693	9.7681	-7.0357
10	4.5866	11.6826	745.4569	19.1916	11.1033	-1.6074
11	4.6806	11.6337	727.2762	20.2701	12.3862	7.0276
12	4.9087	11.3954	689.4537	21.3292	13.6503	23.2090
13	5.2738	11.1132	630.8956	22.3537	14.8892	52.2112
14	5.6786	10.9131	556.1864	23.2908	15.4999	88.3196
15	6.0875	11.0674	471.2644	24.1341	15.8680	131.6701
16	6.5304	11.6417	377.3431	24.9410	15.9338	182.0316
17	6.9661	12.6905	276.5250	25.7543	15.6826	230.3792
18	7.3372	14.1285	181.2225	26.5173	15.2383	268.0991
19	7.5877	16.4221	87.1346	27.2053	14.8076	244.8814
20	7.7689	19.6602	20.1070	27.8657	14.3973	199.4090
21	7.9271	23.6976	-24.4311	28.5349	13.9511	143.6851
22	8.0648	28.3233	-50.0745	29.2103	13.5707	76.3042
23	8.1881	33.4029	-57.0004	29.8871	13.4766	-13.3201
24	8.2387	38.5627	-34.8618	30.5668	13.7559	-114.1675
25	8.3651	43.4232	23.0147	31.2505	14.3894	-214.1358
26	8.6138	54.6389	389.8174	33.5359	13.2943	-315.8062

LINK NO.	Q (RAD)	QDT (RAD/SEC)	QDDT (RAD/SEC2)
1	-0.1745	0.0	0.0
2	-0.0933	-0.5420	-33.7862
3	-0.0054	-0.9652	-65.7652
4	-0.0271	-1.1800	-85.4232
5	0.0517	-1.2617	-89.8319
6	0.0445	-1.1135	-80.2875
7	0.0704	-1.0024	-54.8557
8	0.0501	-0.5840	-18.4321
9	-0.0094	-0.2721	-2.1778
10	-0.0465	0.0581	13.4926
11	-0.1548	0.3213	30.8877
12	-0.2975	0.4689	50.7237
13	-0.4022	0.4297	73.0043
14	-0.4123	0.1083	93.0640
15	-0.5057	-0.3550	108.9760
16	-0.4904	-0.9097	117.9964
17	-0.4896	-1.5033	120.0893
18	-0.3819	-2.0766	117.7694
19	-0.2797	-3.6755	85.2351
20	-0.2452	-4.9361	53.6201
21	-0.2087	-5.8463	25.0049
22	-0.1883	-6.3823	-4.2992
23	-0.1684	-6.4583	-42.4719
24	-0.1140	-6.0947	-88.3781
25	-0.1124	-5.3371	-140.2374
26	-0.1070	-4.6957	-171.9690

T=0.090 SEAT LOAD= 763.7 STRAP= 13.4 LAP= 0.0 HEAD ANGLE=-0.133 KOUNT= 50

LINK NO.	AXIAL FORCE (LB)	SHEAR FORCE (LB)	MOMENT (IN-LB)	FACET FORCE (LB)
1	-763.7117	0.0	-0.0	0.0
2	-210.4504	12.8216	-32.2205	-143.2214
3	-196.6515	2.8529	-27.1760	-133.8572
4	-193.4446	-7.7478	-13.0297	-113.4443
5	-197.7909	-9.8431	1.1467	-100.2056
6	-210.3434	-26.5008	25.5245	-77.2534
7	-237.9029	-33.9778	33.2498	-40.8062
8	-247.6327	-59.2568	70.8910	-20.8472
9	-229.4880	-54.9282	141.6212	-30.6763
10	-227.2589	-45.1316	176.9440	-21.9620
11	-219.4710	-42.3594	193.4901	-17.7299
12	-209.1841	-25.6779	193.9437	-17.6222
13	-191.3145	-0.9502	173.5248	-23.4650
14	-198.2962	22.5743	114.2113	-2.2349
15	-165.0163	21.7477	83.1323	-5.3952
16	-132.1431	32.7434	48.3151	-6.4114
17	-101.4855	25.8731	21.3172	-8.3523
18	-72.0315	19.1487	-0.3849	-9.7121
19	-32.5800	7.7069	27.3791	-14.8446
20	-27.6457	5.7664	18.2829	-16.6424
21	-24.8505	6.0404	8.7232	-15.9452
22	-20.3217	5.3553	1.0257	-16.4188
23	-13.1862	3.9613	-3.4723	-19.5818
24	-9.6597	3.3489	-7.5520	-20.7452
25	-8.1465	3.2321	-11.3611	-20.5842
26	-14.5798	30.5424	-19.9835	-12.[illegible]112

LINK	U	UDT	UDDT	W	WDT	WDDT

NO.	(INS)	(IN/SEC)	(IN/SEC2)	(INS)	(IN/SEC)	(IN/SEC2)
1	4.2000	0.0	0.0	3.5922	0.1291	-3.0852
2	4.7752	0.4129	10.1643	7.1269	0.9407	-40.6062
3	4.8817	1.9144	57.6527	8.7966	1.7415	-73.5209
4	4.9130	4.1472	109.3552	10.4714	2.6608	-104.3531
5	4.91[illegible]	6.7602	165.3182	12.1449	3.6714	-136.2581
6	4.8412	9.4000	233.7420	13.7661	4.8955	-167.8758
7	4.7601	11.7392	323.6825	15.2834	6.2950	-198.6097
8	4.6699	13.5159	428.0369	16.6986	7.7525	-224.4255
9	4.6299	14.5722	529.3512	18.0168	9.1123	-247.7969
10	4.6538	15.0872	607.8789	19.2460	10.4052	-271.1690
11	4.7475	15.1079	649.8116	20.3309	11.6599	-291.9440
12	4.9742	14.7875	656.6574	21.3963	12.9255	-309.0739
13	5.3373	14.2811	627.8057	22.4273	14.2215	-317.1333
14	5.7403	13.7617	577.0511	23.3678	14.9558	-305.2434
15	6.1489	13.5310	509.6716	24.2134	15.4925	-282.5024
16	6.5935	13.6624	428.2386	25.0212	15.7740	-247.9792
17	7.0332	14.2139	332.0320	25.8338	15.7519	-206.3597
18	7.4103	15.1550	229.6692	26.5951	15.5003	-166.7481
19	7.6710	16.8965	101.0577	27.2807	15.0031	-163.7628
20	7.8673	19.6603	-27.3691	27.9385	14.4256	-179.7161
21	8.0448	23.2965	-148.7083	28.6049	13.7625	-207.5429
22	8.2051	27.5919	-256.1611	29.2777	13.0998	-252.0312
23	8.3533	32.4221	-343.1405	29.9529	12.5961	-325.7512
24	8.4736	37.494[illegible]	-389.2320	30.6328	12.3740	-423.2640
25	8.5808	42.499[illegible]	-378.3699	31.3183	12.4678	-534.5191
26	8.8904	55.6972	45.8969	33.5967	10.7640	-677.4621

LINK NO.	0 (RAD)	ODT (RAD/SEC)	ODDT (RAD/SEC2)
1	-0.1745	0.0	0.0
2	-0.0964	-0.6960	-26.6394
3	-0.0109	-1.2098	-30.6526
4	-0.0338	-1.4740	-32.1327
5	0.0445	-1.5806	-38.1993
6	0.0381	-1.4442	-52.0553
7	0.0646	-1.3048	-65.2310
8	0.0468	-0.8193	-73.9621
9	-0.0111	-0.4482	-65.0004
10	-0.0463	-0.0324	-46.7243
11	-0.1530	0.3474	-18.8097
12	-0.2346	0.6277	11.6820
13	-0.3993	0.7188	40.3763
14	-0.4107	0.5095	65.4557
15	-0.5062	0.1385	86.4681
16	-0.4935	-0.3480	104.5151
17	-0.4356	-0.8970	120.7069
18	-0.3908	-1.4450	134.3579
19	-0.2968	-3.1173	143.3067
20	-0.2689	-4.4738	137.6878
21	-0.2372	-5.4951	118.2677
22	-0.2199	-6.1770	83.0117
23	-0.2009	-6.4772	26.8374
24	-0.1454	-6.4144	-47.8611
25	-0.1408	-6.0244	-138.3677
26	-0.1328	-5.6622	-211.9927

T=0.095 SEAT LOAD= 706.4 STRAP= 14.8 LAP= 0.0 HEAD ANGLE=-0.164 KOUNT= 50

LINK NO.	AXIAL FORCE (LB)	SHEAR FORCE (LB)	MOMENT (IN-LB)	FACET FORCE (LB)

1	-706.4282	0.0	-0.0	0.0
2	-182.7843	9.1868	-17.2721	-112.9920
3	-166.3634	1.4693	-16.9679	-106.2363
4	-159.2102	-7.4950	-7.6836	-90.0690
5	-161.8242	-9.3265	3.7058	-78.8177
6	-171.4075	-22.9902	23.7904	-59.3833
7	-132.2703	-28.8342	31.5220	-30.1887
8	-199.4616	-48.9545	62.2261	-13.7533
9	-183.1292	-45.8380	122.4563	-22.5050
10	-181.0829	-39.0047	153.7979	-14.7642
11	-175.0625	-37.6470	170.9114	-10.7112
12	-167.4561	-25.3210	175.9952	-10.0872
13	-153.6479	-5.7231	165.1282	-14.8113
14	-161.0144	13.5493	121.0000	3.4824
15	-134.3228	14.1359	98.3683	0.8987
16	-108.6004	25.9048	69.5912	0.5730
17	-83.2845	22.6056	45.9245	-1.7257
18	-58.7991	20.0682	24.6414	-2.9674
19	-32.3426	10.0437	46.6062	-1.8552
20	-26.5818	8.0904	34.4763	-5.4063
21	-22.8136	9.0362	21.6336	-6.3921
22	-17.5106	8.7255	10.6129	-8.4566
23	-10.3816	6.8239	2.3692	-12.3669
24	-6.5900	6.0604	-5.3897	-14.2880
25	-4.4889	6.1234	-12.5656	-15.2141
26	-5.5062	39.6856	-21.0215	-12.9267

LINK NO.	U (INS)	UDT (IN/SEC)	UDDT (IN/SEC2)	W (INS)	WDT (IN/SEC)	WDDT (IN/SEC2)
1	4.2000	0.0	0.0	3.5928	0.1081	-5.3000
2	4.7773	0.4280	-6.5470	7.1310	0.7035	-52.1463
3	4.8918	2.0381	-16.4649	8.8042	1.3107	-97.6116
4	4.9345	4.3594	-29.2726	10.4832	2.0258	-149.6363
5	4.9512	7.0931	-26.1213	12.1612	2.8169	-205.1652
6	4.8300	9.9483	2.8846	13.7881	3.8052	-265.1634
7	4.8216	12.6697	69.8323	15.3118	4.9640	-327.6741
8	4.7416	14.9817	171.9239	16.7339	6.2031	-386.7685
9	4.7084	16.6311	293.5880	18.0584	7.3695	-440.3918
10	4.7361	17.6503	406.0842	19.2936	8.4705	-493.6515
11	4.8307	17.9958	490.6101	20.3844	9.5827	-545.6042
12	5.0560	17.8319	548.1083	21.4558	10.6290	-599.6073
13	5.4164	17.3032	572.6134	22.4930	11.7770	-650.4825
14	5.8163	16.6367	568.6151	23.4371	12.4948	-669.3779
15	6.2231	16.1425	533.0153	24.2856	13.0859	-669.8680
16	6.6674	15.9070	467.6297	25.0952	13.5011	-649.4292
17	7.1087	15.9853	373.1842	25.9082	13.6758	-610.6764
18	7.4892	16.3925	261.4288	26.6638	13.6355	-565.1453
19	7.7567	17.4203	109.3485	27.3521	13.2507	-526.7672
20	7.9650	19.4061	-64.1143	28.0070	12.6942	-505.4522
21	8.1590	22.2692	-241.5851	28.6698	11.9808	-499.0470
22	8.3390	25.8649	-406.0461	29.3389	11.1671	-514.1789
23	8.5100	30.1169	-547.1592	30.0108	10.3477	-564.5419
24	8.6610	34.8519	-638.0306	30.6884	9.6663	-648.7058
25	8.7372	39.8441	-658.4255	31.3729	9.2053	-758.2657
26	9.1682	55.2309	-218.7602	33.6409	6.6728	-947.1032

LINK NO.	O (RAD)	ODT (RAD/SEC)	ODDT (RAD/SEC2)
1	-0.1745	0.0	0.0
2	-0.1001	-0.7644	2.9865

3	-0.0172	-1.2665	7.1105
4	-0.0414	-1.5417	-0.3400
5	0.0362	-1.6942	-13.8272
6	0.0303	-1.6589	-37.5211
7	0.0573	-1.6267	-60.3690
8	0.0416	-1.2469	-86.5697
9	-0.0143	-0.8621	-90.0408
10	-0.0473	-0.3678	-82.6209
11	-0.1517	0.1380	-64.9792
12	-0.2916	0.5599	-41.5355
13	-0.3954	0.7947	-13.5765
14	-0.4075	0.7315	20.6107
15	-0.5045	0.4991	57.4650
16	-0.4940	0.1433	93.5702
17	-0.4385	-0.2836	125.9640
18	-0.3963	-0.7299	150.9402
19	-0.3103	-2.2587	192.5879
20	-0.2892	-3.5900	205.4250
21	-0.2529	-4.7021	190.0000
22	-0.2495	-5.5901	147.3660
23	-0.2327	-6.2211	76.0572
24	-0.1780	-6.5893	-18.4369
25	-0.1727	-6.7122	-132.0514
26	-0.1639	-6.7787	-230.0392

T=0.100 SEAT LOAD= 663.6 STRAP= 16.4 LAP= 0.0 HEAD ANGLE=-0.201 KOUNT= 50

LINK NO.	AXIAL FORCE (LB)	SHEAR FORCE (LB)	MOMENT (IN-LB)	FACET FORCE (LB)
1	-663.6204	0.0	-0.0	0.0
2	-164.7094	5.8929	-2.8146	-37.7251
3	-145.7225	0.0281	-7.0877	-83.4616
4	-135.3623	-7.9956	-1.4895	-70.7246
5	-136.6820	-9.4346	7.6454	-61.0146
6	-143.9688	-20.6966	24.3454	-44.2833
7	-159.0687	-24.4276	31.8581	-21.2829
8	-165.6634	-39.4718	55.9206	-8.2109
9	-147.9594	-36.8871	104.2989	-16.8310
10	-145.3112	-32.3528	129.2898	-10.3826
11	-140.0915	-32.6618	144.5455	-6.7623
12	-134.4360	-23.8810	152.6266	-5.7080
13	-124.1306	-8.9875	149.8019	-9.2173
14	-131.7913	6.1973	119.0446	6.6991
15	-110.5872	7.1908	104.2665	4.8322
16	-90.6664	13.8972	31.8640	5.1869
17	-69.7341	17.9623	62.5616	2.9440
18	-49.3098	18.4431	43.5567	1.3334
19	-32.3531	10.5613	63.3638	8.6116
20	-26.7832	8.4801	49.8772	4.0245
21	-22.6373	9.8398	35.3925	2.0956
22	-17.0116	9.8864	22.6486	-0.9436
23	-9.8027	7.9224	12.3850	-5.5392
24	-5.7968	7.2384	2.3903	-8.0442
25	-3.3057	7.3705	-6.9438	-9.6947
26	-1.7426	38.4232	-15.9872	-10.2638

LINK NO.	U (INS)	UDT (IN/SEC)	UDDT (IN/SEC2)	W (INS)	WDT (IN/SEC)	WDDT (IN/SEC2)
1	4.2000	0.0	0.0	3.5933	0.0764	-7.2849
2	4.7793	0.3416	-25.2602	7.1339	0.4276	-58.4792
3	4.9014	1.7490	-88.7871	8.8095	0.7717	-117.4167

4	4.9554	3.8944	-141.6671	10.4913	1.1725	-189.0858
5	4.9858	6.6010	-155.4211	12.1725	1.6358	-262.8286
6	4.9391	9.5885	-133.7419	13.8035	2.2807	-338.5922
7	4.8852	12.6156	-81.0936	15.3321	3.0805	-417.3689
8	4.8179	15.3594	-12.7934	16.7595	3.9729	-495.5528
9	4.7942	17.5311	71.6313	18.0891	4.8080	-572.4137
10	4.8284	19.0865	169.7326	19.3291	5.5786	-649.3043
11	4.9259	19.9123	273.2322	20.4245	6.3234	-726.5422
12	5.1514	20.1673	379.9841	21.5004	7.0627	-809.1785
13	5.5097	19.9303	470.0714	22.5426	7.8673	-892.9192
14	5.9064	19.3873	522.1237	23.4900	8.4218	-937.7025
15	6.3105	18.8099	524.8364	24.3414	8.9636	-956.5995
16	6.7529	18.2966	481.9015	25.1532	9.4547	-948.1685
17	7.1934	17.9206	399.5818	25.9676	9.8151	-915.5671
18	7.5745	17.7712	294.0554	26.7285	10.0046	-872.3135
19	7.8453	18.0382	145.7069	27.4105	9.8401	-826.4721
20	8.0613	19.1402	-30.7465	28.0629	9.4336	-791.0855
21	8.2673	21.0809	-218.6522	28.7224	8.8088	-764.8131
22	8.4632	23.7958	-402.5331	29.3873	7.9864	-755.5372
23	8.6535	27.2532	-574.5320	30.0545	6.9690	-777.7165
24	8.8268	31.4217	-706.0094	30.7278	5.9448	-838.5183
25	8.9775	36.1952	-770.7913	31.4087	4.9601	-936.5694
26	9.4408	53.6633	-390.8428	33.6615	1.3805	-1164.1740

LINK NO.	O (RAD)	ODT (RAD/SEC)	ODDT (RAD/SEC2)
1	-0.1745	0.0	0.0
2	-0.1038	-0.6707	30.2285
3	-0.0233	-1.1605	31.9743
4	-0.0491	-1.5113	11.7100
5	0.0276	-1.7531	-8.7413
6	0.0215	-1.8355	-31.3207
7	0.0485	-1.8848	-41.3511
8	0.0344	-1.6112	-57.4348
9	-0.0197	-1.2762	-72.9343
10	-0.0592	-0.8091	-90.1455
11	-0.1520	-0.2860	-101.0399
12	-0.2395	0.2049	-97.5973
13	-0.3318	0.5723	-72.9425
14	-0.4038	0.7113	-27.8930
15	-0.5014	0.7087	24.2811
16	-0.4922	0.5732	73.3809
17	-0.4984	0.3334	114.1671
18	-0.3980	0.0230	143.5236
19	-0.3191	-1.2717	195.9995
20	-0.3045	-2.5136	219.3491
21	-0.2339	-3.6772	214.3833
22	-0.2754	-4.7552	181.2506
23	-0.2627	-5.7306	116.1371
24	-0.2110	-6.5793	21.1029
25	-0.2078	-7.3006	-100.8480
26	-0.2006	-7.9069	-214.7001

T=0.105 SEAT LOAD= 639.7 STRAP= 18.2 LAP= 0.0 HEAD ANGLE=-0.243 KOUNT= 50

LINK NO.	AXIAL FORCE (LB)	SHEAR FORCE (LB)	MOMENT (IN-LB)	FACET FORCE (LB)
1	-639.7242	0.0	-0.0	0.0
2	-157.5443	3.0581	8.8451	-70.6459
3	-137.7457	-1.3808	2.5143	-67.1080
4	-125.5274	-9.4854	6.5604	-56.2456

5	-125.6502	-9.8274	13.5664	-47.8591
6	-130.7581	-19.1722	27.1420	-33.4782
7	-140.9635	-29.4618	33.0854	-15.5243
8	-143.0166	-32.3088	51.3816	-5.3274
9	-127.4365	-29.7774	90.0449	-14.0055
10	-123.7875	-26.4009	108.9543	-8.6825
11	-118.3850	-27.4211	120.6862	-5.6270
12	-113.2292	-20.9821	128.3389	-4.4855
13	-104.7204	-9.4885	128.6285	-7.0997
14	-111.3327	2.1740	106.3741	6.8615
15	-94.2312	1.8783	97.6332	5.7741
16	-78.2883	11.8023	82.1475	6.8339
17	-60.7088	11.4842	69.0680	5.2782
18	-43.4223	13.6592	55.0767	3.9991
19	-34.1363	9.1657	76.8499	16.4246
20	-27.9836	6.8582	63.7854	11.5821
21	-24.0086	8.3300	49.3907	9.4710
22	-18.4963	8.6439	36.6326	6.1217
23	-11.2270	7.0435	26.2543	1.0247
24	-7.1608	6.6528	15.7821	-1.8120
25	-4.5684	6.7122	5.8562	-3.7615
26	-3.9641	25.0430	-4.2571	-4.0941

LINK NO.	U (INS)	UDT (IN/SEC)	UDDT (IN/SEC2)	W (INS)	WDT (IN/SEC)	WDDT (IN/SEC2)
1	4.2000	0.0	0.0	3.5936	0.0369	-8.2573
2	4.7807	0.2237	-15.7271	7.1352	0.1137	-65.4113
3	4.9090	1.3160	-59.9238	8.8118	0.1480	-128.3638
4	4.9730	3.2001	-84.4825	10.4947	0.1778	-207.6657
5	5.0167	5.8552	-75.7523	12.1773	0.2541	-288.1816
6	4.9853	8.9360	-71.0761	13.8105	0.5046	-361.0883
7	4.9470	12.1335	-82.7517	15.3421	0.8901	-445.3630
8	4.8940	15.0448	-83.4011	16.7730	1.3646	-534.5477
9	4.8821	17.5013	-51.8322	18.1057	1.7836	-622.8599
10	4.9251	19.4657	10.4079	19.3485	2.1378	-711.2000
11	5.0280	20.7914	98.0934	20.4466	2.4639	-798.7661
12	5.2562	21.6182	206.8657	21.5252	2.7535	-892.5024
13	5.6146	21.9145	317.4215	22.5702	3.0927	-931.7589
14	6.0095	21.7332	404.4059	23.5197	3.3756	-1054.2521
15	6.4108	21.2751	449.4693	24.3735	3.7685	-1095.7977
16	6.8593	20.6529	452.5428	25.1878	4.2402	-1114.5667
17	7.2881	19.9675	416.5886	26.0043	4.7042	-1109.9118
18	7.6672	19.3768	351.2277	26.7666	5.0632	-1057.5731
19	7.9376	18.3651	233.7460	27.4483	5.1107	-1051.7127
20	8.1570	19.2131	75.6164	28.0992	4.8832	-1018.5081
21	8.3703	20.2309	-103.1163	28.7559	4.4057	-988.9778
22	8.5775	22.0215	-284.9454	29.4169	3.6559	-972.2402
23	8.7829	24.5979	-461.9137	30.0789	2.5849	-982.7124
24	8.9754	28.0654	-597.9446	30.7463	1.2781	-1029.2139
25	9.1490	32.4435	-700.2428	31.4211	-0.1637	-1115.4139
26	9.7033	51.5039	-455.1363	33.6530	-4.9328	-1357.3467

LINK NO.	O (RAD)	ODT (RAD/SEC)	ODDT (RAD/SEC2)
1	-0.1745	0.0	0.0
2	-0.1068	-0.5209	23.5754
3	-0.0237	-0.9894	29.2307
4	-0.0564	-1.4432	-6.0389
5	0.0188	-1.7889	-17.9503
6	0.0120	-1.9630	-10.1002

7	0.0387	-2.0124	-1.4869
8	0.0257	-1.8270	-25.6355
9	-0.0269	-1.5925	-50.0148
10	-0.0553	-1.2491	-81.3443
11	-0.1548	-0.8217	-105.5910
12	-0.2898	-0.3508	-115.9890
13	-0.3900	0.1107	-105.9803
14	-0.4007	0.4557	-73.4870
15	-0.4978	0.7030	-29.9046
16	-0.4886	0.8126	16.5386
17	-0.4955	0.7851	59.6602
18	-0.3963	0.6350	94.0986
19	-0.3231	-0.3539	164.2232
20	-0.3144	-1.4429	202.6791
21	-0.2996	-2.6028	210.0586
22	-0.2969	-3.8233	187.3662
23	-0.2398	-5.1005	133.1006
24	-0.2435	-6.3985	50.3670
25	-0.2454	-7.7016	-56.8547
26	-0.2426	-8.8566	-158.4996

T=0.110 SEAT LOAD= 636.1 STRAP= 20.2 LAP= 0.0 HEAD ANGLE=-0.289 KOUNT= 50

LINK NO.	AXIAL FORCE (LB)	SHEAR FORCE (LB)	MOMENT (IN-LB)	FACET FORCE (LB)
1	-636.0864	0.0	-0.0	0.0
2	-162.5156	1.3534	18.7340	-61.5493
3	-143.0567	-3.4447	11.8673	-57.7060
4	-130.5690	-11.4184	16.4388	-47.2219
5	-128.5845	-9.8420	20.1633	-40.9309
6	-131.0713	-18.2163	30.2896	-29.0549
7	-138.3723	-17.9572	33.8900	-13.8975
8	-138.8381	-28.5072	49.0009	-5.2628
9	-123.0211	-25.7917	81.7303	-14.0323
10	-118.1908	-22.4922	95.8776	-9.4825
11	-111.5528	-23.4374	102.6787	-7.0725
12	-105.4637	-17.7173	106.7358	-6.1736
13	-96.9994	-7.9012	105.3309	-8.2900
14	-102.8706	1.3497	86.0988	4.3407
15	-86.6357	-1.3080	80.6783	3.9439
16	-72.4786	5.6155	71.3408	5.5777
17	-56.8992	4.1370	65.1598	5.1575
18	-41.5893	6.3228	58.1544	4.8174
19	-35.8890	6.0132	86.1244	21.0675
20	-30.2279	3.3553	75.3103	16.7775
21	-27.0149	4.6114	62.8163	15.2673
22	-22.0621	5.0935	51.8160	12.2731
23	-14.7314	4.2950	43.2085	6.8599
24	-10.7253	4.4105	33.9529	3.9403
25	-8.2907	4.2665	24.9322	2.1101
26	-10.6160	0.5297	13.2455	5.0609

LINK NO.	U (INS)	UDT (IN/SEC)	UDDT (IN/SEC2)	W (INS)	WDT (IN/SEC)	WDDT (IN/SEC2)
1	4.2000	0.0	0.0	3.5936	-0.0032	-7.9885
2	4.7818	0.2207	8.3508	7.1349	-0.2504	-81.8304
3	4.9153	1.2879	49.2930	8.8109	-0.5544	-151.7979
4	4.9885	3.1413	66.8890	10.4929	-0.8806	-203.6736
5	5.0455	5.7496	24.6230	12.1750	-1.1490	-265.2095
6	5.0294	8.7339	-27.4692	13.8086	-1.2517	-339.4447
7	5.0068	11.8038	-57.1032	15.3411	-1.2864	-421.1745

8	4.9682	14.6342	-75.1514	16.7732	-1.2570	-594.3947
9	4.9688	17.1557	-77.5795	18.1069	-1.2821	-590.4551
10	5.0223	19.3437	-52.9745	19.3503	-1.3685	-675.3853
11	5.1128	21.0208	-3.5539	20.4490	-1.4813	-761.2349
12	5.3663	22.3079	69.8663	21.5278	-1.6619	-853.3748
13	5.7275	23.1069	159.8012	22.5733	-1.8299	-956.3377
14	6.1226	23.3778	251.2977	23.5234	-1.8824	-1026.7144
15	6.5223	23.2242	325.3010	24.3785	-1.7494	-1088.0525
16	6.9589	22.7467	378.6540	25.1948	-1.4529	-1138.3358
17	7.3331	22.0441	408.5304	26.0135	-1.0576	-1172.5993
18	7.7688	21.2893	410.9644	26.7778	-0.5804	-1133.3197
19	8.0359	20.4422	359.1699	27.4600	-0.5341	-1190.1927
20	8.2547	20.0321	259.2657	28.1101	-0.6529	-1185.0155
21	8.4710	20.2502	127.5264	28.7647	-1.0207	-1174.3807
22	8.6850	21.1969	-22.1918	29.4222	-1.7059	-1158.7728
23	8.9011	22.9148	-185.0513	30.0787	-2.8313	-1182.0023
24	9.1090	25.6318	-338.1438	30.7390	-4.3564	-1223.3572
25	9.3933	29.4788	-459.4965	31.4056	-6.2004	-1298.2074
26	9.9553	49.2854	-414.3796	33.6107	-12.1414	-1516.3744

LINK NO.	0 (RAD)	ODT (RAD/SEC)	O DDT (RAD/SEC2)
1	-0.1745	0.0	0.0
2	-0.1092	-0.5106	-24.2925
3	-0.0335	-0.9833	-24.0635
4	-0.0637	-1.4377	12.4111
5	0.0098	-1.7468	26.7644
6	0.0023	-1.9155	13.7935
7	0.0287	-1.9508	11.1013
8	0.0164	-1.8683	3.0972
9	-0.0354	-1.7582	-16.9921
10	-0.0625	-1.5610	-41.3723
11	-0.1600	-1.2598	-66.7873
12	-0.2930	-0.8706	-88.9487
13	-0.3308	-0.4193	-102.3814
14	-0.3995	0.0182	-97.0340
15	-0.4349	0.4174	-81.0084
16	-0.4846	0.7125	-55.7683
17	-0.4911	0.8774	-24.8368
18	-0.3922	0.8979	7.0611
19	-0.3232	0.2831	82.2238
20	-0.3133	-0.5753	134.5963
21	-0.3101	-1.6498	162.4731
22	-0.3137	-2.9295	164.2520
23	-0.3136	-4.4204	136.3303
24	-0.2747	-6.0691	81.7014
25	-0.2844	-7.8426	3.3164
26	-0.2886	-9.4340	-67.7618

T=0.115 SEAT LOAD= 652.0 STRAP= 22.5 LAP= 0.0 HEAD ANGLE=-0.336 KOUNT= 50

LINK NO.	AXIAL FORCE (LB)	SHEAR FORCE (LB)	MOMENT (IN-LB)	FACET FORCE (LB)
1	-652.0031	0.0	-0.0	0.0
2	-181.9460	0.1262	30.9958	-57.3036
3	-160.6926	-4.2791	20.7690	-55.0985
4	-146.1275	-12.8694	23.7859	-46.3719
5	-142.7151	-9.9700	25.2593	-41.4495
6	-144.0379	-18.4055	33.8469	-30.5454
7	-150.5712	-16.6003	34.8818	-15.9078
8	-149.8806	-26.5675	48.1321	-8.1548

9	-135.6123	-23.6613	77.9552	-17.0146
10	-127.5523	-19.8196	88.7490	-12.8998
11	-119.3585	-20.4446	91.0553	-10.9893
12	-111.7038	-14.3334	90.7503	-10.3912
13	-102.1963	-4.6702	85.3570	-12.2831
14	-106.3998	3.5668	64.5317	0.0722
15	-89.9920	-1.9153	59.7601	0.1728
16	-75.3235	1.8750	54.3309	2.1257
17	-60.0259	-2.0582	53.6670	2.8959
18	-45.1423	-1.5309	53.4275	3.7524
19	-38.9785	1.9003	91.0765	21.8876
20	-34.1110	-1.3059	83.7463	18.7480
21	-32.1273	-0.6368	74.4925	13.4972
22	-28.9683	-0.2389	66.7173	16.4073
23	-20.5572	-0.0032	61.6061	10.7569
24	-16.6637	0.7230	55.1442	7.9547
25	-14.6149	0.2252	48.4213	6.6599
26	-23.3243	-32.5376	34.5509	15.9828

LINK NO.	U (INS)	UDT (IN/SEC)	UDDT (IN/SEC2)	W (INS)	WDT (IN/SEC)	WDDT (IN/SEC2)
1	4.2000	0.0	0.0	3.5935	-0.0417	-7.1585
2	4.7830	0.2914	18.1402	7.1326	-0.6700	-80.4520
3	4.9226	1.6520	81.1171	8.8062	-1.2912	-136.9438
4	5.0054	3.6447	113.2329	10.4360	-1.8725	-187.9075
5	5.0750	6.1338	112.9495	12.1660	-2.4131	-237.3115
6	5.0732	8.8601	77.5192	13.7982	-2.8354	-289.6386
7	5.0653	11.6598	13.5748	15.3296	-3.2517	-355.8138
8	5.0405	14.3225	-44.5255	16.7608	-3.6141	-430.4508
9	5.0536	16.7883	-71.6540	18.0934	-4.0256	-500.4359
10	5.1182	18.9965	-84.8036	19.3354	-4.4982	-569.3663
11	5.2375	20.8008	-80.5533	20.4325	-5.0099	-641.7686
12	5.4782	22.3456	-49.5926	21.5093	-5.6279	-722.1278
13	5.8444	23.5236	11.6003	22.5527	-6.2897	-814.3934
14	6.2420	24.2443	99.0770	23.5017	-6.5983	-885.5993
15	6.6419	24.5080	190.4515	24.3566	-6.9054	-958.5855
16	7.0770	24.3983	281.5733	25.1737	-6.9286	-1033.3484
17	7.5183	23.9945	367.4119	25.9937	-6.7924	-1100.5650
18	7.8805	23.4213	433.9773	26.7595	-6.5373	-1151.4538
19	8.1431	22.5052	455.5360	27.4423	-6.5928	-1210.3296
20	8.3589	21.8038	439.1894	28.0916	-6.8059	-1254.3632
21	8.5750	21.5600	389.2733	28.7444	-7.2170	-1283.7610
22	8.7921	21.9165	308.2791	29.3983	-7.9360	-1306.0221
23	9.0149	22.9205	193.0795	30.0490	-9.1631	-1336.2186
24	9.2345	24.8991	58.4617	30.7012	-10.8967	-1381.1675
25	9.4464	28.0846	-74.7887	31.3577	-13.0886	-1442.9229
26	10.1975	47.5604	-253.2687	33.5306	-19.9584	-1591.3683

LINK NO.	O (RAD)	ODT (RAD/SEC)	ODDT (RAD/SEC2)
1	-0.1745	0.0	0.0
2	-0.1122	-0.6997	-35.6723
3	-0.0387	-1.1115	-21.3036
4	-0.0708	-1.4208	-6.7376
5	0.0014	-1.6248	13.5694
6	-0.0070	-1.7379	26.1822
7	0.0192	-1.8352	37.8965
8	0.0072	-1.8405	13.9789
9	-0.0443	-1.7868	2.7551
10	-0.0706	-1.6819	-10.7858

11	-0.1670	-1.5089	-35.5842
12	-0.2983	-1.2569	-66.6242
13	-0.3942	-0.9153	-95.8668
14	-0.4007	-0.5065	-112.0478
15	-0.4340	-0.0896	-119.6100
16	-0.4820	0.2745	-115.7354
17	-0.4[illegible]74	0.5505	-101.4600
18	-0.3880	0.7075	-79.1812
19	-0.3212	0.4234	-25.6648
20	-0.3209	-0.1705	24.0757
21	-0.3167	-1.0597	67.3327
22	-0.3265	-2.2532	98.2596
23	-0.3341	-3.7892	107.8677
24	-0.3039	-5.6081	96.7986
25	-0.3233	-7.6630	63.9763
26	-0.3361	-9.5001	43.1426

T=0.120 SEAT LOAD= 684.7 STRAP= 25.0 LAP= 0.0 HEAD ANGLE=-0.383 KOUNT= 50

LINK NO.	AXIAL FORCE (LB)	SHEAR FORCE (LB)	MOMENT (IN-LB)	FACET FORCE (LB)
1	-684.7328	0.0	-0.0	0.0
2	-214.1454	-0.2059	46.3674	-56.4691
3	-183.0762	-3.7150	28.8279	-58.6348
4	-170.3244	-13.5956	29.3957	-52.0953
5	-165.6884	-9.5833	28.4704	-48.6965
6	-166.4308	-19.0124	36.4594	-38.0518
7	-174.5474	-16.4815	34.9539	-21.4984
8	-173.6339	-27.1166	48.6007	-13.4731
9	-156.5696	-23.9889	77.2197	-22.6364
10	-149.3507	-19.3525	85.8806	-18.6975
11	-139.7773	-19.8241	85.6288	-16.9520
12	-130.6648	-12.5348	82.3034	-16.4938
13	-119.6663	-1.6132	72.5920	-18.3663
14	-123.9723	7.1789	46.9203	-4.9974
15	-104.9615	-0.7142	40.6882	-4.6465
16	-88.0553	0.9923	36.3443	-2.6707
17	-71.5122	-5.8258	38.6202	-0.9669
18	-55.5783	-7.9348	43.1879	0.9998
19	-44.7761	-2.1406	93.0125	18.4312
20	-40.6815	-6.1147	89.3593	16.6705
21	-40.1127	-6.3129	83.6710	18.1038
22	-36.9773	-6.3452	79.7727	17.2252
23	-28.8941	-5.1338	79.3124	11.2080
24	-25.0120	-3.8385	76.7858	8.6051
25	-23.4826	-4.8437	73.3841	8.1947
26	-41.3620	-69.4590	56.4319	26.8825

LINK NO.	U (INS)	UDT (IN/SEC)	UDDT (IN/SEC2)	W (INS)	WDT (IN/SEC)	WDDT (IN/SEC2)
1	4.2000	0.0	0.0	3.5932	-0.0729	-5.1193
2	4.7847	0.3612	-0.1700	7.1284	-0.9976	-49.9231
3	4.9317	1.9171	14.2015	8.7982	-1.8802	-97.2077
4	5.0248	4.0669	42.0882	10.4744	-2.6990	-139.3901
5	5.1070	6.6077	59.1534	12.1512	-3.4687	-180.9660
6	5.1185	9.2585	61.2809	13.7807	-4.1224	-222.4773
7	5.1240	11.8455	42.0302	15.3092	-4.8209	-269.7500
8	5.1118	14.2149	-11.6363	16.7378	-5.4907	-318.1437
9	5.1367	16.4202	-79.8139	18.0675	-6.2202	-372.8636
10	5.2119	18.4710	-129.0727	19.3064	-7.0061	-428.8474
11	5.3402	20.2398	-144.6969	20.4000	-7.8392	-485.6496

12	5.5889	21.8799	-131.2096	21.4728	-8.8164	-549.1563
13	5.9617	23.3108	-86.4247	22.5118	-9.9039	-626.6100
14	6.3639	24.4477	-7.3777	23.4579	-10.6526	-691.2929
15	6.7564	25.1843	87.6664	24.3109	-11.2303	-764.8306
16	7.2021	25.5828	195.4497	25.1268	-11.6539	-847.6307
17	7.6326	25.6940	310.7384	25.9467	-11.9339	-929.9456
18	8.0030	25.5598	415.3683	26.7128	-12.0016	-999.5193
19	8.2615	24.8899	489.2728	27.3945	-12.4143	-1098.8898
20	8.4740	24.2934	545.5159	28.0420	-12.9582	-1183.0869
21	8.6886	24.0155	581.3890	28.6922	-13.5190	-1252.1949
22	8.9067	24.1874	590.6861	29.3422	-14.5379	-1303.5489
23	9.1335	24.8232	563.6978	29.9862	-15.9853	-1366.3246
24	9.3615	26.2916	501.8240	30.6291	-17.9664	-1419.3695
25	9.5878	28.3825	403.7546	31.2739	-20.4503	-1474.5348
26	10.4333	46.9885	47.4298	33.4110	-27.6036	-1515.8797

LINK NO.	O (RAD)	ODT (RAD/SEC)	ODDT (RAD/SEC2)
1	-0.1745	0.0	0.0
2	-0.1160	-0.8001	-7.3587
3	-0.0446	-1.2156	-18.1483
4	-0.0781	-1.4768	-13.3207
5	-0.0066	-1.6079	-4.4124
6	-0.0157	-1.7157	3.3570
7	0.0104	-1.6713	27.7905
8	-0.0017	-1.6744	46.2635
9	-0.0531	-1.6912	37.4091
10	-0.0791	-1.6869	11.3204
11	-0.1749	-1.6373	-17.6631
12	-0.3054	-1.5403	-49.0752
13	-0.3999	-1.3655	-83.9932
14	-0.4046	-1.0726	-111.5425
15	-0.4960	-0.7347	-133.5820
16	-0.4822	-0.3906	-144.4845
17	-0.4361	-0.0779	-144.0133
18	-0.3858	0.1631	-133.2396
19	-0.3198	0.0655	-113.3179
20	-0.3219	-0.3275	-84.9977
21	-0.3216	-1.0084	-48.0273
22	-0.3370	-2.0140	-6.9940
23	-0.3520	-3.4264	30.7853
24	-0.3309	-5.1855	65.2372
25	-0.3606	-7.2367	102.2655
26	-0.3826	-9.0073	150.8200

T=0.125 SEAT LOAD= 729.1 STRAP= 27.6 LAP= 0.0 HEAD ANGLE=-0.425 KOUNT= 50

LINK NO.	AXIAL FORCE (LB)	SHEAR FORCE (LB)	MOMENT (IN-LB)	FACET FORCE (LB)
1	-729.9851	0.0	-0.0	0.0
2	-254.4208	-0.4329	62.5206	-59.2020
3	-223.6359	-3.1663	37.5962	-65.7123
4	-202.9629	-14.0538	34.7118	-62.0278
5	-195.6559	-6.6797	30.8370	-60.5724
6	-195.7019	-19.3930	38.1427	-50.2804
7	-226.5832	-16.2962	32.7839	-30.5711
8	-205.9292	-28.4525	47.6147	-21.8373
9	-188.8829	-25.9718	78.6176	-30.3373
10	-181.0612	-20.7252	88.4457	-25.9871
11	-170.3429	-21.1611	87.4843	-24.1116
12	-159.3269	-12.2085	82.0856	-23.7250

13	-147.1351	1.1368	68.4598	-25.7692
14	-152.0829	11.7467	35.8729	-10.1620
15	-130.1754	1.9323	26.8289	-9.7943
16	-109.9418	2.9192	20.9478	-8.0558
17	-91.0892	-6.7446	23.4925	-5.8059
18	-73.0541	-11.8001	30.3919	-3.0016
19	-54.0751	-5.2975	93.9986	11.0348
20	-50.5415	-10.2087	93.4514	10.5462
21	-51.3665	-11.3176	90.7313	13.8346
22	-48.8938	-11.9607	90.3726	14.1863
23	-39.5006	-9.9571	94.6591	7.3912
24	-35.2455	-8.1939	96.1111	4.8549
25	-34.1221	-9.7577	95.9974	5.4580
26	-62.9597	-102.6024	74.6073	35.5892

LINK NO.	U (INS)	UDT (IN/SEC)	UDDT (IN/SEC2)	W (INS)	WDT (IN/SEC)	WDDT (IN/SEC2)
1	4.2000	0.0	0.0	3.5928	-0.0934	-3.2287
2	4.7664	0.3206	-7.2729	7.1229	-1.1877	-27.4438
3	4.9412	1.8584	-22.8696	8.7878	-2.2591	-54.8399
4	5.0453	4.0631	-31.8845	10.4594	-3.2655	-85.5503
5	5.1404	6.6842	-29.3333	12.1318	-4.2163	-114.8405
6	5.1653	9.3771	-27.9217	13.7576	-5.0373	-141.1949
7	5.1835	11.8924	-42.2916	15.2822	-5.9244	-169.3538
8	5.1825	14.0272	-80.2090	16.7069	-6.7854	-198.6590
9	5.2176	15.9194	-129.4470	18.0323	-7.7304	-230.4639
10	5.3025	17.7070	-174.3903	19.2667	-8.7396	-263.2609
11	5.4393	19.3570	-201.3789	20.3555	-9.8214	-303.3678
12	5.6964	21.0529	-194.4870	21.4227	-11.0838	-354.3677
13	6.0769	22.7177	-147.4384	22.4553	-12.5256	-419.2533
14	6.4858	24.2489	-67.4922	23.3968	-13.5826	-478.5892
15	6.8931	25.4550	26.1398	24.2460	-14.5146	-546.6295
16	7.3322	26.3931	133.4888	25.0589	-15.3449	-625.4936
17	7.7647	27.1019	255.2816	25.6764	-16.0069	-708.2808
18	8.1358	27.5393	377.3262	26.6411	-16.4750	-783.1903
19	8.3921	27.3452	492.9201	27.3195	-17.4298	-896.1723
20	8.6025	27.2011	617.3774	27.9631	-18.4500	-997.4116
21	8.8166	27.3206	740.3922	28.6090	-19.5115	-1084.9275
22	9.0361	27.7832	847.1542	29.2536	-20.7671	-1158.2762
23	9.2662	28.5401	921.8143	29.8896	-22.5348	-1224.1241
24	9.5012	29.9265	952.7122	30.5219	-24.7819	-1268.4975
25	9.7395	32.2159	919.7576	31.1537	-27.4602	-1299.9101
26	10.6705	48.2293	464.4387	33.2540	-34.7747	-1237.3458

LINK NO.	O (RAD)	ODT (RAD/SEC)	ODDT (RAD/SEC2)
1	-0.1745	0.0	0.0
2	-0.1201	-0.8029	6.3989
3	-0.0508	-1.2514	5.1973
4	-0.0856	-1.5322	-2.2453
5	-0.0148	-1.6466	-2.7540
6	-0.0243	-1.7118	2.1743
7	0.0024	-1.5528	18.8705
8	-0.0095	-1.4686	30.5546
9	-0.0610	-1.[illegible]004	29.6480
10	-0.0873	-1.5849	19.9951
11	-0.1833	-1.6971	-8.3818
12	-0.3137	-1.7807	-47.7703
13	-0.4078	-1.7805	-84.3572
14	-0.4114	-1.6214	-110.1619

15	-0.5014	-1.3984	-132.1074
16	-0.4860	-1.1274	-143.6890
17	-0.4384	-0.8437	-159.9632
18	-0.3868	-0.5859	-164.2144
19	-0.3212	-0.6876	-186.4450
20	-0.3251	-1.0131	-188.1566
21	-0.3277	-1.5462	-166.1846
22	-0.3476	-2.3403	-122.5149
23	-0.3691	-3.5076	-61.8141
24	-0.3562	-4.9811	14.1176
25	-0.3955	-6.7041	114.8859
26	-0.4254	-8.0504	223.8637

T=0.130 SEAT LOAD= 780.5 STRAP= 30.7 LAP= 0.0 HEAD ANGLE=-0.463 KOUNT= 50

LINK NO.	AXIAL FORCE (LB)	SHEAR FORCE (LB)	MOMENT (IN-LB)	FACET FORCE (LB)
1	-780.4655	0.0	-0.0	0.0
2	-298.7920	-0.3769	78.1055	-64.9423
3	-263.7541	-2.5916	46.3948	-75.3597
4	-240.0044	-14.6177	40.4448	-74.1605
5	-230.1485	-7.5694	33.1611	-74.9496
6	-229.1514	-19.6427	39.4273	-65.2648
7	-243.3313	-16.0419	29.2288	-41.7938
8	-243.0335	-30.2741	45.6777	-32.1467
9	-226.5619	-29.0474	80.4756	-39.4793
10	-218.6542	-23.6209	93.9219	-34.3105
11	-207.7632	-24.4733	95.9887	-31.7798
12	-196.4095	-13.4413	90.7360	-31.2418
13	-181.8023	3.3350	73.2941	-33.7241
14	-188.0647	16.8776	31.5647	-15.0312
15	-162.6775	5.3977	18.6815	-14.8601
16	-138.5240	6.6229	9.7528	-13.4548
17	-116.7181	-5.6281	11.1586	-10.9003
18	-95.3518	-13.1205	18.6227	-7.4995
19	-66.4174	-6.9988	96.4276	1.3422
20	-63.0249	-12.8781	97.7293	1.7047
21	-64.9333	-14.6817	96.5246	6.6938
22	-62.6308	-15.9082	98.3499	8.0249
23	-51.0659	-13.4045	106.3117	-0.0702
24	-45.3158	-11.3291	110.6631	-2.8182
25	-44.9091	-13.3821	112.7694	-1.3174
26	-84.7152	-124.9924	85.7407	40.5499

LINK NO.	U (INS)	UDT (IN/SEC)	UDDT (IN/SEC2)	W (INS)	WDT (IN/SEC)	WDDT (IN/SEC2)
1	4.2000	0.0	0.0	3.5923	-0.1051	-1.3232
2	4.7380	0.3071	-2.9355	7.1167	-1.2746	-7.5554
3	4.9502	1.7513	-23.5048	8.7760	-2.4284	-12.9574
4	5.0651	3.8219	-65.0943	10.4423	-3.5270	-18.7707
5	5.1731	6.3046	-121.4645	12.1097	-4.5750	-27.5123
6	5.2112	8.8666	-177.6033	13.7311	-5.4994	-41.8295
7	5.2418	11.2544	-220.3559	15.2509	-6.4987	-58.2695
8	5.2511	13.2522	-241.8017	16.6710	-7.4701	-75.1016
9	5.2352	15.0067	-246.9562	17.9914	-8.5316	-91.2110
10	5.3886	16.6734	-244.0272	19.2203	-9.5645	-108.8873
11	5.5335	18.2759	-232.5885	20.3033	-10.8967	-129.8654
12	5.7991	20.0272	-209.1432	21.3637	-12.3611	-159.3702
13	6.1885	21.9069	-167.1328	22.3833	-14.0816	-203.5741
14	6.6060	23.8218	-96.1621	23.3239	-15.4152	-252.8863
15	7.0206	25.4942	-5.1477	24.1676	-16.6726	-314.0629

16	7.4657	26.9764	106.4006	24.9753	-17.8876	-389.6350
17	7.9033	28.3150	239.7182	25.7885	-18.9615	-473.0198
18	8.2782	29.4048	381.3586	26.5499	-19.8101	-551.2544
19	8.5350	29.8874	536.9216	27.2221	-21.3010	-647.3351
20	8.7466	30.5143	717.1514	27.8594	-22.8025	-732.6747
21	8.9631	31.4352	908.5239	28.4990	-24.2875	-809.2663
22	9.1867	32.6393	1091.5324	29.1363	-25.8913	-870.6578
23	9.4218	33.9926	1249.8235	29.7628	-27.9362	-910.7881
24	9.6545	35.7330	1354.4096	30.3834	-30.3378	-927.1631
25	9.9142	38.0547	1418.5253	31.0017	-33.0263	-885.9362
26	10.9194	51.7237	934.4721	33.0664	-39.8722	-779.0066

LINK NO.	O (RAD)	ODT (RAD/SEC)	ODDT (RAD/SEC2)
1	-0.1745	0.0	0.0
2	-0.1240	-0.7606	7.9407
3	-0.0569	-1.1843	19.5233
4	-0.0932	-1.4622	28.9091
5	-0.0229	-1.5773	31.2479
6	-0.0327	-1.6494	25.6229
7	-0.0052	-1.4771	15.2117
8	-0.0166	-1.3892	1.4272
9	-0.0683	-1.4360	-6.0770
10	-0.0951	-1.5676	-15.7507
11	-0.1919	-1.7758	-28.7520
12	-0.3231	-2.0104	-46.8472
13	-0.4177	-2.1859	-74.8841
14	-0.4209	-2.1689	-105.2131
15	-0.5100	-2.0662	-134.6241
16	-0.4936	-1.8909	-159.3389
17	-0.4947	-1.6856	-180.2170
18	-0.3815	-1.4809	-196.2348
19	-0.3272	-1.7747	-245.0711
20	-0.3328	-2.1675	-266.3591
21	-0.3380	-2.6224	-255.5670
22	-0.3613	-3.1944	-211.1898
23	-0.3878	-4.0136	-135.3938
24	-0.3811	-5.0193	-24.3747
25	-0.4276	-6.1576	90.8244
26	-0.4627	-6.8604	242.6160

T=0.135 SEAT LOAD= 834.0 STRAP= 34.0 LAP= 0.0 HEAD ANGLE=-0.494 KOUNT= 50

LINK NO.	AXIAL FORCE (LB)	SHEAR FORCE (LB)	MOMENT (IN-LB)	FACET FORCE (LB)
1	-834.0085	0.0	-0.0	0.0
2	-343.7827	-0.1434	92.7649	-72.2828
3	-304.2989	-1.8393	54.0667	-86.8358
4	-277.8354	-15.1995	45.3108	-87.8382
5	-265.9282	-6.7859	35.2575	-90.4273
6	-264.4646	-20.4973	41.1926	-80.7860
7	-282.4086	-16.5066	26.6792	-53.1068
8	-282.6456	-33.0377	45.2873	-42.3354
9	-266.3700	-32.9562	84.4521	-48.8653
10	-258.4658	-27.4033	101.9605	-42.8040
11	-247.5036	-28.9150	107.8733	-39.5110
12	-235.6136	-15.9508	104.2867	-38.6832
13	-219.3863	4.3523	84.8216	-41.5614
14	-227.7336	21.2390	34.4002	-19.0733
15	-198.5126	8.5929	17.7968	-19.1481
16	-170.0498	11.0899	4.9914	-18.0307

17	-144.6388	-3.1354	4.2903	-15.3674
18	-120.2096	-12.1570	10.8576	-11.6023
19	-79.7142	-7.0797	101.6893	-8.0809
20	-75.9189	-13.8042	103.1864	-7.4535
21	-78.3351	-15.9264	101.6242	-1.2094
22	-75.5918	-17.5409	103.6750	0.6964
23	-61.3120	-14.8736	113.3868	-9.0026
24	-54.3781	-12.6649	118.8787	-12.2169
25	-53.6567	-15.0298	121.6193	-10.1236
26	-102.3772	-133.4124	88.7541	41.4674

LINK NO.	U (INS)	UDT (IN/SEC)	UDDT (IN/SEC2)	W (INS)	WDT (IN/SEC)	WDDT (IN/SEC2)
1	4.2000	0.0	0.0	3.5918	-0.1068	0.4802
2	4.7894	0.2637	-11.5450	7.1103	-1.2655	11.9698
3	4.9586	1.5686	-54.5943	8.7638	-2.3973	25.5289
4	5.0832	3.3655	-124.5719	10.4247	-3.4707	40.5822
5	5.2027	5.4642	-218.6530	12.0868	-4.5096	52.5601
6	5.2527	7.6322	-314.1220	13.7035	-5.4621	55.8675
7	5.2946	9.7158	-386.4038	15.2181	-6.5032	56.7614
8	5.3135	11.6056	-406.7275	16.6332	-7.5292	53.7707
9	5.3665	13.4138	-382.6541	17.9482	-8.6341	53.8703
10	5.4685	15.2257	-336.9555	19.1713	-9.8161	52.6404
11	5.6218	16.9965	-281.7718	20.2479	-11.1095	49.9398
12	5.8166	18.9630	-219.4723	21.3007	-12.6747	38.5667
13	6.2360	21.1030	-151.0497	22.3163	-14.5595	14.8415
14	6.7240	23.3782	-72.6321	23.2446	-16.1101	-25.3604
15	7.1480	25.4959	19.4719	24.0813	-17.6472	-77.4252
16	7.6010	27.5491	137.0031	24.8820	-19.2302	-148.7984
17	8.0480	29.6034	287.6760	25.6888	-20.7312	-234.9559
18	8.4302	31.4742	455.4803	26.4449	-21.9881	-318.8956
19	8.6316	32.8447	653.4789	27.1087	-23.8622	-374.1760
20	8.9089	34.4743	871.9855	27.7375	-25.6900	-417.1394
21	9.1324	36.4475	1097.2420	28.3688	-27.4771	-459.4007
22	9.3645	38.6646	1313.0755	28.9975	-29.3134	-439.6548
23	9.6086	40.9229	1510.1230	29.6134	-31.4642	-488.5414
24	9.8615	43.3332	1657.5091	30.2220	-33.8083	-461.5923
25	10.1235	45.9772	1750.3391	30.8274	-36.2695	-377.6819
26	11.1916	57.5092	1362.1983	32.8595	-42.4500	-254.3651

LINK NO.	O (RAD)	ODT (RAD/SEC)	ODDT (RAD/SEC2)
1	-0.1745	0.0	0.0
2	-0.1277	-0.7032	19.5760
3	-0.0625	-1.0536	35.0714
4	-0.1000	-1.2618	50.3723
5	-0.0303	-1.3558	54.5170
6	-0.0406	-1.4602	46.2074
7	-0.0123	-1.3850	19.5839
8	-0.0236	-1.4358	-17.2762
9	-0.0757	-1.5529	-36.4540
10	-0.1033	-1.7441	-52.6237
11	-0.2013	-2.0044	-62.2908
12	-0.3339	-2.2985	-71.2434
13	-0.4296	-2.5653	-84.2069
14	-0.4330	-2.6803	-106.4039
15	-0.5220	-2.7406	-137.8966
16	-0.5051	-2.7274	-173.8793
17	-0.5055	-2.6634	-207.5756
18	-0.4019	-2.5626	-232.6858

19	-0.3343	-3.1041	-281.7987
20	-0.3472	-3.6000	-299.6249
21	-0.3545	-4.0023	-287.2720
22	-0.3801	-4.3543	-242.5949
23	-0.4097	-4.7769	-162.7371
24	-0.4367	-5.2300	-47.9451
25	-0.4571	-5.6716	81.4865
26	-0.4941	-5.7111	209.8266

T=0.140 SEAT LOAD= 885.4 STRAP= 37.4 LAP= 0.0 HEAD ANGLE=-0.520 KOUNT= 55

LINE NO.	AXIAL FORCE (LB)	SHEAR FORCE (LB)	MOMENT (IN-LB)	FACET FORCE (LB)
1	-885.3574	0.0	-0.0	0.0
2	-385.7088	0.0562	105.2322	-80.6553
3	-341.3919	-1.2205	60.1438	-99.0134
4	-312.9960	-15.9084	48.8106	-101.8595
5	-299.7952	-6.6589	37.1018	-105.4471
6	-298.6971	-22.3213	43.8450	-94.9225
7	-320.6215	-18.2954	26.7299	-62.7615
8	-321.6962	-37.3251	48.4238	-50.4349
9	-304.6339	-37.8156	93.0412	-57.0405
10	-296.4168	-31.8122	114.0303	-50.1362
11	-284.7898	-33.8430	122.5576	-46.2268
12	-272.0552	-19.1896	120.3683	-45.1244
13	-254.2086	4.1698	100.0285	-48.3295
14	-264.3117	23.9677	43.0519	-21.8481
15	-231.3055	10.4159	24.5059	-21.9542
16	-199.1855	15.0608	8.5220	-20.8191
17	-169.6171	0.1232	5.1888	-19.2036
18	-140.9182	-9.1307	9.0997	-14.3933
19	-99.3483	-5.5388	109.8449	-14.3292
20	-86.0896	-12.8504	109.6954	-14.1126
21	-88.3119	-14.9278	105.9817	-7.3382
22	-94.7055	-16.7503	106.3440	-5.3409
23	-67.8774	-14.3019	115.6759	-16.5528
24	-69.1511	-12.1563	120.5019	-20.3509
25	-53.4747	-14.6166	122.3616	-18.0992
26	-112.2343	-128.8056	84.8688	33.1755

LINE NO.	U (INS)	UDT (IN/SEC)	UDDT (IN/SEC2)	W (INS)	WDT (IN/SEC)	WDDT (IN/SEC2)
1	4.2000	0.0	0.0	3.5913	-0.1001	2.4157
2	4.7706	0.1866	-22.8709	7.1042	-1.1365	41.7130
3	4.9655	1.1629	-109.6967	8.7524	-2.1442	79.3999
4	5.0980	2.5042	-222.9184	10.4081	-3.0948	114.3184
5	5.2268	4.0721	-338.6855	12.0652	-4.0284	144.5524
6	5.2864	5.7468	-436.0293	13.6773	-4.9199	166.0745
7	5.3378	7.4857	-496.9793	15.1868	-5.9015	189.7388
8	5.3660	9.3048	-502.8406	16.5969	-6.8855	210.4888
9	5.4284	11.2712	-465.9705	17.9064	-7.9340	233.5820
10	5.5401	13.3503	-404.9714	19.1237	-9.0704	253.5981
11	5.7030	15.4604	-327.4095	20.1939	-10.3310	268.6371
12	5.9886	17.8266	-230.9232	21.2387	-11.9168	269.8603
13	6.3397	20.4170	-119.2459	22.2446	-13.8994	251.8784
14	6.8402	23.1708	-2.0774	23.1647	-15.5663	203.3057
15	7.2761	25.8248	122.8125	23.9930	-17.4730	145.1115
16	7.7418	28.5105	260.4016	24.7849	-19.4135	71.4509
17	8.2101	31.3340	417.6100	25.5832	-21.3370	-12.2391
18	8.5938	34.0459	583.8408	26.3320	-23.0038	-91.3442
19	8.8646	36.4418	737.1646	26.9858	-25.0401	-101.6574

20	9.0927	39.1875	1003.8869	27.6052	-26.9740	-102.2886
21	9.3290	42.2993	1223.4367	28.2272	-28.8839	-110.6799
22	9.5749	45.6030	1433.8982	28.8465	-30.7929	-111.9898
23	9.8328	48.8626	1633.0609	29.4518	-32.8523	-78.4963
24	10.0197	52.0639	1795.9289	30.0492	-34.9413	-12.8797
25	10.3762	55.1991	1907.3274	30.6433	-36.9769	84.4721
26	11.4975	65.0986	1641.4561	32.6461	-42.5571	184.9546

LINE NO.	O (RAD)	ODT (RAD/SEC)	ODDT (RAD/SEC2)
1	-0.1745	0.0	0.0
2	-0.1308	-0.5447	43.4432
3	-0.0673	-0.8094	63.4470
4	-0.1056	-0.9643	67.6757
5	-0.0363	-1.0648	59.5770
6	-0.0473	-1.2278	44.3193
7	-0.0190	-1.3033	11.5931
8	-0.0311	-1.5414	-24.4772
9	-0.0340	-1.7612	-44.9328
10	-0.1128	-2.0495	-65.9666
11	-0.2122	-2.3800	-85.3026
12	-0.3464	-2.7326	-102.8473
13	-0.4436	-3.0738	-120.9993
14	-0.4479	-3.2990	-143.2297
15	-0.5376	-3.4917	-164.9160
16	-0.5299	-3.6259	-186.6830
17	-0.5214	-3.7090	-208.9838
18	-0.4176	-3.7336	-230.8910
19	-0.3584	-4.5034	-267.2757
20	-0.3689	-5.0748	-278.4291
21	-0.3780	-5.4100	-265.9553
22	-0.4048	-5.5432	-226.5314
23	-0.4356	-5.5732	-153.4605
24	-0.4335	-5.4919	-54.2639
25	-0.4845	-5.2931	61.3783
26	-0.5203	-4.8156	145.2936

T=0.145 SEAT LOAD= 928.8 STRAP= 47.8 LAP= 0.0 HEAD ANGLE=-0.543 KOUNT= 50

LINK NO.	AXIAL FORCE (LB)	SHEAR FORCE (LB)	MOMENT (IN-LB)	FACET FORCE (LB)
1	-928.8215	0.0	-0.0	0.0
2	-419.0922	0.0650	113.2452	-89.7951
3	-372.6441	-1.2287	64.2497	-110.3602
4	-342.2845	-17.2451	51.8747	-113.6735
5	-328.6662	-7.5330	39.7606	-117.2939
6	-328.4126	-25.0669	48.0398	-105.2220
7	-353.5248	-21.1112	30.1087	-69.2300
8	-355.4074	-42.5875	55.1736	-55.1979
9	-336.5142	-43.1522	106.6831	-62.7063
10	-327.8921	-36.5410	131.3289	-54.8629
11	-315.3913	-38.8556	142.0662	-50.3713
12	-301.4232	-22.6241	140.9191	-49.0456
13	-281.6316	3.4199	119.8159	-52.6578
14	-294.0478	25.8160	57.1541	-22.7636
15	-256.9803	11.8665	36.6504	-22.9440
16	-220.1227	18.8176	17.6360	-21.6433
17	-186.6458	4.7500	11.0533	-19.2460
18	-153.6503	-3.2978	6.1534	-16.4228
19	-97.4444	-1.4140	121.9511	-14.5102
20	-99.3936	-9.5233	117.0648	-15.8531

21	-92.3283	-11.7186	109.6102	-9.5308
22	-87.7354	-13.8445	106.7772	-7.9749
23	-69.1946	-11.9913	113.7677	-20.2374
24	-60.5097	-10.0772	115.4135	-24.6028
25	-58.3191	-12.4323	116.2223	-22.6497
26	-112.1726	-114.6927	76.4833	35.0053

LINK NO.	U (INS)	UDT (IN/SEC)	UDDT (IN/SEC2)	W (INS)	WDT (IN/SEC)	WDDT (IN/SEC2)
1	4.2000	0.0	0.0	3.5908	-0.0803	5.6351
2	4.7912	0.0441	-32.0124	7.0992	-0.8345	79.3209
3	4.9697	0.4964	-150.6059	8.7429	-1.5744	147.3301
4	5.1074	1.1894	-291.4621	10.3944	-2.2931	207.1531
5	5.2425	2.1437	-420.1655	12.0474	-3.0206	260.4019
6	5.3093	3.3422	-515.4696	13.6553	-3.7509	303.8913
7	5.3687	4.8224	-560.7840	15.1604	-4.5508	352.9135
8	5.4061	6.6685	-544.0553	16.5659	-5.3665	398.9275
9	5.4788	8.8672	-485.0013	17.8705	-6.2394	445.3941
10	5.6017	11.2943	-403.0371	19.0824	-7.2253	484.3433
11	5.7762	13.8420	-302.9319	20.1466	-8.3778	511.3786
12	6.0750	16.7658	-176.4163	21.1835	-9.9481	515.6017
13	6.5006	20.0176	-26.8932	22.1793	-12.0325	491.6526
14	6.9565	23.4479	123.6558	23.0898	-14.0800	426.2892
15	7.4073	26.8021	283.3316	23.9084	-16.2158	341.9421
16	7.8383	30.2331	465.0739	24.6896	-18.5717	219.5520
17	8.3527	33.8707	594.3775	25.4771	-20.9587	118.9353
18	8.7718	37.1392	469.9646	26.2167	-22.9194	198.3039
19	9.0571	40.3695	425.3606	26.8604	-24.9426	172.6144
20	9.3015	44.2780	735.7282	27.4702	-26.8102	179.2704
21	9.5560	48.4760	1101.2219	28.0826	-28.7109	181.1659
22	9.8208	52.7578	1391.2589	28.6924	-30.5957	178.7145
23	10.0074	56.9424	1572.2905	29.2879	-32.4601	212.7331
24	10.3824	60.9356	1719.4717	29.8758	-34.1996	274.5557
25	10.6759	64.6310	1838.6645	30.4609	-35.7526	373.5299
26	11.8440	73.5421	1692.8295	32.4368	-40.9581	412.1510

LINK NO.	O (RAD)	ODT (RAD/SEC)	ODDT (RAD/SEC2)
1	-0.1745	0.0	0.0
2	-0.1329	-0.2766	62.1351
3	-0.0704	-0.4365	82.3590
4	-0.1035	-0.5941	79.2490
5	-0.0403	-0.7627	62.1378
6	-0.0529	-1.0185	40.9047
7	-0.0255	-1.2765	-0.4932
8	-0.0331	-1.6918	-37.8083
9	-0.0934	-2.0096	-57.6499
10	-0.1239	-2.4064	-80.0944
11	-0.2253	-2.8534	-105.7467
12	-0.3614	-3.3215	-131.0083
13	-0.4606	-3.7687	-153.3098
14	-0.4663	-4.1001	-174.8913
15	-0.5572	-4.3848	-196.1028
16	-0.5415	-4.6037	-200.6961
17	-0.5426	-4.6291	74.1288
18	-0.4385	-3.8994	403.1171
19	-0.3839	-5.5215	89.2782
20	-0.3975	-6.2799	-177.3133
21	-0.4081	-6.5689	-206.5248
22	-0.4352	-6.5438	-173.8123

23	-0.4652	-6.2664	-119.7761
24	-0.4616	-5.7623	-46.8753
25	-0.5103	-5.0512	28.6019
26	-0.5428	-4.2693	73.8375

T=0.150 SEAT LOAD= 956.3 STRAP= 71.7 LAP= 0.0 HEAD ANGLE=-0.564 KOUNT= 50

LINK NO.	AXIAL FORCE (LB)	SHEAR FORCE (LB)	MOMENT (IN-LB)	FACET FORCE (LB)
1	-956.2733	0.0	-0.0	0.0
2	-437.6326	-0.3629	115.1408	-98.3345
3	-391.1864	-2.3241	66.3277	-118.4713
4	-361.3815	-19.5258	55.1659	-120.4463
5	-348.4871	-9.6907	44.0514	-123.0377
6	-349.5110	-28.7023	54.3216	-108.9999
7	-376.3232	-24.7380	37.7056	-70.7744
8	-378.9654	-48.2359	65.8623	-55.2424
9	-357.5627	-48.2624	125.5107	-64.6307
10	-349.0622	-40.8101	154.2012	-55.8452
11	-336.3167	-42.8357	167.7789	-50.8343
12	-322.0060	-24.5961	167.7620	-49.4791
13	-301.0309	4.8340	145.9840	-53.8214
14	-315.0054	31.7285	76.9538	-21.6008
15	-274.5030	22.4340	46.8767	-23.2712
16	-231.6356	33.0178	10.1471	-24.5172
17	-193.6665	15.4689	-9.5110	-23.8888
18	-157.0524	-0.4713	-19.2084	-21.2300
19	-100.2421	5.6175	143.2698	-4.6998
20	-91.1140	-2.4219	131.3755	-8.7505
21	-89.8772	-3.7527	116.3657	-4.8151
22	-83.5483	-6.5451	107.0340	-5.1176
23	-64.4970	-6.6971	108.8230	-18.3240
24	-55.4616	-5.6183	107.4665	-23.5570
25	-52.8023	-7.8510	103.9305	-22.6609
26	-101.6078	-91.9256	64.2037	29.6533

LINK NO.	U (INS)	UDT (IN/SEC)	UDDT (IN/SEC2)	W (INS)	WDT (IN/SEC)	WDDT (IN/SEC2)
1	4.2000	0.0	0.0	3.5905	-0.0439	8.7534
2	4.7310	-0.1149	-30.1295	7.0962	-0.3588	107.6104
3	4.9703	-0.2675	-147.7154	8.7371	-0.6929	199.3395
4	5.1097	-0.2889	-289.4300	10.3859	-1.0534	281.0511
5	5.2470	0.0044	-423.7366	12.0360	-1.4561	355.0209
6	5.3195	0.7106	-524.2497	13.6409	-1.9167	415.6362
7	5.3857	1.9711	-563.5636	15.1427	-2.4217	478.6922
8	5.4326	3.9607	-518.2084	16.5447	-2.9714	531.2874
9	5.5172	6.5592	-410.8988	17.8457	-3.5874	578.1458
10	5.6535	9.5202	-272.2416	19.0532	-4.3830	604.6687
11	5.8422	12.6932	-117.0674	20.1119	-5.4417	604.4542
12	6.1573	16.3863	69.5848	21.1408	-7.0912	559.7243
13	6.6014	20.5513	286.3778	22.1256	-9.4828	465.3234
14	7.0765	24.8710	456.3189	23.0248	-12.0107	380.3935
15	7.5463	28.9640	474.8812	23.8313	-14.5497	418.2003
16	8.0459	32.6797	387.2398	24.5999	-17.0357	491.6607
17	8.5381	36.0813	341.7577	25.3757	-19.2418	528.5479
18	8.9624	38.9992	334.2129	26.1063	-20.9448	537.7452
19	9.2639	42.2186	345.5393	26.7406	-22.6694	603.0181
20	9.5292	46.4648	283.7900	27.3410	-24.4696	622.9082
21	9.8074	51.5002	308.6928	27.9436	-26.4764	610.3954
22	10.0971	56.9363	452.2561	28.5436	-28.5682	555.3509
23	10.3381	62.5292	704.3027	29.1298	-30.5414	482.3523

24	10.7062	67.9190	1034.4468	29.7093	-32.2345	452.6112
25	11.0205	72.7960	1341.1019	30.2873	-33.5433	479.5717
26	12.2322	81.5470	1441.0175	32.2374	-38.8025	422.0181

LINK NO.	O (RAD)	ODT (RAD/SEC)	ODDT (RAD/SEC2)
1	-0.1745	0.0	0.0
2	-0.1335	0.0444	62.6653
3	-0.0715	-0.0163	83.4603
4	-0.1115	-0.1844	83.6239
5	-0.0439	-0.4387	67.0164
6	-0.0574	-0.8059	43.0040
7	-0.0319	-1.3041	-12.6623
8	-0.0481	-1.9431	-65.7211
9	-0.1043	-2.3762	-92.9780
10	-0.1370	-2.8854	-115.3443
11	-0.2410	-3.4594	-144.9270
12	-0.3798	-4.0672	-185.6983
13	-0.4816	-4.6795	-218.0395
14	-0.4892	-5.0480	-95.0511
15	-0.5812	-4.8934	122.0960
16	-0.5648	-4.5039	0.2168
17	-0.5639	-4.1415	83.4623
18	-0.4573	-3.7513	-118.4689
19	-0.4115	-5.6387	-51.3898
20	-0.4307	-7.0105	-87.4436
21	-0.4440	-7.7650	-184.9126
22	-0.4711	-7.9466	-269.4862
23	-0.4991	-7.5420	-319.2083
24	-0.4319	-6.6405	-280.2940
25	-0.5358	-5.3169	-118.7107
26	-0.5636	-4.0812	-3.9567

T=0.155 SEAT LOAD= 961.2 STRAP= 96.8 LAP= 0.0 HEAD ANGLE=-0.584 KOUNT= 50

LINK NO.	AXIAL FORCE (LB)	SHEAR FORCE (LB)	MOMENT (IN-LB)	FACET FORCE (LB)
1	-961.1892	0.0	-0.0	0.0
2	-437.5696	-1.3695	110.9121	-104.1094
3	-394.0878	-4.4998	66.2982	-121.3618
4	-367.1483	-22.6901	58.4909	-120.5857
5	-356.6810	-13.2631	50.0854	-121.0189
6	-360.1461	-33.3971	63.1459	-104.5271
7	-387.5756	-29.3110	50.8643	-66.0604
8	-391.6454	-54.1085	81.8934	-49.4073
9	-367.3985	-52.4801	151.1615	-62.1764
10	-360.4272	-43.3435	183.4995	-52.8765
11	-349.4173	-44.1780	201.3911	-47.5733
12	-335.3242	-22.9405	200.7880	-46.8358
13	-310.6303	11.1007	166.6187	-53.5300
14	-320.2093	42.0994	75.0519	-22.7788
15	-275.3540	30.6964	34.1994	-25.7957
16	-229.6193	37.6294	-5.7187	-27.5719
17	-190.1113	17.4350	-28.7548	-27.1179
18	-152.6213	-2.1129	-37.7568	-23.9251
19	-99.3933	11.2030	167.9235	10.6287
20	-88.1431	3.1841	149.5693	4.0409
21	-84.4493	3.1726	127.9103	5.5968
22	-75.8306	1.3051	111.3734	3.1853
23	-55.9206	0.4300	104.7751	-10.5879
24	-45.3012	1.2308	95.5662	-16.7502

25	-41.3743	-0.2894	85.1219	-17.6781
26	-78.7180	-55.6725	46.8436	22.1350

LINK NO.	U (INS)	UDT (IN/SEC)	UDDT (IN/SEC2)	W (INS)	WDT (IN/SEC)	WDDT (IN/SEC2)
1	4.2962	0.0	0.0	3.5904	0.0027	8.8378
2	4.7901	-0.2459	-22.2306	7.0958	0.1753	94.1547
3	4.9672	-0.9356	-119.5621	8.7362	0.2935	173.5022
4	5.1048	-1.6318	-245.9832	10.3842	0.3175	237.7612
5	5.2428	-1.9762	-359.8515	12.0331	0.2522	293.4727
6	5.3168	-1.7219	-433.1046	13.6364	0.0524	336.0438
7	5.3389	-0.5728	-437.6023	15.1364	-0.1840	382.2947
8	5.4465	1.7649	-343.5123	16.5362	-0.5176	419.0034
9	5.5457	5.0443	-174.3264	17.8346	-0.9450	450.4159
10	5.6988	8.8532	36.9352	19.0384	-1.6498	459.9907
11	5.9055	12.9732	262.6594	20.0917	-2.7481	454.9837
12	6.2418	17.7104	448.4597	21.1119	-4.5728	475.0724
13	6.7091	22.6979	491.2227	22.0841	-7.0386	555.8299
14	7.2067	27.1721	422.7055	22.9704	-9.5345	592.1505
15	7.6964	31.0139	388.1603	23.7649	-11.8692	617.1692
16	8.2138	34.4498	326.1076	24.5216	-14.1518	658.5891
17	8.7226	37.6145	271.9970	25.2868	-16.1718	697.2053
18	9.1609	40.3343	216.6992	26.0092	-17.7364	729.2427
19	9.4786	43.6307	262.9746	26.6356	-19.1872	760.5583
20	9.7654	48.0401	366.7814	27.2273	-20.9243	759.5215
21	10.0694	53.3772	441.8404	27.8194	-23.0942	715.3698
22	10.3876	59.3470	493.8636	28.4082	-25.5029	657.8449
23	10.7130	65.7403	541.8521	28.9836	-27.8219	590.3381
24	11.0570	72.0785	592.6620	29.5541	-29.7862	524.2096
25	11.3988	77.9035	615.6070	30.1256	-31.1941	423.7352
26	12.6555	87.2225	794.7875	32.0481	-37.0475	267.1004

LINK NO.	O (RAD)	ODT (RAD/SEC)	ODDT (RAD/SEC2)
1	-0.1745	0.0	0.0
2	-0.1326	0.3308	51.5699
3	-0.0706	0.3809	73.6402
4	-0.1114	0.2132	70.2659
5	-0.0453	-0.1350	43.2832
6	-0.0610	-0.6489	15.9894
7	-0.0387	-1.4535	-48.0395
8	-0.0589	-2.3918	-116.3320
9	-0.1175	-2.9809	-154.3513
10	-0.1532	-3.6530	-198.0283
11	-0.2605	-4.3985	-198.8436
12	-0.4026	-4.9606	-64.0009
13	-0.5065	-4.9944	88.1549
14	-0.5141	-4.8318	21.6077
15	-0.6048	-4.5886	87.4331
16	-0.5368	-4.2263	67.7108
17	-0.5340	-3.8387	61.0609
18	-0.4755	-3.5408	86.8014
19	-0.4399	-5.7027	-59.3748
20	-0.4666	-7.3296	-83.1802
21	-0.4345	-8.3919	-86.4367
22	-0.5133	-8.7995	-78.6689
23	-0.5387	-8.4578	-64.4763
24	-0.5276	-7.4286	-71.3098
25	-0.5637	-5.8124	-72.0432
26	-0.5844	-4.3525	-105.5134

T=0.160 SEAT LOAD= 947.5 STRAP=122.4 LAP= 0.0 HEAD ANGLE=-0.608 KOUNT= 55

LINK NO.	AXIAL FORCE (LB)	SHEAR FORCE (LB)	MOMENT (IN-LB)	FACET FORCE (LB)
1	-947.4686	0.0	-0.0	0.0
2	-423.0558	-2.7401	101.6128	-107.2931
3	-384.6703	-7.5175	64.2254	-119.9127
4	-362.6347	-26.9633	62.1474	-114.9632
5	-356.1791	-18.5207	58.2816	-111.9674
6	-363.1269	-39.7034	75.2371	-92.1786
7	-389.8699	-35.5011	70.6042	-55.0713
8	-395.6205	-61.1192	104.8451	-37.2991
9	-367.1127	-56.3346	186.0604	-55.1318
10	-361.2820	-43.9659	218.8558	-45.9220
11	-343.3952	-41.6216	227.8367	-42.3694
12	-329.8919	-17.2915	209.9781	-44.3349
13	-302.4877	17.4438	163.8388	-52.4627
14	-300.9352	48.4815	66.5646	-23.4434
15	-264.3102	36.1616	19.6566	-27.2835
16	-217.9978	39.7003	-21.9083	-29.6095
17	-179.0738	17.4814	-44.6774	-28.8776
18	-142.3735	-4.2242	-52.0482	-25.1986
19	-96.8433	18.0335	196.0571	30.5172
20	-83.0560	10.3447	169.7128	20.5171
21	-76.5925	11.6258	140.1827	18.7660
22	-66.0082	10.1535	115.8552	13.5751
23	-46.3154	7.7695	100.8823	-0.8829
24	-35.9736	7.9238	84.1834	-8.1369
25	-30.9194	6.9405	67.1816	-11.0699
26	-54.6968	-20.4223	31.2302	14.9782

LINK NO.	U (INS)	UDT (IN/SEC)	UDDT (IN/SEC2)	W (INS)	WDT (IN/SEC)	WDDT (IN/SEC2)
1	4.2000	0.0	0.0	3.5905	0.0331	3.5136
2	4.7886	-0.3581	-23.2511	7.0976	0.5236	51.3698
3	4.9611	-1.4878	-99.9320	8.7395	0.9440	96.2025
4	5.0938	-2.7260	-185.3870	10.3882	1.2207	134.5255
5	5.2288	-3.5203	-245.3655	12.0375	1.3783	167.2764
6	5.3034	-3.4910	-249.8929	13.6402	1.3430	189.4131
7	5.3315	-2.1812	-159.3732	15.1395	1.2976	215.4538
8	5.4523	0.8597	46.1211	16.5381	1.0994	234.3976
9	5.5705	5.2468	310.5736	17.8346	0.7777	254.7953
10	5.7456	10.2608	522.7116	19.0350	0.1414	295.4443
11	5.9754	15.2558	590.9711	20.0832	-0.7255	384.3968
12	6.3366	20.2874	543.6562	21.0950	-2.1742	457.3258
13	6.8285	25.0663	477.1425	22.0559	-4.2481	546.6434
14	7.3478	29.2227	386.3229	22.9303	-6.4959	617.2189
15	7.8560	32.7422	307.3138	23.7137	-8.5582	678.0460
16	8.3398	35.8840	249.9641	24.4596	-10.5916	721.9439
17	8.9133	38.8402	223.1692	25.2152	-12.4542	737.3175
18	9.3654	41.4393	195.2671	25.9300	-13.9466	749.4451
19	9.6997	44.7527	143.7993	26.5490	-15.4624	736.7582
20	10.0092	49.3055	95.6426	27.1317	-17.3319	714.4557
21	10.3405	54.7332	35.1690	27.7125	-19.6969	679.1818
22	10.6888	60.6610	-39.7683	28.2886	-22.3567	624.0642
23	11.0521	66.9372	-112.2356	28.8517	-24.9829	554.8034
24	11.4217	73.1748	-163.9832	29.4114	-27.3167	473.0594
25	11.7927	78.3877	-186.2706	29.9749	-29.1547	376.7203
26	13.0986	83.4574	108.0631	31.8654	-36.1600	85.1300

LINK NO.	Q (RAD)	QDT (RAD/SEC)	QDDT (RAD/SEC2)
1	-0.1745	0.0	0.0
2	-0.1303	0.5581	38.7484
3	-0.0679	0.6933	48.4102
4	-0.1096	0.4926	38.1868
5	-0.0455	0.0236	8.3191
6	-0.0642	-0.6722	-38.2477
7	-0.0468	-1.8346	-119.5832
8	-0.0726	-3.1496	-191.7139
9	-0.1347	-3.9129	-184.5803
10	-0.1739	-4.5287	-83.5151
11	-0.2839	-4.7391	52.6816
12	-0.4271	-4.7330	57.6477
13	-0.5307	-4.6750	110.3840
14	-0.5374	-4.4263	96.7181
15	-0.6267	-4.1724	98.2710
16	-0.6071	-3.9013	45.0259
17	-0.5026	-3.6476	37.2316
18	-0.4927	-3.3778	53.1129
19	-0.4687	-5.7645	57.7173
20	-0.5038	-7.4361	56.1084
21	-0.5269	-8.4423	52.5589
22	-0.5576	-8.8222	25.8632
23	-0.5823	-8.5399	-10.3891
24	-0.5653	-7.6773	-60.4022
25	-0.5939	-6.3086	-124.8588
26	-0.6079	-5.1173	-196.2639

T=0.165 SEAT LOAD= 924.8 STRAP=148.3 LAP= 0.0 HEAD ANGLE=-0.636 KOUNT= 50

LINK NO.	AXIAL FORCE (LB)	SHEAR FORCE (LB)	MOMENT (IN-LB)	FACET FORCE (LB)
1	-924.8330	0.0	-0.0	0.0
2	-399.6205	-4.8526	88.5848	-109.6300
3	-367.3423	-11.8340	61.3426	-115.4803
4	-351.5519	-32.8431	67.226[illegible]	-104.4391
5	-350.3520	-25.7951	69.8382	-96.3438
6	-361.4703	-47.8492	91.9642	-71.9395
7	-385.2302	-42.5093	97.7094	-37.8824
8	-391.1527	-67.1304	133.1496	-19.7654
9	-354.0739	-56.4524	214.8562	-46.0596
10	-345.6506	-40.5613	234.4730	-38.9981
11	-329.4774	-36.2657	230.3206	-37.4308
12	-309.9632	-12.3178	206.4895	-40.2647
13	-281.7137	21.1909	154.1237	-49.0385
14	-287.3353	50.8731	57.6511	-22.6819
15	-244.1182	39.0245	9.2817	-26.8702
16	-200.2485	41.1196	-32.9270	-29.7825
17	-164.3350	19.0784	-57.6672	-29.5374
18	-130.8562	-4.4955	-66.5675	-26.2625
19	-95.1347	24.2407	223.7143	49.8753
20	-78.9668	16.6570	189.7549	36.5854
21	-69.9808	19.0490	152.9315	31.6825
22	-57.5730	17.8341	121.7128	23.7835
23	-38.1609	13.9688	99.3664	8.7049
24	-27.5878	13.5171	76.1731	0.4888
25	-21.6323	12.9342	53.5794	-4.2286
26	-34.0015	7.3342	19.8251	9.7187

LINK	U	UDT	UDDT	W	WDT	WDDT

NO.	(INS)	(IN/SEC)	(IN/SEC2)	(INS)	(IN/SEC)	(IN/SEC2)
1	4.2000	0.0	0.0	3.5907	0.0502	4.3835
2	4.7365	-0.4657	-18.4324	7.1008	0.7723	55.6453
3	4.9526	-1.8997	-57.8217	8.7453	1.3964	97.3755
4	5.0782	-3.3889	-56.3093	10.3959	1.8297	119.8599
5	5.2093	-4.1561	45.7840	12.0462	2.1025	132.1517
6	5.2843	-3.7030	242.1520	13.6491	2.1473	143.7205
7	5.3709	-1.4902	498.4038	15.1484	2.2098	166.4215
8	5.4599	2.7518	705.4698	16.5462	2.1318	193.0623
9	5.6130	8.1800	795.6300	17.8415	1.9974	239.0664
10	5.8047	13.5958	766.5951	19.0394	1.6217	271.9260
11	6.0595	18.4683	691.8070	20.0841	1.0080	295.1175
12	6.4451	23.1590	595.4857	21.0895	-0.1371	352.4064
13	6.9599	27.4520	466.4788	22.0411	-1.7714	410.6350
14	7.4335	31.0479	362.1615	22.9052	-3.6819	464.4472
15	8.0233	34.1555	260.9277	23.6789	-5.4964	514.3235
16	8.5721	36.9796	168.3419	24.4151	-7.3419	564.9808
17	9.1103	39.6237	68.0203	25.1617	-9.0413	620.7843
18	9.5742	41.8840	-48.0483	25.8693	-10.3805	680.0926
19	9.9241	44.7024	-189.4315	26.4808	-11.3073	716.1967
20	10.2551	48.6659	-345.4996	27.0541	-13.6831	732.3409
21	10.6122	53.4867	-503.0819	27.6228	-16.1419	733.4506
22	10.9889	58.8478	-649.9552	28.1850	-19.0176	703.5908
23	11.3824	64.6346	-778.4901	28.7340	-22.0316	622.0182
24	11.7825	70.5472	-857.4753	29.2808	-24.9055	498.0370
25	12.1823	76.2690	-892.5680	29.8335	-27.4056	326.5713
26	13.5447	88.4463	-494.9656	31.6849	-36.1896	-83.8379

LINK NO.	Q (RAD)	QDT (RAD/SEC)	QDDT (RAD/SEC2)
1	-0.1745	0.0	0.0
2	-0.1271	0.7096	20.8770
3	-0.0633	0.8450	8.0971
4	-0.1069	0.5097	-45.8266
5	-0.0457	-0.1894	-105.4134
6	-0.0685	-1.1480	-146.0801
7	-0.0578	-2.6143	-150.0427
8	-0.0907	-3.9953	-77.5855
9	-0.1557	-4.3254	20.0819
10	-0.1966	-4.4336	64.6181
11	-0.3069	-4.4450	88.5414
12	-0.4498	-4.2568	134.3886
13	-0.5525	-4.0360	113.0877
14	-0.5533	-3.6730	118.7319
15	-0.6465	-3.7239	125.3255
16	-0.6258	-3.5025	115.5086
17	-0.6200	-3.2121	146.9426
18	-0.5087	-2.8929	157.5279
19	-0.4962	-5.1398	180.6227
20	-0.5397	-6.8069	179.1739
21	-0.5680	-7.9201	153.4007
22	-0.6011	-8.5090	96.5315
23	-0.6250	-8.5299	12.2325
24	-0.6046	-8.0388	-88.7396
25	-0.6273	-7.1025	-181.7091
26	-0.6362	-6.2708	-262.4175

T=0.170 SEAT LOAD= 889.5 STRAP=173.7 LAP= 0.0 HEAD ANGLE=-0.671 KOUNT= 50

LINK NO.	AXIAL FORCE (LB)	SHEAR FORCE (LB)	MOMENT (IN-LB)	FACET FORCE (LB)

1	-889.4754	0.0	-0.0	0.0
2	-366.5167	-8.0883	73.9019	-109.1710
3	-344.2285	-17.6526	50.4405	-105.6020
4	-336.7974	-40.3953	77.8559	-86.0417
5	-341.0205	-33.5300	86.4665	-73.1060
6	-354.7781	-54.7313	111.2610	-46.0623
7	-372.0325	-45.9381	123.9959	-18.8979
8	-375.9068	-67.5870	154.6895	-3.1305
9	-330.9593	-51.8249	226.8357	-37.7514
10	-321.6548	-35.0042	236.3610	-32.5312
11	-305.0273	-30.1101	224.7413	-32.3753
12	-285.8367	-7.2586	196.6596	-35.9706
13	-259.1416	24.2194	143.7379	-44.8047
14	-263.4406	52.8114	48.8058	-21.5484
15	-224.0757	42.3543	-1.5629	-26.3785
16	-183.5342	43.3812	-45.8927	-30.3268
17	-151.3675	20.9649	-73.6521	-30.8667
18	-121.9012	-5.5566	-83.6607	-28.0012
19	-94.9262	29.0923	250.1141	67.0822
20	-76.9625	21.4087	210.0917	50.9945
21	-66.1782	24.6950	167.4758	43.5202
22	-52.4351	23.7702	130.8469	33.2852
23	-33.1077	18.8600	102.6322	17.3367
24	-22.1784	18.0515	73.8713	8.1233
25	-15.3544	17.7905	46.2444	1.8399
26	-18.4910	27.4226	13.2063	6.6023

LINK NO.	U (INS)	UDT (IN/SEC)	UDDT (IN/SEC2)	W (INS)	WDT (IN/SEC)	WDDT (IN/SEC2)
1	4.2000	0.0	0.0	3.5910	0.0792	5.8570
2	4.7841	-0.4720	28.3928	7.1054	1.0453	31.4426
3	4.9429	-1.8284	128.3706	8.7534	1.8092	27.4642
4	5.0619	-2.7866	359.9074	10.4063	2.2248	-2.9099
5	5.1313	-2.3796	699.1218	12.0580	2.4781	-16.7143
6	5.2721	-0.5284	1002.9552	13.6612	2.6046	6.2683
7	5.3728	2.8066	1148.7404	15.1611	2.7959	30.3919
8	5.4945	7.3824	1097.8986	16.5591	2.8849	54.2585
9	5.6546	12.5654	948.4143	17.8540	2.8185	52.3795
10	5.8827	17.6287	815.6161	19.0502	2.5016	58.1590
11	6.1608	22.0276	695.3780	20.0921	2.0126	65.2136
12	6.5582	26.0856	574.9936	21.0922	1.0194	82.7969
13	7.1029	29.7665	450.6537	22.0363	-0.4087	123.3885
14	7.6582	32.7815	317.4438	22.8914	-2.0496	191.9792
15	8.1971	35.2963	168.9079	23.6568	-3.5380	278.7906
16	8.7585	37.4445	7.6651	24.3847	-4.9638	383.0424
17	9.3082	39.3360	-178.3341	25.1238	-6.2023	510.5397
18	9.7318	40.8545	-367.6641	25.8257	-7.1280	622.7518
19	10.1437	42.8355	-564.8693	26.4306	-8.3325	670.3342
20	10.4924	45.9309	-745.2624	26.9948	-10.0894	696.9633
21	10.8715	49.9005	-916.6522	27.5513	-12.5113	710.0247
22	11.2731	54.4776	-1075.6682	28.0987	-15.4948	698.6778
23	11.6938	59.5590	-1224.5244	28.6317	-18.8623	643.9480
24	12.1223	64.9706	-1343.5514	29.1626	-22.3396	533.4382
25	12.5502	70.4897	-1368.0658	29.7008	-25.6671	386.2943
26	13.9785	84.7048	-977.3275	31.5025	-36.8161	-149.6794

LINK NO.	O (RAD)	ODT (RAD/SEC)	ODDT (RAD/SEC2)
1	-0.1745	0.0	0.0
2	-0.1234	0.7143	-34.3235

3	-0.0600	0.6433	-108.6909
4	-0.1055	-0.0823	-183.0588
5	-0.0484	-0.9808	-181.4885
6	-0.0761	-1.8549	-108.5073
7	-0.0720	-2.9296	13.7193
8	-0.1105	-3.7498	120.1718
9	-0.1767	-4.0034	116.6298
10	-0.2178	-3.9955	127.4204
11	-0.3276	-3.8092	117.7526
12	-0.4695	-3.6334	127.7803
13	-0.5711	-3.4092	140.0307
14	-0.5761	-3.1868	176.4221
15	-0.6632	-2.9080	202.1139
16	-0.6412	-2.5760	223.8186
17	-0.6339	-2.2349	250.4536
18	-0.5208	-1.8957	253.9107
19	-0.5194	-4.0912	230.0601
20	-0.5713	-5.8202	202.3020
21	-0.6056	-7.1117	163.0598
22	-0.6423	-7.9977	104.6516
23	-0.5675	-3.4472	19.5173
24	-0.6459	-8.4739	-81.8106
25	-0.6653	-8.1126	-226.9560
26	-0.6711	-7.7188	-313.5491

T=0.175 SEAT LOAD= 345.0 STRAP=197.7 LAP= C.0 HEAD ANGLE=-0.714 KOUNT= 53

LINK NO.	AXIAL FORCE (LB)	SHEAR FORCE (LB)	MOMENT (IN-LB)	FACET FORCE (LB)
1	-345.0054	0.0	-0.0	0.0
2	-332.6818	-11.1819	64.5532	-102.1152
3	-322.5429	-23.5119	66.4629	-87.9031
4	-323.3557	-46.9665	93.7258	-62.2718
5	-329.1161	-38.0826	102.6214	-48.8101
6	-341.6701	-57.1767	124.6814	-23.6790
7	-352.2612	-45.5405	139.8566	-4.3558
8	-355.0367	-64.8563	165.7576	8.8744
9	-307.4928	-46.7196	234.9657	-29.8700
10	-298.6528	-29.0014	236.9320	-26.3675
11	-282.7240	-23.1620	219.3479	-27.6072
12	-264.0215	-0.8009	185.5142	-32.4077
13	-213.4902	29.1032	128.9057	-41.7252
14	-241.1351	56.5295	33.0503	-21.8666
15	-205.9485	46.0263	-19.6336	-27.3470
16	-163.9522	44.4222	-64.8653	-32.3061
17	-141.3253	20.4214	-92.8772	-33.1244
18	-116.4788	-9.1961	-100.8014	-30.1589
19	-97.3942	32.3774	276.9254	82.0712
20	-77.3770	24.4650	232.1017	63.6468
21	-65.7041	28.4906	184.6658	54.1905
22	-50.8018	27.7841	143.6421	42.0349
23	-31.1247	22.1157	111.0128	24.9849
24	-19.7462	21.1085	77.9676	14.8181
25	-12.1934	21.0154	46.3959	7.3174
26	-10.5101	37.0236	12.7674	6.4089

LINK NO.	U (INS)	UDT (IN/SEC)	UDDT (IN/SEC2)	W (INS)	WDT (IN/SEC)	WDDT (IN/SEC2)
1	4.2000	0.0	0.0	3.5914	0.0867	-3.3214
2	4.7824	-0.1191	108.0849	7.1105	0.8640	-110.0895
3	4.9368	-0.2893	483.7222	8.7619	1.3719	-199.0839

4	5.0549	0.4388	892.7419	10.4164	1.6245	-230.5940
5	5.1305	2.4511	1167.5368	12.0692	1.7903	-255.7928
6	5.2838	5.4416	1317.9503	13.6732	1.9632	-269.4080
7	5.4024	9.1786	1351.8302	15.1742	2.1731	-238.8842
8	5.5360	13.3929	1264.6639	16.5728	2.2993	-295.9449
9	5.729[illegible]	17.7036	1086.2006	17.8674	2.2557	-296.8614
10	5.9811	21.7856	879.9928	19.0621	1.9642	-291.3953
11	6.2794	25.4102	689.3684	20.1015	1.4806	-274.7614
12	6.7057	28.8250	511.2705	21.0970	0.5243	-232.9755
13	7.2570	31.8016	344.3743	22.0346	-0.5008	-150.1252
14	7.8255	34.0234	162.2623	22.8826	-1.6857	-37.3581
15	8.3750	35.6837	-28.3381	23.6418	-2.6243	93.1702
16	8.9448	36.9059	-229.0180	24.3641	-3.3882	245.3220
17	9.5016	37.7923	-441.6515	25.0987	-3.9289	398.0418
18	9.9303	38.3326	-639.0162	25.7974	-4.2437	526.0190
19	10.3495	39.2441	-849.4147	26.3971	-5.1289	606.0101
20	10.7111	41.3279	-1054.8171	26.9529	-6.6706	671.7534
21	11.1073	44.3912	-1247.7073	27.4976	-8.9465	723.6602
22	11.5304	48.1794	-1416.4962	28.0301	-11.9131	744.4805
23	11.9748	52.5481	-1560.9512	28.5457	-15.4882	713.8304
24	12.4283	57.4140	-1656.9624	29.0580	-19.4488	628.5140
25	12.8838	62.6699	-1709.3538	29.5775	-23.5482	466.1340
26	14.3883	78.9413	-1306.2711	31.3166	-37.5740	-146.5866

LINK NO.	O (RAD)	ODT (RAD/SEC)	ODDT (RAD/SEC 2)
1	-0.1745	0.0	0.0
2	-0.1209	0.1539	-198.1444
3	-0.0588	-0.3075	-252.2701
4	-0.1083	-1.0364	-180.3192
5	-0.0553	-1.7064	-105.1386
6	-0.0364	-2.2146	-43.3434
7	-0.0864	-2.7976	37.0458
8	-0.1277	-3.1546	123.2951
9	-0.1948	-3.2078	155.0773
10	-0.2360	-3.2385	167.1218
11	-0.3452	-3.1315	170.3854
12	-0.4860	-2.9414	163.5459
13	-0.5862	-2.5560	197.2185
14	-0.58[illegible]	-2.1618	232.8308
15	-0.6749	-1.7285	260.9600
16	-0.6510	-1.2973	275.4738
17	-0.6418	-0.9101	275.2136
18	-0.5270	-0.5817	265.3987
19	-0.5367	-2.8214	262.1813
20	-0.5377	-4.7212	237.8981
21	-0.6301	-6.2655	186.3665
22	-0.6810	-7.4780	108.1730
23	-0.7095	-8.3645	9.9988
24	-0.6893	-8.9338	-106.0142
25	-0.7036	-9.2169	-225.0817
26	-0.7133	-9.3591	-337.3458

T=0.130 SEAT LOAD= 814.0 STRAP=219.7 LAP= 0.0 HEAD ANGLE=-0.765 KOUNT= 52

LINK NO.	AXIAL FORCE (LB)	SHEAR FORCE (LB)	MOMENT (IN-LB)	FACET FORCE (LB)
1	-314.0241	0.0	-0.0	0.0
2	-320.2457	-14.4657	74.5230	-84.5777
3	-311.8646	-25.3529	77.3592	-69.1599
4	-312.0353	-49.6359	104.1970	-44.9815

5	-317.4788	-39.6684	111.5426	-32.4535
6	-328.7458	-57.4382	131.0919	-9.2159
7	-334.7234	-44.1200	147.1664	4.7330
8	-336.4108	-61.4495	169.1230	15.9065
9	-288.3005	-42.2896	235.5389	-24.4926
10	-280.1400	-24.2237	233.6876	-22.0216
11	-264.9978	-17.4415	212.5122	-24.2246
12	-246.1909	5.1264	172.5735	-30.1130
13	-220.3765	34.2843	108.0211	-40.1777
14	-220.6525	60.2287	9.8397	-23.7849
15	-189.2585	48.2964	-44.1016	-29.6023
16	-156.1053	42.9447	-87.4041	-35.1891
17	-133.0392	16.9908	-112.6571	-35.7235
18	-112.9300	-15.4132	-116.0858	-32.2731
19	-101.4469	33.7864	303.8742	95.2264
20	-80.7593	25.4836	255.8481	75.0658
21	-67.7972	30.0483	204.9804	64.3557
22	-52.0833	29.6209	160.8203	50.8461
23	-31.6991	23.7280	125.1373	32.6014
24	-19.7549	22.8185	88.8720	21.5723
25	-11.5883	22.8041	54.2144	13.1583
26	-7.3988	35.8294	18.8911	9.5421

LINK NO.	U (INS)	UDT (IN/SEC)	UDDT (IN/SEC2)	W (INS)	WDT (IN/SEC)	WDDT (IN/SEC2)
1	4.2000	0.0	0.0	3.5918	0.0499	-9.3509
2	4.7334	0.5164	133.5567	7.1130	0.0856	-174.3268
3	4.9423	2.5376	573.1446	8.7657	0.0791	-286.3170
4	5.0692	5.3937	999.8315	10.4299	0.0849	-359.1162
5	5.2184	8.8178	1312.4031	12.0741	0.0442	-416.8366
6	5.3283	12.4795	1466.2799	13.6787	0.0861	-452.2321
7	5.4656	16.1865	1453.6783	15.1804	0.1237	-500.0790
8	5.6190	19.8359	1336.5128	16.5793	0.1211	-543.9580
9	5.8323	23.3011	1169.0763	17.8736	-0.0203	-573.5620
10	6.1015	26.4589	972.1093	19.0669	-0.2900	-576.7172
11	6.4154	29.0530	755.0678	20.1042	-0.6233	-543.8934
12	6.8560	31.3035	488.1906	21.0962	-1.1469	-459.4672
13	7.4197	33.1228	195.1660	22.0293	-1.7422	-327.5166
14	7.9968	34.2851	-58.7441	22.8729	-2.2752	-177.1437
15	8.5520	34.9279	-274.3715	23.6292	-2.5112	-32.8355
16	9.1255	35.1283	-480.2653	24.3497	-2.4927	124.2625
17	9.6840	34.9561	-691.9830	25.0835	-2.2470	281.7867
18	10.1629	34.5016	-884.4442	25.7823	-1.8904	413.6435
19	10.5340	34.4038	-1069.1301	26.3787	-2.2872	521.4815
20	10.9037	35.5194	-1247.6112	26.9278	-3.4098	617.9109
21	11.3135	37.6949	-1411.8590	27.4619	-5.3402	699.7949
22	11.7530	40.7103	-1554.5810	27.9800	-8.1191	751.3852
23	12.2174	44.3928	-1681.2135	28.4774	-11.7674	754.0364
24	12.6946	48.7531	-1780.0828	28.9689	-16.1221	691.4816
25	13.1751	53.7551	-1831.4261	29.4661	-20.9605	557.0752
26	14.7657	71.8080	-1533.9874	31.1270	-38.2426	-117.5644

LINK NO.	O (RAD)	ODT (RAD/SEC)	ODDT (RAD/SEC2)
1	-0.1745	0.0	0.0
2	-0.1230	-1.0177	-227.2689
3	-0.0636	-1.6010	-250.4983
4	-0.1158	-1.9666	-199.7695
5	-0.0651	-2.2042	-112.6494
6	-0.0478	-2.3345	-26.3075

7	-0.0997	-2.5041	59.5899
8	-0.1420	-2.5630	106.0376
9	-0.2032	-2.5232	144.8935
10	-0.2500	-2.3666	179.3553
11	-0.3586	-2.1187	235.7337
12	-0.4981	-1.7942	283.0849
13	-0.5962	-1.3703	291.3798
14	-0.5373	-0.8901	276.4066
15	-0.6802	-0.3752	275.9407
16	-0.6540	0.0978	282.4252
17	-0.6428	0.4883	275.2936
18	-0.5265	0.7634	257.2984
19	-0.5475	-1.4780	259.3318
20	-0.6183	-3.5141	235.6523
21	-0.6681	-5.3139	186.6262
22	-0.7170	-6.8949	116.3031
23	-0.7511	-8.2724	23.4329
24	-0.7353	-9.4210	-88.2756
25	-0.7575	-10.3427	-218.2018
26	-0.7648	-11.0388	-329.1941

T=0.185 SEAT LOAD= 805.6 STRAP=238.8 LAP= 0.0 HEAD ANGLE=-0.824 KOUNT= 50

LINK NO.	AXIAL FORCE (LB)	SHEAR FORCE (LB)	MOMENT (IN-LB)	FACET FORCE (LB)
1	-805.6473	0.0	-0.0	0.0
2	-334.9839	-16.7620	105.6112	-58.6067
3	-315.5281	-24.6786	91.7439	-53.5234
4	-308.2854	-48.1016	109.7966	-36.4734
5	-310.6345	-37.5302	112.6938	-27.1093
6	-320.2143	-55.1444	129.7376	-5.9339
7	-325.0775	-42.0059	145.4251	6.5657
8	-326.5270	-58.3127	165.8512	17.0888
9	-278.7069	-33.6183	227.2881	-23.2496
10	-269.8229	-20.0429	220.6989	-21.6841
11	-253.6810	-12.4880	193.7710	-24.8060
12	-234.4767	9.6122	150.1733	-31.0986
13	-209.3142	37.3247	84.0430	-40.7674
14	-207.9872	61.7792	-13.1445	-26.4738
15	-178.1936	48.8909	-68.0019	-32.3481
16	-146.3213	40.0569	-109.2336	-38.3233
17	-126.6367	11.5332	-130.4443	-39.1734
18	-109.9366	-23.8306	-127.3884	-33.7972
19	-105.7922	33.4700	330.7561	107.7980
20	-84.2611	24.6759	281.0300	86.4519
21	-70.9954	29.5820	228.1117	75.0284
22	-54.9208	29.4461	182.0831	60.6393
23	-33.8460	23.7748	144.7276	41.1821
24	-21.4160	23.2149	106.3561	29.3617
25	-12.7998	23.2033	69.5055	20.2559
26	-8.3326	23.6798	31.8035	16.1737

LINK NO.	U (INS)	UDT (IN/SEC)	UDDT (IN/SEC2)	W (INS)	WDT (IN/SEC)	WDDT (IN/SEC2)
1	4.2000	0.0	0.0	3.5919	0.0059	-7.5384
2	4.7874	1.0088	46.3921	7.1114	-0.6631	-118.3104
3	4.9611	4.7578	279.5590	8.7626	-1.2625	-237.4220
4	5.1075	9.5998	628.6424	10.4169	-1.7012	-343.4343
5	5.2779	14.7170	995.6832	12.0689	-2.1363	-445.3195
6	5.4986	19.5242	1311.2764	13.6732	-2.3713	-519.7529
7	5.5659	23.6347	1494.4554	15.1743	-2.6365	-538.2845

8	5.7355	26.9032	1462.1792	16.5727	-2.8570	-623.3808
9	5.9639	29.4477	1264.4234	17.8658	-3.1432	-648.1113
10	6.2462	31.4464	1008.1003	19.0577	-3.4311	-643.2457
11	6.5701	32.7928	725.2091	20.0938	-3.6157	-612.3755
12	7.0185	33.6147	420.4565	21.0842	-3.7114	-530.2096
13	7.5874	33.8745	104.3606	22.0161	-3.6046	-391.9934
14	8.1668	33.6195	-189.2968	22.8591	-3.2997	-216.7663
15	8.7223	33.0264	-460.6595	23.6161	-2.7415	-47.0586
16	9.2941	32.1372	-697.1089	24.3386	-1.9395	114.2601
17	9.8492	30.9467	-901.3884	25.0755	-0.9722	249.7471
18	10.3235	29.6017	-1063.9143	25.7777	-0.0283	350.9095
19	10.6920	28.6587	-1213.1717	26.3733	0.0586	431.6742
20	11.0651	28.9748	-1353.4039	26.9180	-0.6026	513.1175
21	11.4839	30.4182	-1481.4470	27.4435	-2.1173	590.0567
22	11.9363	32.7912	-1593.6421	27.9484	-4.6048	647.8537
23	12.4182	35.8952	-1695.3482	28.4278	-8.1641	675.6384
24	12.9159	39.7957	-1788.6930	28.8969	-12.7237	647.3685
25	13.4208	44.5027	-1835.2116	29.3684	-18.1185	564.5949
26	15.1043	63.6834	-1714.1926	30.9344	-38.7748	-104.3409

LINK NO.	O (RAD)	ODT (RAD/SEC)	ODDT (RAD/SEC2)
1	-0.1745	0.0	0.0
2	-0.1395	-1.8814	-116.9464
3	-0.0746	-2.7491	-196.5147
4	-0.1282	-3.0062	-215.7436
5	-0.0778	-2.9604	-195.7094
6	-0.1103	-2.7471	-141.6550
7	-0.1118	-2.4009	-16.7260
8	-0.1534	-1.9846	128.8997
9	-0.2198	-1.7013	182.8872
10	-0.2594	-1.3382	235.9922
11	-0.3661	-0.8757	267.4295
12	-0.5034	-0.3429	290.5561
13	-0.5992	0.2012	317.9992
14	-0.5979	0.6763	333.7349
15	-0.6784	1.1038	317.0285
16	-0.6501	1.4707	273.3986
17	-0.6371	1.7622	236.6882
18	-0.5197	1.9301	204.6749
19	-0.5518	-0.3075	202.4583
20	-0.6331	-2.4466	184.9119
21	-0.6924	-4.4576	148.7059
22	-0.7500	-6.3524	96.0620
23	-0.7321	-8.1497	25.1971
24	-0.7834	-9.8109	-60.5938
25	-0.8117	-11.3219	-181.2869
26	-0.8239	-12.5895	-283.9965

T=0.190 SEAT LOAD= 815.0 STRAP=254.7 LAP= 0.0 HEAD ANGLE=-0.890 KOUNT= 50

LINK NO.	AXIAL FORCE (LB)	SHEAR FORCE (LB)	MOMENT (IN-LB)	FACET FORCE (LB)
1	-815.0082	0.0	-0.0	0.0
2	-368.5125	-20.2671	147.9480	-30.8680
3	-335.9611	-23.1790	113.4860	-38.0423
4	-317.2218	-45.1890	117.7536	-31.7970
5	-313.1079	-32.2311	111.8080	-28.7313
6	-318.0353	-48.9484	122.7675	-12.5222
7	-322.2811	-35.4910	131.5908	-0.6266
8	-322.6432	-51.0570	148.6837	8.6491

9	-278.6589	-33.7255	203.9347	-27.7307
10	-268.8846	-16.2943	195.2310	-26.4952
11	-252.0493	-9.2752	166.1946	-29.7055
12	-232.2218	11.9000	121.1668	-35.7624
13	-207.2985	37.9846	54.8312	-44.4821
14	-205.2819	60.0176	-38.0465	-30.6571
15	-176.0751	45.0026	-88.5043	-35.5088
16	-145.1245	33.9769	-123.8422	-40.8833
17	-125.3507	4.2602	-139.7860	-39.6483
18	-108.9565	-32.7031	-130.9688	-34.2574
19	-110.8140	31.9795	358.3732	120.1802
20	-88.3392	22.5563	307.5518	98.0275
21	-74.8916	27.5241	253.3894	86.3162
22	-58.6037	27.4957	206.3889	71.4762
23	-36.4579	22.3302	168.4342	51.0141
24	-24.0928	22.2816	129.0602	38.6143
25	-15.2309	22.1717	91.0349	29.0752
26	-12.2008	0.4976	51.0500	26.1165

LINK NO.	U (INS)	UDT (IN/SEC)	UDDT (IN/SEC2)	W (INS)	WDT (IN/SEC)	WDDT (IN/SEC2)
1	4.2000	0.0	0.0	3.5919	-0.0267	-5.7814
2	4.7927	1.0810	7.4147	7.1069	-1.1237	-69.3152
3	4.9873	5.5333	84.4525	8.7537	-2.2599	-161.9674
4	5.1516	11.7515	287.4852	10.4042	-3.2955	-283.0876
5	5.3623	18.7243	622.7020	12.0527	-4.3134	-405.6386
6	5.5215	25.3375	981.6592	13.6548	-4.9574	-493.2943
7	5.7012	30.6241	1240.0536	15.1538	-5.5613	-560.0383
8	5.8880	33.9134	1277.8877	16.5507	-5.9090	-577.5734
9	6.1267	35.5396	1123.5687	17.8422	-6.2504	-575.8625
10	6.4156	36.2298	875.8142	19.0328	-6.4503	-545.9018
11	6.7426	36.1272	591.3972	20.0684	-6.4287	-432.7188
12	7.1912	35.3839	280.2548	21.0594	-6.0397	-396.5669
13	7.7575	34.0720	-29.3606	21.9935	-5.3144	-264.6386
14	8.3321	32.4164	-293.0607	22.8401	-4.2013	-115.8779
15	8.8314	30.5414	-526.2498	23.6020	-2.8518	24.9691
16	9.4457	28.4713	-746.4393	24.3305	-1.2571	171.6737
17	9.9922	26.2021	-965.1503	25.0740	0.4080	312.3590
18	10.4577	23.9872	-1153.9089	25.7821	1.8734	422.8808
19	10.8137	22.3218	-1307.9102	26.3791	2.2741	473.4651
20	11.1328	22.0476	-1421.0745	26.9213	1.9211	517.9917
21	11.6175	22.9829	-1505.9423	27.4400	0.6980	556.9402
22	12.0810	24.9018	-1576.8890	27.9331	-1.5788	578.5347
23	12.5767	27.5497	-1653.1107	28.3949	-5.0564	574.1004
24	13.0928	31.0059	-1728.2351	28.8409	-9.7568	534.3151
25	13.6203	35.3257	-1852.1886	29.2843	-15.5898	433.2539
26	15.4011	54.6834	-1881.5452	30.7391	-39.3774	-140.9128

LINK NO.	O (RAD)	ODT (RAD/SEC)	ODDT (RAD/SEC2)
1	-0.1745	0.0	0.0
2	-0.1410	-2.2351	-35.3701
3	-0.0904	-3.4797	-102.2804
4	-0.1459	-4.0545	-184.9848
5	-0.0953	-4.0495	-212.5357
6	-0.1261	-3.5969	-178.7430
7	-0.1242	-2.6066	-61.4587
8	-0.1618	-1.3979	96.1510
9	-0.2259	-0.7453	180.2827
10	-0.2630	-0.1033	244.5651

11	-0.3670	0.5320	283.6858
12	-0.5014	1.1518	301.7742
13	-0.5943	1.7405	294.6271
14	-0.5905	2.2403	287.8502
15	-0.6690	2.6404	281.8976
16	-0.6392	2.8985	279.2317
17	-0.6252	3.0160	263.9321
18	-0.5074	2.9942	229.3076
19	-0.5510	0.6111	182.8879
20	-0.6433	-1.6730	136.3889
21	-0.7131	-3.8506	95.6165
22	-0.7807	-5.9578	56.4468
23	-0.8326	-8.0439	9.4176
24	-0.8332	-10.0811	-57.9661
25	-0.8703	-12.0605	-107.6144
26	-0.8901	-13.8986	-197.9175

T=0.195 SEAT LOAD= 837.1 STRAP=267.0 LAP= 0.0 HEAD ANGLE=-0.961 KOUNT= 53

LINK NO.	AXIAL FORCE (LB)	SHEAR FORCE (LB)	MOMENT (IN-LB)	FACET FORCE (LB)
1	-837.0840	0.0	-0.0	0.0
2	-412.5217	-24.0740	194.5873	-4.8224
3	-368.4940	-22.4755	141.4979	-22.2595
4	-339.0005	-42.7720	132.6718	-26.3986
5	-324.3134	-24.7117	113.0248	-32.8056
6	-320.6267	-33.8931	112.5432	-25.5796
7	-322.5411	-23.5236	106.7880	-15.3869
8	-319.7610	-37.7624	116.7743	-9.0414
9	-282.9013	-25.7182	161.0260	-37.7378
10	-272.3922	-11.8347	153.6573	-36.1604
11	-256.0064	-7.0330	128.4604	-38.4111
12	-236.6088	12.3232	87.6816	-43.2365
13	-212.6131	36.6963	25.7814	-50.2486
14	-210.5080	56.5159	-61.8733	-35.6465
15	-179.9892	39.1140	-107.6201	-39.2074
16	-147.9656	25.6392	-135.8625	-43.5232
17	-127.1212	-5.8285	-143.6918	-40.5353
18	-109.7447	-43.3621	-126.1707	-33.5364
19	-117.6799	29.4998	388.1088	132.3069
20	-94.1806	19.4951	336.5633	109.5884
21	-80.5096	24.6096	281.2306	97.8237
22	-63.3381	24.7183	233.3782	82.6250
23	-41.2042	20.2264	195.2190	61.0543
24	-28.0783	20.7800	155.3307	46.0613
25	-19.0693	20.4714	116.7224	38.1806
26	-18.9001	-29.2478	73.8074	37.8453

LINK NO.	U (INS)	UDT (IN/SEC)	UDDT (IN/SEC2)	W (INS)	WDT (IN/SEC)	WDDT (IN/SEC2)
1	4.2000	0.0	0.0	3.5917	-0.0486	-2.5078
2	4.7983	1.1704	24.2277	7.1005	-1.3394	-41.2066
3	5.0160	6.0035	120.6053	8.7406	-2.9019	-97.9559
4	5.2236	13.0221	254.2345	10.3847	-4.4326	-169.1328
5	5.4626	21.2241	410.6911	12.0266	-5.9865	-251.0808
6	5.6586	29.1802	567.0466	13.6244	-7.0486	-319.1939
7	5.8677	35.5142	689.5407	15.1196	-7.9605	-368.3569
8	6.0715	39.0472	726.8290	16.5145	-8.3710	-376.7258
9	6.3169	40.1445	669.0134	17.8044	-8.6752	-364.4453
10	6.6066	39.8702	538.9827	18.9945	-8.5339	-326.1663
11	6.9298	38.5433	354.6909	20.0310	-8.3664	-265.5804

12	7.3710	36.3966	123.4064	21.0249	-7.5363	-171.3612
13	7.9270	33.6624	-126.2100	21.9645	-6.1004	-42.6462
14	8.4902	30.7640	-358.8370	22.8185	-4.2825	91.2157
15	9.0273	27.7971	-568.5895	23.5888	-2.2795	214.3092
16	9.5787	24.7117	-756.9721	24.3270	-0.0288	328.6735
17	10.1115	21.4562	-928.3944	25.0804	2.2385	422.4028
18	10.5634	18.3864	-1070.3138	25.7971	4.1669	488.1642
19	10.9151	15.9383	-1211.9072	26.3966	4.7562	504.1302
20	11.2853	15.0143	-1344.3343	26.9375	4.5772	524.1706
21	11.7135	15.4457	-1457.0169	27.4505	3.4961	541.8137
22	12.1856	16.9715	-1548.3297	27.9324	1.2451	535.2268
23	12.6837	19.2697	-1625.6835	28.3765	-2.3728	492.2681
24	13.2263	22.3857	-1702.8602	28.7983	-7.3998	409.4138
25	13.7743	26.3333	-1763.4773	29.2113	-13.7590	309.3981
26	15.6503	44.9115	-2020.3689	30.5403	-40.1158	-138.2951

LINK NO.	O (RAD)	ODT (RAD/SEC)	ODDT (RAD/SEC2)
1	-0.1745	0.0	0.0
2	-0.1526	-2.4221	-54.2273
3	-0.1089	-3.9114	-81.0766
4	-0.1681	-4.7529	-96.4966
5	-0.1178	-4.8496	-97.3805
6	-0.1460	-4.3023	-82.9818
7	-0.1389	-2.9011	-38.5916
8	-0.1678	-1.0698	34.2993
9	-0.2277	-0.0538	92.9887
10	-0.2607	0.9394	155.2921
11	-0.3610	1.8101	208.7074
12	-0.4921	2.5323	240.2954
13	-0.5820	3.1246	254.9623
14	-0.5759	3.5892	257.2164
15	-0.6524	3.9487	242.8445
16	-0.6214	4.1541	218.5757
17	-0.6071	4.1822	190.7904
18	-0.4897	4.0238	166.0591
19	-0.5457	1.5112	159.6237
20	-0.6500	-0.9865	130.8739
21	-0.7312	-3.4134	84.3729
22	-0.8100	-5.7793	28.6018
23	-0.8729	-8.1212	-24.8234
24	-0.8843	-10.4054	-61.8145
25	-0.9321	-12.6121	-95.6375
26	-0.9612	-14.5426	-96.0921

T=0.200 SEAT LOAD= 863.1 STRAP=276.0 LAP= 0.0 HEAD ANGLE=-1.035 KOUNT= 52

LINK NO.	AXIAL FORCE (LB)	SHEAR FORCE (LB)	MOMENT (IN-LB)	FACET FORCE (LB)
1	-863.1495	0.0	-0.0	0.0
2	-461.3360	-23.5257	246.7153	23.1159
3	-405.7395	-21.4719	172.1554	-6.1473
4	-363.6539	-39.9059	148.9554	-21.5330
5	-338.3390	-16.2138	114.0866	-32.4133
6	-323.8061	-27.4131	100.6260	-41.3258
7	-322.7520	-9.4312	77.4400	-33.1578
8	-315.3792	-21.4506	78.2262	-30.8146
9	-286.3553	-15.3583	105.0323	-50.6401
10	-274.0973	-6.1904	97.6750	-48.8189
11	-258.4968	-4.7607	78.0775	-49.6847
12	-240.3325	11.4568	45.5684	-52.5207

13	-218.2611	33.1023	-7.5476	-57.0560
14	-217.0410	49.8737	-85.8342	-40.9237
15	-185.7130	30.1422	-123.5329	-42.6356
16	-153.2012	15.1566	-142.4949	-45.4219
17	-131.3435	-17.0864	-141.1973	-40.5510
18	-112.9656	-54.0402	-114.8503	-31.9911
19	-127.2795	26.2018	418.6351	142.4723
20	-103.0284	15.4342	367.3160	119.4826
21	-89.5512	20.6911	311.4366	108.1295
22	-72.4173	21.1915	263.0611	92.7164
23	-48.0383	17.8245	224.7108	69.6848
24	-34.1230	19.2017	183.9044	55.9902
25	-24.6998	13.7474	144.1614	45.7970
26	-28.6284	-59.7863	97.0060	49.4539

LINK NO.	U (INS)	UDT (IN/SEC)	UDDT (IN/SEC2)	W (INS)	WDT (IN/SEC)	WDDT (IN/SEC2)
1	4.2000	0.0	0.0	3.5914	-0.0512	1.3683
2	4.8045	1.3149	32.9291	7.0932	-1.5380	-13.7352
3	5.0478	6.7264	149.6228	8.7251	-3.2431	-34.2814
4	5.2920	14.3369	245.4746	10.3609	-4.9800	-47.3131
5	5.5733	22.9388	256.8679	11.9943	-6.7733	-63.1953
6	5.8101	31.1238	209.0351	13.5862	-8.0258	-71.2736
7	6.0515	37.5290	131.7479	15.0764	-9.0548	-67.3249
8	6.2731	41.0215	76.4125	16.4693	-9.4587	-52.4788
9	6.5234	41.9450	48.4151	17.7578	-9.6760	-29.5027
10	6.8106	41.3193	26.5640	18.9483	-9.5274	-1.6378
11	7.1255	39.4459	-16.3340	19.9870	-8.9503	40.2030
12	7.5537	36.5016	-107.0570	20.9862	-7.7108	106.3842
13	8.0934	32.7591	-252.7556	21.9345	-5.6972	201.6756
14	8.6393	28.8262	-421.6612	22.7991	-3.2948	292.8193
15	9.1591	24.9055	-582.8967	23.5808	-0.7661	374.2118
16	9.6928	20.9722	-729.2319	24.3315	1.9487	445.0055
17	10.2072	16.9721	-857.2641	25.0972	4.5662	494.7255
18	10.6424	13.3163	-952.4922	25.8242	6.7110	518.8891
19	10.9804	10.3340	-1026.5267	26.4266	7.2104	467.4369
20	11.3446	8.9195	-1089.0300	26.9666	6.9734	426.2265
21	11.7737	8.9060	-1150.5403	27.4743	5.8746	400.0491
22	12.2524	10.0078	-1225.2351	27.9447	3.5503	379.8898
23	12.7703	11.8143	-1338.4381	28.3702	-0.2629	352.4724
24	13.3177	14.3749	-1485.8114	28.7660	-5.5136	312.5317
25	13.8843	17.7177	-1662.9796	29.1459	-12.4219	252.6648
26	15.8493	34.6265	-2063.1726	30.3384	-40.5353	-5.9334

LINK NO.	O (RAD)	ODT (RAD/SEC)	ODDT (RAD/SEC2)
1	-0.1745	0.0	0.0
2	-0.1655	-2.7567	-66.5968
3	-0.1235	-4.3057	-68.9283
4	-0.1928	-5.0452	-21.6737
5	-0.1427	-5.0262	19.1953
6	-0.1680	-4.3797	43.1514
7	-0.1527	-2.8891	42.4168
8	-0.1729	-0.9542	25.5955
9	-0.2272	0.2022	19.6898
10	-0.2547	1.3942	35.1493
11	-0.3499	2.5115	77.0696
12	-0.4768	3.4780	131.9125
13	-0.5635	4.2347	175.1464
14	-0.5549	4.7316	186.1465

15	-0.6299	5.0169	176.9663
16	-0.5982	5.0883	155.9168
17	-0.5841	4.9649	125.7269
18	-0.4678	4.6685	95.5431
19	-0.5365	2.0864	70.3933
20	-0.6535	-0.5136	55.8195
21	-0.7473	-3.0622	53.5735
22	-0.8384	-5.5681	55.6316
23	-0.9136	-8.0749	46.0952
24	-0.9368	-10.5131	24.5650
25	-0.9759	-12.8567	-2.2588
26	-1.0347	-14.7942	-7.6115

END OF SIMULATION. IHLF= 0

STOP 0
EXECUTION TERMINATED